Molecular pharmacology of altered cardiopulmonary function in inflammation

El-Awady, Mohammed

Award date:
2008

Awarding institution:
University of Bath

Molecular Pharmacology of Altered Cardiopulmonary Function in Inflammation

Mohammed Shaaban Hassan El-Awady

A thesis submitted for the degree of Doctor of Philosophy

University of Bath

Department of Pharmacy and Pharmacology

November 2008

Acknowledgements

I wish to express my sincere gratitude and appreciation to my supervisors,
Dr. Malcolm Watson and Dr. Sergey Smirnov for their continuous guidance, help and support. Their guidance helped me in critically analyzing scientific literature, planning and executing experimental strategies, and writing, presenting, and publishing my results.

I sincerely thank my Egyptian colleagues and friends (Osama, Hassan, Mostafa, Hany, Hanan) for their help, advice and sharing good moments throughout these years.

I would also like to thank Dr. Mike Storm and Dr. Adrian Roger for their technical help and advice. Thanks also to all the colleagues in the department, the technicians and the staff of the animal house for their assistance and support.

I sincerely thank the Egyptian Cultural Bureau in London, the Mission Department in Cairo and My Department of Pharmacology & Toxicology, University of Mansoura, Egypt for the financial support, assistance and advice.

Finally and most importantly, I thank my family for their invaluable support and sharing both good and bad moments of life throughout these past four years.

Publications

Original papers:

1- El-Awady MSH, Smirnov SV, Watson ML (2008). Desensitization of the soluble guanylyl cyclase/cGMP pathway by lipopolysaccharide in isolated rat pulmonary artery but not aorta. *Br J Pharmacol*, **155**, 1164–1173.

2- El-Awady MSH, Smirnov SV, Watson ML. Voltage-independent calcium channels mediate lipopolysaccharide-induced hyporeactivity to endothelin-1 in the rat aorta. Submitted.

Abstracts:

1- El-Awady MSH, Smirnov SV, Watson ML. Mechanisms of LPS-induced changes in vascular reactivity to endothelin-1 in rat aortic and pulmonary vessels. Presented at BPS Winter Meeting (2006) and published in pA_2Online, Vol4Issue2abst020P.

2- El-Awady MSH, Smirnov SV, Watson ML. Desensitization of NO/cGMP pathway in isolated rat pulmonary artery but not aorta by lipopolysaccharide. Presented at 5^{th} James Black Conference "Cutting Edge Concepts in Lung Pharmacology" (2007).

3- El-Awady MSH, Smirnov SV, Watson ML. Lipopolysaccharide-induced vascular hypocontractility to endothelin-1 in rat is dependent on non-voltage-gated calcium channels but not on calcium sensitization. Presented at EPHAR2008 and published in *Fundamental & Clinical Pharmacology*, 22 (Suppl. 2), 74.

Abstract

Inflammation has incompletely characterized effects on cardiopulmonary vascular reactivity. Sepsis is a major inflammatory disease characterized by two main vasomotor complications, generalized vasodilation with hyporesponsiveness to vasoconstrictors and pulmonary hypertension. The main aim of this study is to examine the molecular mechanisms involved in cardiopulmonary vascular reactivity changes induced by the powerful inflammatory stimulus lipopolysaccharide (LPS). Pulmonary and aortic rings from male Wistar rats (250-300g) were isolated and incubated for 20 h in culture medium (DMEM+10% FBS) with or without LPS (*E. coli* O55:B5, 10 $\mu g.ml^{-1}$). The effect of organ culture and LPS type, concentration and incubation time in addition to tissue contraction to endothelin-1 (ET-1), phenylephrine, 80 mM KCl, and U46619; and relaxation responses to ACh, sodium nitroprusside (SNP), 8-pCPT-cGMP, BAY 41-2272, T-0156, nifedipine, SKF-96365, Ro-31-8425, and Y-27632 were measured by standard organ bath techniques. Nitric oxide (NO) production was measured by the Griess method and SNP-induced cGMP production was measured by ELISA. mRNAs expression levels of eNOS, iNOS, ET-1, ET_A and ET_B were measured by qRT-PCR and the expression levels of PKC, $sGC_{\alpha 1}$, $sGC_{\beta 1}$ and PDE5 and phosphorylation of MLC_{20}, ROKα, CPI-17 and MYPT1 were measured by immunoblotting. The effect of endothelium removal, indomethacin, trolox, external Ca^{2+} removal, 1400W, ODQ, glibenclamide, iberiotoxin and cycloheximide in addition to changes in intracellular Ca^{2+} ($[Ca^{2+}]_i$) in aortic vascular smooth muscle cells (VSMCs) induced by ET-1 were also measured. LPS selectively induced vascular hyporeactivity to different vasoconstrictors in rat aorta but not in the pulmonary artery, which is not due to organ culturing and is not affected by changing the LPS type, but is enhanced by increasing LPS concentration or the incubation time. This aortic hypocontractility to ET-1 is largely mediated by NO-independent activation of sGC and depends on external Ca^{2+} influx through non-VOCCs, but not on ET-1 receptor expression or Ca^{2+} sensitization. In addition, this aortic hyporeactivity to ET-1 is dependent on protein synthesis. The pulmonary artery is not affected because LPS induces a desensitization of the sGC/cGMP dependent pathway by decreasing protein expression levels of $sGC_{\beta 1}$, and hence sGC activity, and increasing PDE5 activity. Neither the endothelium, cyclooxygenase, reactive oxygen species nor K^+ channels are involved in these LPS effects. Therefore, it is likely that both Ca^{2+} homeostasis and the sGC/cGMP pathway play important roles in vasomotor complications in sepsis. sGC and/or PDE5-selective inhibitors, together with manipulating VSMC $[Ca^{2+}]_i$, could be important in controlling systemic and pulmonary vasomotor complications in sepsis.

Contents

List of Tables

List of Figures

Abbreviations

$[Ca^{2+}]_i$	Intracellular calcium
ACh	Acetylcholine
AngII	Angiotensin-II
BH_4	Tetrahydrobiopterin
BK	Large-conductance Ca^{2+}-activated K^+ (K_{Ca}) channels
BSA	Bovine serum albumin
CaMKII	Ca^{2+}/calmodulin-dependent protein kinase II
cGMP	3',5'-cyclic guanosine monophosphate (cGMP)
COX	Cyclooxygenase
CPI-17	PKC-potentiated phosphatase inhibitor protein-17 kDa
DAG	Diacylglycerol
DMEM	Dulbecco's modified Eagle's medium
ECs	Endothelial cells
EDHF	Endothelium-dependent hyperpolarizing factor
E_{max}	Maximum response
eNOS	Endothelial nitric oxide synthase
ET-1	Endothelin-1
FAD	Flavin adenine dinucleotide
HRP	Horseradish peroxidase
iNOS	Inducible nitric oxide synthase
IP_3	Inositol 1,4,5- trisphosphate
K_{ATP}	ATP-sensitive K^+ channels
LBP	LPS-binding protein
LPS	Lipopolysaccharide
MAPK	Mitogen-activated protein kinase
MLC_{20}	20 kDa regulatory myosin light chain
MLCK	Myosin light chain kinase
MLCP	Myosin light chain phosphatase
MYPT1	Myosin phosphatase targeting subunit 1
NADPH	Reduced nicotinamide adenine dinucleotide phosphate
NF-κB	Nuclear factor-κB

NO	Nitric Oxide
NSCCs	Non-selective cation channels
$O_2^{\cdot -}$	Superoxide anion
PDE5	Phosphodiesterase-5
pEC_{50}	Negative log the concentration producing 50% of maximal response
PGI_2	Prostacyclin
PKA	Protein kinase A
PKC	Protein kinase C
PKG	Protein kinase G
PLA_2	Phospholipase A_2
PLCβ	Phospholipase Cβ
PLD	Phospholipase D
PSS	Physiological salt solution
qRT-PCR	Quantitative reverse-transcriptase polymerase chain reaction
ROCCs	Receptor-operated Ca^{2+} channels
ROK/ROCK	Rho-activated kinase
ROS	Reactive oxygen species
SDS-PAGE	Sodium dodecyl sulphate-polyacrylamide gel electrophoresis
SEM	Standard error of mean
SERCA	The sarcoplasmic reticulum (SR) Ca^{2+}-ATPase pump
sGC	Soluble guanylyl cyclase
SNP	Sodium nitroprusside
SOCCs	Store-operated Ca^{2+} channels
TBSN	Tris-buffered saline-Nonidet-P40
TLR	Toll-like receptors
TRP	Transient receptor potential channel
TxA_2	Thromboxane A_2
VC	Vasoconstriction
VD	Vasodilation
VOCCs	Voltage-operated Ca^{2+} channels
VSMC	Vascular smooth muscle cell

To my wife, my children

and the soul of my mother and my father

Chapter 1

Introduction

Chapter 1

1.1 Inflammation, Lipopolysaccharide and vascular reactivity

Inflammation is a series of local vascular and lymphatic changes occurring in living organisms. The main features of the inflammatory response include vasodilation, increased vascular permeability, cellular infiltration and activation of cells of the immune system (Ryan & Majno, 1977). Inflammation normally leads to recovery from infections, limits tissue injury and initiates healing and repair. However, if inflammation is not properly controlled, it can lead to persistent tissue damage (Webster & Galley, 2003). The role of vascular cells is critically important in inflammatory diseases, including atherosclerosis, hypertension, ischemia-reperfusion and septic shock (Tedgui & Mallat, 2001).

1.1.1 Inflammation and vascular reactivity

Cardiovascular homeostasis is, in part, governed by blood pressure, expressed as the product of total peripheral resistance and cardiac output (Reddi & Carpenter, 2005). The contraction of vascular smooth muscle cells (VSMCs) controls vascular tone, and thus regulates total peripheral resistance, blood pressure and tissue perfusion. The vascular tone depends on a complex interplay between endothelial cells (ECs) and VSMCs through the release of different vasoconstrictors [endothelin-1 (ET-1), thromboxane A_2 (TxA_2), prostaglandin H_2, angiotensin-II (AngII) and superoxide anion ($O_2^{\cdot -}$)] and vasodilators [nitric oxide (NO), endothelium-dependent hyperpolarizing factor (EDHF), prostacyclin (PGI_2) and prostaglandin E_2] (Davis *et al.*, 2003; Vila & Salaices, 2005).

Inflammatory stimuli, such as inflammatory cytokines and bacterial endotoxins, have multiple and diverse effects on both ECs ands VSMCs, leading to altered vascular reactivity and selective permeability, leukocyte adhesion, platelet activation and conversion to procoagulant state, VSMC proliferation and extracellular matrix deposition (Tan *et al.*, 1999; Aird, 2003).

One of the major examples of inflammatory diseases affecting the vascular system is sepsis, which is a complex dysregulation of inflammation arising when the host is unable to successfully contain an infection (Buras *et al.*, 2005). Sepsis has two stages: an early hyperdynamic stage characterized by increased heart rate, cardiac output, vascular resistance and proinflammatory cytokines; and a later hypodynamic stage characterized by decreased heart rate, cardiac output and vascular resistance and increased levels of anti-inflammatory cytokines (Hoesel & Ward, 2004). Complications arising from sepsis include disseminated intravascular coagulation, systemic vascular collapse, multi-organ failure, and development of vascular leak syndromes, including acute respiratory distress syndrome (Bannerman & Goldblum, 2003). The two main vasomotor complications are septic shock and pulmonary hypertension (Parsons *et al.*, 1989; Manthous *et al.*, 1993; Lorente *et al.*, 1993). The mechanism of this difference in vascular reactivity between the systemic and the pulmonary vascular beds in sepsis is unclear.

1.1.2 Lipopolysaccharide

Lipopolysaccharide (LPS) or endotoxin is a major component of the Gram-negative bacterial cell wall released, as example, by cell lysis. LPS is a di-phosphorylated polar macromolecule composed of an *O*-specific hydrophilic polysaccharides chain, a core oligosaccharide region and a hydrophobic lipid A component which is responsible for the proinflammatory properties of LPS (Alexander & Rietschel, 2001). LPS forms microaggregates in biologic fluids and then rapidly interacts with a variety of serum or membrane-bound lipophilic proteins (Opal, 2007). LPS is the key molecule involved in the initiation of sepsis. The administration of LPS, both in humans (Suffredini *et al.*, 1989) and in animals (Ruetten *et al.*, 1996; Peters & Lewis, 1996; Gardiner *et al.*, 1996b), has been used as a model to study sepsis and septic shock.

1.1.2.1 LPS recognition and signalling

LPS binds to a 60-kDa LPS-binding protein (LBP) which is an acute phase protein primarily synthesized by hepatocytes (Schumann *et al.*, 1990). The LPS-LBP

complex is recognized by CD14, which is either expressed by monocytes/macrophages (mCD14) or released as a soluble form by monocytes (sCD14) (Hiki *et al.*, 1998). sCD14-LPS complexes have been shown to stimulate mCD14-negative cells, such as epithelial cells, ECs, fibroblasts and SMCs (Pugin *et al.*, 1993; Heine *et al.*, 2001). The CD14-LPS complexes induce cell signalling through toll-like receptors (TLRs) (Akira *et al.*, 2006). Ten TLRs subtypes have been identified in human: TLR-4 mediates the responses to LPS, while TLR2 mediates responses to toxins from Gram-positive bacteria, yeast and mycobacteria (Akira *et al.*, 2006). Endothelial cells express two of the known TLRs, predominantly TLR4 and very low levels of TLR2 and the expression of both is regulated by the transcription factor nuclear factor-κB (NF- κB) and interferon-γ (Faure *et al.*, 2000). Activation of TLR4 leads to stimulation of both MyD88-dependent and MyD88-independent pathways (Figure 1.1). These pathways involve signalling through NF-κB, mitogen-activated protein kinases (MAPKs) and phosphatidylinositol-3-kinase (Dauphinee & Karsan, 2006).

Further LPS recognition molecules may involve CD11/CD18 (β_2-integrin), selectins, scavenger receptors, membrane-organizing extension spike protein (moesin) and heptose-specific lipopolysaccharide receptors (Van Amersfoort *et al.*, 2003). Generally, LPS recognition and signalling involve various membrane molecules as well as intracellular receptors (Heine *et al.*, 2001). Different recognition systems such as scavenger receptors contribute to the clearance of LPS in the circulation mainly by Kupffer cells and hepatocytes in the liver (Hampton *et al.*, 1991; Satoh *et al.*, 2008).

1.1.2.2 LPS and inflammation

LPS is a powerful stimulator of inflammatory pathways with the generation of pro- and anti-inflammatory mediators, including cytokines, coagulation factors, cell adhesion molecules, myocardial depressants and heat shock proteins (Heine *et al.*, 2001; Peters *et al.*, 2003). The degree of cytokine expression in response to inflammatory stimuli such as LPS is principally regulated by NF-κB which is also responsible for the regulation of cell adhesion molecules, immunoreceptors,

procoagulants, acute phase proteins, NO production, and VSMCs migration and proliferation (Collins & Cybulsky, 2001).

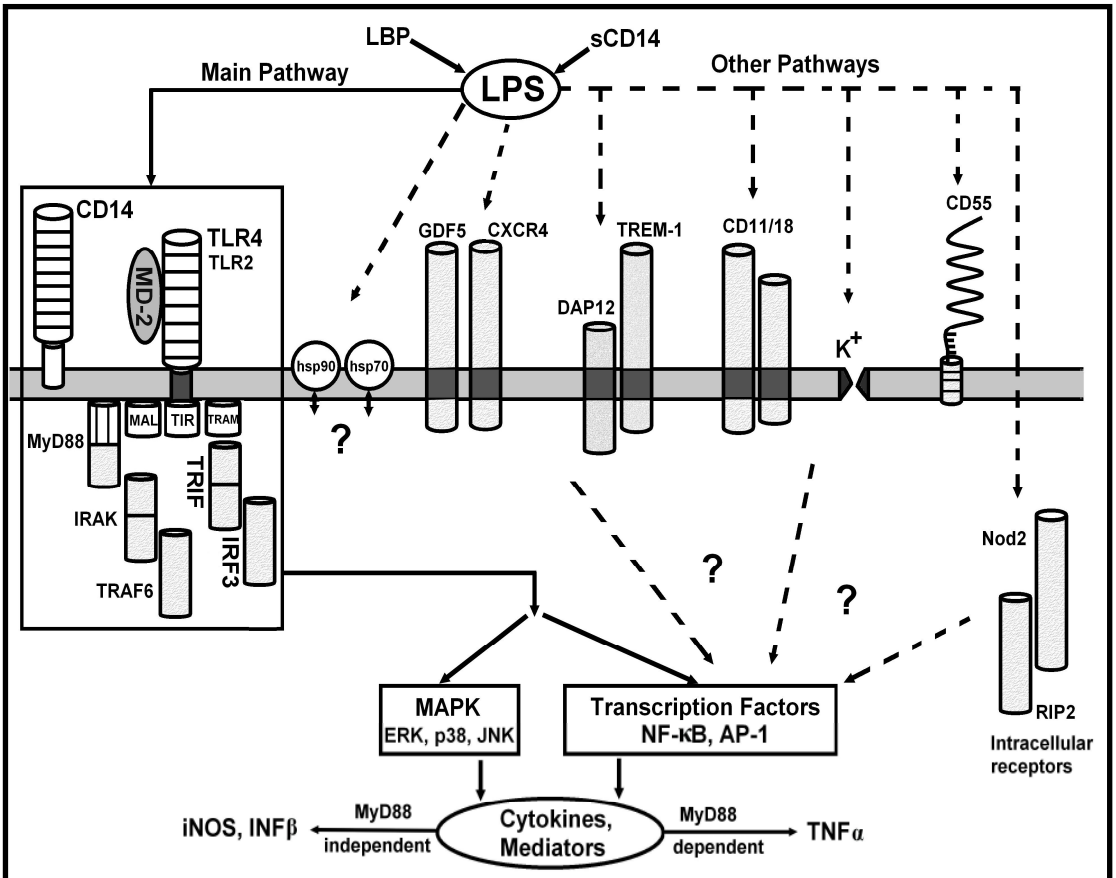

Figure 1.1 LPS recognition and signalling. The main LPS signalling pathway through TLR is boxed, comprising both MyD88-dependent and -independent pathways, while alternative pathways are shown by shaded lines. AP-1, activator protein-1; CXCR4, chemokines receptor 4; DAP-12, DNAX-activating protein; ERK, extracellular signal-regulated kinase; GDF5, growth differentiation factor 5; hsp70/90, heat shock protein 70/90; IRAK, IL-1 receptor-associated kinase; IRF3, interferon (INF) regulatory factor 3; JNK, c-jun NH2-terminal kinase; K^+, potassium channels; LBP, LPS-binding protein; MAPK, mitogen-activated protein kinase; MyD-88, myeloid differentiation factor 88; NF-κB, nuclear factor-κB; Nod2, nucleotide-binding oligomerization domain protein-2; RIP2, receptor interacting protein 2; TLR, Toll-like receptors;TRAF6, tumor necrosis factor (TNF) receptor-associated factor 6; TREM-1, Triggering receptor expressed on myeloid cells-1; TIR, TLR-IL-1 receptor domain (adapted from (Heine *et al.*, 2001; Mitchell *et al.*, 2007).

1.1.2.3 LPS and vascular reactivity

Different models have been developed to study LPS-induced changes in vascular reactivity. Examples include *in vitro* models (McKenna, 1990; Hall *et al.*, 1996; O'Brien *et al.*, 2001; Piepot *et al.*, 2002; Boer *et al.*, 2005), *in vivo* models (Curzen *et al.*, 1995; Gardiner *et al.*, 1995; Ruetten *et al.*, 1996; Griffiths *et al.*, 1997; Mitaka *et al.*, 1999; Hirata & Ishimaru, 2002) and *ex vivo* models using vessels harvested from endotoxic animals (Schneider *et al.*, 1992; Gunnett *et al.*, 1998; Wu *et al.*, 2004). Although vascular hyporeactivity was induced by LPS in most models, some models using smaller rodent vessels were unable to demonstrate diminished responses to vasoconstrictors (Mitchell *et al.*, 1993; Glembot *et al.*, 1995; Wu *et al.*, 2004). Table 1.1 represents the variability of vascular reactivity responses to LPS. This variability may be attributed to the difference in experimental models. However, different vascular beds respond variably to different vasoconstrictors in the same model (Piepot *et al.*, 2002; Farmer *et al.*, 2003), suggesting that complex mechanisms are present depending on the type of vascular bed and the vasoconstrictor. Exploring these mechanisms using a suitable model is important in understanding vascular reactivity changes induced by LPS.

Of the several mediators suspected to be involved in LPS-induced vascular reactivity changes, NO and ET-1 play major roles in systemic hypotension, vascular hyporesponsiveness and pulmonary hypertension induced by LPS (Pittet *et al.*, 1991; Lorente *et al.*, 1993; Szabo *et al.*, 1995; Curzen *et al.*, 1997; Liu *et al.*, 1997; Fujii *et al.*, 2000; Piechota *et al.*, 2007).

Table 1.1 Variability of LPS effects on vascular reactivity

Reference	Study type	Animal/ human tissue	Main LPS-induced effects
(Biguad *et al.*, 1990)	*ex vivo*	Rat aorta	- Hyporeactivity to phenylephrine, KCl, Bay K 8644 and calimycin
(Farmer *et al.*, 2003)	*ex vivo*	Rat aorta, mesenteric and renal arteries	- Hyporeactivity to methoxamine in aorta and mesenteric, but not in renal arteries - KCl, caffeine and U46619 not affected
(Umans *et al.*, 1993)	*ex vivo*	Rat and rabbit aortas	- Hypocontractility to phenylephrine, AngII, KCl and serotonin - Impaired relaxation to ACh and A23187
(Gardiner *et al.*, 1996b)	*in vivo*	Rat	- Depressor and dilator effects of LPS infusion was opposed by AngII in first 1-2 h, ET-1 between 2-8h and vasopressin after 24 h
(Guc *et al.*, 1990)	*in vivo*	Rat	- Hypocontractility to phenylephrine, vasopressin, cirazoline and serotonin, but not to ET-1
(Wakabayashi *et al.*, 1987)	*ex vivo*	Rat aorta	- Hypocontractility to norepinephrine, KCl and serotonin
(Piepot *et al.*, 2002)	*in vitro*	Rat coronary, mesenteric, hepatic and renal arteries	-Hyporeactivity to KCl in all vessels tested, to noradrenaline in mesenteric and hepatic and to U46619 in coronary
(Buyukafsar *et al.*, 2004)	*ex vivo*	Rat mesenteric arteries	- Hyporeactivity to phenylephrine, AngII, but enhanced responses to ET-1
(Mitchell *et al.*, 1993)	*ex vivo*	Rat perfused mesenteric vascular bed	- Responses to ET-1, phenylephrine, U46619 and serotonin were not affected

1.2 Nitric oxide

NO is one of the most ubiquitous substances in mammalian species, involved in the control of many cellular functions in different parts of the body. NO, being one of the most important endogenous vasodilators, plays an important role in inflammatory diseases. For example, it has been shown to contribute to the development of delayed hypotension, vasoplegia and acute lung injury in patients with septic shock (Manthous *et al.*, 1993; Lorente *et al.*, 1993; Feihl *et al.*, 2001; Lopez *et al.*, 2004) as well as in animals injected with LPS (Szabo *et al.*, 1995; Griffiths *et al.*, 1995; Bishop-Bailey *et al.*, 1997).

The recognition that exogenous NO gas as well as NO generated from various nitrocompounds has biological activity through activating soluble guanylyl cyclase (sGC) and inducing smooth muscle relaxation (Arnold *et al.*, 1977), was followed by the discovery of an endothelium-derived relaxing factor (EDRF) (Furchgott & Zawadzki, 1980). Ten years later, it was confirmed that NO represents EDRF in the vasculature (Ignarro *et al.*, 1987).

1.2.1 Synthesis of NO

NO is synthesized from the amino acid L-arginine by a family of heme containing enzymes named the NO synthases (NOS) (Nathan & Hibbs, Jr., 1991). The substrate L-arginine is metabolized by NOS to produce NO in addition to L-citrulline (Ignarro *et al.*, 1987; Michel & Feron, 1997). The synthesis of NO by NOS involves the transfer of electrons between various co-factors including molecular oxygen, flavin adenine dinucleotide (FAD) and mononucleotide, tetrahydrobiopterin (BH4), reduced nicotinamide adenine dinucleotide phosphate (NADPH) and a heme moiety, with one atom of oxygen finally binding with the terminal guanidine nitrogen from arginine to form NO (Stuehr, 1999). In addition, a small amount of NO is non-enzymatically produced from the chemical reduction of nitrite (Weitzberg & Lundberg, 1998).

1.2.2 NO synthases

At least 3 NOS isoforms have been identified, namely neuronal NOS (nNOS, or NOS I), inducible NOS (iNOS, or NOSII) and endothelial NOS (eNOS, or NOS III) (Alderton *et al.*, 2001). Both nNOS and eNOS isoforms are constitutively expressed and are activated by calcium (Ca^{2+})-calmodulin. iNOS is regulated primarily at the transcriptional level, independent of agonist stimulation and intracellular Ca^{2+} ($[Ca^{2+}]_i$). Constitutive nNOS and eNOS require an increase in resting $[Ca^{2+}]_i$ for their binding of calmodulin and subsequent full activation (Michel & Feron, 1997). However, iNOS is able to bind calmodulin with extremely high affinity even at the low $[Ca^{2+}]_i$ characteristic of resting cells and therefore its activation is not regulated by alterations in $[Ca^{2+}]_i$ (Xie & Nathan, 1994).

eNOS, expressed in ECs, is the predominant NOS isoform in the vessel wall (Alderton *et al.*, 2001). ET-1 and Ang II (Li *et al.*, 1999; Alderton *et al.*, 2001) have been shown to upregulate eNOS expression. Cytokines and LPS, potent upregulators of iNOS expression, appear to have the opposite effect on eNOS (Li *et al.*, 2002). At high concentrations, NO itself works in a negative feedback manner to inhibit both activity and expression of eNOS (Abu-Soud *et al.*, 2000).

The $[Ca^{2+}]_i$ required to activate constitutive NOS also inhibits GC (Coleman, 2001). Therefore cells in which constitutive NOS is activated cannot respond to the NO produced. Cells expressing iNOS probably utilise glutathione as their defence against NO (Coleman, 2001).

1.2.3 Metabolism of NO

NO is an extremely unstable molecule, remaining effective for only few seconds (Griffith *et al.*, 1984), due to rapid oxidation of NO by O_2 and free oxygen radicals forming inactive nitrogen dioxide, which is converted to nitrite then nitrate. Both nitrite and nitrate are eliminated in urine within 5 hours, with basal nitrates concentration in blood 100 fold higher (30 mmol L^{-1}) than nitrites (Moncada & Higgs, 1993).

In the blood, NO is rapidly inactivated by binding to hemoglobin, forming methaemoglobin, therefore keeping the concentration of NO in the nanomolar range (Beckman & Koppenol, 1996). However, hemoglobin is rapidly regenerated by red blood cell methaemoglobin reductase with nitrate as a by-product. The high affinity of NO for hemoglobin and its inactivation by binding to hemoglobin means that its physiological actions remain localized to the site of its generation and are rapidly terminated (Anggard, 1994).

1.2.4 Mechanism of Action of NO

NO is a gas at physiological temperature and pressure, with a complete lack of reactivity with water making it lipophilic, and thus rapidly diffuses to interact with molecular targets in cells in the vascular wall and lumen (Grisham *et al.*, 1999; Hughes, 2008). NO interacts with metal centres and thiol groups within diverse protein targets, including membrane receptors, ion channels, cytosolic enzymes, and transcription factors such as AP-1 and NF-κB (Stamler, 1994). S-Nitrosylation of thiol groups in plasma proteins such as albumin generates a circulating pool of NO-donating groups (Keaney, Jr. *et al.*, 1993), whereas S-nitrosylation of hemoglobin in the lung provides nitrosothiol groups to the peripheral vasculature and regulates oxygen delivery (Gow *et al.*, 1999).

The most important receptor molecule for NO is NO-sensitive sGC, which catalyzes the formation of 3',5'-cyclic guanosine monophosphate (cGMP). The biological effects of cGMP are mediated by protein kinase G (PKG), cGMP-gated ion channels and cGMP-regulated phosphodiesterases (PDEs) (Beavo, 1995; Hofmann *et al.*, 2006).The amplitude and duration of a cGMP signal are determined by the activity of sGC, a heterodimeric cGMP-forming enzyme, and PDEs which degrade cGMP (Juilfs *et al.*, 1999). Only two sGC isoforms, $\alpha_1/\ \beta_1$ and $\alpha_2/\ \beta_1$ exist with the $\alpha_1/\ \beta_1$ sGC heterodimer being the predominant isoform in most tissues including lung (Friebe & Koesling, 2003). The major cGMP-degrading PDE isoform in vascular smooth muscle is the cGMP-binding PDE5 (Beavo, 1995; Maurice *et al.*, 2003).

1.2.5 Dysfunction of NO pathway

Dysfunction of NO can occur as a result of decreased production, enhanced degradation and decreased sensitivity. In vascular diseases such as hypertension and atherosclerosis, the NO substrate L-arginine may be depleted secondary to an increase in arginase activity (Loscalzo, 2000). In addition, asymmetric dimethylarginine can act as an endogenous competitive NOS inhibitor (Cooke, 2000). At suboptimal concentrations of the cofactor BH_4 or the substrate L-arginine, NOS becomes 'uncoupled', leading to the production of $O_2^{\cdot -}$ and hydrogen peroxide thus decreasing NO production and increasing its inactivation (Xia *et al.*, 1998; Cai & Harrison, 2000). Furthermore, dysfunction of the NO pathway can occur by a decrease in the expression of eNOS (Alderton *et al.*, 2001).

The interaction between NO and $O_2^{\cdot -}$ or lipid peroxides deplete NO levels by directly forming peroxynitrites or indirectly by attenuating NO release (Hogg & Kalyanaraman, 1999; Cai & Harrison, 2000). Oxidized LDL, hypertension, ageing and hyperglycaemia have all been shown to decrease the expression of sGC (Friebe & Koesling, 2003). Altering the redox state of sGC itself makes it unresponsive to both endogenous and exogenous NO (Stasch *et al.*, 2006).

1.2.6 Physiological effects of NO

Direct NO effects occur at low (nanomolar) concentrations of NO resulting from the constitutive NOS isoforms. These include relaxation of vascular and non-vascular smooth muscle, inhibition of platelet aggregation, and inhibition of leukocyte adhesion to the endothelium (Nathan & Xie, 1994). NO, at high concentrations produced from iNOS, competes with O_2 leading to inhibition of constitutive isoforms of NOS (Griscavage *et al.*, 1995), and downregulates the activity of key enzymes in oxidative metabolism, thus negatively influencing cellular energetics in conditions such as sepsis (Gardner *et al.*, 1997). In contrast with this potentially deleterious action, NO may be highly protective against oxidative stress by scavenging several free radicals such as $O_2^{\cdot -}$, hydroxyl radical and hydrogen peroxide (Grisham *et al.*, 1999).

Indirect effects of NO occur at high (micromolar) concentrations of NO resulting from iNOS through the formation of other mediators. These involve the carcinogenic compounds N-nitrosamines (Hecht, 1997), and S-nitrosothiols that play significant roles in a large number of biological processes (Broillet, 1999). In addition, the highly reactive and cytotoxic oxidant species peroxynitrite depletes glutathione, nitrates tyrosine residues in proteins and causes DNA damage and activation of the nuclear enzyme poly(ADP-ribose) polymerase, a pathway increasingly recognized as a major mechanism of NO/peroxynitrite-mediated cytotoxicity (Szabo & Dawson, 1998).

1.2.7 Role of NO in inflammation and sepsis

NO may exert either anti- or pro-inflammatory effects. NO is proinflammatory at low concentrations by inducing vasodilation and the recruitment of neutrophils, whereas at high concentrations it downregulates cell adhesion molecules, suppresses activation and induces apoptosis of inflammatory cells (Coleman, 2001). NO can interact with the pathways of gene expression controlled by the transcription factor NF-kB. When activated by various extracellular inflammatory triggers (e.g., stimulation of CD14 by LPS), NF-kB translocates to the nucleus, where it induces the transcription of numerous genes coding for proteins involved in inflammation, such as cytokines, cell adhesion molecules, and iNOS (Janssen-Heininger *et al.*, 2000). Both activation (Kalra *et al.*, 2000) and inhibition (DelaTorre *et al.*, 1997) of NF-kB activity by NO have been described.

Excessive NO production, derived mainly from iNOS, has been shown to contribute to the development of delayed hypotension, vasoplegia and acute lung injury in patients with septic shock (Feihl *et al.*, 2001; Lopez *et al.*, 2004) as well as in animals injected with LPS (Szabo *et al.*, 1995; Bishop-Bailey *et al.*, 1997). Different strategies have been used to control excessive NO production in sepsis, such as inhibiting NO production with various NOS inhibitors or by inhibiting NO-dependent pathways such as sGC, however results have been conflicting. Table 1.2 represents variable results relating to the involvement of NO in LPS-induced vascular dysfunction.

Table 1.2 Variability of the role of NO in LPS-induced changes in vascular reactivity

Reference	Study type	Animal/ human tissue	Main findings
(Peters & Lewis, 1996)	*in vivo*	Rat hindquarter bed	- Relaxation responses to ACh and sodium nitroprusside (SNP) impaired by LPS
(Parker *et al.*, 1994)	*ex vivo*	Guinea pig aorta	- Relaxation responses to ACh, but not to SNP, impaired by LPS
(Mitolo-Chieppa *et al.*, 1996)	*ex vivo*	Rat perfused mesenteric vascular bed	- L-NAME failed to restore reactivity to norepinephrine after LPS
(Yen *et al.*, 1995)	*ex vivo*	Rat aorta	- L-NAME and aminoguanidine partially restored reactivity to norepinephrine after LPS
(Hernanz *et al.*, 2004)	*in vitro*	Rat superior mesenteric artery	- 1400W restored reactivity to noradrenaline after LPS
(Boyle, III *et al.*, 2000)	*ex vivo*	Mouse mesenteric resistance arteries	- iNOS knockout protected against LPS-induced hyporeactivity to norepinephrine
(Virdis *et al.*, 2005)	*ex vivo*	Rat mesenteric resistance arteries	- LPS increases iNOS mRNA, but eNOS not affected
(Tsai *et al.*, 2006)	*ex vivo*	Rat pulmonary artery and aorta	- LPS increases iNOS mRNA in the pulmonary artery, but not the aorta

1.3 Endothelins

ET-1, being the most powerful endogenous vasoconstrictor identified to date, has been suggested to play an important role in vascular changes in diseases involving inflammation, such as sepsis and associated syndromes and pulmonary hypertension (Wanecek *et al.*, 2000; Luscher & Barton, 2000; Dhaun *et al.*, 2007). ET-1 was isolated, characterized and cloned from the culture medium of porcine ECs (Yanagisawa *et al.*, 1988). ET-1 was subsequently demonstrated to be one of a family of potent vasoactive peptides, designated ET-1, ET-2 and ET-3, which have been shown to be encoded by three distinct genes (Inoue *et al.*, 1989). A similar peptide has been discovered following genomic cloning in mice (Saida *et al.*, 1989) and termed vasoactive intestinal contractor or β-endothelin. This has subsequently been found to be a murine and rat homolog of human ET-2 (Bloch *et al.*, 1991). Apart from this example, data suggest that there are little interspecies differences in the sequences of the ET subtypes.

1.3.1 ET structure

ETs are 21 amino acid peptides containing four cysteine residues forming two disulphide bonds between Cys^{1}-Cys^{15} and Cys^{3}-Cys^{11}, which hold the peptide chains in a hairpin loop configuration (Inoue *et al.*, 1989). ET-2 differs from ET-1, the major isoform, by 2 amino acids, while ET-3 differs from ET-1 by 6 amino acids (Figure 1.2).

The three ETs isopeptides show a remarkable resemblance, both in structure (~ 67% sequence homology) and biological activity, to sarafotoxins, a family of peptides isolated from the venom of *Atractaspis engaddenis* (Landan *et al.*, 1991).

1.3.2 ET biosynthesis and secretion

ET isopeptides arise from post-translational, proteolytic processing of large precursor peptides termed preproendothelins -1, -2 and -3, which consists of approximately 200 amino acids (Yanagisawa *et al.*, 1988; Itoh *et al.*, 1988). The preproETs undergo cleavage to produce a 38 (human) or 39 (porcine) amino acid

peptides known as bigETs (proETs) (Figure 1.2). The bigETs are then cleaved at Trp^{21}-Val^{22} by ET convering enzymes (ECEs) to produce the active peptides (Schmidt *et al.*, 1994; Emoto & Yanagisawa, 1995).

ET-1 is the main isoform released from the endothelium, and is also produced by airway epithelial cells, VSMCs, macrophages, fibroblasts, cardiomyocytes and neurons (Nakamura *et al.*, 1990; Luscher & Barton, 2000). ET-2 is expressed by intestinal epithelial cells, while ET-3 is produced by brain neurons, intestinal epithelial cells and renal tubular epithelial cells (Matsumoto *et al.*, 1989; Kedzierski & Yanagisawa, 2001).

Regulation of the ET system takes place mainly at the synthesis level, particularly during transcription, because cells do not store endothelins (Matsumoto *et al.*, 1989; Teder & Noble, 2000; Hynynen & Khalil, 2006; Dhaun *et al.*, 2007). ET-1 mRNA can be upregulated or downregulated by several factors (Figure 1.2).

1.3.3 ET metabolism/clearance

ET-1 concentration in vascular tissue is approximately 100 times higher than that in plasma and its half life in blood is 4 to 7 minutes because of quick binding to tissues and rapid metabolism by neutral endopeptidase present in the lung, kidney and central nervous system (Abassi *et al.*, 1992; Mateo & De Artinano, 1997). Other forms of ET metabolism may involve its uptake and lysosomal targeting by endothelial ET_B receptors that could function as "clearance receptors" (Bremnes *et al.*, 2000; Kedzierski & Yanagisawa, 2001).

Prolonged exposure of cells to ET can lead to a reduction in the responsiveness to a second exposure to ET i.e. desensitization can occur (Le Monnier de Gouville & Cavero, 1991). It has been shown also that ETs can indirectly decrease the stability of ET_B receptor mRNA (Sakurai *et al.*, 1992) and alter receptor expression, leading to receptor internalization/downregulation (Marsault *et al.*, 1991).

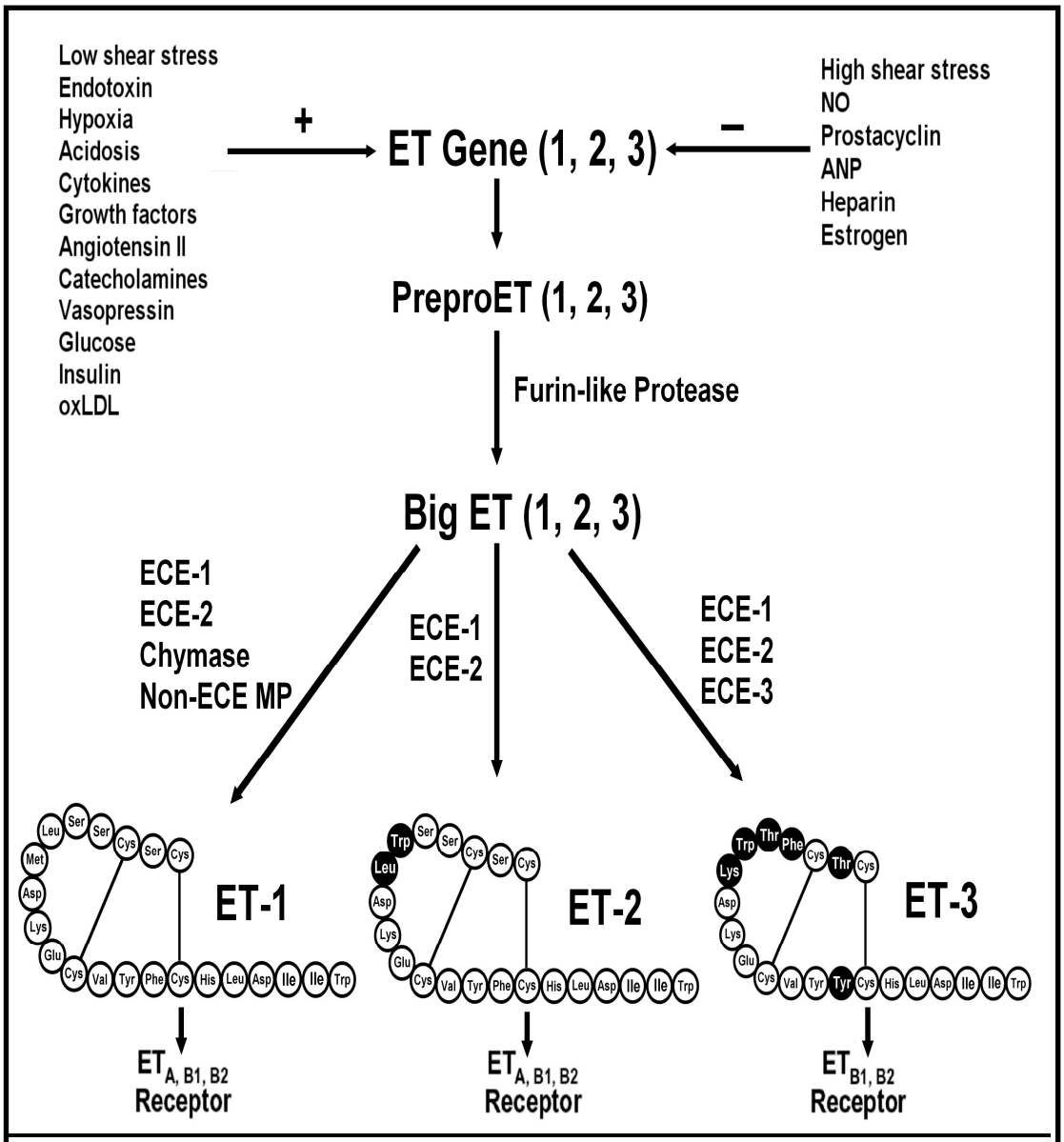

Figure 1.2 Schematic diagram of endothelins synthesis pathways. Amino acids in dark circles are different compared to ET-1. ANP, atrial natriuretic peptide; ECE, endothelin-converting enzyme; ET, endothelin; MP, metalloprotease; oxLDL, oxidised LDL (adapted from (Luscher & Barton, 2000; Hynynen & Khalil, 2006; Dhaun *et al.*, 2007).

1.3.4 ET receptors

There are two main known ET receptors, ET_A and ET_B, in addition to another two proposed ones, ET_C and ET_{AX}. ET_A and ET_B receptors are widely expressed in vascular tissues, airway smooth muscle, cardiomyocytes, hepatocytes, neurons, osteoblasts, reproductive system and some regions of the kidney (Kedzierski & Yanagisawa, 2001). ET_A and ET_B share 63% amino acid identity and are encoded by distinct genes located on chromosomes 4 and 13, respectively (Hynynen & Khalil, 2006). In VSMCs, the ET_A/ET_B ratio is often considered to increase with vessel size (Kirkby *et al.*, 2008). ET_A receptors mediate vasoconstriction and cell proliferation and show a great affinity for ET-1 and ET-2 over ET-3 (Luscher & Barton, 2000). The prolonged persisting contractile response mediated through ET_A receptors may be due its extremely slow dissociation from ET-1, which acts essentially as an irreversible ligand (Bremnes *et al.*, 2000). ET_B receptors show equal affinity for ET isoforms and are important for ET clearance, EC survival, release of NO and PGI_2, inhibition of ECE-1 and promotion of natriuresis and diuresis (Nakamura *et al.*, 1991; Dhaun *et al.*, 2007). The ET_C receptor has been cloned from *Xenopus leavis* dermal melanophores and shows selectivity for ET-3 over ET-1 (Karne *et al.*, 1993), and an ET_{AX} receptor has been cloned from *Xenopus* heart (Kumar *et al.*, 1994). ET_C and ET_{AX} receptors have no mammalian equivalent (Kirkby *et al.*, 2008).

Based on their in vivo pharmacology, ET_B receptors have been subdivided into ET_{B1}, located on the ECs and mediating vasorelaxation through release of NO and PGI_2, and ET_{B2}, located directly on the VSM and mediating vasoconstriction (Sudjarwo *et al.*, 1993).

1.3.5 ET receptor-mediated signalling pathways

ET peptides evoke complex, tightly regulated pathways of signal transduction that result in both short-term (e.g. contraction, secretion) and long-term (e.g. mitogenesis) biological effects. ET receptors belong to the superfamily of seven transmembrane receptors linked to G proteins (Davenport *et al.*, 1995). ET_A receptors are functionally coupled to $G_{q/11}$ protein to activate phospholipase Cβ (PLCβ), and to G_i protein to inhibit adenylyl cyclase (Figure 1.3) (Robin *et al.*,

2002). ET_A receptor-mediated activation of $G_{q/11}$ and PLCβ result in the breakdown of phosphatidylinositol 4,5-bisphosphate, and the generation of inositol 1,4,5-trisphosphate (IP_3) and diacylglycerol (DAG). IP_3 acts on specific receptors on the $[Ca^{2+}]_i$ stores and stimulates Ca^{2+} release, while DAG stimulates protein kinase C (PKC) activity (Neylon, 1999; McNair *et al.*, 2004).

ET also activates plasma membrane Ca^{2+} channels, including voltage-operated Ca^{2+} channels (VOCCs), receptor-operated Ca^{2+} channels (ROCCs) and store-operated Ca^{2+} channels (SOCCs), and thus stimulates Ca^{2+} influx from the extracellular space (Miwa *et al.*, 2005). ET_A receptor stimulation can also activate phospholipase D (PLD) with generation of DAG, phospholipase A_2 (PLA_2) resulting in release of arachidonic acid, the Na^+/H^+ exchanger, as well as tyrosine kinases, MAPKs and phosphatidylinositol 3-kinase (Hynynen & Khalil, 2006) that are involved both in vasoconstriction and mitogenesis (Figure 1.3). ET-1 has also been shown also to inhibit ATP-sensitive K^+ (K_{ATP}) channels (Satoh, 1995).

Stimulation of endothelial ET_B receptors activates signalling pathways that promote the release of relaxing factors such as NO, PGI_2 and EDHFs (Figure 1.3). The ET_B receptor-mediated release of NO from ECs may account for the transient vasodilator action of ET-1.

1.3.6 ET physiological and pathophysiological actions

ETs are postulated to be involved in the maintenance of basal vascular tone, regulation of water balance, local and systemic role in haemorrhage, and paracrine-, autocrine-, and endocrine signalling, embryonic development, gastrointestinal and endocrine function and prostate growth (Rubanyi & Polokoff, 1994; Luscher & Barton, 2000). Pathological conditions thought to involve ETs include coronary and cerebral vasospasm, myocardial ischemia, congestive heart failure, sepsis and associated syndromes, gastric ulceration, bronchial asthma and pulmonary hypertension (Wanecek *et al.*, 2000; Luscher & Barton, 2000; Dhaun *et al.*, 2007; Kirkby *et al.*, 2008).

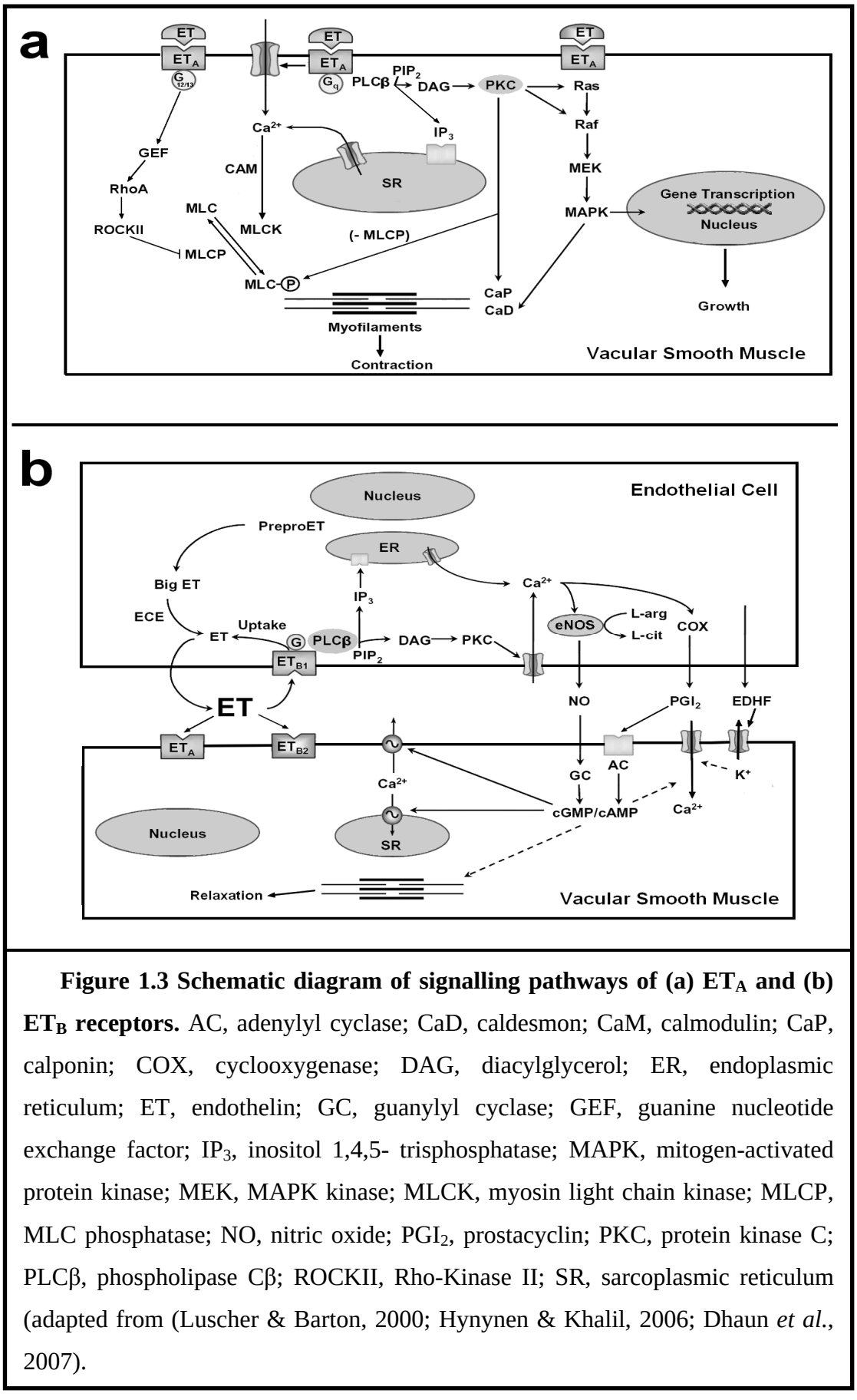

Figure 1.3 Schematic diagram of signalling pathways of (a) ET_A and (b) ET_B receptors. AC, adenylyl cyclase; CaD, caldesmon; CaM, calmodulin; CaP, calponin; COX, cyclooxygenase; DAG, diacylglycerol; ER, endoplasmic reticulum; ET, endothelin; GC, guanylyl cyclase; GEF, guanine nucleotide exchange factor; IP_3, inositol 1,4,5- trisphosphatase; MAPK, mitogen-activated protein kinase; MEK, MAPK kinase; MLCK, myosin light chain kinase; MLCP, MLC phosphatase; NO, nitric oxide; PGI_2, prostacyclin; PKC, protein kinase C; PLCβ, phospholipase Cβ; ROCKII, Rho-Kinase II; SR, sarcoplasmic reticulum (adapted from (Luscher & Barton, 2000; Hynynen & Khalil, 2006; Dhaun *et al.*, 2007).

1.3.7 ET interactions with NO

There are close interactions between NO and ET-1 in the vascular wall. NO inhibits the production of ET-1 in ECs (Boulanger & Luscher, 1990) and ET-1 is known to stimulate the release of NO via activation of the ET_B receptors located on ECs (Clozel *et al.*, 1992). However, ET-1 may reduce the bioavailability of NO in the vessel wall, through increasing $O_2^{\cdot -}$ production (Maczewski & Beresewicz, 2000). ET-1 may also reduce iNOS activity (Ikeda *et al.*, 1997), an effect that can be restored in dogs by dual ET_A/ET_B receptor blockade (Shaw *et al.*, 2001).

1.3.8 ET role in inflammation and sepsis

ET-1 is suggested to act as a proinflammatory cytokine because it stimulates macrophages and monocytes to release ROS and cytokines (McMillen & Sumpio, 1995; Fujii *et al.*, 2000; Luscher & Barton, 2000). ET-1 also induces neutrophil adhesion, platelet aggregation, chemotaxis of macrophages, and mast cell activation (McMillen & Sumpio, 1995; Fujii *et al.*, 2000; Luscher & Barton, 2000). In addition, ET-1 has been shown to have mitogenic activity for SMCs, myocytes and fibroblasts (Battistini *et al.*, 1993).

ET-1 is suggested to play an important role in the inflammatory response to sepsis since plasma ET-1 levels are elevated in animal models of sepsis (Takahashi *et al.*, 1990; Weitzberg *et al.*, 1996; Mitaka *et al.*, 1999; Fujii *et al.*, 2000; Hirata & Ishimaru, 2002) and in septic patients, where its level correlates with the severity of illness (Pittet *et al.*, 1991). Also, vascular ET-1 mRNA expression and arterial ET-1 concentration are elevated after LPS treatment in rats (Curzen *et al.*, 1997).

Interestingly, the use of different ET receptors antagonists to counteract the increased ET-1 levels in sepsis has resulted in conflicting results (Gardiner *et al.*, 1995; Weitzberg *et al.*, 1996; Curzen *et al.*, 1997; Fujii *et al.*, 2000; Hirata & Ishimaru, 2002; Konrad *et al.*, 2004). Table 1.3 represents variable results relating to the involvement of ET in in LPS-induced vascular dysfunction.

Table 1.3 Variability of the role of ET-1 in LPS-induced changes in vascular reactivity

Reference	Study type	Animal/ human tissue	Main findings
(Ros *et al.*, 1997)	*in vitro*	Human vascular ECs	- LPS increases ET-1 release in culture medium
(Schuetz *et al.*, 2007)	*in vivo*	Human	- Plasma ET-1 increases in sepsis and its levels correlate with severity of sepsis
(Forni *et al.*, 2005)	*ix vivo*	Pig	- LPS treatment increases plasma ET-1 levels
(Curzen *et al.*, 1997)	*ex vivo*	Rat pulmonary artery and aorta	- LPS increases ET-1 mRNA and protein levels
(Gardiner *et al.*, 1996a)	*in vivo*	Rat	- Non-selective ET_A/ET_B blocker increases hypotension induced by LPS
(Wanecek *et al.*, 1997)	*in vivo*	Pig	- Non-selective ET_A/ET_B blocker abolishes pulmonary hypertension induced by LPS, but plasma ET-1 levels remains elevated
(Ruetten *et al.*, 1996)	*in vivo*	Rat	- Selective ET_A blocker do not attenuate hypotension and vascular hyporeactivity induced by LPS

1.4 Regulation of VSM contraction

Since vascular reactivity is changed in inflammation, the identification of mechanisms that control VSM contraction are important to understand how inflammatory stimuli, either directly or through the release of vasoactive mediators, affect vascular tone. The contraction of VSM is primarily regulated by the reversible phosphorylation of the 20 kDa regulatory myosin light chain (MLC_{20}) (Ikebe *et al.*, 1987). MLC_{20} is specifically phosphorylated by Ca^{2+}/calmodulin-dependent myosin light chain kinase (MLCK), which in turn is activated by the release of Ca^{2+} from internal stores (Adelstein & Hathaway, 1979; Sommerville & Hartshorne, 1986) or the influx of Ca^{2+} across the plasmalemma through different Ca^{2+} channels (Hughes, 1995). The degree of MLC_{20} phosphorylation is further regulated by myosin light chain phosphatase (MLCP) (Bialojan *et al.*, 1985; Haeberle *et al.*, 1985).

When a greater contraction is produced for a given elevation of $[Ca^{2+}]_i$, this phenomenon is referred to as "Ca^{2+} sensitization of the contractile apparatus", which occurs with several receptor-mediated contractile stimulations (Somlyo & Somlyo, 1994). Therefore, vascular tone depends on the regulation of $[Ca^{2+}]_i$ and Ca^{2+} sensitization of the contractile apparatus (Figure 1.4). This section will describe the principal mechanisms regulating VSM contraction.

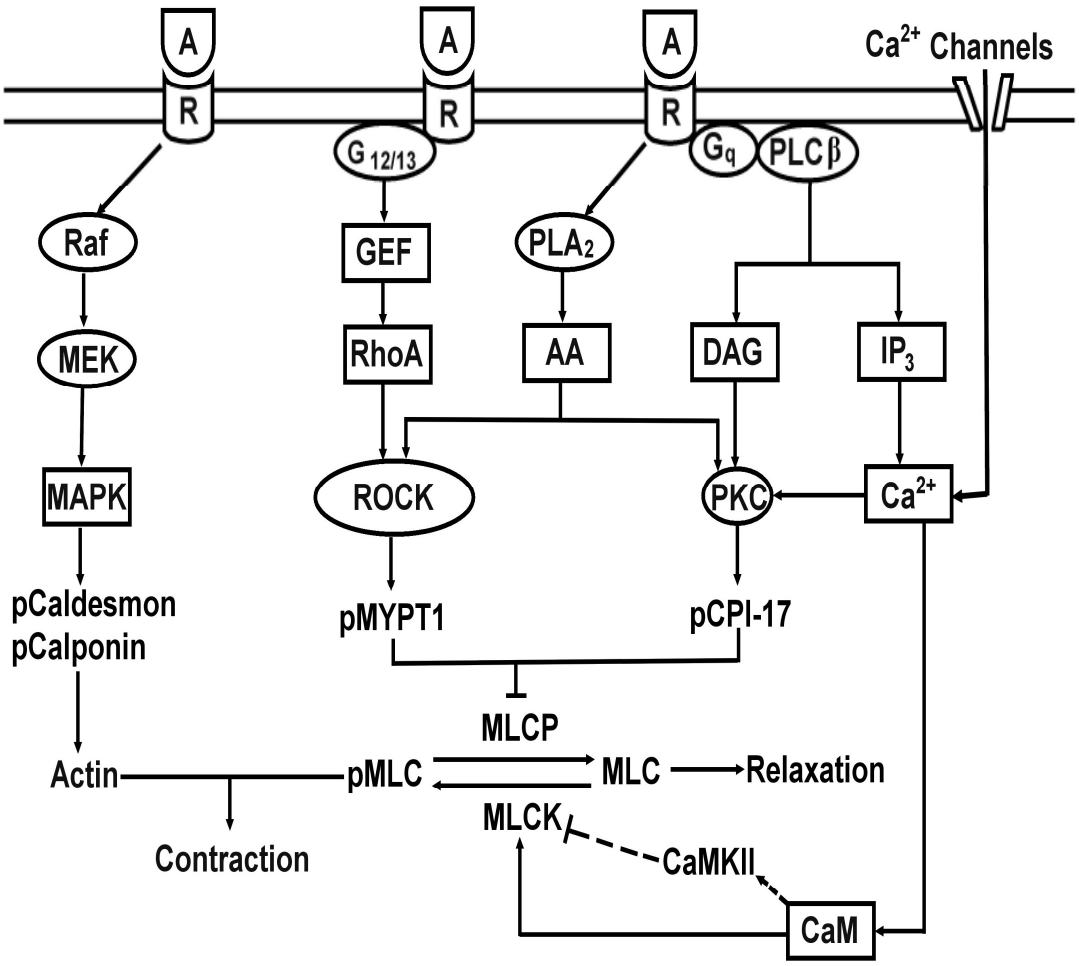

Figure 1.4 Schematic diagram of signal transduction pathways involved in contraction of VSMCs. A, agonist; AA, arachidonic acid; CaM, calmodulin; CaMKII, Ca^{2+}/CaM-dependent protein kinase II; CPI-17, PKC-potentiated phosphatase inhibitor protein-17 kDa; DAG, diacylglycerol; GEF, guanine nucleotide exchange factor; GPCR, G protein-coupled receptor; IP_3, inositol 1,4,5- trisphosphate; MAPK, mitogen-activated protein kinase; MEK, MAPK kinase R, receptor; MLCK, myosin light chain kinase; MYPT1, myosin phosphatase targeting subunit 1; PKC, protein kinase C; PLA_2, phospholipase A_2; PLCβ, phospholipase Cβ; PP1Cδ, δ-isoform of type 1 protein phosphatase catalytic subunit; ROCK, Rho-activated kinase (adapted from (Salamanca & Khalil, 2005; Woodsome *et al.*, 2006).

1.4.1 Intracellular Ca^{2+} regulation

At rest, $[Ca^{2+}]_i$ is much lower within VSMCs than in the extracellular fluid (Orallo, 1996). In response to vasoconstrictor stimuli, Ca^{2+} is mobilized from either intracellular stores such as the sarcoplasmic reticulum (SR) or the extracellular space to increase $[Ca^{2+}]_i$ in VSMCs. The majority of contractile agonists such as norepinephrine, AngII, ATP and ET-1 evoke contraction via binding to G-protein-coupled receptors to activate PLC-β resulting in the breakdown of phosphatidylinositol 4,5-bisphosphate and the generation of IP_3 and DAG (Sanders, 2001). IP_3 diffuses from the cell membrane into the cytosol and stimulates IP_3-sensitive receptors (IP_3R) on SR to release Ca^{2+} (Neylon, 1999; McNair *et al.*, 2004). The IP_3-mediated increase in $[Ca^{2+}]_i$, in turn, may induce further Ca^{2+} release from SR via a Ca^{2+}-induced Ca^{2+}-release mechanism (McPherson & Campbell, 1993). DAG, which can also be generated by the PLD-mediated hydrolysis of phosphatidylcholine, remains in the cell membrane and stimulates PKC activity (Galizzi *et al.*, 1987). Thus, the initial rapid phasic component observed in contractile response to these agonists reflects the IP_3-mediated Ca^{2+} release from the SR, followed by a tonic increase in $[Ca^{2+}]_i$, which is dependent on extracellular Ca^{2+} (Hashimoto *et al.*, 1986; Karaki *et al.*, 1997).

1.4.1.1 Ca^{2+} release from SR

In VSMCs, Ca^{2+} is stored intracellularly in the SR, which contains at least two types of voltage-independent Ca^{2+}-release channels, those sensitive to IP_3 (IP_3R) and those sensitive to the plant alkaloid ryanodine (ryanodine receptor, RyR) (Iino, 1990; Laporte & Laher, 1997). The IP_3R function can be modulated by $[Ca^{2+}]_i$, cytosolic ATP and phosphorylation by various protein kinases, including cyclic adenosine 3′,5′-monophosphate (cAMP)-dependent protein kinase (protein kinase A, PKA) and PKC (Marin *et al.*, 1999). The RyR is regulated mainly by Ca^{2+} in addition to cyclic adenosine diphosphoribose (McPherson & Campbell, 1993; Jaggar *et al.*, 1998; Lesh *et al.*, 1998).

1.4.1.2 Ca^{2+} influx across the plasmalemma

VOCCs, ROCCs and SOCCs are responsible for Ca^{2+} influx across the plasmalemma. L-type channels are the most important VOCCs and the most important route of Ca^{2+} influx in VSMC (Hofmann *et al.*, 1994). Contractile agonists may directly activate non-selective cation channels (NSCCs), and thereby cause membrane depolarization (Guibert *et al.*, 2008). On the other hand, Ca^{2+} released from the SR and/or entering through NSCCs may activate Ca^{2+}-dependent cation channels and/or Cl^- channels, eliciting membrane depolarization. However, the rise in $[Ca^{2+}]_i$ could also activate Ca^{2+}-dependent K^+ channels, thus opposing the depolarizing effects of the activation of Ca^{2+}-dependent Cl^- channels (Nilsson, 1998).

ROCCs may be subdivided into ligand-gated Ca^{2+} channels and second messenger-operated Ca^{2+} channels (Somlyo & Somlyo, 1968; Bolton, 1979; Felder *et al.*, 1994). The ligand-gated Ca^{2+} channels are probably NSCCs with some degree of selectivity for divalent cations, coupled to specific receptors and are directly activated by receptor agonists, including ATP, norepinephrine, vasopressin, ET, AngII, and serotonin (Orallo, 1996; Nilsson, 1998). Second messenger-operated Ca^{2+} channels are indirectly activated by diffusible second messengers such as IP_3, or Ca^{2+} following receptor activation, but there is limited evidence for their existence in VSMCs (Felder *et al.*, 1994; Hughes, 1995).

Depletion of the intracellular SR Ca^{2+} stores by diverse mechanisms (receptor agonists, Ca^{2+}-induced Ca^{2+}-release activators, SR-Ca^{2+} ATPase inhibitors, Ca^{2+} ionophores) has been reported to cause capacitive Ca^{2+} entry through SOCCs in a wide range of cell types, including VSMCs (Gibson *et al.*, 1998; Putney, Jr., 1999). Unlike receptor-operated NSCCs, SOCCs are highly selective for Ca^{2+} over other cations (Hoth & Penner, 1992). Transient receptor potential (TRP) channels have been suggested as excellent candidates for SOCCs and also ROCCs in mammalian cells (Walker *et al.*, 2001; Clapham *et al.*, 2001). Current research suggests that TRP1, TRP3, TRP6, and TRP7 encode NSCCs, that TRP2, TRP4, and TRP5 are SOCCs, and that TRP3, TRP4, TRP6, and TRP7 can be expressed in VSMCs (Walker *et al.*, 2001; Clapham *et al.*, 2001).

1.4.1.3 Mechanisms that reduce $[Ca^{2+}]_i$

Several mechanisms exist that reduce cytosolic free Ca^{2+} level, including the plasma membrane Ca^{2+}-ATPase (PMCA) pump, the SR Ca^{2+}-ATPase (SERCA) pump, the Na+/Ca^{2+} exchanger (NCX), and cytosolic Ca^{2+}-binding proteins (Juhaszova *et al.*, 1996; Laporte & Laher, 1997).

PMCA utilizes energy from ATP hydrolysis to produce Ca^{2+} efflux. The PMCA activity can be increased by binding to CaM and phosphorylation by several protein kinases such as PKA, PKC, cGMP-dependent protein kinase (protein kinase G; PKG) and Ca^{2+}/CaM-dependent protein kinase (CaMK), while autoinhibition occurs when CaM is absent (Gonzalez *et al.*, 1996).

Like the PMCA, the SERCA pump also utilizes the energy supplied by the hydrolysis of ATP to accumulate Ca^{2+} inside the SR. Once Ca^{2+} is taken up into the SR lumen, it is bound by several small hydrophilic proteins, such as calreticulin or calsequestrin that are capable of binding large amounts of Ca^{2+} (Marin *et al.*, 1999). The SERCA pump is regulated by the transmembrane protein phospholamban and sarcolipin, instead of CaM (Traaseth *et al.*, 2008). The phosphorylation of phospholamban by PKA, PKG and CaMK increases SERCA Ca^{2+} affinity and the rate of its Ca^{2+} transport (Raeymaekers *et al.*, 1990; Traaseth *et al.*, 2008).

The NCX may contribute to either Ca^{2+} extrusion or even Ca^{2+} influx, depending on the conditions, and its physiological significance in VSMCs has been questioned (Juhaszova *et al.*, 1996).

The myoplasma of the smooth muscle contains many Ca^{2+}-binding proteins that may provide a mechanism for the rapid removal of Ca^{2+} and limiting its diffusion (Horowitz *et al.*, 1996). These include CaM, troponin C, saponin, calbindin, calretinin, parvalbumin and the annexin family (Heizmann, 1992; Niki *et al.*, 1996). The myoplasma also contains many inorganic compounds or other small organic molecules such as amino acids, nucleotides and organic acids which have the ability to bind to Ca^{2+} (Toescu, 1995).

1.4.2 Mechanisms controlling the Ca^{2+} sensitization of the contractile apparatus

Ca^{2+} sensitivity can be regulated by either MLC_{20} phosphorylation-dependent or -independent mechanisms. The phosphorylation-dependent mechanism involves mediators controlling MLCP activity, such as Rho-kinase (Rho-activated kinase/ROKα/ROCKII), PKC, arachidonic acid and telokin, in addition to the CaMKII that regulates MLCK activity (Somlyo & Somlyo, 2000; Hirano, 2007). The phosphorylation-independent mechanism depends on cross-bridge regulation by thin filament-associated proteins, such as caldesmon and calponin (Morgan & Gangopadhyay, 2001).

MLCP is composed of three subunits: a catalytic subunit of type 1 phosphatase (PP1Cδ; ~37 kDa); and two noncatalytic subunits, a large 110-130 kDa regulatory subunit termed myosin phosphatase target subunit (MYPT1) or myosin-binding subunit and a 20-kDa subunit of unknown function (Hartshorne, 1998; Ito *et al.*, 2004). RhoA, a small monomeric G-protein, activates Rho-kinase that phosphorylates the MYPT1 and inhibits its catalytic activity, increasing MLC_{20} phosphorylation and, hence, contraction (Feng *et al.*, 1999). In addition, Rho-kinase may phosphorylate and activate CPI-17, leading to the inhibition of PP1Cδ, and thereby inhibiting MLCP (Koyama *et al.*, 2000).

PKC is another important regulator of MLCP. PKC is a family of closely related serine/threonine kinases. The PKC family can be divided into four major groups (classical, novel, atypical and group D) depending on the requirement for Ca^{2+}, DAG, and/or phosphatidylserine for activation in addition to sensitivity to phorbol esters (Walsh *et al.*, 1996). DAG and arachidonic acid can activate PKC leading to phosphorylation of CPI-17 with subsequent inhibition of MLCP (Li *et al.*, 1998). Arachidonic acid, released through the activation of PLA_2 and/or PLD (Parmentier *et al.*, 2001), was shown to directly activate Rho-kinase independent of RhoA (Feng *et al.*, 1999) and PKC (Kitazawa *et al.*, 2000).

The 17 kDa protein telokin represents another regulator of MLCP. It mediates Ca^{2+} desensitization through activation of MLCP in VSMCs, which lead to a

decreased MLC_{20} phosphorylation with subsequent relaxation (Wu *et al.*, 1998b; Choudhury *et al.*, 2004).

In addition to MLCP, MLCK can play a role in Ca^{2+} desensitization. The activity of MLCK is primarily regulated by the Ca^{2+}-CaM complex. However, the phosphorylation of MLCK, by CaMKII, in the region of its CaM-binding domain decreases its affinity for the Ca^{2+}-CaM complex and, hence, its phosphorylating activity (Stull *et al.*, 1993).

The thin-filament-associated proteins caldesmon and calponin possess actin- and CaM-binding activities, and the capability to inhibit the actomyosin ATPase activity and, hence, crossbridge cycling (Winder *et al.*, 1998). When phosphorylated, their inhibitory action on actomyosin ATPase can be reversed, possibly leading to enhanced crossbridge cycling and thus to an enhanced contractile response without an increase in MLC_{20} phosphorylation (Winder *et al.*, 1998). Thus, these thin-filament-associated proteins may participate in the regulation of myofilament Ca^{2+} sensitivity through their phosphorylation by MAPKs and/or other kinases such as PKC, CaMKII, or p21-activated kinase (Morgan & Gangopadhyay, 2001).

1.4.3 Other mechanisms regulating VSM contraction

1.4.3.1 Cyclic nucleotides

An increase in the cytosolic level of cGMP (by NO, carbon monoxide (CO), or natriuretic peptides) or cAMP (by β-adrenergic agonists, PGI_2 or adenosine) in VSMCs is considered one of the major mechanisms that mediate vasodilation through reduction of both $[Ca^{2+}]_i$ and Ca^{2+} sensitivity in VSMCs (Vaandrager & de Jonge, 1996; Polson & Strada, 1996; Levin *et al.*, 1998). The increase in cGMP levels leads to the activation of PKG, which in turn reduces $[Ca^{2+}]_i$ through activation of SERCA, PMCA and NCX, inhibition of IP_3R/ IP_3 synthesis, activation of K^+ channels and inhibition of VOCCs (Vaandrager & de Jonge, 1996). The PKG-induced reduction of myofilament Ca^{2+} sensitivity is possibly due to the upregulation of MLCP (Vaandrager & de Jonge, 1996; Somlyo & Somlyo, 2000). Similarly, the increase in cAMP levels exerts profound influences on cellular Ca^{2+} mobilization

through the activation of PKA, including inhibition of the activation of PLC and Ca^{2+} channels, stimulation of PMCA, SERCA and the NCX and activation of K^+ channels (Minami *et al.*, 1993; Takuwa, 1996). In addition, the increase in cAMP reduces myofilament Ca^{2+} sensitivity, presumably by phosphorylating MLCK and thereby decreasing its affinity for the Ca^{2+}-CaM complex (Takuwa, 1996).

1.4.3.2 Potassium channels

In VSMCs potassium (K^+) channels play a fundamental role in maintaining the membrane potential, a major determinant of vascular tone, particularly in systemic resistance vessels. Specifically, the blockade of K^+ channels results in membrane depolarization and increased Ca^{2+} influx through VOCCs, leading to vasoconstriction. Conversely, the activation of K^+ channels results in plasmalemmal K^+ efflux, membrane hyperpolarization, and reduced Ca^{2+} influx through VOCCs, leading to vasodilation (Nelson & Quayle, 1995; Takuwa, 1996). Therefore, K^+ channels may serve to limit membrane depolarization in response to vasoconstrictor stimuli (as ET-1, AngII, vasopressin or TxA_2) and their activation may be involved in response to vasodilator stimuli (as NO, EDHF, PGI_2 or adenosine) (Waldron & Cole, 1999).

Several K^+ channels exist in VSMCs, such as voltage-gated K^+ (K_V), Ca^{2+}-activated K^+ (K_{Ca}), ATP-sensitive K^+ (K_{ATP}) and inward rectifying K^+ (K_{ir}) channels. Depolarization activates K_V and K_{Ca}, $[Ca^{2+}]_i$ activates K_{Ca}, hyperpolarization activates K_{ir} while ATP inhibits K_{ATP} channels (Brayden, 1996; Clapp & Tinker, 1998). Membrane hyperpolarization by K^+ channel opening, mainly the large-conductance K_{Ca} (BK) and K_{ATP} channels, has been shown to account for the observed vascular hyporeactivity of septic shock (Chen *et al.*, 2000; Farias *et al.*, 2002; Wu *et al.*, 2004; O'Brien *et al.*, 2005; Pickkers *et al.*, 2006). BK is the most abundant K^+ channel in VSMCs (Ledoux *et al.*, 2006) that can be upregulated in hypertension (Rusch *et al.*, 1996).

1.4.3.3 Chloride channels

Chloride (Cl^-) channels also play an important role in the regulation of $[Ca^{2+}]_i$ in VSMCs as they are abundantly distributed in the VSM membrane. Two types of Cl^- channels exist in VSMCs including volume-regulated Cl^- (Cl_v) and Ca^{2+}-dependent Cl^- (Cl_{Ca}) channels (Large & Wang, 1996; Yamazaki *et al.*, 1998). Vascular distension caused by a rise in blood pressure would activate Cl_v channels leading to membrane depolarization and subsequent opening of VOCCs resulting in vasoconstriction. Thus, the Cl_v channel may play a protective role in maintaining tissue integrity against mechanical stretch (Yamazaki *et al.*, 1998; Kitamura & Yamazaki, 2001). The Cl_{Ca} channels have been reported to be activated by an increase in $[Ca^{2+}]_i$ and contribute to the contractile response to norepinephrine in some vascular beds (Large & Wang, 1996; Kitamura & Yamazaki, 2001).

1.5 Aim of the work

Inflammation has incompletely characterised effects on cardiopulmonary vascular reactivity. Both hypo- and hyper-responsiveness to vasoactive agents have been reported, depending on the experimental system used. The changes reported in vascular reactivity are likely to be a consequence of altered expression of vasoactive substances and alterations in signalling transduction events in vascular tissue. The aim of this project is to characterise the relationships between changed vascular reactivity induced by LPS, as a powerful inflammatory stimulus, and the expression and activity of vasoactive mediators and associated signalling events.

A better understanding of the relationship between inflammation and vascular smooth muscle function will provide the basis for novel therapeutic strategies in the treatment of cardiopulmonary pathologies associated with inflammatory disease.

Objectives:

1- to establish and optimize an *in vitro* model that can be easily controlled to determine the effects and mechanisms of LPS on vascular reactivity.

2- to examine the effect of LPS on vascular reactivity to different vasoconstrictors and vasodilators in the developed *in vitro* model, using different arteries representing the systemic and pulmonary circulations.

3- to determine the vasoactive mediators that could be involved in vascular reactivity changes induced by LPS.

4- to investigate the possible alterations in signalling transduction events involved in VSM contraction that could be induced by LPS, including the role of specific receptor expression, $[Ca^{2+}]_i$ and Ca^{2+} sensitization.

These objectives will be used to test the hypothesis that LPS induces changes in VSM reactivity through affecting signalling events, such as specific receptor expression, Ca^{2+} influx, $[Ca^{2+}]_i$ and/or Ca^{2+} sensitization, and these changes depend on the type of vascular tissue and the vasoactive mediator being tested.

Chapter 2

Methods & Materials

Chapter 2

2.1 Tissue preparation

Male Wistar rats of 8-9 weeks age (250-300 g) from the University of Bath Animal House (Bath, UK) were used. Animal housing and care was carried out in accordance with UK Home Office legislation and guidelines [Animals (Scientific procedures) Act 1986]. Standard animal facilities were used, including constant temperature (20±2°C), relative humidity (55±10%) and alternating 12 h light and dark cycles in addition to providing food and water *ad libitum*.

Rats were humanely killed by cervical dislocation and the side branches of the pulmonary artery and the descending thoracic aorta were separated and placed in ice-cold HEPES-buffered physiological salt solution (PSS) (see Table 2.1 for composition). The vessels were dissected free of fat and connective tissue, and cut into rings (2-4 mm in length).

2.2 Organ tissue culture

Under sterile tissue culture conditions in a class 2 microflow safety biological cabinet (Astec Environmental Systems, North Somerset, UK), vascular rings were gently washed in Dulbecco's modified Eagle's medium (DMEM) before being placed into 48-well tissue culture plates, with each well containing 1 ring in 1 ml DMEM supplemented with penicillin (100 unit.ml^{-1}), streptomycin (100 μg ml^{-1}) and 10% certified and heat-inactivated foetal bovine serum (FBS). After 1 h stabilization, vascular rings were transferred to a fresh medium of the same composition (control group) or supplemented with LPS (10 μg ml^{-1}; LPS-treated group) and incubated for 20 h at 37^{o}C in humidified atmosphere of 5% CO_2 in air using a Leec CO_2 incubator (Leec Limited, Nottingham, UK). Different vasoactive reagents and inhibitors used in this study are listed in Table 2.2.

Table 2.1 Composition of physiological salt solutions (PSS)

	Krebs-Henseleit	HEPES-buffered	Ca^{2+}-free HEPES-buffered
NaCl	118	118	118
KCl	4.7	4.7	4.7
Glucose	11.1	11.1	11.1
KH_2PO_4	1.2	—	—
$NaHCO_3$	25	—	—
$MgSO_4$	1.2	—	—
$MgCl_2$	—	1.2	1.2
HEPES	—	10	10
$CaCl_2$	2.5	1.5	—

All values are expressed in mM. The pH of HEPES-buffered PSS was adjusted to 7.4 with NaOH, while that of Krebs-Henseleit solution was adjusted to the same value with continuous bubbling with carbogen mixture (5% CO_2 + 95% O_2). For $[Ca^{2+}]_i$ measurements, HEPES-buffered PSS was used, but with $CaCl_2$ 2.5 mM instead of 1.5 mM.

2.3 *In vitro* vascular reactivity studies

Following 20 h of incubation, arterial rings from the control and the LPS-treated groups were suspended in an organ bath between 2 stainless steel parallel hooks, one of which was fixed and the other attached to an isometric tension transducer. The organ bath was filled with 18 ml of Krebs-Henseleit solution at a temperature of 37^{o}C and continuously bubbled with a mixture of 95% O_2 and 5% CO_2. Rings were allowed to equilibrate under 12 (aorta) and 7 (pulmonary artery) mN resting tension for 60 minutes, during which time the bath solution was replaced every 15 minutes and the resting tension was readjusted when necessary. Isometric tension generated by the VSM was measured using a force displacement transducer (K30, Hugo-sachs Elektronik, March, Germany) and recorded with a MacLab 4S unit linked to a PC running Chart v4.2 software (ADInstruments Ltd., Chalgrove, Oxfordshire, UK). The software was adjusted to record 20 samples per second at 2mV sensitivity and a 20 Hz filter was applied to remove electronic noise.

At the beginning of each experiment, arterial ring responsiveness was assessed by measuring contraction to 80 mM KCl and this procedure was repeated until consistent responses were obtained, and then rings were washed until tension returned to the base line.

To measure vasoconstriction, cumulative concentration-response curves were constructed to ET-1 (0.3-100 nM), phenylephrine (1 nM-10 µM) and U46619 (3 nM-1 µM). Contraction to ET-1 was also measured in absence of external Ca^{2+} (Ca^{2+} was omitted from PSS and 1 mM EGTA was added) or in presence of different inhibitors (Table 2.2).

To measure vasorelaxation, rings were first preconstricted with 30 nM ET-1 and after reaching a steady state contraction (plateau), relaxation responses to ACh (1 nM- 30 µM), SNP (1 nM-30 µM), 8-pCPT-cGMP (0.1 µM-100 µM), BAY 41-2272 (1 nM-10 µM), T-0156 (0.1 nM-100 nM), Ro-31-8425 (300 nM), nifedipine (10 nM-30 µM), SKF-96365 (10 µM), and Y-27632 (0.1 µM-30 µM) were measured (Table 2.2).

In some preparations, endothelium was removed by gentle mechanical rubbing, and denudation was confirmed by absence of relaxation to 1 µM ACh. Appropriate vehicle control experiments were also conducted.

Table 2.2 Different vasoactive mediators and inhibitors used in this study

Compound	Function	Solubility	Final concentration
ET-1	ET receptor agonist, VC	H_2O	0.3–100 nM
Phenylephrine	α_1-adrenoceptor agonist, VC	H_2O	10 nM-30 µM
U46619	TxA_2 mimetic, VC	DMSO	3 nM-1 µM
KCl	Depolarizing agent, receptor-independent VC	H_2O	80 mM
ACh	eNOS stimulant, VD	H_2O	1 nM-30 µM
SNP	NO releasing agent	H_2O	1 nM-30 µM
1400W	Specific iNOS inhibitor	DMSO	1 µM
8-pCPT-cGMP	PDE-resistant cGMP analogue	H_2O	0.1 µM-100 µM
BAY 41-2272	Direct sGC activator, VD	DMSO	1 nM-10 µM
ODQ	sGC inhibitor	DMSO	10 µM
T-0156	PDE5 inhibitor	DMSO	0.1 nM-100 nM
Y-27632	ROCK inhibitor	H_2O	0.1 µM-30 µM
Ro-31-8425	PKC inhibitor	DMSO	300 nM
Indomethacin	COX inhibitor	Na_2CO_3 (5 mM)	10 µM
Trolox	Antioxidant, ROS inhibitor	Ethanol	200 µM
Cycloheximide	Protein synthesis inhibitor	Ethanol	10 µM
Glybenclamide	K^+_{ATP} channel blocker	DMSO	10 µM
Iberiotoxin	BK channel blocker	H_2O	100 nM
EGTA	Ca^{2+}-chelating agent	H_2O	1 mM
Nifedipine	L-type VOCC blocker	DMSO	10 nM-30 µM
SKF-96365	ROCCs & SOCCs blocker	H_2O	10 µM

VC, vasoconstrictor; VD, vasodilator. Stock solutions were normally prepared as 1000x of the maximum concentration required.

2.4 Measurement of NO release

In aqueous solutions, NO has a very short half-life and is oxidized to nitrite and nitrate, therefore, NO production was determined by measuring the accumulation of these breakdown products in the culture medium (Bishop-Bailey *et al.*, 1997). Nitrate was first reduced to nitrite and the total nitrite was measured spectrophotometrically by the Greiss reaction.

Pulmonary and aortic rings were divided into four groups: control, LPS, LPS+L-NAME (100 μM) or LPS+1400W (1 μM). Each ring was incubated in 1 ml medium as described above, but phenol red-free DMEM was used. After 20 h incubation, 60 μl supernatant was taken from each well and samples were incubated for 60 min at 37°C with 0.2 unit ml^{-1} nitrite reductase, 50 μM NADPH and 5 μM FAD to reduce nitrate to nitrite. Remaining NADPH, which absorbs at 550 nm, was oxidized by the addition of 10 unit ml^{-1} lactate dehydrogenase and 10 mM sodium pyruvate for a further 10 min at 37°C. A final sample volume of 100 μl was then mixed with an equal volume of modified Greiss reagent for 5 min in 96-well plates. Absorbance was measured at 550 nm by Versamax tunable microplate reader with Softmax Pro software (Molecular Devices, USA) and total nitrite concentration was calculated using the standard curves of sodium nitrate (0-128 nmole ml^{-1}) in culture medium run simultaneously in parallel.

2.5 Assay of SNP-induced cGMP production

To assess changes in cGMP production, a NO donor (100 μM SNP) was used to stimulate production of cGMP in the presence of a non-selective PDE inhibitor (100 μM IBMX) to prevent cGMP degradation (Toward *et al.*, 2005; Fernandes *et al.*, 2006). This assay is based on the competitive binding technique in which cGMP present in a sample competes with a fixed amount of horseradish peroxidase (HRP)-labeled cGMP for sites on a rabbit polyclonal antibody. During the incubation, the polyclonal antibody becomes bound to the goat anti-rabbit antibody coated onto the microplate. Following a wash, to remove excess conjugate and unbound sample, a substrate solution is added to the wells to determine the bound enzyme activity. The colour development is stopped and the absorbance is read at

450 nm. The intensity of the colour is inversely proportional to the concentration of cGMP in the sample.

Rings from control and LPS groups were transferred to a HEPES-buffered PSS and incubated for 1 h at 37^{o}C. Rings were then incubated with the non-selective PDE inhibitor 100 μM IBMX for 30 min followed by incubation with 100 μM SNP for an additional 10 min further incubation. Rings were then quickly frozen and homogenized in ice-cold 6% trichloroacetic acid to give a 10% (w/v) homogenate. Homogenates were centrifuged at 2000 g for 15 min at 4°C, the supernatant was recovered and the pellet discarded. The supernatant was washed 4 times with 5 volumes of water saturated diethyl ether and the upper ether layer was discarded after each wash. The remaining aqueous extract was heated at 60^{o}C for 10 min to remove any traces of ether, then lyophilised using Edwards modulyo freeze dryer (Edwards high vacuum international, Sussex, UK) attached to a vacuum pump (RV8, Edwards, UK) with samples placed in 1.5 microfuge tubes with open caps in a Savant SVC-100H Speed Vac Concentrator (Savant, Farmingdale, NY, USA). The dried extract was dissolved in a suitable volume of assay buffer and cGMP was measured in duplicate by ELISA using a commercially available enzyme immunoassay (R&D Systems Europe Ltd., Abingdon, UK) according to the manufacturer's instructions. Results were expressed as picomoles of cGMP per milligram of tissue weight.

2.6 Measurement of changes in $[Ca^{2+}]_i$ in isolated aortic VSMCs

2.6.1 Isolation of VSMCs

Aortic rings (4-6 mm in length) were separated and incubated as before (control and LPS 10 μg ml^{-1}) for 20 h. After incubation, the endothelium was removed mechanically by gentle rubbing and aortic rings were washed with Ca^{2+}-free HEPES-buffered PSS (Table 2.1) for 15 min at 37^{o}C with continuous shaking. Vascular rings were digested by transferring into 2 ml enzymatic solution composed of Ca^{2+}-free HEPES-buffered PSS plus the components shown in Table 2.3 and incubated at 37^{o}C for 45 min with continuous shaking. The digested rings were carefully washed 3 times in fresh Ca^{2+}-free PSS (each 5 min), then tissues were placed in fresh Ca^{2+}-free HEPES-buffered PSS and gently triturated by a fire-polished Pasteur pipette to

release VSMCs. Undispersed pieces of tissue were removed by syringe filtration through a nylon mesh (95 μm) very slowly. The Ca^{2+} concentration was increased gradually in the final cell suspension to 0.5 mM. The viability of the cells were tested with trypan blue exclusion, with >85% of the cells viable considered as acceptable. Suspended VSMCs were then incubated at room temperature for 1 h over glass coverslips, coated with poly-L-lysine overnight, in a 6-well plate.

Table 2.3 Enzymatic solution to separate aortic VSMCs

Component	Concentration (mg ml^{-1})
Papain	1
Collagenase-P	2
Soyabean trypsin inhibitor	0.5
Dithiothrietol	1
Bovine serum albumin (BSA)	1

2.6.2 Measurement of $[Ca^{2+}]_i$

VSMCs were loaded for 1 h at room temperature with 5 μM membrane-permeant Fura-2 AM in HEPES-buffered PSS but with Ca^{2+} 2.5 mM (Table 2.1) containing 0.02% Pluronic F-127 at room temperature in the dark. The ratiometric nature of the Fura-2 dye allows for assessment of $[Ca^{2+}]_i$ that are independent of diameter changes. The coverslips with attached fura-2 loaded cells were placed in a 0.25-ml chamber on the stage of a Zeiss Axiovert S 100 inverted microscope with a 40x/1.30 Fluar oil immersion objective. The cells were excited alternately at 340- and 380-nm wavelengths of ultraviolet light at a frequency of 0.75 Hz by using a Spectramaster I variable excitation wavelength generator (EG&G Wallac LSR, Cambridge, UK). Emitting fluorescence was collected through a 510-580nm band pass emission filter and cell images were acquired using an Ultrapix (PDCI) CCD camera (1024x1024 max pixels) and analysed using Ultraview software version 4 (Perkin-Elmer, USA). The background fluorescence signal was subtracted by measuring emitted fluorescence from an area on the coverslip with no cells.

The cells were perfused with either HEPES-buffered PSS (2.5 mM $CaCl_2$) or Ca^{2+}-free HEPES-buffered PSS (with 1 mM EGTA added) at 2 ml min^{-1} at 37°C for 10 min. $[Ca^{2+}]_i$ baseline was recorded for 30 s before the perfusion of ET-1 (100 nM). At the end of the experiment, 2 μM ionomycin with 10 mM Ca^{2+} followed by 2 mM EGTA were added to obtain the fluorescence intensity maximum (F_{max}) and the fluorescence intensity minimum (F_{min}) respectively.

The $[Ca^{2+}]_i$ was determined from the Grynkiewicz equilibrium equation (Grynkiewicz *et al.*, 1985):

$$\mathbf{[Ca^{2+}]_i = K_D \times \beta \times (R - R_{min})/(R_{max} - R)}$$

R, the experimental value of fluorescence ratio,

$\mathbf{K_D}$, the dissociation constant for fura-2 (224 nM at 37°C),

β is the ratio of fluorescence of fura-2 when excited at 380 nM in the zero and saturating Ca^{2+}.

The $[Ca^{2+}]_i$ during sustained phase was expressed as % of the transient peak $[Ca^{2+}]_i$.

2.7 Immunoblotting

Immunoblotting or Western blotting is a technique that allows visualisation of the relative amounts of specific proteins in a given sample. Samples are lysed using different buffers containing detergents, solubilising agents and different protease inhibitors. To fully dissociate proteins into their polypeptide subunits, samples are heated with sodium dodecyl sulphate (SDS) and thiol reagent. The negative charge associated with protein by the bound detergent enables proteins to migrate through a polyacrylamide gel strictly according to polypeptide size. Following electrophoresis, separated proteins are transferred into a membrane, and then probed with primary antibodies raised against specific proteins. Secondary antibodies, tagged with an enzyme such as HRP, are then added to bind specifically to the primary antibodies. The enzyme bound to the secondary antibodies catalyses a chemiluminescence reaction that enables the antibodies to be detected using photosensitive film.

2.7.1 Tissue lysis

After 20 h of incubation with either control or LPS, pulmonary and aortic rings were rapidly frozen in liquid nitrogen, either directly or after reaching maximal contraction to ET-1, and collected at the plateau of maximal contraction in organ bath and then stored at -80 ^{o}C until used. Vascular tissue was mechanically homogenized using PowerGen 125 homogenizer (Fisher Scientific, UK) in 10 volumes per weight (between 200-400 µl) of an ice-cold lysis buffer (see Table 2.4 for composition). Homogenates were rotated at 4 ^{o}C for 30 min to allow inhibition of proteases and then centrifuged (18000 g for 15 min at 4 ^{o}C) and supernatant was used as described below.

Table 2.4 Immunoblotting buffers

Buffer	Composition
Lysis buffer I	150 mM NaCl, 1 mM EDTA, 50 mM Tris HCl pH 7.5, 1% Nonidet-P40, 10% glycerol, 1 mM sodium orthovanadate, 10 mM sodium fluoride, 1 mM PMSF and 1% protease inhibitor cocktail
Lysis buffer II	1x RIPA buffer, 10 mM sodium fluoride, 1 mM sodium molybdate, 1 mM PMSF and 1% protease inhibitor cocktail
Sample buffer	10% SDS, 200 mM Tris HCl pH 6.8, 50% glycerol, 0.01% bromophenol blue and 5% 2-mercaptoethanol (added just prior use)
Running buffer	192 mM glycine, 25 mM Trizma base, 0.1% (w/v) SDS, ultrapure water
Semi-dry transfer buffer	39 mM glycine, 48 mM Trizma base, 0.0375% SDS, 20% (v/v) methanol, ultrapure water
Tris-buffered saline (TBS)	20 mM Tris-HCl pH 7.5 and 150 mM NaCl
TBSN	TBS + 0.05% Nonidet-P40

2.7.2 Determination of protein concentrations in lysates

In order to provide similar amounts of proteins in the same volume of each sample, supernatant protein concentration was quantified by the BioRad protein assay (Bio-Rad, Hercules, USA) which is based on the Bradford protein

quantification assay (Bradford, 1976; Zor & Selinger, 1996). A 1 mg ml^{-1} solution of BSA was used to construct the standard curve at concentrations of 0-32 μg μl^{-1}. Equal volumes (2 μl) of each lysate sample or the standard were added to 250 μl of Quickstart Bradford dye reagent 1x (BioRad) in triplicate in a 96-well microtitre plate. Protein concentration was measured at 595 nm using Versamax tunable microplate reader with Softmax Pro software (Molecular Devices, USA). The protein concentrations of the lysate samples were then calculated from the standard curve by linear regression with additional compensation for any dilutions.

2.7.3 Immunoblotting sample preparation

After determining protein concentrations, lysate samples containing higher concentrations of proteins were diluted with ice-cold lysis buffer to equalize the protein concentrations between all samples. Samples (100-200 μl each) were mixed with 5x SDS sample buffer (see Table 2.4 for composition) in 4 to 1 volumes respectively, heated at 100 ^{o}C for 5 min using Techne dri-block DB-2A (Techne Cambridge Limited, Cambridge, UK), placed on ice for 5 min and then stored at -20 ^{o}C until used.

2.7.4 Polyacrylamide gel electrophoresis

One-dimensional polyacrylamide gels were prepared using BioRad Mini Protean II gel electrophoresis with attached PowerPac 300 unit (Bio-Rad Labs, Hemel Hempstead, UK) and assembled according to the manufactures guidelines, utilising pre-cleaned glass plates. The resolving gel was prepared at the desired percentage of acrylamide depending on the relative size of the proteins under investigation (Table 2.5), where 7.5% gel was used for all proteins studied except those less than 30 kDa (MLC_{20} and CPI-17) in which 15% gel was used. The resolving gel was poured between the glass plates and overlaid with water to achieve a uniform line and left to polymerise for 40 min. The water was then aspirated and the stacking gel poured on top, with a 10-well comb inserted between the plates to create the wells for the loading of protein samples, and left for 20 min to polymerize. The wells were thoroughly cleaned with water to remove any residual stacking gel before being filled with lx SDS-PAGE running buffer (Table 2.4). Protein samples

(40 µg per lane) were then loaded into the wells with one well loaded with 10 µl of pre-stained molecular weight markers to serve as a guide to ease protein band identification at a later stage. Pre-cast gels were then placed into a gel tank with lx SDS-PAGE running buffer in the top and bottom reservoirs and electrophoresis was run at 80 volts until the bromophenol blue present in the lysate samples entered the resolving gel. At that time, the voltage was increased to 180 volts. Gels were run until the bromophenol blue dye reached the bottom of the resolving gel or the desired separation of bands in reference to the molecular weight markers was achieved, then gels were removed and placed into semi-dry transfer buffer.

Table 2.5 Recipes for electrophoresis gels

	Running gel		Stacking gel 5%
	7.5%	**15%**	
30% acrylamide/Bis-acrylamide	3.75	7.5	1.67
MilliQ H_2O	5.6	1.85	6.0
1M Tris-HCl pH 8.8	5.6	5.6	—
1M Tris-HCl pH 6.8	—	—	1.25
10% SDS	0.25	0.25	0.15

All values are expressed in ml. Total volume of the running gel is sufficient for three 1 mm thick mini gels, while that of stacking gel is sufficient for four 1 mm thick mini gels. 50 µl ammonium persulfate (10% w/v) and 20 µl TEMED are added to running and stacking gel mixtures just before pouring into the gel cassettes.

2.7.5 Semi-dry transfer of proteins to nitrocellulose membrane

Following gel electrophoresis, the separated proteins were transferred onto nitrocellulose membranes by semi-dry transfer using Bio-Rad Transblot SD cell (BioRad, USA). This approach was achieved by removing the gel from the pre-assembled gel apparatus and soaked in semi-dry transfer buffer (Table 2.4). In order to ensure efficient transfer of the proteins, the bottom (positive) graphite electrode was dampened with transfer buffer. A gel-membrane sandwich composed of four pieces of 3MM Whatman paper, a piece of nitrocellulose membrane, the gel and finally another four pieces of Whatman paper, all of the same size as the gel and

all pre-soaked in the semi-dry transfer buffer, were placed on the bottom electrode and rolled to gently expel any air bubbles then the upper negative electrode, which was dampened with transfer buffer, was gently lowered into place. The proteins were transferred at a rate of 0.8 mA cm^{-2} (40 mA per gel) for 1 hour.

2.7.6 Antibody probing and immunoblot developing

Once the transfer had finished, the transfer apparatus was disassembled and the nitrocellulose membrane was washed in TBSN (See Table 2.10) prior to the addition of water soluble Ponceau S to check for successful and even transfer of proteins and to mark the molecular weight standards. Excess stain was removed by washing the membrane in TBSN. The non-specific binding of antibody was blocked by incubation of the membranes for 1 h with TBSN containing 5% non-fat milk with gentle shaking on a Stuart rocking platform (Sterilin LTD, Staffordshire, UK) at room temperature. The membranes were then subjected to wash in TBSN before incubation overnight at 4 ^{o}C with one of the primary antibodies (see Table 2.6 for conditions used for different antibodies) with gentle shaking. The next day, blots were washed three times each for five min with TBSN before being incubated for 1 h with HRP-conjugated secondary antibodies (1: 10000-20000 dilution in TBSN with 2% milk, Dako, Glostrup, Denmark). Immunoreactive protein bands were detected by ECL or ECL Advance kit (Amersham Biosciences) and visualized on an X-Ray film (Fujifilm Corporation, Tokyo, Japan). The intensity of the specific bands was quantified by densitometric analysis using Labimage software (Kapelan Bio-imaging Solutions, Halle, Germany).

2.7.7 Membrane stripping and reprobing

In order to probe for a different molecule in the lysate samples of a nitrocellulose membrane that had already been used, the used membranes were stripped free of antibody before reusing. Membranes were first washed with TBSN for 10 min at room temperature in a rocking platform, and then they were stripped using Re-Blot Plus solution (Chemicon, USA) according to manufacturer instruction. After washing several times with TBSN, membranes were blocked and reprobed with antibodies as described before. This procedure of stripping and reprobing was

specifically used for examining equal loading of phospho-proteins using antibodies specific for their non-phospho proteins. For other non-phosphorylated proteins, an antibody against abundant protein in the lysate samples, such as rabbit polyclonal anti-β-actin antibody, was used usually without stripping if there is an appropriate size difference between β-actin and the desired protein, otherwise stripping was applied.

Table 2.6 Immunoblotting conditions for primary antibodies

Molecule targeted by antibody	Primary antibody species	MW (kDa)	Primary antibody conc.	Secondary antibody conc
CPI-17	rabbit	17	1 μg ml^{-1}	1:10000
MLC_{20}	rabbit	20	1:1000	1:10000
MYPT1	rabbit	130	1:200	1:10000
Phospho-CPI-17 (Thr38)	rabbit	17	2 μg ml^{-1}	1:10000
Phosphodiesterase 5	mouse	85/95	1:500	1:10000
Phospho-MLC_{20} (Ser19)	rabbit	20	1:1000	1:10000
Phospho-MYPT1 (Thr850)	rabbit	130	1 μg ml^{-1}	1:10000
Phospho-ROCK α (The396)	rabbit	160	2 μg ml^{-1}	1:10000
PKC	rabbit	80	1:200	1:10000
sGCα_1	rabbit	80	1:10000	1:10000
sGCβ_1	rabbit	69	1:4000	1:10000
β-actin	rabbit	45	1:1000	1:10000

All antibodies used are polyclonal except anti-phosphodiesterase 5 which is monoclonal. Primary antibody concentration represents the antibody dilution in TBSN with 0.01% (w/v) sodium azide (10 ml per each membrane). Secondary antibody concentration represents the antibody dilution in TBSN with 2% (w/v) skimmed milk (10 ml per each membrane).

2.8 Quantitative RT-PCR

To measure changes induced by LPS in the gene expression of NO and ET-1 systems, RNA was extracted from aortic and pulmonary arterial rings after culturing, reverse-transcribed (RT) to cDNA and then quantified using gene specific primers for eNOS, iNOS, ET-1, ET_A and ET_B by real-time polymerase chain reaction (PCR).

2.8.1 RNA isolation and purification

After 20 h of incubation with either control or LPS, pulmonary and aortic rings were rapidly frozen in liquid nitrogen and then stored at -80 ^{o}C until used. Vascular tissue was mechanically homogenized using PowerGen 125 homogenizer (Fisher Scientific, UK) in 2 ml RNAase free microfuge tube with rounded bottom containing 1 ml TRIZOL reagent (Invitrogen, USA). The homogenized samples were then incubated for 5 minutes at 15-30°C before adding 0.2 ml chloroform in an Airone PCR-640 UV cabinet (Safelab Systems, Bristol, UK), vortexing, incubating at 15-30°C for 2-3 min and centrifugation at 15,400g for 15 min at 4°C using Beckman GS-15R centrifuge. Following centrifugation, the upper colourless aqueous phase containing RNA was transferred to 1.5 ml RNAase free microfuge tube and the RNA was precipitated by adding 0.5 ml of isopropyl alcohol. Samples were incubated at 15-30°C for 10 minutes and then centrifuged at 15,400g for 10 min at 4°C. The precipitated gel-like RNA pellet was washed once by adding 1 ml of 75% ethanol, vortexed and then centrifuged at 15,400g for 5 min at 4°C. The RNA pellet was dried in air for 5-10 min prior to being resuspended in 50-100 µl of sterile water and heating the samples to 55°C for 10 minutes to break secondary structures within the RNA and enhancing its solubility. The produced RNA pellet was further purified using High Pure RNA Tissue Kit (Roche Applied Science, Mannheim, Germany) which contains DNase digest step to remove any genomic DNA according to manufacturer's instructions.

RNA concentration and purity for each sample was determined using a 1:100 dilution of the RNA and the absorbance measured at 260nm and 280nm using the GeneQuant II spectrophotometer.

The concentration of RNA was determined as following:

Concentration of RNA (µg ml^{-1}) = dilution factor x 40* x A260

***** The standard consideration is that 40 µg $m1^{-1}$ of RNA has an absorbance of 1 at 260 nm

Ratio values of 1.8-2.0 verified acceptable RNA purity. RNA samples were then stored at -80°C.

2.8.2 cDNA synthesis

RNA samples (1 µg each) were reverse-transcribed using Omniscript RT kit (Quiagen GmbH, Hilden, Germany) with anchored oligo dT primers (ABgene, Surrey, UK) in the presence of an RNase inhibitor (RNasin Plus, Promega, Madison, WI, USA) according to manufacturer's instructions using a Perkin Elmer GeneAmp PCR System 2400 thermal cycler. The reaction mixture (Table 2.7) was setup at 40°C for 60 minutes followed by 70°C for 10 minutes to inactivate the reverse-transcriptase. RT-negative samples, in which no reverse-transcriptase was added, were also prepared to identify any possible genomic DNA contamination within RNA samples. cDNAs produced were stored at -20°C.

Table 2.7 Reverse-transcriptase (RT) reaction mixture

Component	Volume (µl)
10x RT buffer	2
dNTP (5 mM)	2
Anchored oligo dT primers (500 ng ml^{-1})	2
RNasin plus	0.25
Reverse transcriptase (RT)	1
RNA template	1-12
PCR grade H_2O	to 20

2.8.3 Primers

Primers were designed using Primer3 software (Whitehead Institute for Biomedical Research, Cambridge, MA, USA) and ProbeFinder Version 2.04 software (Roche Applied Science, Mannheim, Germany), after retrieving gene

specific sequences and intron-exon information from Pubmed (Entrez Gene) and Ensembl v37 (Rattus norvegicus genome). Primers were analysed by NetPrimer software (PREMIER Biosoft International, Palo Alto, CA, USA) to detect any primer-dimer, haipins or other secondary structures. Each primer was then blasted on Pubmed/Ensembl to ensure its specificity to the gene required. All primers were intron-spanning to avoid amplification of any genomic DNA and their product sizes are less than 150 bp which is optimal size for real-time PCR. The primers used in this study are presented in Table 2.8.

Table 2.8 Primers used in this study

Primer		Sequence	Annealing temp. (°C)	Amplicon size (bp)
ET-1	Forward	CTACTTCTGCCACCTGGACAT	55	66
	Reverse	CCTAGTCCATACGGGACGAC		
ET_A	Forward	ATCTCTGCGCTCTCAGTGTG	55	71
	Reverse	GATCCCGATTCCTTGAACC		
ET_B	Forward	CTGTTGGCTTCCCCTTCAC	57	107
	Reverse	TGTAGTCCAAAACCAGCAAAAA		
eNOS	Forward	TGACCCTCACCGATACAACA	55	60
	Reverse	CGGGTGTCTAGATCCATGC		
iNOS	Forward	TGGTGGTGACAAGCACATTT	55	95
	Reverse	GGTATGCCCGAGTTCTTTCA		
β-actin	Forward	CCCGCGAGTACAACCTTCT	55	72
	Reverse	CGTCATCCATGGCGAACT		

Annealing temperature was determined by software (NetPrimer and Primer3) and tested using PCR

2.8.4 PCR

PCR is an *in vitro* method for the enzymatic synthesis of specific DNA sequences, using two oligonucleotide primers that bind to opposite strands and flank the region of interest in the target DNA. Numerous cycles involving template denaturation to open the double stranded DNA, primer annealing, and the extension

of the annealed primer by a DNA polymerase are performed using a thermal cycler. The products synthesized at the end of each cycle then serve as the template in the next round, hence the number of target DNA copies doubled at every cycle (exponential accumulation).

All PCR reactions were set-up in 25 µl reaction volumes (Table 2.9), in thin walled PCR tubes. The PCR reaction was amplified using a Perkin Elmer GeneAmp PCR System 2400 thermocycler, and the amplification cycles are illustrated in Table 2.10. At the beginning of each run, the samples were incubated at 95°C to enable activation of the thermostable recombinant Taq DNA polymerase (Hot Start DNA polymerase, Promega) by the removal of specific blocking groups. Thus, the enzyme is completely activated at a temperature where primers can not bind non-specifically. PCR products were then analysed by agarose gel electrophoresis.

Table 2.9 PCR reaction mixture

Component	Volume (µl)
PCR Master Mix (Promega)	12.5
Sense primer (0.5 µM final)	0.5
Antisense primer (0.5 µM final)	0.5
cDNA template	1-2.5
PCR grade H_2O	to 25

Table 2.10 PCR amplification cycles

Cycle		Temp. °C	Time (min)	No. of cycles
Initial denaturation (hot start)		94	5	1
Amplification	**Denaturation**	94	0.5	40
	Annealing	55	0.5	
	Elongation	72	0.5	
Final elongation		72	10	1
Hold		4	∞	1

2.8.5 Agarose gel electrophoresis

Electrophoresis-grade agarose was dissolved in 1x Tris-Borate EDTA (TBE) at a concentration of 1.8 %. For small 8-samples gel, 0.9 g of agarose was added to 50 ml TBE buffer in a flask covered with aluminium foil to prevent spillover, heated in microwave for 1.5-2 min at medium power, cooled to around 50°C and the volume was readjusted to 50 ml with warm ultrapure water, and then poured into horizontal gel cast apparatus with a comb inserted to form wells and allowed to set at 4°C. The comb was removed and the buffer solution was poured into the gel box up to 2-3 mm above the gel. The wells were loaded with the samples (6x TrackIt loading buffer 3.3 µl, DNA sample 2.7-6.7 µl, H_2O to 20 µl) alongside low-molecular weight DNA ladder markers. The gel was run in Kodac Biomax QS 710 gel electrophoresis chamber attached to BioRad PowerPac 300 unit at 80 V for ~ 1.5 h until bands were clearly separated, as visualised by the migration of orangeG at 50 bp and bromophenol blue at 300 bp. The gel was then placed into the staining tray with ethidium bromide (50 µl in 100 ml TBE buffer to obtain final concentration of 0.5µg/ml) for 10-20 min and then rinsed once with TBE buffer. DNA was visualised on a UV transilluminator (at 254 nm) and photographed with GeneGenius Gel Documentation System (Syngene Inc., Cambridge, UK).

2.8.6 Real-time PCR

Real-time or quantitative PCR is a system for monitoring the PCR kinetics as PCR products accumulate, based on the property that the intercalator SYBR Green l which binds to the minor groove of the double stranded DNA produced during each amplification reaction and fluoresces once bound. The fluorescence is recorded at the end of the elongation phase at 530mn using a special PCR thermocycler coupled with fluorescence acquisition system. Amplification enhances the amount of double-stranded DNA generated which SYBR Green I binds, thus resulting in an increase in fluorescence. This elevated fluorescence is monitored throughout the 40 cycles, thus by plotting the increase in fluorescence versus cycle number; the system provides a complete picture of the PCR process in comparison to assaying product accumulation. To prove that only the desired PCR product has been amplified, melt curve analysis was performed. Melt curve analysis was carried out by heating the

PCR product slowly at a rate of 0.1°C sec^{-1} from 65°C to 95°C which causes melting of double-stranded DNA and a corresponding decrease in SYBR Green I fluorescence. The real-time PCR machine continuously monitors the fluorescence signal and displays it as melting peaks. Each specific peak represents the characteristic melting temperature of a particular DNA product. The resultant PCR product can also be analysed on an agarose gel and stained with ethidium bromide then visualised under a UV transilluminator to provide further confirmation of product identity.

Real-time PCR amplification and on-line monitoring was performed using LightCycler® FastStart DNA Master SYBRgreen I in LightCycler® 1.5 thermal cycler (Roche Applied Science, Mannheim, Germany) according to manufacturer's instructions. A master mix composed of 0.4 μM primers, 3.5 mM $MgCl_2$, 2 μl SYBR Green Master Mix and PCR-grade water (to 18 μl) was added to pre-chilled capillaries, prior to the addition of 2 μl of 10^{-1} diluted cDNA. The capillaries were centrifuged at 3000 g for 30 seconds at 4°C before loading into the LightCycler. Each template was analyzed in duplicate within the same run. Following 40 amplification cycles, melt-curve analyses were performed to verify specific amplification. PCR efficiency of both the target and reference genes was calculated from the derived slopes of standard curves by LightCycler software (v4.0). These PCR efficiency values were used to calculate the relative quantification values for calibrator-normalized target gene expression as following:

$$\textbf{Efficiency (E)} = [10^{(-1/\text{slope})}-1]$$

$$\textbf{Normalized Ratio} = \frac{\textbf{Cp target unknown / Cp reference unknown}}{\textbf{Cp target calibrator / Cp reference calibrator}}$$

- **Cp or Ct =** Crossing point or threshold cycle at which florescence starts linear part
- **Control=** Calibrator = Exogenous standard
- **Unknown=** Sample
- **Normalizer=** Endogenous standard = Reference = Housekeeping Gene

$$\Delta Ct_{target}(Control-Unknown)$$

$$\Delta Ct_{Norm}(Control-Unknown)$$

$$\text{Normalized } \frac{\text{Unknown}}{\text{Control}} = \frac{(1+E_{target})^{-\Delta Ct_{target}}}{(1+E_{norm})^{-\Delta Ct_{norm}}}$$

In all cases transcript levels were normalized to β-actin. The real-time PCR amplification cycles and melt curve analysis program are shown in Table 2.11.

Table 2.11 Lightcycler PCR program

Analysis Mode	Cycles	Segment	Target Temperature	Hold Time	Acquisition Mode
Pre-Incubation					
None	1		95°C	10 min	none
Amplification					
Quantification	40	Denaturation	95°C	10 s	none
		Annealing	primer dependent	5 s	none
		Extension	72°C	= (amplicon [bp]/25) s	single
Melting Curve					
Melting Curves	1	Denaturation	95°C	0 s	none
		Annealing	65°C	15 s	none
		Melting	95°C slope = 0.1°C/sec)	0 s	continuous
Cooling					
None	1		40°C	30 s	none

According to LightCycler® FastStart DNA Master SYBRgreen I manual instructions.

2.9 Data analysis

Data are expressed as mean ± standard error of mean (SEM), where (n) equals the number of animals, except in qRT-PCR (n= number of independent experiments, each using duplicate PCR reactions from the same sample prepared from pooled tissue lysates of 2 animals) and in $[Ca^{2+}]_i$ experiments (n= number of VSM cells from at least 3 animals). The $[Ca^{2+}]_i$ during the sustained phase is expressed as a % of the transient $[Ca^{2+}]_i$ phase. Vascular relaxation is calculated as % of maximal steady state contraction induced by 30 nM ET-1. The highest response obtained is considered as the maximum response (E_{max}). pEC_{50} (= negative log the concentration producing 50% of maximal response) was determined from non-linear regression analysis (4-parameter curve fit) carried out using Graphpad Prism software (V 4.03, Graphpad Software Inc., San Diego, USA). Significant differences between groups were determined with paired Student's *t*-test or one-way ANOVA with Dunnett's, Tukey-Kramer's or Student-Newman-Keuls Multiple Comparisons *post-hoc* tests as appropriate.

2.10 Materials

Material	Catalogue No.	Company
1400W	1415	Tocris Bioscience
2-Mercaptoethanol	M3148	Sigma-Aldrich
2-Propanol	P/7507/17	Fisher Scientific
30 ml container sterile	128C	Sterilin
30% Acrylamide/Bis-acrylamide solution	161-0158	BioRad
60 ml container sterile	TP35-004	Fisher Scientific
7 ml Bijou	129B	Fisher Scientific
8-pCPT-cGMP	C5438	Sigma-Aldrich
Absolute ethanol	E/0650DF/17	Fisher Scientific
Acetylcholine chloride	15917-0050	Fisher Scientific
Agarose 1000	10975-035	Invitrogen
Albumin from bovine serum	A4919	Sigma-Aldrich
Ammonium persulphate	A9164	Sigma-Aldrich
Anchored oligo dT	AB-1247	ABgene
Anti-CPI-17 antibody	07-344	Upstate
Anti-MLC_{20} antibody	3672	Cell Signaling Technology
Anti-MYPT1 (H-130) antibody	Sc-25618	Santa Cruz Biotechnology
anti-phospho-CPI-17 (Thr38) antibody	36-006	Upstate
Anti-phosphodiesterase 5 antibody	611498	BD Biosciences
Anti-phospho-MLC_{20} (Ser19) antibody	3671	Cell Signaling Technology
Anti-phospho-MYPT1 (Thr850) antibody	36-003	Upstate
Anti-phospho-ROCK α (The396) antibody	Ab24843	Abcam
Anti-PKC (H-300) antibody	Sc-10800	Santa Cruz Biotechnology
Anti-soluble guanylyl cyclase α_1 antibody	Ab50358	Abcam
Anti-soluble guanylyl cyclase β_1 antibody	Ab50333	Abcam
Anti-β-actin antibody	4967	Cell Signaling Technology
BAY 41-2272	196876	Calbiochem
Bromophenol blue	B8026	Sigma-Aldrich
Calcium Chloride 1M solution	190464K	BDH
Cell culture 24-multiwell plates	662160	Greiner bio-one
Cell culture 6-multiwell plates	657160	Greiner bio-one
Cell culture 96-multiwell plates	137101	NUNC
Cell culture dishes, 30 mm	153066	Nunc
Chloroform	C/4960/17	Fisher Scientific

Chromotography paper 3MM 46*57 cm	3030917	Whatman
Collagenase-P	1213857	Roche Applied Science
Coverslips, borosilicate glass,	———	BDH
Cryotube vials 1.8 ml	368632	Nunc
Custom primers (25 nmole)	———	Invitrogen
Cycloheximide	239764	Calbiochem
Deltiazem	D2521	Sigma-Aldrich
Diethylether	D/2450/17	Fisher Scientific
Dimethyl sulphoxide (DMSO)	D8418	Sigma-Aldrich
Disposable serological pipets 10 ml	607180	Greiner bio-one
Disposable serological pipets 25 ml	760180	Greiner bio-one
Dithiothreitol	D0632	Sigma-Aldrich
DMEM	21969-035	Gibco
DMEM without phenol red	31053	Gibco
ECL advance Western Blotting detection kit	RPN2135	GE Healthcare
ECL Western Blotting detection kit	RPN2209	GE Healthcare
EDTA	E5134	Sigma-Aldrich
EGTA	E4378	Sigma-Aldrich
Endothelin-1 (ET-1)	88-1-10A	American peptide company
Ethidium Bromide solution	H5041	Promega
FAD	F6625	Sigma-Aldrich
Filter tips P2/P10 racked	771288	Greiner bio-one
Filter tips P20 racked	774288	Greiner bio-one
Filter tips P200 racked	772288	Greiner bio-one
Foetal bovine serum (FBS) certified (heat-inactivated)	10082-139	Gibco
Fuji Medical X-Ray Film	2731261	Fisher Scientific
Fura-2 AM	F1221	Molecular Probes
Glucose anhydrous	284508W	BDH
Glybenclamide	G0639	Sigma-Aldrich
Glycerol	G5516	Sigma-Aldrich
Glycine	50046	Sigma-Aldrich
Griess reagent (modified)	G4410	Sigma-Aldrich
HEPES	H3375	Sigma-Aldrich
High Pure RNA tissue kit	2033674	Roche Applied Science
Horseradish peroxidase-conjugated goat anti-mouse secondary antibody	P0447	Dako
Horseradish peroxidase-conjugated goat anti-rabbit secondary antibody	P0448	Dako

Horseradish peroxidase-conjugated rabbit anti-goat secondary antibody	P0449	Dako
Hydrochloric acid 37%	H/1150/PB17	Fisher Scientific
Iberiotoxin	L8211	Latoxan
IBMX	410957	Calbiochem
Indomethacin	I-7378	Sigma-Aldrich
Ionomycin calcium	I0634	Sigma-Aldrich
K_2HPO_4, anhydrous	P/5240/53	Fisher Scientific
KH_2PO_4	P/4760/53	Fisher Scientific
Lactate dehydrogenase from rabbit muscle	L1254	Sigma-Aldrich
Lightcycler capillaries 20 ul	1909339	Roche Applied Science
LightCycler FastStart DNA Master SYBR Green I kit	2239264	Roche Applied Science
Lipopolysaccharide (LPS) from *E.coli 055:B5*	L2880	Sigma-Aldrich
Lipopolysaccharide (LPS) from *Salmonella typhimurium*	L6511	Sigma-Aldrich
L-NAME hydrochloride	N-5751	Sigma-Aldrich
Low Molecular Weight DNA Ladder	N3233S	New England Biolabs
Magnesium chloride 1M solution	220933M	BDH
Magnesium sulphate	M/1000/60	Fisher Scientific
Methanol	M/4056/17	Fisher Scientific
Microcentrifuge tubes 0.5 ml amber	TUL-150-130T	Fisher Scientific
Microcentrifuge tubes 0.5 ml Clear	TUL-150-010G	Fisher Scientific
Microcentrifuge tubes 1.5 ml amber	TUL-150-270D	Fisher Scientific
Microcentrifuge tubes 1.5 ml Clear	TUL-150-150N	Fisher Scientific
Microcentrifuge tubes 2 ml Clear	FB74111	Fisher Scientific
NADPH	481973	Calbiochem
Natural gel saver II tips (1-200 ul)	FB56205	Fisher Scientific
Nifedipine	N7634	Sigma-Aldrich
Nitrate reductase (Aspergillus)	N7265	Sigma-Aldrich
Nitrile Gloves	52003M	Kimberly Clark
Nonidet P-40	56009	Sigma-Aldrich
Non-sterile 96-well plate	260836	NUNC
ODQ	0880	Tocris Bioscience
Omniscript RT Kit	205111	Quiagen
Papain	P4762	Sigma-Aldrich
Parameter cGMP assay Kit	KGE003	R&D Systems
Pasteur pipettes, disposable 3 ml	FB55354	Fisher Scientific
PCR Master Mix	M7502	Promega

Penicillin/streptomycin	15140-122	Invitrogen
Petri Dish, 90 mm, sterile	101VR20	Sterilin
Phenylephrine	P6126	Sigma-Aldrich
Phenylmethanesulfonylfluoride (PMSF)	P7626	Sigma-Aldrich
Phosphate buffered saline (PBS, 10X)	3082920A	Invitrogen
Pipet tips 0.1-10 µl	FB34521	Fisher Scientific
Pipette tips blue 200-1000 µl	740295	Greiner bio-one
Pipette tips Clear 1-5 ml	745290	Greiner bio-one
Pipette tips yellow 10-200 µl	739295	Greiner bio-one
Pluronic acid F-127 20% in DMSO	P3000MP	Invitrogen
Poly-L-Lysine solution 70000-150000 KDa	3438-100-01	R&D Systems
Ponceau S solution	P7170	Sigma-Aldrich
Potassium chloride	P/4240/53	Fisher Scientific
Protease inhibitor cocktail for mammalian/tissue extracts	P8340	Sigma-Aldrich
Protein Standards (Precision Plus, ALL Blue)	161-0373	BioRad
Quickstart Bradford dye reagent 1X	500-0205	BioRad
Reblot Plus Strong antibody stripping solution 10X	2504	Millipore
RIPA buffer 10X	9806	Cell Signaling Technology
RNasin Plus RNase inhibitor	N2611	Promega
Ro-31-8425	557514	Calbiochem
SKF-96365	1147	Tocris Bioscience
Skimmed Milk	LP0031	Oxoid
Sodium azide	S2360	Sigma-Aldrich
Sodium bicarbonate	S/4200/63	Fisher Scientific
Sodium carbonate	S/2920/53	Fisher Scientific
Sodium Chloride	S/3105/63	Fisher Scientific
Sodium dodecyl sulphate	L4390	Sigma-Aldrich
Sodium fluoride	S7920	Sigma-Aldrich
Sodium hydroxide	22146-5	Sigma-Aldrich
Sodium molybdate	S6646	Sigma-Aldrich
Sodium nitrate	71752	Sigma-Aldrich
Sodium nitroprusside	71778	Sigma-Aldrich
Sodium orthovanadate	567540	Calbiochem
Sodium pyruvate 100 mM sterile liquid	S8636	Sigma-Aldrich
Syringe driven filter unit (0.22 µm)	SLGP033RS	Millipore
Syringes, plastipack, different volumes	——	BD Biosciences
T-0156	1676	Tocris Bioscience

TEMED	T9281	Sigma-Aldrich
Thapsigargin	586005	Calbiochem
TrackIT Cyan/Orange loading buffer	10482-028	Invitrogen
Trans-Blot nitrocellulose membrane 0.45 µm	162-0115	BioRad
Trichloroacetic acid	T9159	Sigma-Aldrich
Trizma base	T87602	Sigma-Aldrich
Trolox	648471	Calbiochem
Tryban blue	T6146	Sigma-Aldrich
Trypsin inhibitor from soybean	T9003	Sigma-Aldrich
Tubes 15 ml polypropylene, sterile	188261	Greiner bio-one
Tubes 50 ml polypropylene, sterile	227270	Greiner bio-one
U46619	16450.1	Cayman
Ultrapure H_2O (MilliQ)	——	Millipore
Ultrapure TBE buffer 10X	15558-042	Invitrogen
Y-27632	1254	Tocris Bioscience

Company addresses:

Abcam (Cambridge, UK), ABgene (Surrey, UK), American peptide company (Sunnyvale, CA, USA), BD Biosciences (Oxford, UK), BDH (VWR International, Lutterworth, UK), BioRad (Hercules, CA, USA), Calbiochem (Nottingham, UK), Cayman/Axxora (Nottingham, UK), Cell Signaling Technology (Danvers, MA, USA), Dako (Glostrup, Denmark), Fisher Scientific (Loughborough, UK), GE Healthcare (Little Chalfont, UK), Gibco/Molecular Probes/Invitrogen (Carlsbad, USA), Greiner bio-one (Frickenhausen, Germany), Kimberly Clark (Zaventem, Belgium), Latoxan (Valence, France), Upstate/Millipore (Billerica, MA, USA), New England Biolabs (Ipswich, MA, USA), NUNC (Roskilde, Denmark), Oxoid (Basingstoke, UK), Promega (Madison, WI, USA), R&D Systems (Abingdon, UK), Roche Applied Science (Mannheim, Germany), Santa Cruz Biotechnology (Santa Cruz, CA, USA), Sigma-Aldrich (Poole, UK), Sterilin/Barloworld (Stone, UK), Tocris Bioscience (Avonmouth, UK), Whatman (Maidstone, UK).

Chapter 3

Result I: LPS-induced Changes in Vascular Reactivity

Chapter 3

3.1 Introduction

LPS is a powerful stimulator of inflammatory pathways and a key molecule involved in the initiation of sepsis and associated syndromes (Heine *et al.*, 2001; Buras *et al.*, 2005). The administration of LPS, both in humans (Suffredini *et al.*, 1989) and in animals (Ruetten *et al.*, 1996; Peters & Lewis, 1996; Gardiner *et al.*, 1996b), has been used as a model to study sepsis and septic shock, which is a complex pathophysiological state characterized by systemic vasodilation and hyporesponsiveness to different vasoconstrictor agents (Wakabayashi *et al.*, 1987; Guc *et al.*, 1990; Umans *et al.*, 1993; Sirmagul *et al.*, 2006; Matsuda & Hattori, 2007).

Different models have been developed to study LPS-induced changes in vascular reactivity. These include *in vitro* models (McKenna, 1990; Hall *et al.*, 1996; O'Brien *et al.*, 2001; Piepot *et al.*, 2002; Miyamoto *et al.*, 2004; Boer *et al.*, 2005) and *in vivo* models (Gardiner *et al.*, 1995; Griffiths *et al.*, 1995; Ruetten *et al.*, 1996; Weitzberg *et al.*, 1996; Ruetten & Thiemermann, 1996; Curzen *et al.*, 1997; Griffiths *et al.*, 1997; Rees *et al.*, 1998; Mitaka *et al.*, 1999; Hirata & Ishimaru, 2002) as well as *ex vivo* models using vessels harvested from endotoxic animals (Schneider *et al.*, 1992; Gunnett *et al.*, 1998; Wu *et al.*, 2004).

The results of the previous studies are highly variable. For example, LPS induces hyporeactivity to phenylephrine in rat *in vivo* (Guc *et al.*, 1990), in rat superior mesenteric artery *in vitro* (O'Brien *et al.*, 2001) and in rat and rabbit aortas *ex vivo* (Umans *et al.*, 1993), but not in rat pulmonary arteries *ex vivo* (McIntyre, Jr. *et al.*, 1997; Pulido *et al.*, 2000) and not in rat perfused mesenteric vascular bed *ex vivo* (Mitchell *et al.*, 1993). ET-1 induced vasoconstriction is increased by LPS treatment in rat mesenteric artery *ex vivo* (Buyukafsar *et al.*, 2004) and guinea pig coronary and mesenteric arteries *ex vivo* (Jones *et al.*, 1999), but is decreased in rat pulmonary arteries *ex vivo* (Curzen *et al.*, 1995) and not affected in rat *in vivo* (Guc *et al.*, 1990).

Even in the same model, there is variability in LPS-induced changes in vascular reactivity between different blood vessels towards different vasoconstrictors (Piepot *et al.*, 2002; Farmer *et al.*, 2003). This suggests that the type of blood vessel, mechanism of action of the vasoactive agent and the experimental conditions all affect the vascular reactivity observed in endotoxemic models.

The *in vivo* studies represent real pathological features, but it is difficult to controlling experimental conditions due to multiple factor interactions including neurological, blood components and metabolic factors. On the other hand, in the *in vitro* studies using cultures of dispersed VSMCs, it is easy to control the experimental conditions, although these do not represent cell to cell interaction in real tissue architecture and real pathological conditions. An organ culture system has the distinct advantages of better preservation of tissue architecture, cell-to-cell interactions, extracellular matrix and cell morphology and function (Ozaki & Karaki, 2002). In addition, organ culture has been shown to preserve tissue structure and contractility (Adner *et al.*, 1998; Guibert *et al.*, 2005). Thus, the organ culture study has several advantages over the classical, *in vivo* and *in vitro* methodologies.

This study focused mainly on LPS-induced changes in contractile responses to ET-1 since plasma levels of this powerful vasoconstrictor are elevated in animal models of sepsis (Curzen *et al.*, 1997; Fujii *et al.*, 2000) and in septic patients (Pittet *et al.*, 1991) and its level correlates with the severity of illness (Pittet *et al.*, 1991; Piechota *et al.*, 2007). An organ culture method was used to study the effect of LPS on vascular reactivity of the pulmonary artery and the aorta, studied under similar experimental conditions. The main objectives were:

- establish an organ culture model to examine if LPS is capable of changing vascular reactivity and study the different factors that could affect vascular reactivity in this model, such as LPS type, concentration and incubation time.
- examine a pulmonary and a systemic blood vessel under the same experimental conditions, since they respond differently in sepsis which could help in finding contributing mechanisms involved in sepsis-induced vascular complications.

3.2 Methods

Pulmonary and aortic arterial rings were incubated with LPS (10 µg ml^{-1}, 20 h) before measuring the contractile responses to ET-1 (0.3 nM-100 nM), 80 mM KCl, phenylephrine (1 nM-10 µM) or U46619 (3 nM-1 µM). In addition, the effect of organ culture on vascular contractile responses to ET-1 was measured by comparing fresh control to cultured control vascular rings. The effect of LPS type was investigated by measuring changes in responses to ET-1 and 80 mM KCl induced by either *E.coli 055:B5* or *Salmonella typhimurium* LPS. Responses to different LPS concentrations were also investigated. The effect of incubation time was investigated by measuring iNOS expression at different time points (4, 8 and 20 h) using qRT-PCR.

3.3 Effect of organ culture on vascular reactivity

In control experiments, there were no significant differences between freshly isolated and 20h-incubated pulmonary or aortic vascular rings in the contractile responses to ET-1 (Figure 3.1), indicating that tissue responsiveness was not adversely influenced by prolonged incubation.

3.4 Effect of LPS type on vascular reactivity changes

The vascular changes induced by LPS in both the pulmonary artery and the aorta were similar when incubating with either *E.coli 055:B5* or *Salmonella typhimurium* LPS. Neither type of LPS affected the contractile response of the pulmonary artery to either ET-1 (Figure 3.2a and 3.2b) or 80 mM KCl (Figure 3.2e and 3.2f). On the other hand, the contractile responses of the aortic rings to either ET-1 (Figure 3.2c and 3.2d) or 80 mM KCl (Figure 3.2e and 3.2f) were decreased by incubation with either type of LPS. These results suggest that LPS-induced changes in vascular reactivity are not dependent on the type of LPS, but on a common pathway induced by different LPS types.

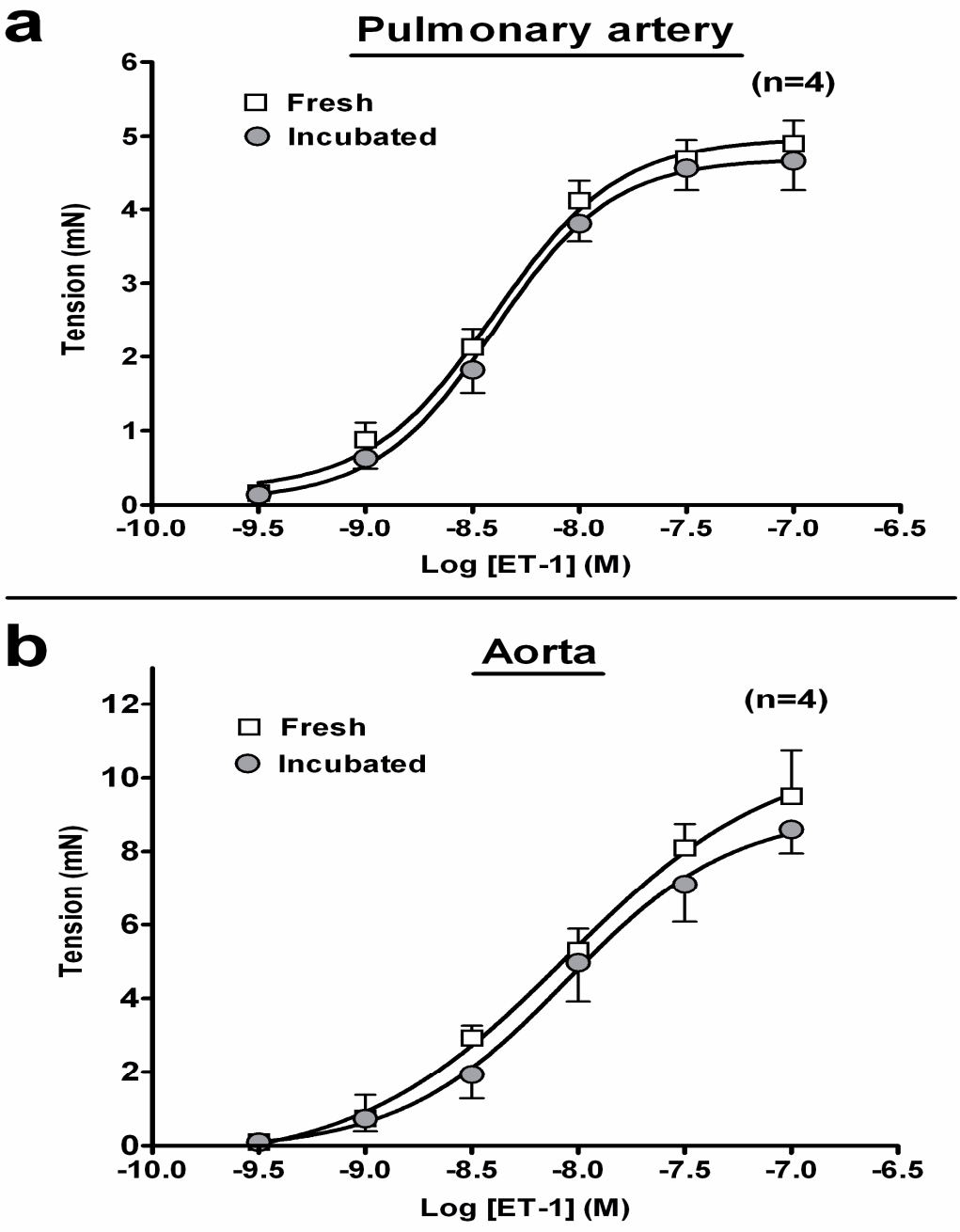

Figure 3.1 Effect of organ culture on contractile responses to ET-1 in pulmonary and aortic rings. Contraction to ET-1 (0.3 nM-100 nM) was measured in pulmonary (a) and aortic (b) rings before and after incubation with control culture medium for 20 h. Data are expressed as mean ± s.e.m., where (n) equals the number of animals.

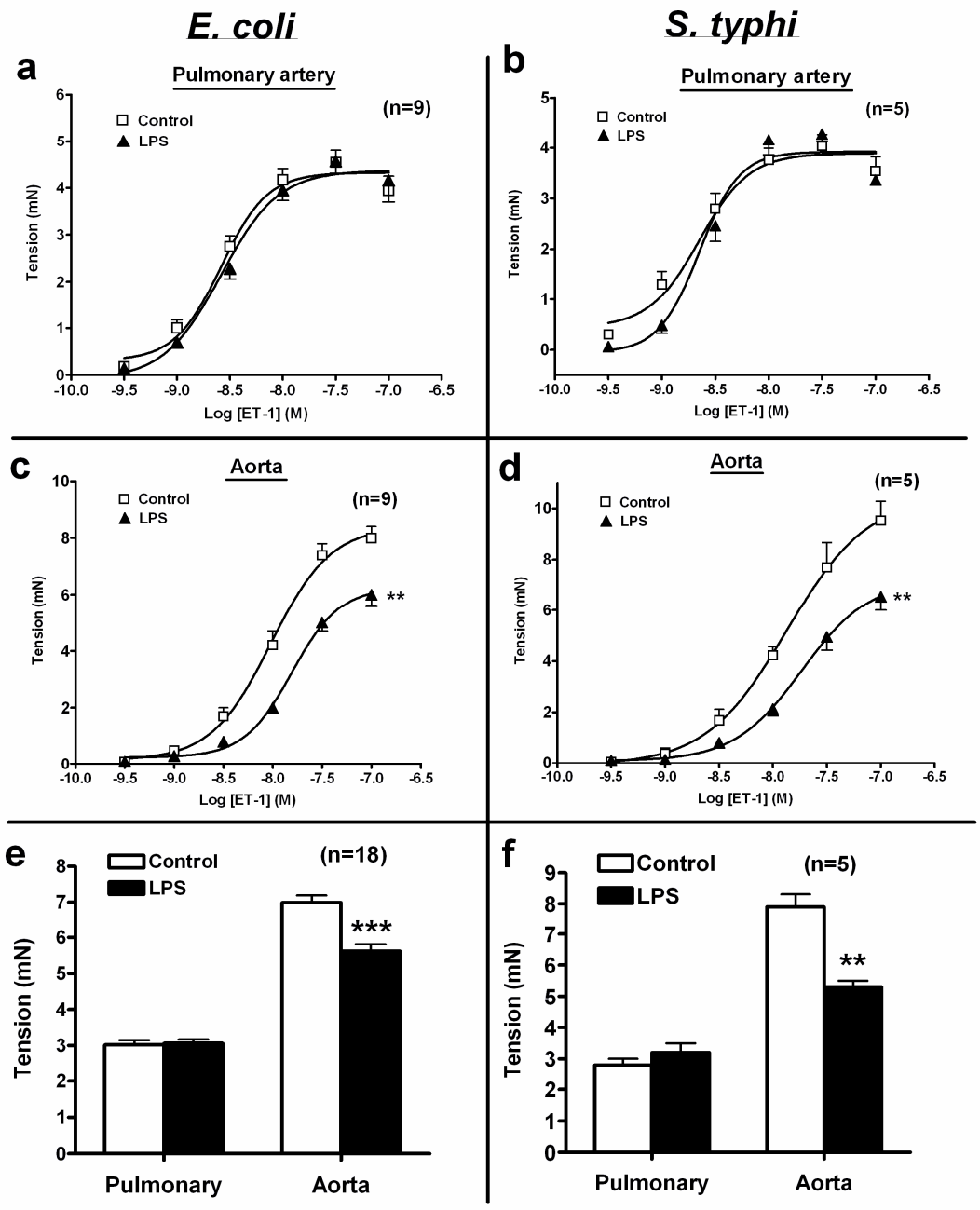

Figure 3.2 Effect of LPS type on vascular reactivity of the pulmonary artery and the aorta. Contraction to ET-1 (0.3 nM-100 nM) and 80 mM KCl in the pulmonary artery and the aorta was measured after incubation with LPS (10 µg ml^{-1}, 20 h) either from *E.coli 055:B5* (a, c, e) or *Salmonella typhimurium* (b, d, f). Data are expressed as mean ± s.e.m., where (n) equals the number of animals.

** $p<0.01$, ***$p<0.001$ for E_{max} and pEC_{50} values compared with control group using paired Student's *t*-test.

3.5 Effect of LPS concentration on vascular reactivity changes

Increasing the concentration of LPS significantly enhanced aortic hyporeactivity to ET-1 (Figure 3.3). The decrease in E_{max} was 16±3 %, 25±4% and 31±5% for LPS concentrations of 1, 10 and 100 µg ml^{-1}, respectively (n=4). All three LPS concentrations caused hyporeactivity to ET-1, but the hyporeactivity induced by LPS 10 µg ml^{-1} was not significantly different from that induced by LPS 100 µg ml^{-1}. This result suggests that an LPS concentration of 10 µg ml^{-1} caused near maximal response, therefore, this concentration was chosen for subsequent experiments in this study.

3.6 Effect of incubation time on the mRNA expression iNOS

Continuous incubation with LPS resulted in enhanced gene expression of iNOS both in the pulmonary artery (Figure 3.4a) and the aorta (Figure 3.4b). This increase in iNOS gene expression was 666±103 % in the pulmonary artery and 1287±447% in the aorta when compared to their respective controls at 20 h. The presence of matching time controls ensures that the increase in iNOS was only due to LPS and not due to incubation itself. Moreover, all the time point controls and LPS-treated groups for each sample were pooled exactly from the same animals to prevent any changes due to different genetic backgrounds of different animals. These results suggest that increasing incubation time had a cumulative effect on vascular expression of iNOS, with the 20 h timepoint showing the highest increase in iNOS gene expression by LPS in the present model.

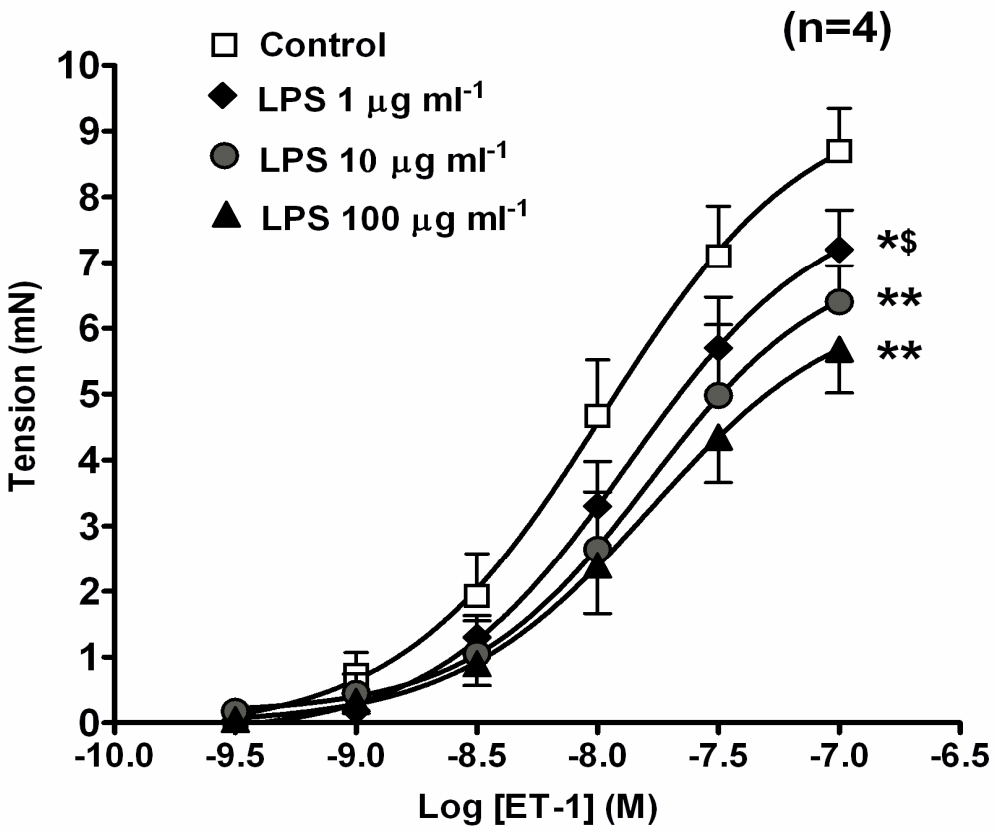

Figure 3.3 Effect of LPS concentration on aortic hyporeactivity to ET-1. Contraction to ET-1 (0.3 nM-100 nM) was measured after incubation with LPS (1, 10 or 100 μg ml^{-1}, 20 h) in the aortic rings. Data are expressed as mean ± s.e.m., where (n) equals the number of animals. For E_{max} and pEC_{50} values: * $p<0.05$, ** $p<0.01$ compared with control group; \$$p<0.05$ compared with LPS 100 μg group using one-way ANOVA followed by Tukey Kramer's *post-hoc* test.

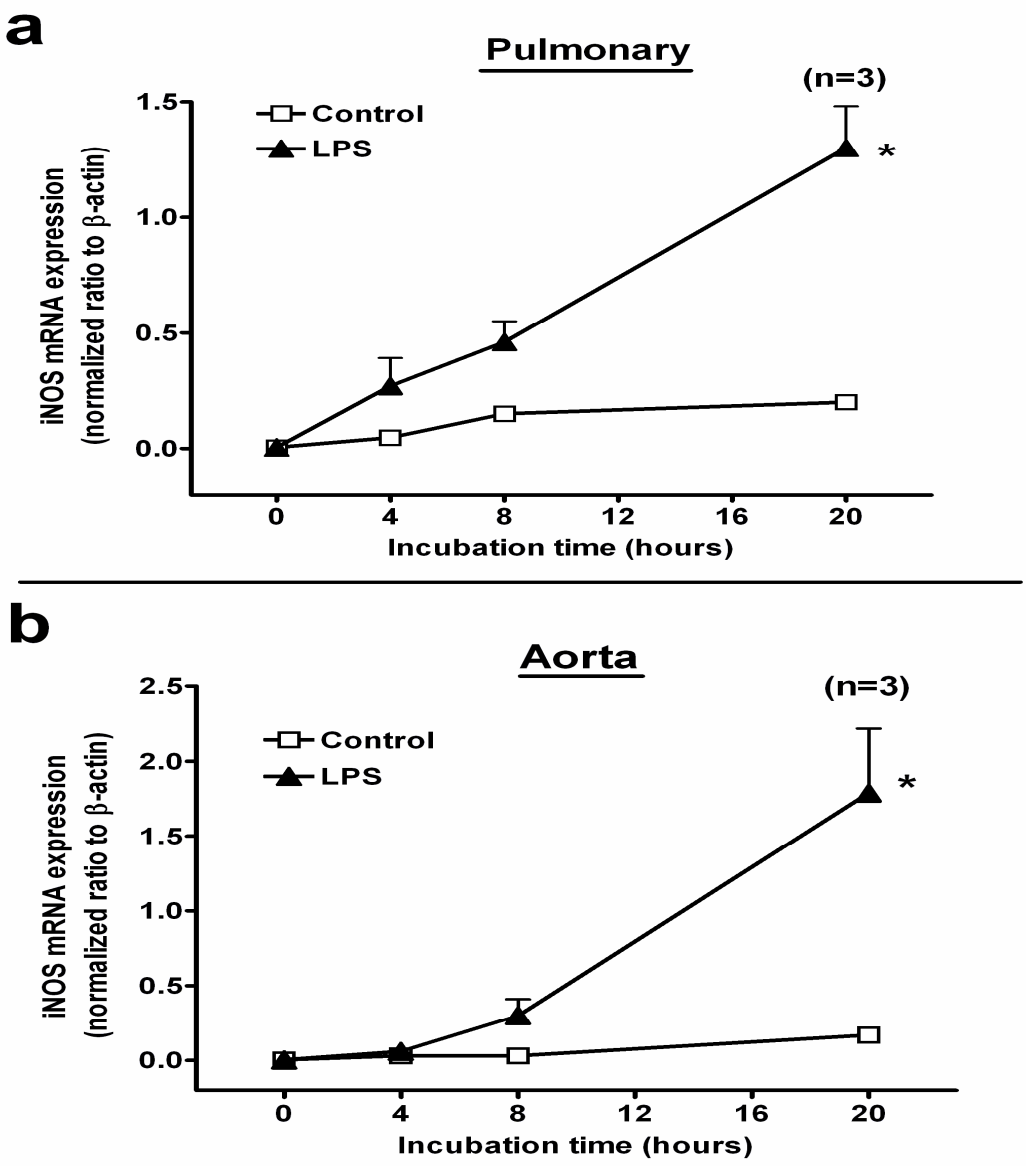

Figure 3.4 Effect of LPS incubation on mRNA expression of iNOS in the pulmonary artery and aorta. RNA was extracted from control and LPS (10 µg ml^{-1}, 20 h)-treated vascular rings at 4, 8 and 20 h and reverse-transcribed into cDNA before carrying out quantitative RT-PCR to detect changes in the gene expression of iNOS in the pulmonary artery (a) and aorta (b). Data are expressed as mean ± s.e.m., where (n) equals the number of independent experiments, each using duplicate PCR reactions from the same sample prepared from pooled tissue lysates of 2 animals. * $p<0.05$ compared with matching time-control using paired Student's *t*-test.

3.7 Effect of LPS on vascular reactivity to different vasoconstrictors

Incubation of arterial rings with LPS had a differential effect on the responses to different vasoconstrictors. In the pulmonary artery, no significant changes in contraction induced by ET-1 were found between control and LPS-treated groups (Figure 3.5a). In the aorta, however, a significant decrease in tissue contractility to ET-1 was observed in the LPS-treated group compared with the control group ($p<0.01$, $n=9$) (Figure 3.5b). This hyporeactivity to ET-1 was manifested by a 26±4 % decrease in E_{max} from 8.41±0.40 mN to 6.26±0.32 mN and an increase in EC_{50} from 9.6±0.5 nM to 15.7±0.8 nM in the control and LPS-treated groups, respectively.

Similar aortic hyporeactivity to other vasoconstrictors was also observed. For KCl, a receptor-independent vasoconstrictor, maximal contraction induced by 80 mM KCl was significantly decreased by 20±2 % in LPS-treated aortic rings compared to control ($P<0.001$, $n=18$), whereas pulmonary artery responses were unchanged (Figure 3.6).

The maximal contractile response to the α-adrenergic agonist phenylephrine was unchanged in the pulmonary artery (Figure 3.7a), but it was reduced by 78±2 % in LPS-treated aortic rings compared to control ($P<0.001$, $n= 5$) (Figure 3.7b). In contrast, the contraction induced by the TxA_2 mimetic U46619 was not affected by incubation with LPS either in the pulmonary artery (Figure 3.8a) or in the aorta (Figure 3.8b), suggesting that the mechanisms of contraction induced by U46619 were not affected by LPS.

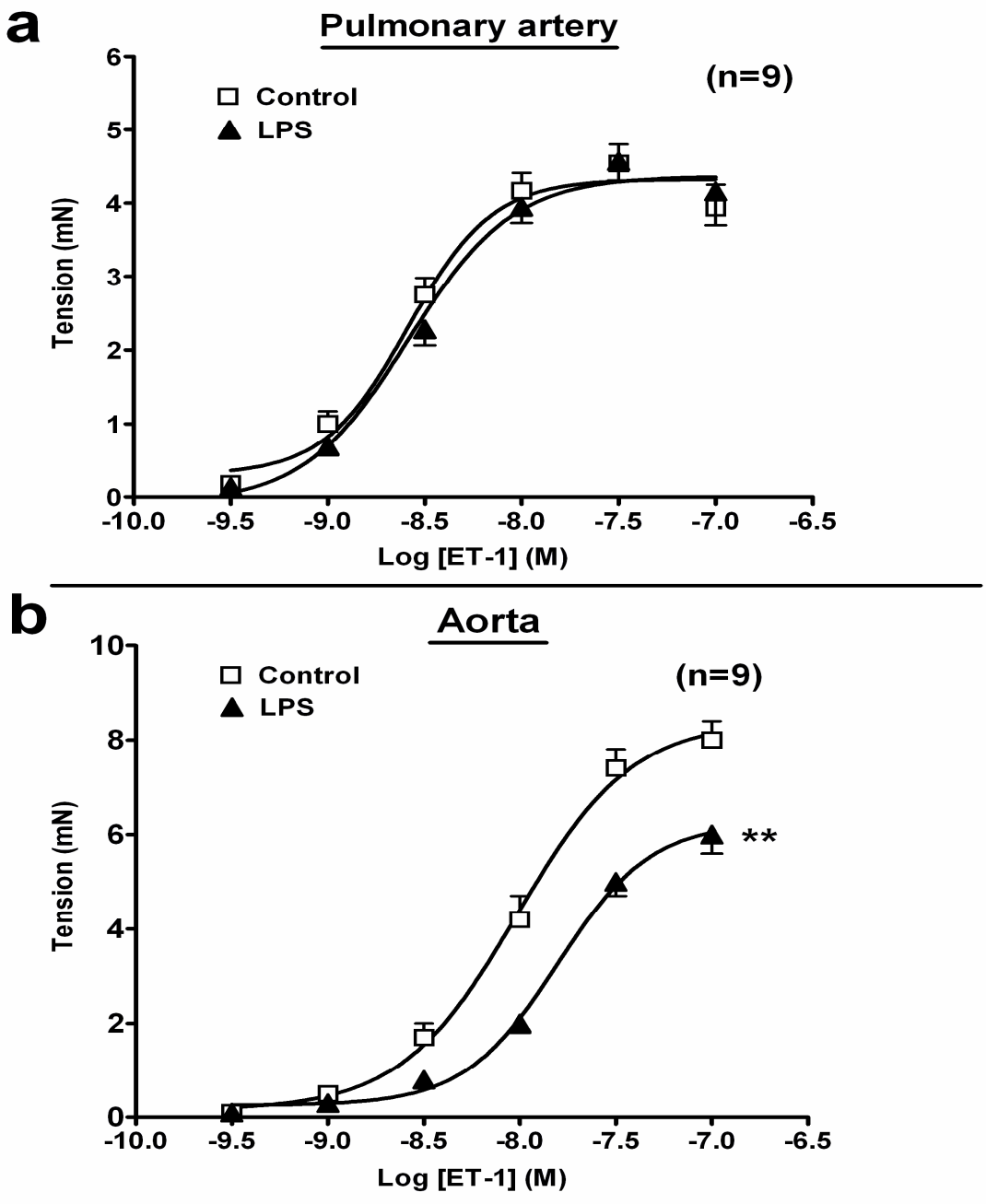

Figure 3.5 Effect of LPS on contractile responses to ET-1 in the pulmonary artery and the aorta. Contraction to ET-1 (0.3 nM-100 nM) was measured after incubation with LPS (10 µg ml^{-1}, 20 h) in the pulmonary (a) and aortic (b) arterial rings. Data are expressed as mean ± s.e.m., where (n) equals the number of animals. ** $p<0.01$ for E_{max} and pEC_{50} values compared with control group using paired Student's *t*-test.

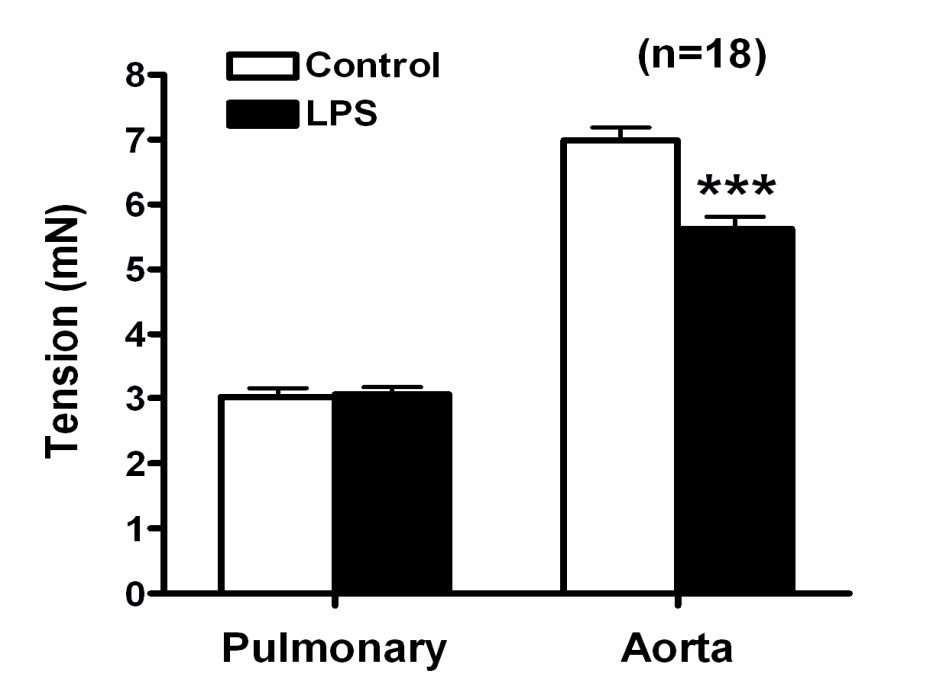

Figure 3.6 Effect of LPS on contractile responses to 80 mM KCl in the pulmonary artery and the aorta. Contraction to 80 mM KCl was measured after incubation with LPS (10 µg ml^{-1}, 20 h) in the pulmonary (a) and aortic (b) arterial rings. Data are expressed as mean ± s.e.m., where (n) equals the number of animals. *** $p<0.001$ for E_{max} values compared with control group using paired Student's *t*-test.

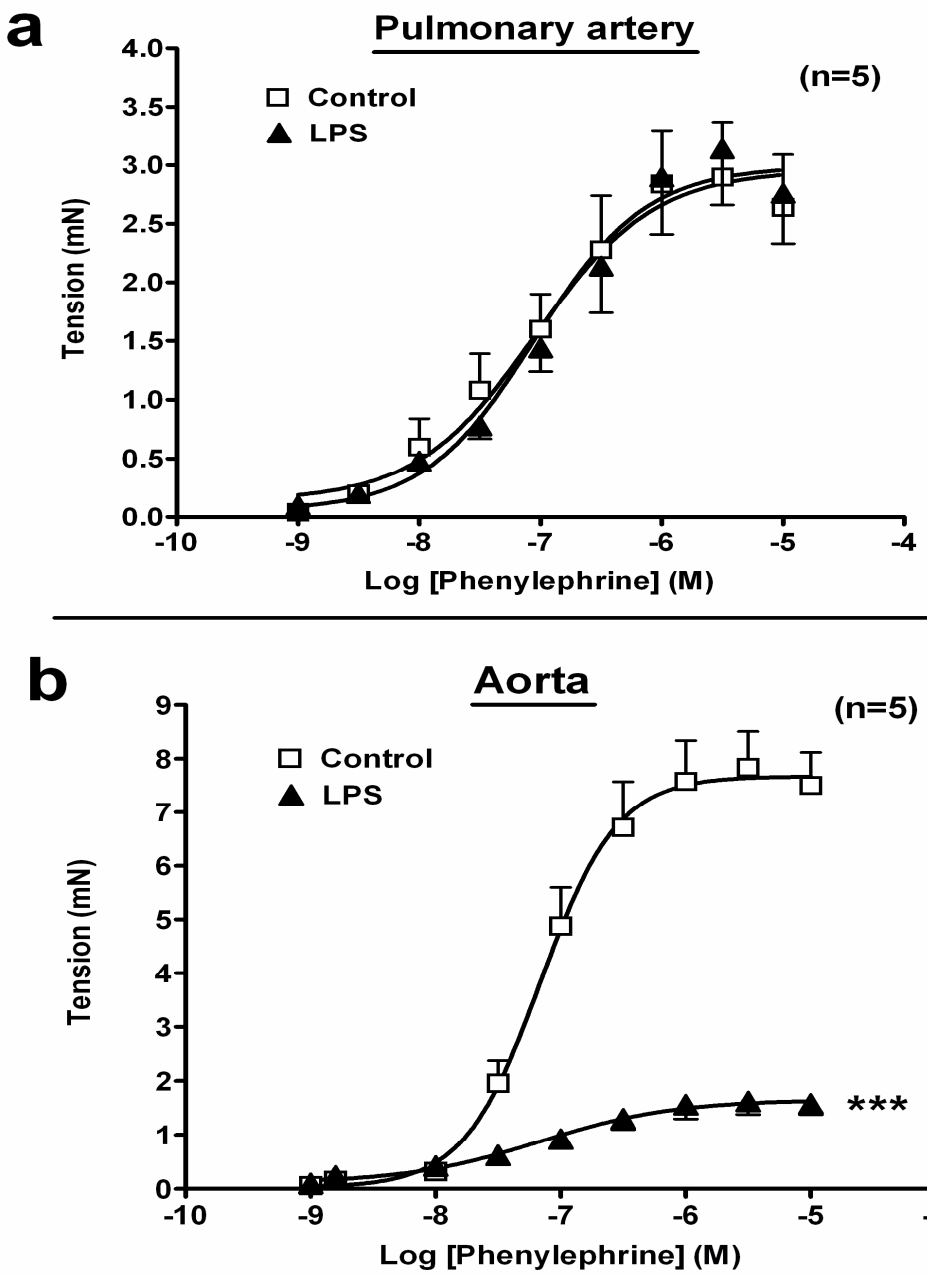

Figure 3.7 Effect of LPS on contractile responses to phenylephrine in the pulmonary artery and the aorta. Contraction to phenylephrine (1 nM-10 µM) was measured after incubation with LPS (10 µg ml^{-1}, 20 h) in the pulmonary (a) and aortic (b) arterial rings. Data are expressed as mean ± s.e.m., where (n) equals the number of animals. *** $p<0.001$ for E_{max} and pEC_{50} values compared with control group using paired Student's *t*-test.

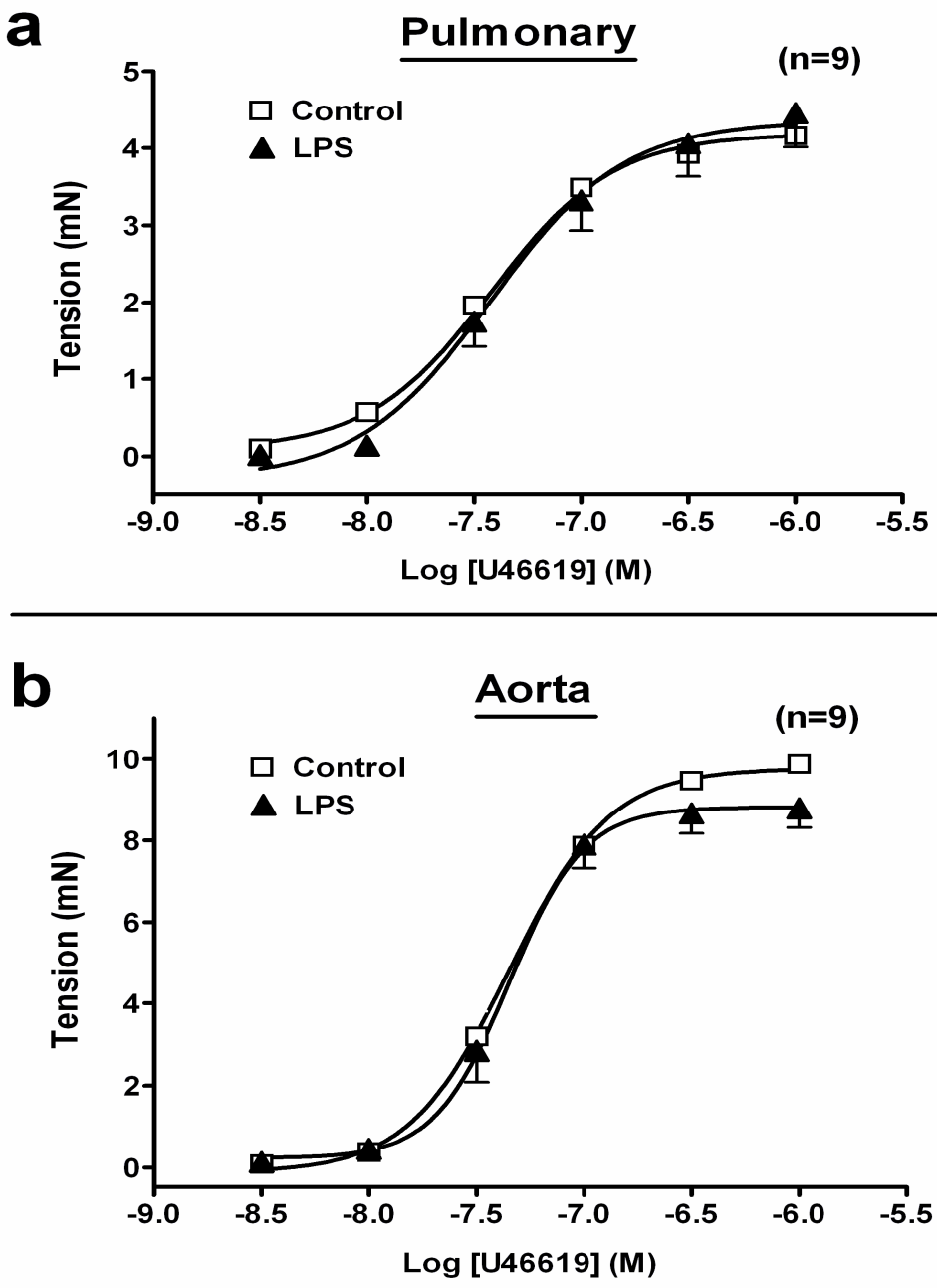

Figure 3.8 Effect of LPS on contractile responses to U46619 in the pulmonary artery and the aorta. Contraction to U46619 (3 nM-1 µM) was measured after incubation with LPS (10 µg ml^{-1}, 20 h) in the pulmonary (a) and aortic (b) arterial rings. Data are expressed as mean ± s.e.m., where (n) equals the number of animals.

3.8 Discussion

The results presented in this chapter show that pulmonary and aortic contractile responses to ET-1 were not affected by organ culture. LPS-induced changes in vascular contractility to ET-1 and KCl were not affected by changing the LPS type, but aortic hypocontractility to ET-1 was increased by increasing LPS concentration. Continuous incubation with LPS *in vitro* resulted in an enhanced gene expression of iNOS in both vessels, indicating a cumulative effect of LPS. Moreover, LPS selectively induces vascular hypocontractility to ET-1, KCl and phenylephrine in isolated rat aorta but not in the pulmonary artery, while the contractile responses to the TxA_2 mimetic U46619 were not affected in either vessel.

The organ culture method used in this study had no effect on vascular reactivity to ET-1 when compared to fresh control, indicating that tissue responsiveness was not adversely influenced by prolonged incubation. Previous studies showed that the contractile responses to ET-1 of human omental arteries (Adner *et al.*, 1995), rat vessels including the aorta and mesenteric artery (Adner *et al.*, 1998) and rat extra- and intrapulmonary vessels (Guibert *et al.*, 2005) were not altered by organ culture. In addition, ACh-induced relaxation was not changed by 20 h organ culture of rat mesenteric artery, although there was a loss in NO and PG-mediated dilatation which is compensated for by EDHF (Alm *et al.*, 2002). In contrast, organ culture has been shown to upregulate ET_B receptors on VSM of different rat blood vessels except the aorta although the contractile responses to ET-1 were not affected (Adner *et al.*, 1998). These studies support the usefulness of organ culture model to study contractile responses, especially at short time points such as 20 h as used in this study.

In addition to the effect of organ culture, LPS type, concentration and incubation time were also studied. The profile of LPS-induced changes in vascular reactivity was similar between different types of LPS, indicating that these vascular changes are independent of LPS type. With regard to LPS concentration, LPS concentration of 10 µg ml^{-1} was optimum in the present model. This LPS concentration was previously reported to give a maximal iNOS induction (Kleschyov *et al.*, 1998; O'Brien *et al.*, 2001). Also, O'Brien *et al.* (2001) found that

hyporeactivity was unaffected by the concentration of LPS over 1 to 100 µg ml^{-1}, although responses were dependent upon incubation time and were prolonged in presence of serum.

The effect of incubation time was examined by measuring vascular expression of iNOS gene, which is known to be upregulated by LPS (Lorente *et al.*, 1993; Szabo *et al.*, 1995; Bishop-Bailey *et al.*, 1997; Liu *et al.*, 1997). Increasing incubation time was found to enhance the expression of iNOS, which was extensively expressed at 20 h.

The findings of this *in vitro* organ culture model are similar to observations in clinical sepsis where systemic vasodilation and pulmonary hypertension occur (Manthous *et al.*, 1993; Lorente *et al.*, 1993) and to an *ex vivo* rat endotoxemic model using phenylephrine (McIntyre, Jr. *et al.*, 1997). In addition, *in vivo* differences in vascular responses to LPS are characterized by systemic vasodilation and hyporesponsiveness to vasoconstrictor agents, but the pulmonary, renal and mesenteric circulations often exhibit various degrees of vasoconstriction (Curzen *et al.*, 1997; Farmer *et al.*, 2003). These results confirm the usefulness of organ culture models to study LPS-induced changes in vascular reactivity.

LPS in this study induced hypocontractility to ET-1, in addition to KCl and phenylephrine, in rat aorta but not in the pulmonary artery. In contrast to ET-1, KCl and phenylephrine, the contractile responses to U46619 were not altered by LPS in either the pulmonary artery or the aorta, indicating that LPS does not affect the contractile pathways induced by U46619. Similar results were obtained previously in rat aorta *ex vivo* (Farmer *et al.*, 2003) and rat mesenteric artery *ex vivo* (Farmer *et al.*, 2003) and *in vitro* (O'Brien *et al.*, 2001). In contrast, contractile responses to U46619 were attenuated *in vitro* in rat coronary arteries (Piepot *et al.*, 2002) and pulmonary artery (Boer *et al.*, 2005). The last two studies utilized higher concentrations of LPS (50 µg ml^{-1}), that is 5 times as the concentration used in this study, which may explain the difference in results.

3.9 Summary and conclusions

By using an organ culture method, the effect of *in vitro* incubation with LPS as a powerful inflammatory stimulus, was examined on the pulmonary artery and the aorta under similar experimental conditions. The main findings are:

1- The pulmonary and aortic contractile responses to ET-1 were not affected by 20 h organ culture.

2- The LPS-induced changes in vascular reactivity to ET-1 and KCL were independent of LPS type.

3- Increasing LPS concentration enhanced aortic hyporeactivity to ET-1, with the concentration of 10 $\mu g\ ml^{-1}$ being optimum in this model.

4- Continuous incubation with LPS induced cumulative iNOS expression in both vessels.

5- LPS caused a selective decrease in contractile responses to ET-1, 80 mM KCl and phenylephrine, but not to the TxA_2 mimetic U46619, in the aorta while the pulmonary artery responses were not affected.

In conclusion, the present organ culture model showed that LPS selectively induced vascular hyporeactivity to different vasoconstrictors in rat aorta but not the pulmonary artery, similar to clinical symptoms *in vivo* in endotoxemia and sepsis. This aortic hyporeactivity was not due to organ culturing per se and was not affected by changing the LPS type. Increasing LPS concentration or the incubation time enhances this aortic hyporeactivity. Therefore, this organ culture model is suitable to study LPS-induced changes in vascular reactivity and can be easily controlled to study the molecular mechanisms involved.

Chapter 4

Result II: Mediators Involved in LPS-induced Changes in Vascular Reactivity

Chapter 4

4.1 Introduction

Several mediators have been suggested to play a major role in sepsis-induced vascular complications, including NO, derivatives of COX and reactive oxygen species (ROS). Excessive NO production, derived mainly from iNOS, has been shown to contribute to the development of acute lung injury, delayed hypotension and vasoplegia in patients with septic shock (Feihl *et al.*, 2001; Lopez *et al.*, 2004) as well as in animals injected with LPS (Szabo *et al.*, 1995; Bishop-Bailey *et al.*, 1997).

In septic shock, inhibition of the activity of eNOS precedes the induction of iNOS (Lu *et al.*, 1996). Moreover, down-regulation of eNOS occurs at time points similar to those where iNOS induction is seen. iNOS has been shown to impair eNOS by limiting availability of a major NOS cofactor, tetrahydrobiopterin (Gunnett *et al.*, 2005) and by producing peroxynitrite which causes nitration of protein tyrosine residues leading to inhibition of different enzymes involved in endothelium-dependent relaxation, such as eNOS (Pasquet *et al.*, 1996). The impaired endothelium-dependent relaxations, either mediated by iNOS or other factors, have been shown in blood vessels from endotoxemic animals (Umans *et al.*, 1993; Myers *et al.*, 1995; Piepot *et al.*, 2000; Wiel *et al.*, 2000; Piepot *et al.*, 2003).

Different experimental strategies have been used to control excessive NO production in sepsis, such as inhibiting NO production preferentially with selective iNOS inhibitors or by inhibiting NO-dependent pathways such as sGC, however results are conflicting. For example, the potent and highly selective iNOS inhibitor 1400W (Garvey *et al.*, 1997) has been shown to prevent LPS-induced hypotension (Bachetti *et al.*, 2003) and delay hypotension and circulatory failure in rats *in vivo* (Cuzzocrea *et al.*, 2006), but only partially reverses LPS-induced hyporeactivity to phenylephrine in rat superior mesenteric artery *in vitro* (O'Brien *et al.*, 2001) and is not effective in rabbits (Bachetti *et al.*, 2003). ODQ, an irreversible and highly selective heme-site inhibitor of sGC (Garthwaite *et al.*, 1995), prevents aortic hypocontractility to norepinephrine *ex vivo* in rat (Chen *et al.*, 2005) and both *in vitro* and *in vivo* in rat and mouse (Zingarelli *et al.*, 1999). Conversely, ODQ is partially effective in restoring vascular reactivity to phenylephrine in the rat superior

mesenteric artery *in vitro* (O'Brien *et al.*, 2001) and *ex vivo* in rat aorta (Wu *et al.*, 1998a).

Previous studies have shown that LPS decreases sGC activity in rat lung and aorta (Fernandes *et al.*, 2006), and in cultured rat aortic (Papapetropoulos *et al.*, 1996) and pulmonary (Scott & Nakayama, 1998) VSMCs. PDE5 activity is increased in rat lung after LPS injection (Holzmann *et al.*, 1996) and 1 h after LPS inhalation in guinea pig lungs (Toward *et al.*, 2005) but is decreased after 48 h in the same model. These studies have examined whole lung tissue or cultured pulmonary VSMCs, but there are no direct measurements published using isolated pulmonary arteries. Furthermore, these changes in NO signalling pathways have not been related to vascular reactivity in the same experimental model.

COX has also been suggested to play a role in LPS-induced changes in vascular reactivity, since enhanced COX-2 expression has been shown in mesenteric vessels from endotoxemic rats (Virdis *et al.*, 2005), in rat pulmonary VSMCs (Ermert *et al.*, 2000), in rat lung and heart in vivo (Liu *et al.*, 1996) and in rat aorta in vitro (Bishop-Bailey *et al.*, 1997). However, inhibition of inducible and/or constitutive COX pathways rarely reverses hypotension (Bernard *et al.*, 1997; Leach *et al.*, 1998; O'Brien *et al.*, 2001)

Similarly, ROS have been shown to be induced by LPS since treatment of rats with LPS enhances vascular expression of xanthine and NADPH oxidases and increases formation of $O_2^{\cdot -}$ and peroxynitrite (Brandes *et al.*, 1999). In addition, reduced plasma levels of different antioxidants and increased levels of markers of oxidative stress have been found in patients with septic shock (Goode *et al.*, 1995; Galley *et al.*, 1997) and in rats (Carbonell *et al.*, 2000). Inhibition of ROS yielded controversial results. For example, LPS-induced vasoconstrictor hyporeactivity can be corrected in human by high doses of vitamin C (Pleiner *et al.*, 2003) and in a rat endotoxic shock model *in vivo* by a peroxynitrite decomposition catalyst (Cuzzocrea *et al.*, 2006). In contrast, inhibition of $O_2^{\cdot -}$ does not restore but further deteriorates relaxation of LPS-treated rat aortic rings (Brandes *et al.*, 1999).

In this chapter the role of different mediators (including the endothelium-derived mediators NO/cGMP, COX and ROS) involved in LPS-induced changes in vascular reactivity to ET-1 was investigated in isolated rat pulmonary artery and aorta.

4.2 Methods

Pulmonary and aortic arterial rings were incubated with LPS (10 µg ml^{-1}, 20 h) in the presence or absence of endothelium, COX inhibitor indomethacin (10 µM), the antioxidant trolox (200 µM), the iNOS inhibitor 1400W (1 µM) and sGC inhibitor ODQ (10 µM) before measuring the contractile responses to ET-1 (0.3 nM-100 nM). Relaxation responses to ACh, SNP, 8-pCPT-cGMP, BAY 41-2272 and T-0156 were also measured. NO production was measured by Griess method and SNP-induced cGMP production was measured by ELISA. The expression of $sGC_{\alpha 1}$, $sGC_{\beta 1}$ and PDE5 proteins were measured by immunoblotting. Appropriate control experiments were done to exclude vehicle effects on vascular tissue responsiveness.

4.3 Effect of endothelium removal on LPS-induced changes in vascular reactivity to ET-1

As previously shown in chapter 3, LPS selectively causes hyporeactivity to ET-1 in the aorta but not in the pulmonary artery (Figure 3.5). The role of endothelium was studied in endothelium-denuded control and LPS-treated aortic rings. In the pulmonary artery, removal of endothelium did not cause a significant difference between control and LPS-treated vascular rings (Figure 4.1a). In the aorta, removal of endothelium did not abolish the decreased contractility to ET-1 in LPS-treated group (Figure 4.1b). This result indicates that endothelium does not play a major role in LPS-induced changes in vascular reactivity to ET-1.

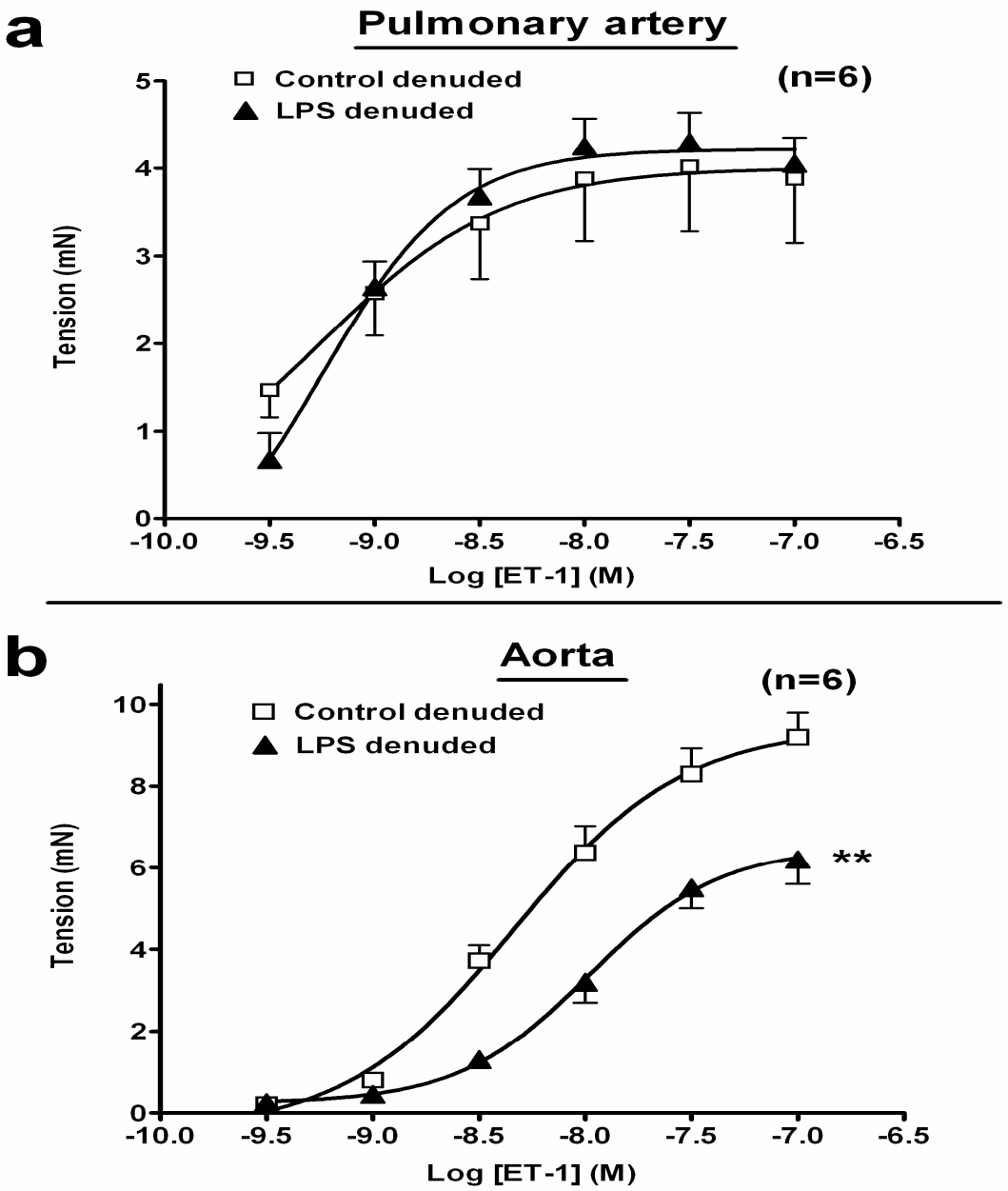

Figure 4.1 Effect of removal of endothelium on LPS-induced changes in vascular reactivity to ET-1 in the pulmonary artery and the aorta. Contraction to ET-1 (0.3 nM-100 nM) was measured in endothelium-denuded pulmonary artery (a) and aorta (b) after incubation with LPS (10 µg ml^{-1}, 20 h). Data are expressed as mean ± s.e.m., where (n) equals the number of animals.

** $p<0.01$ for E_{max} and pEC_{50} values compared with control group using paired Student's *t*-test.

4.4 Effect of COX-inhibition on LPS-induced changes in vascular reactivity to ET-1

Inhibition of COX by 10 µM indomethacin added 1 h before and during LPS incubation did not affect LPS-induced changes in vascular reactivity to ET-1. In the pulmonary artery, inhibition of COX did not cause a significant difference between control and LPS-treated rings (Figure 4.2a). In the aorta, inhibition of COX did not abolish the difference between control and LPS-treated aortic rings in response to ET-1 (Figure 4.2b), since the E_{max} was still reduced by 19±2% in LPS-treated group. Since removal of endothelium and inhibition of COX did not abolish LPS-induced aortic hyporeactivity to ET-1, mediators produced by COX, such as prostaglandins and TxA_2, are not a major pathway involved in vascular hyporeactivity to ET-1 induced by LPS.

4.5 Effect of ROS-inhibition on LPS-induced changes in vascular reactivity to ET-1

Inhibition of ROS by 200 µM trolox (a cell-permeable, water-soluble derivative of vitamin E with potent antioxidant properties) added 1 h before and during LPS incubation did not affect LPS-induced changes in vascular reactivity to ET-1. In the pulmonary artery, inhibition of ROS did not cause a significant difference between control and LPS-treated rings (Figure 4.3a). Similarly, inhibition of ROS did not abolish the difference between control and LPS-treated aortic rings in response to ET-1 (Figure 4.3b), where the E_{max} was still reduced by 20±3%. These results suggest that ROS does not play a major role in LPS-induced changes in vascular reactivity to ET-1.

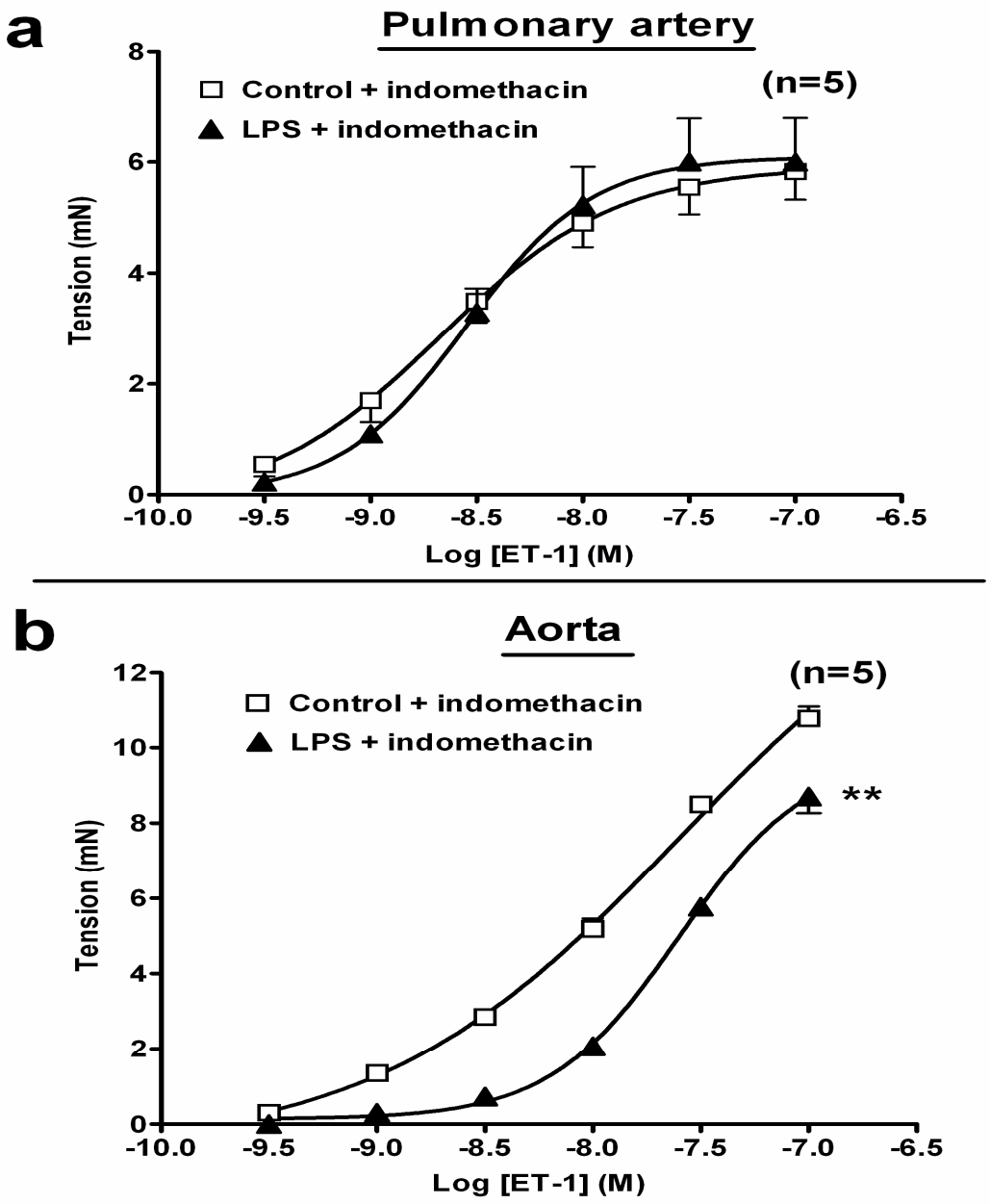

Figure 4.2 Effect of indomethacin on LPS-induced changes in vascular reactivity to ET-1 in the pulmonary artery and the aorta. Contraction to ET-1 (0.3 nM-100 nM) was measured in the pulmonary artery (a) and the aorta (b) after incubation with LPS (10 µg ml^{-1}, 20 h) in the presence of 10 µM indomethacin. Data are expressed as mean ± s.e.m., where (n) equals the number of animals.
** $p<0.01$ for E_{max} and pEC_{50} values compared with control group using paired Student's *t*-test.

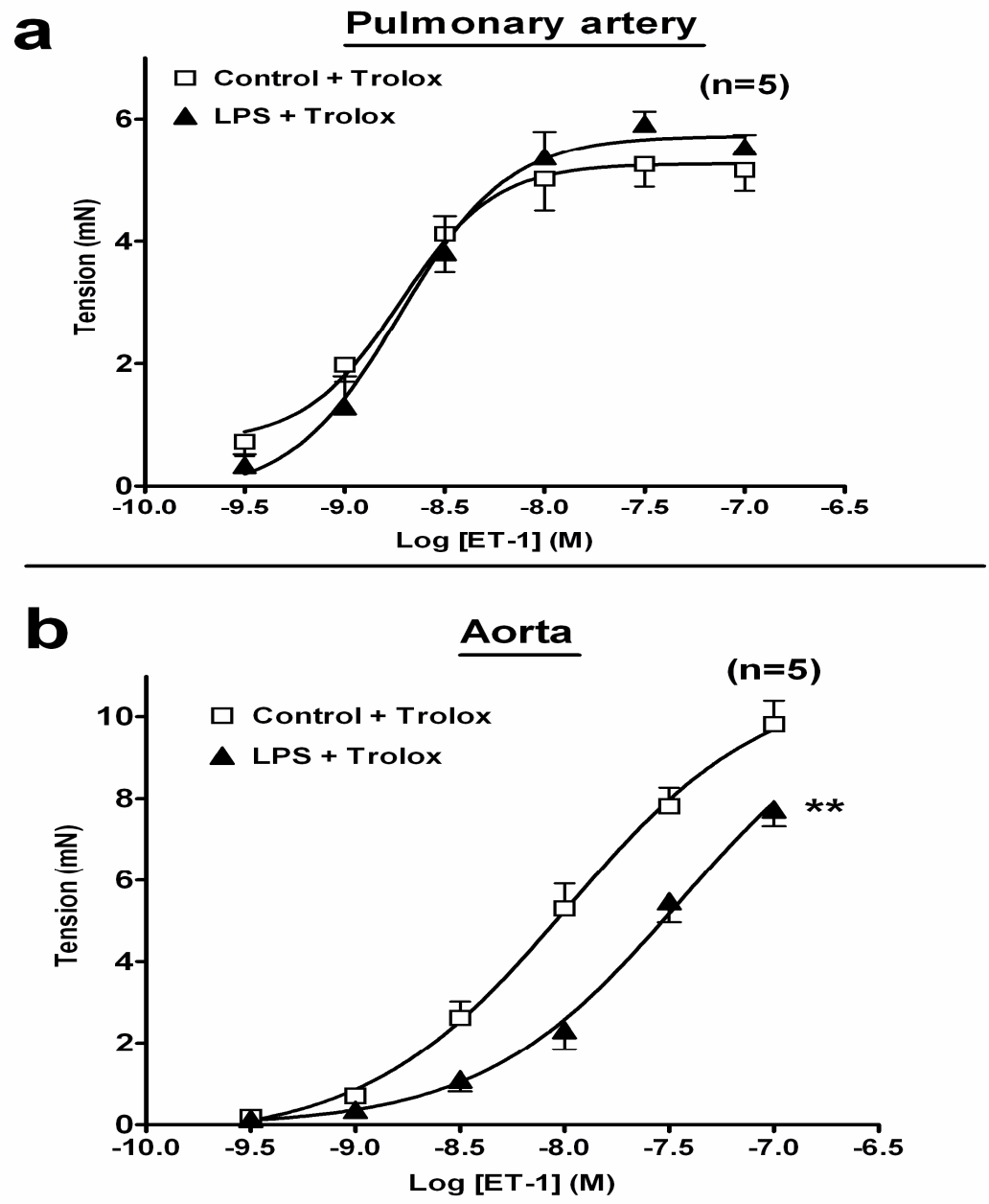

Figure 4.3 Effect of trolox on LPS-induced changes in vascular reactivity to ET-1 in the pulmonary artery and the aorta. Contraction to ET-1 (0.3 nM-100 nM) was measured in the pulmonary artery (a) and the aorta (b) after incubation with LPS (10 µg ml^{-1}, 20 h) in the presence of 200 µM trolox. Data are expressed as mean ± s.e.m., where (n) equals the number of animals. ** $p<0.01$ for E_{max} and pEC_{50} values compared with control group using paired Student's *t*-test.

4.6 Role of NO in LPS-induced changes in vascular reactivity to ET-1

4.6.1 Effect of LPS on eNOS and iNOS gene expression

The PCR primers designed for eNOS, iNOS and the housekeeping gene β-actin were tested first by using standard RT-PCR to detect the presence of the expected products at 60, 95 and 72 bp respectively (Figure 4.4). Melt-curve analyses, verifying specific amplification and the absence of secondary primers products and PCR standard curves of both the target (eNOS and iNOS) and reference (β-actin) genes are shown in Figure 4.5.

Although eNOS mRNA expression was changed by incubation in both the pulmonary artery and the aorta, but changes in eNOS mRNA expression at 4, 8 and 20 h were not significantly different between control and LPS-treated pulmonary (Figure 4.6a) or aortic rings (Figure 4.6b). This result, together with the absence of an effect of endothelium removal, confirms that eNOS is not involved in LPS-induced changes in vascular reactivity to ET-1. Conversely, continuous incubation with LPS resulted in enhanced gene expression of iNOS to a similar extent both in the pulmonary artery (Figure 4.6c) and the aorta (Figure 4.6d). This increase in iNOS gene expression was 666±103 % in the pulmonary artery and 1287±447% in the aorta when compared to their respective controls at 20 h. The presence of matching time controls ensures that the increase in iNOS is only due to LPS and not due to incubation itself. Moreover, all the time point controls and LPS-treated groups for each sample were pooled exactly from the same animals to prevent any changes due to genetic variation between different animals. These results suggest that LPS-induced expression of iNOS may contribute to changes in vascular reactivity to ET-1 through excessive NO production.

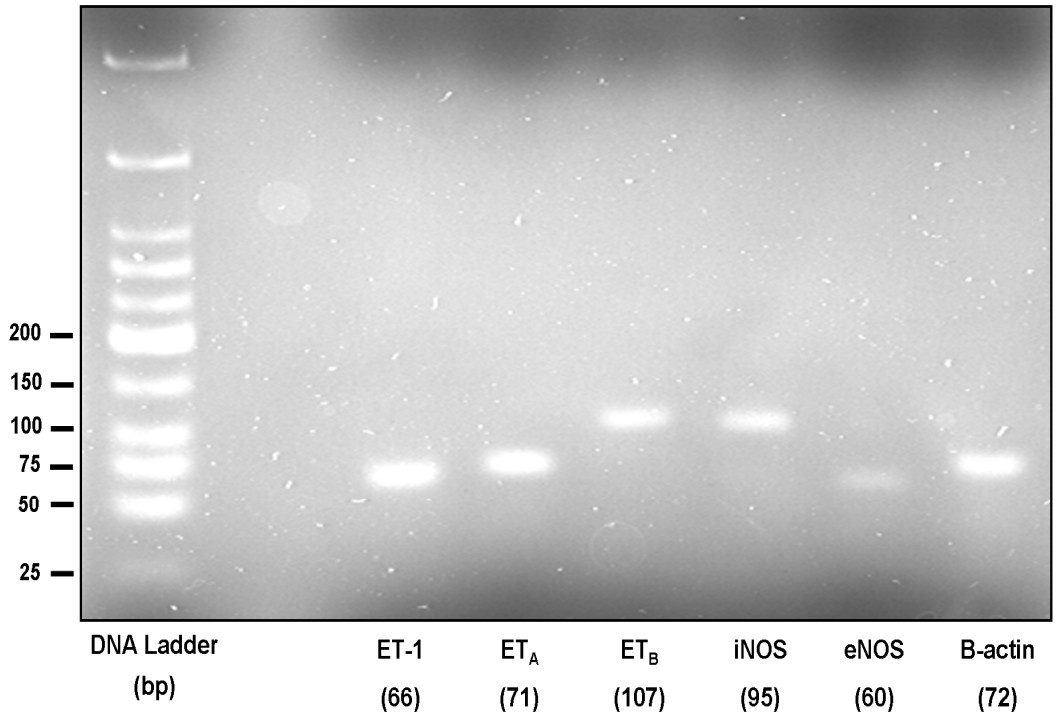

Figure 4.4 Representative PCR gel for eNOS, iNOS, ET-1, ET_A, ET_B and β-actin genes. RNA was extracted from LPS (10 µg ml^{-1})-treated rings after 20 h and reverse-transcribed into cDNA before carrying out standard PCR and detecting the products on agarose gel with ethidium bromide and UV-imaging.

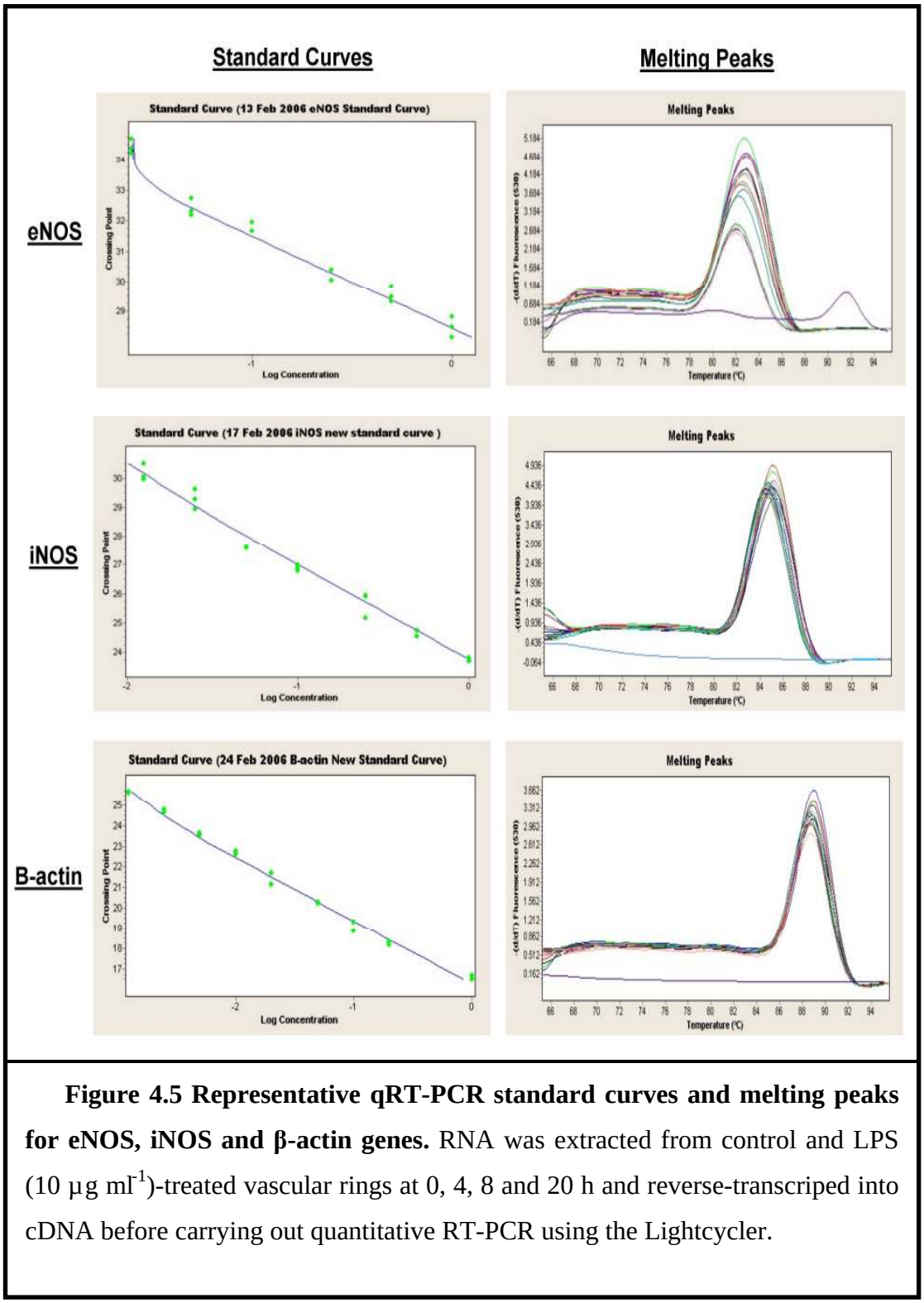

Figure 4.5 Representative qRT-PCR standard curves and melting peaks for eNOS, iNOS and β-actin genes. RNA was extracted from control and LPS (10 µg ml^{-1})-treated vascular rings at 0, 4, 8 and 20 h and reverse-transcriped into cDNA before carrying out quantitative RT-PCR using the Lightcycler.

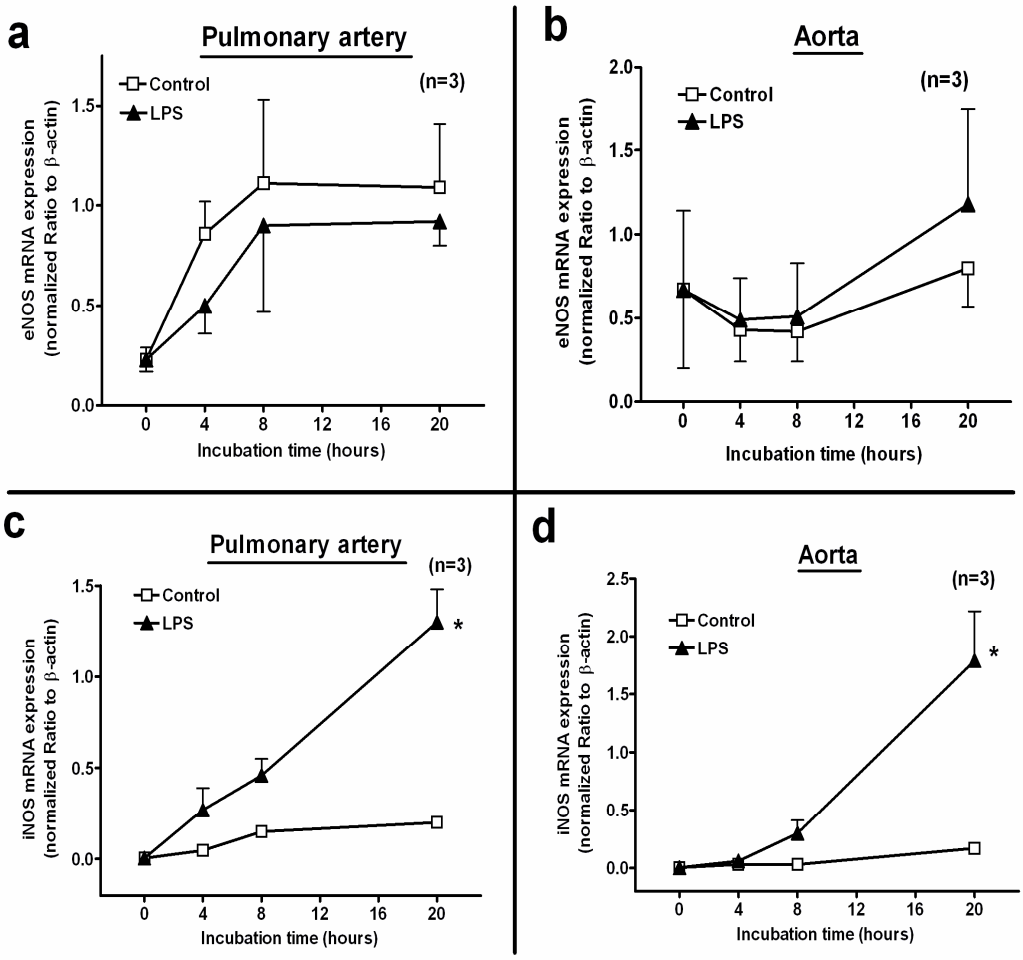

Figure 4.6 LPS-induced changes in gene expression of eNOS and iNOS in the pulmonary artery and the aorta. RNA was extracted from control and LPS (10 µg ml^{-1})-treated vascular rings at 0, 4, 8 and 20 h and reverse-transcribed into cDNA before carrying out qRT-PCR to detect changes in the gene expression of eNOS (a and b) and iNOS (c and d) in the pulmonary artery and aorta. Data are expressed as mean ± s.e.m., where (n) equals the number of independent experiments, each using duplicate PCR reactions from the same sample prepared from pooled tissue lysates of 2 animals. * $p<0.05$ compared with matching time-control using paired Student's *t*-test. Data for iNOS (c and d) was presented before in Figure 3.4.

4.6.2 Effect of LPS on NO release

To detect if the LPS-induced iNOS expression is associated with NO overproduction the accumulation of nitrite and nitrate (NOx), as the breakdown products of NO, was measured in the culture medium. Incubation of the pulmonary artery and the aorta with LPS caused a significant 5- to 10- fold increase in NO release ($p<0.01$, n=5) (Figure 4.7). The increases in NO production were not significantly different between the two preparations. Co-incubation of pulmonary and aortic rings with LPS together with either the non-specific NOS-inhibitor L-NAME (100 μM) or the iNOS-specific inhibitor 1400W (1 μM) prevented the LPS-induced overproduction of NO in both vessels (Figure 4.7). This result confirms that LPS enhances NO release through increasing iNOS expression.

4.6.3 Effect of LPS on endothelium-dependent relaxation

Incubation of the pulmonary artery and the aorta with LPS caused a significant impairment of the endothelium-dependent relaxation. Vascular relaxation to ACh was significantly decreased by LPS in the pulmonary artery, as manifested by a decrease in E_{max} from 68±10 % to 41±5 % in the control and LPS-treated groups respectively ($p<0.01$, n=5) (Figure 4.8a). Similarly, vascular relaxation to ACh was significantly decreased by LPS in the aorta, as manifested by a decrease in E_{max} from 71±5 % to 56±3 % in the control and LPS-treated groups respectively ($p<0.01$, n=5) (Figure 4.8b). This result suggests that either eNOS activity or the downstream signalling of NO in the VSMCs is impaired.

4.6.4 Effect of LPS on endothelium-independent relaxation

Endothelium-independent vascular relaxation induced by SNP was significantly decreased ($p<0.01$, n=6) by LPS in the pulmonary artery, as manifested by a decrease in E_{max} from 64±7 % to 40±3 % in the control and LPS-treated groups respectively (Figure 4.9a). Conversely, there were no significant differences in SNP-induced vasorelaxation between control and LPS-treated groups in the aorta (Figure 4.9b). This result suggests that the downstream signalling of NO is selectively impaired by LPS in the pulmonary artery but not in the aorta.

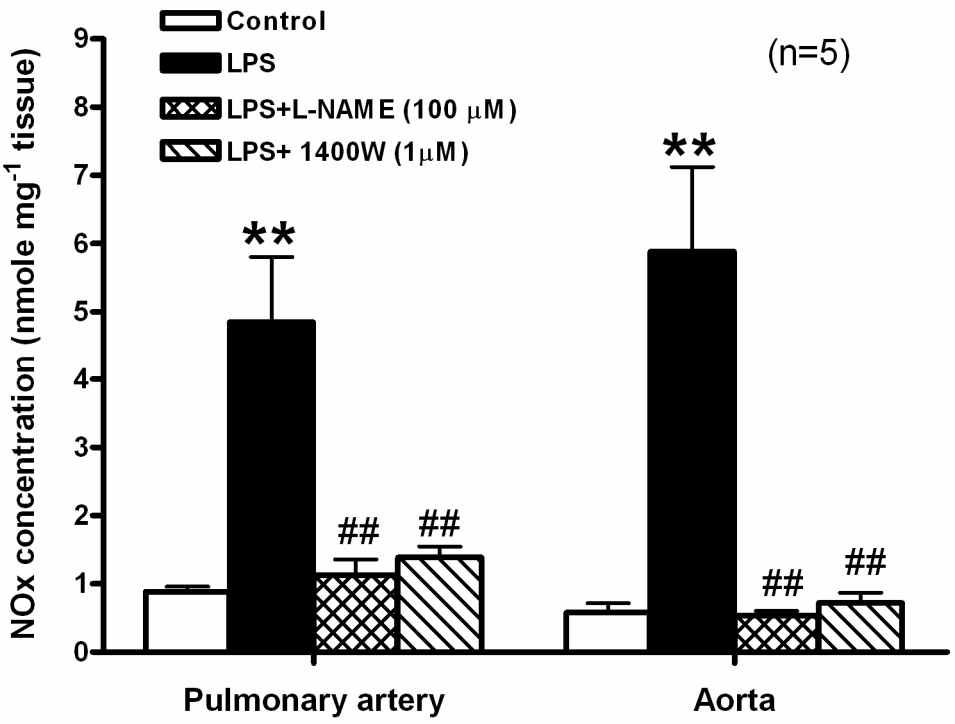

Figure 4.7 Effect of LPS treatment on NO release from isolated rat pulmonary artery and aorta. NO release (total amount of nitrite plus nitrate, NOx) was determined in the supernatant spectrophotometrically using Greiss reagent after reduction of nitrate to nitrite. LPS-induced NO overproduction was inhibited by co-incubation with either L-NAME (100 μM) or 1400W (1 μM). Data are expressed as mean ± s.e.m., where (n) equals the number animals. **p<0.01 compared with control group, $^{\#\#}$ p<0.01 compared with LPS group using one-way ANOVA followed by Dunnett's *post-hoc* test.

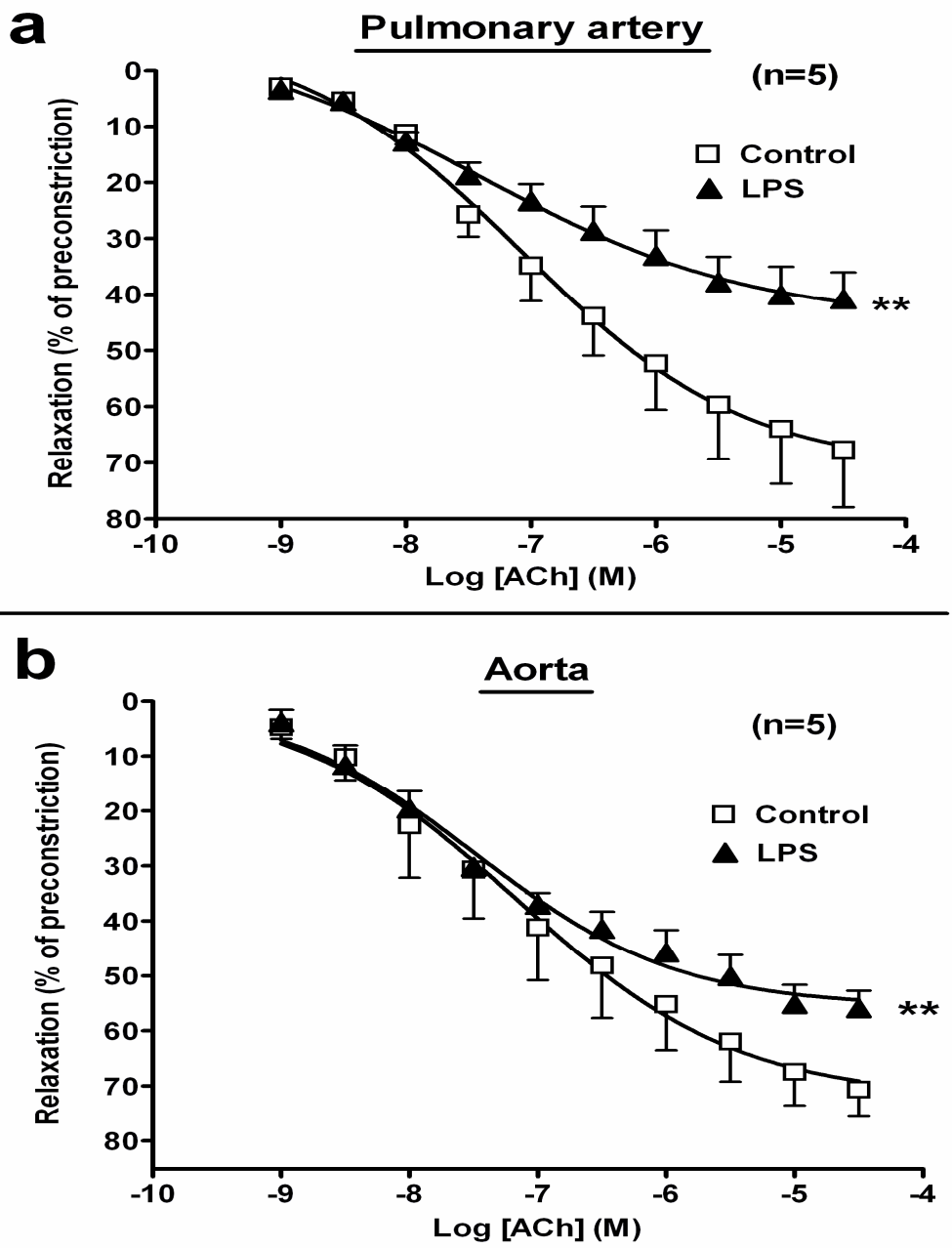

Figure 4.8 Effect of LPS on ACh-induced relaxation in the pulmonary artery and the aorta. LPS (10 µg ml^{-1}, 20 h)-treated pulmonary (a) and aortic (b) arterial rings were preconstricted with 30 nM ET-1 before measuring relaxation responses to ACh (1 nM-30 µM). Data are expressed as mean ± s.e.m., where (n) equals the number animals. **$p<0.01$ for E_{max} and pEC_{50} values compared with control group using paired Student's *t*-test.

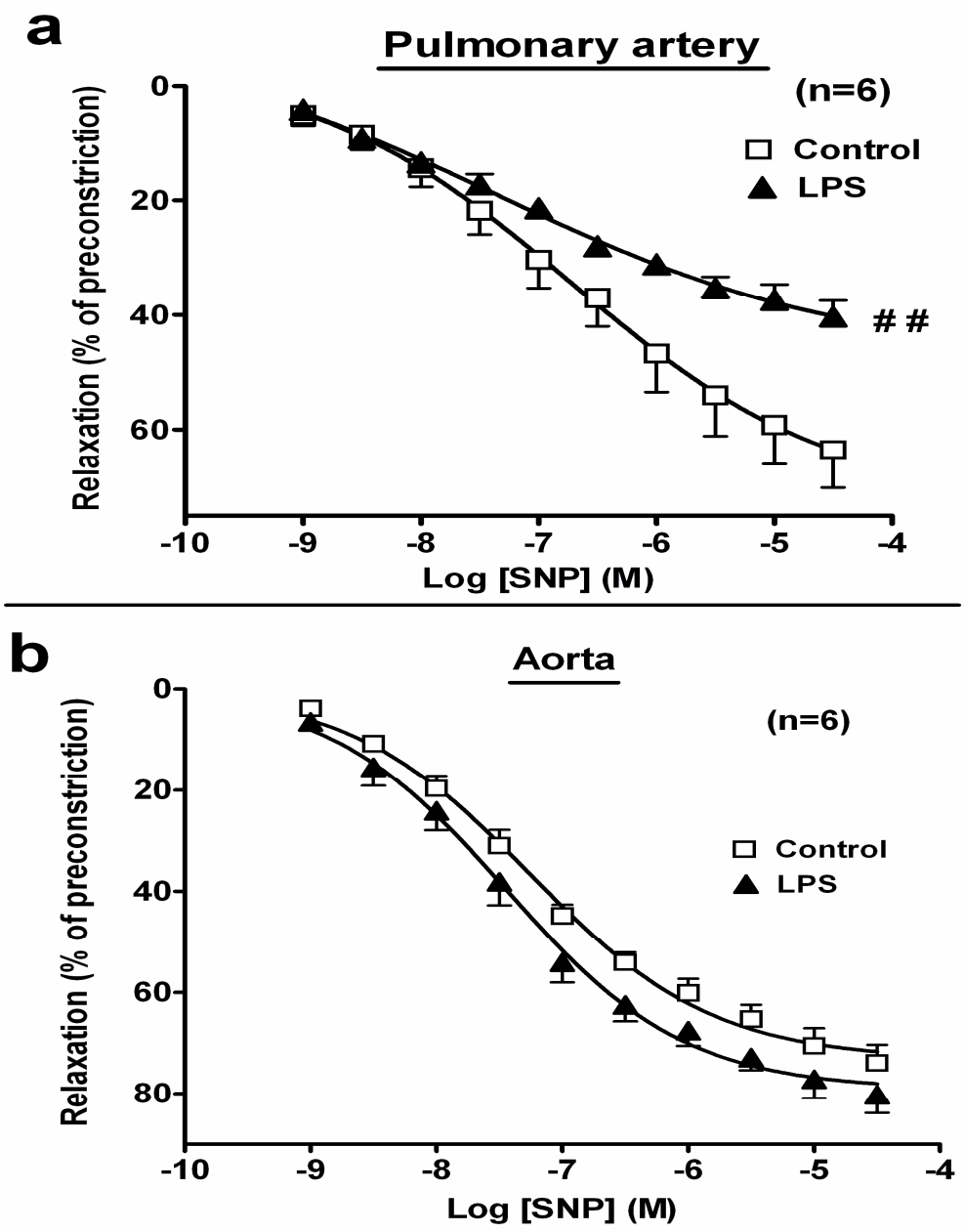

Figure 4.9 Effect of LPS on SNP-induced relaxation in the pulmonary artery and the aorta. LPS (10 µg ml^{-1}, 20 h)-treated pulmonary (a) and aortic (b) arterial rings were preconstricted with 30 nM ET-1 before measuring relaxation responses to SNP (1 nM-30 µM). Data are expressed as mean ± s.e.m., where (n) equals the number animals. ##$p<0.01$ for E_{max} values compared with control group using paired Student's *t*-test.

4.6.5 Effect of LPS on NO-independent direct sGC activation

Incubation of the pulmonary artery and the aorta with LPS caused a differential effect on the relaxation induced by the direct NO-independent sGC activator BAY 41-2272. Vascular relaxation to BAY 41-2272 was significantly decreased ($p<0.01$, $n=4$) by LPS in the pulmonary artery (Figure 4.10a), as manifested by a 32±8 % decrease in E_{max}. Conversely, BAY 41-2272-induced relaxation was significantly increased in the aorta ($p<0.01$, $n=4$) (Figure 4.10b) as manifested by a 15±7 % increase in E_{max}. These results suggest that sGC activation, the main downstream signalling pathway for NO, is impaired by LPS in the pulmonary artery, while it is enhanced in the aorta.

4.6.6 Effect of LPS on relaxation induced by PDE-resistant cGMP analogue

To assess whether LPS-mediated pulmonary hyporeactivity to SNP was due to decreased cGMP or impaired downstream cGMP-effector signalling molecules (such as PKG), the relaxation response to the PDE-resistant cGMP analogue 8-pCPT-cGMP was studied. LPS treatment had no significant effect on relaxation responses to 8-pCPT-cGMP either in the pulmonary artery (Figure 4.11a) or in the aorta (Figure 4.11b). These results suggest that pulmonary hyporeactivity to SNP is likely to be due to either decreased cGMP synthesis by sGC or increased cGMP degradation (mainly by PDE5), or both.

4.6.7 Effect of LPS on SNP-induced cGMP production

Incubation with LPS significantly decreased ($p<0.05$, $n=4$) the SNP-stimulated cGMP production in the pulmonary artery by 24±4 % from 4.15±0.23 to 3.13±0.18 pmole mg^{-1} tissue, whereas cGMP levels in the aorta were not significantly affected (Figure 4.12). These results confirm that cGMP synthesis is impaired by LPS in the pulmonary artery but not in the aorta.

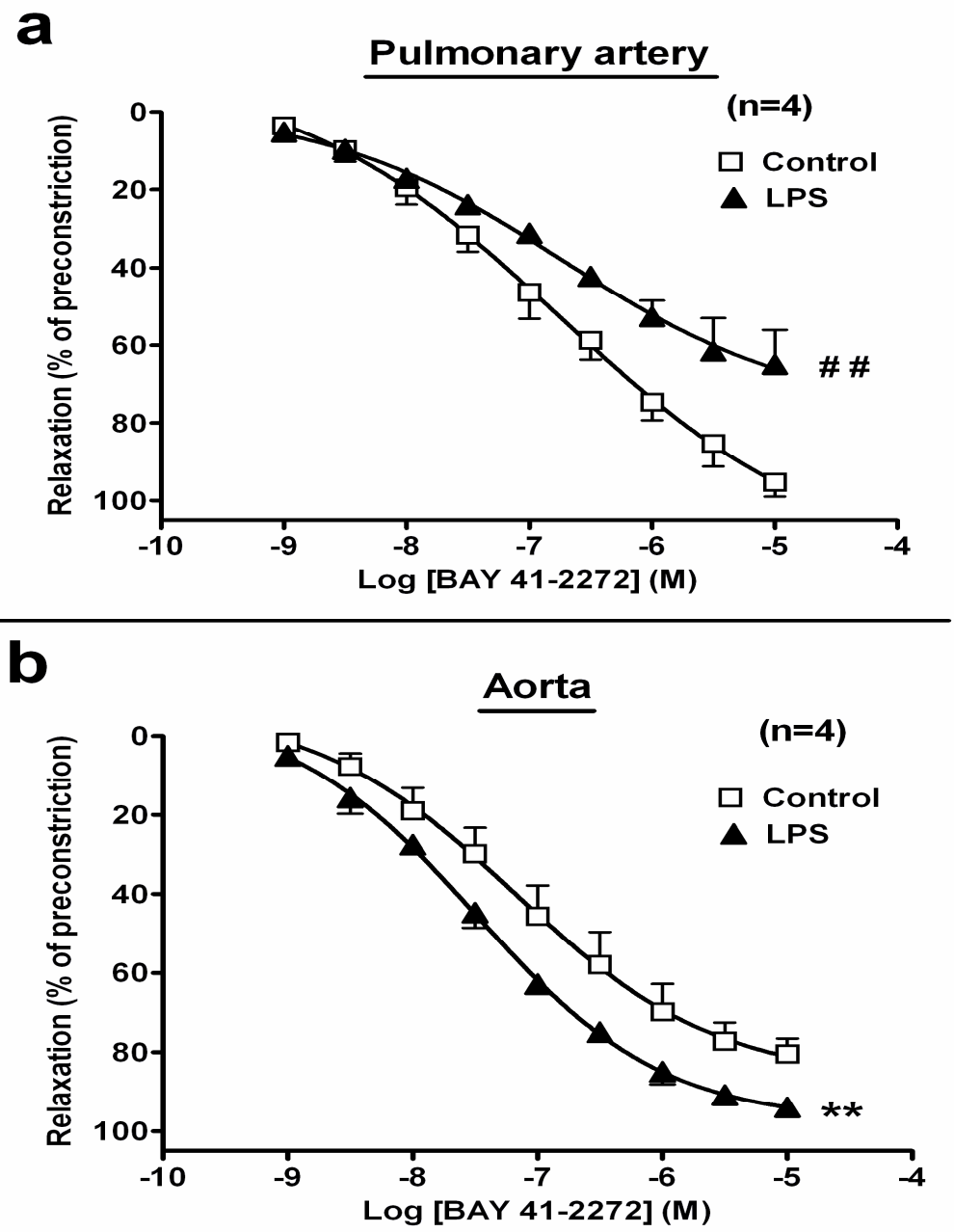

Figure 4.10 Effect of LPS on BAY 41-2272-induced relaxation in the pulmonary artery and the aorta. LPS (10 µg ml^{-1}, 20 h)-treated pulmonary (a) and aortic (b) arterial rings were preconstricted with 30 nM ET-1 before measuring relaxation to BAY 41-2272 (1 nM-10 µM). Data are expressed as mean ± s.e.m., where (n) equals the number animals. ##$p<0.01$ for $E_{max,}$ **$p<0.01$ for E_{max} and pEC_{50} values compared with control group using paired Student's *t*-test.

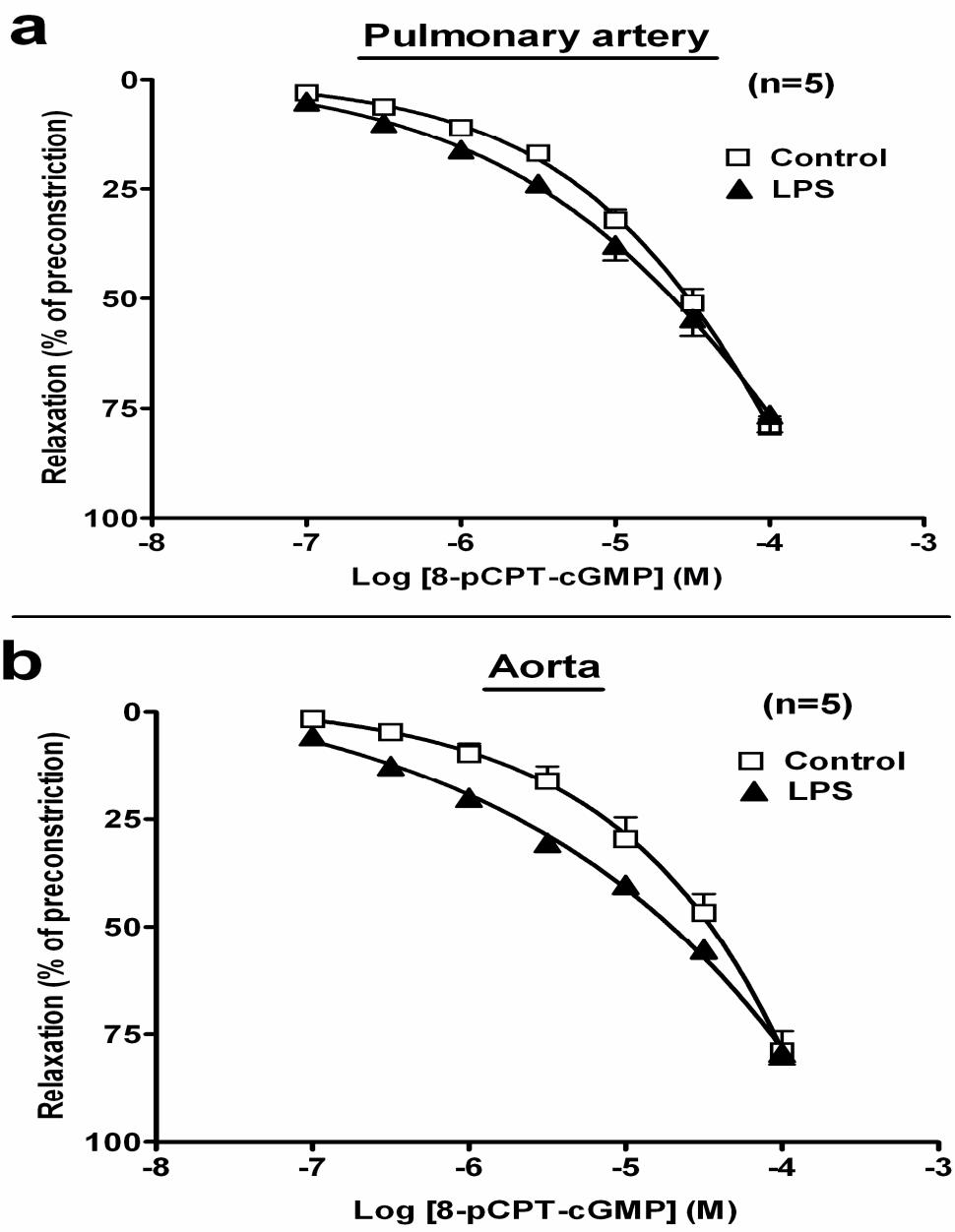

Figure 4.11 Effect of LPS on 8-pCPT-cGMP-induced relaxation in the pulmonary artery and the aorta. LPS (10 µg ml^{-1}, 20 h)-treated pulmonary (a) and aortic (b) arterial rings were preconstricted with 30 nM ET-1 before measuring relaxation to the non-hydrolysable cGMP analogue 8-pCPT-cGMP (0.1 µM-100 µM). Data are expressed as mean ± s.e.m., where (n) equals the number animals.

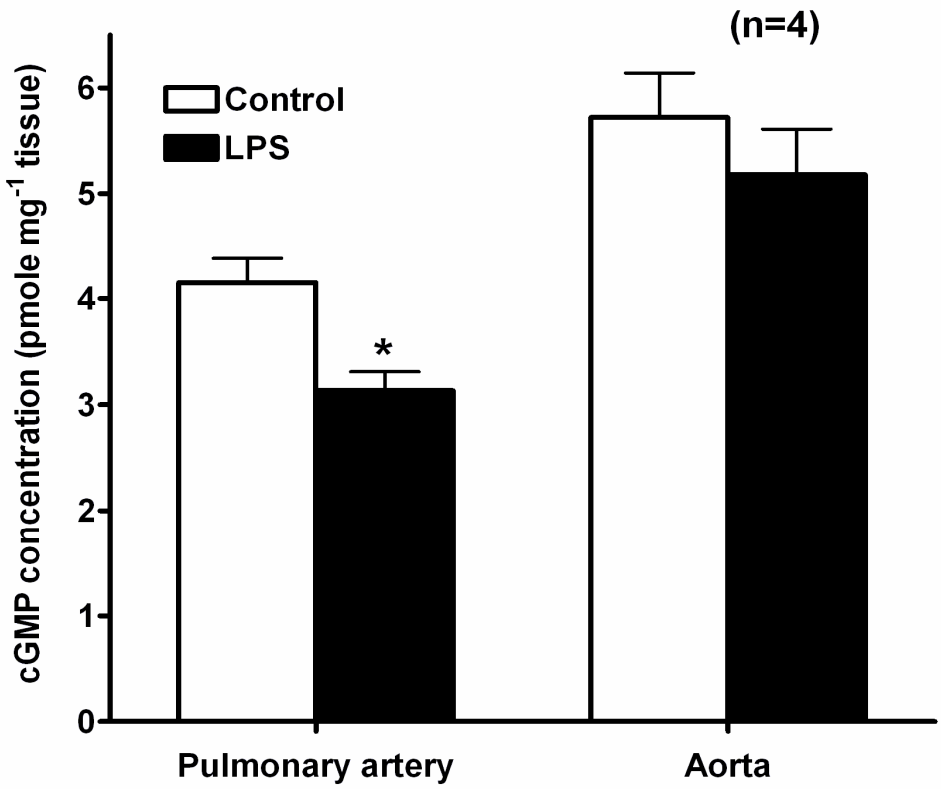

Figure 4.12 Effect of LPS on SNP-induced cGMP production in the pulmonary artery and the aorta. Pulmonary and aortic rings from LPS (10 µg ml^{-1}, 20 h)-treated and control groups were stimulated by SNP (100 µM for 10 min) in the presence of the non-selective PDE-inhibitor IBMX (100 µM), freeze-dried and cGMP levels were determined by ELISA. Data are expressed as mean ± s.e.m., where (n) equals the number animals. *$p<0.05$ compared with control group using paired Student's *t*-test.

4.6.8 Effect of iNOS inhibition on LPS-induced changes in vascular reactivity to ET-1

In the pulmonary artery, inhibition of iNOS did not cause a significant difference between control and LPS-treated rings (Figure 4.13a). In the aorta, inhibition of iNOS did not abolish the difference between control and LPS-treated aortic rings in response to ET-1 (compare Figure 3.5 with Figure 4.13b), where the E_{max} was still reduced by 16±1% as a result of LPS treatment. These results suggest the presence of mediator(s) other than iNOS-derived NO that play a major role in LPS-induced changes in vascular reactivity to ET-1.

4.6.9 Effect of sGC inhibition on LPS-induced changes in vascular reactivity to ET-1

In contrast with iNOS inhibition, inhibition of sGC by incubation with 10 μM ODQ abolished the LPS-induced changes in vascular reactivity to ET-1. In the pulmonary artery, inhibition of sGC did not cause a significant difference between control and LPS-treated rings (Figure 4.14a). In contrast, inhibition of sGC prevented the LPS-induced decrease in contraction to ET-1 in the aorta (Figure 4.14b). These results suggest that LPS induces sGC activation through mediator(s) other than NO, leading to aortic hyporeactivity to ET-1.

4.6.10 Effect of LPS on protein expression level of sGC subunits

In the pulmonary artery, LPS pre-treatment caused a significant decrease ($p<0.01$, $n=4$) in protein expression levels of $sGC_{\beta 1}$ subunit by 36±7 % (protein density ratio to β-actin), while the expression of the $sGC_{\alpha 1}$ subunit was not significantly affected (Figure 4.15). In contrast, LPS did not significantly change the protein expression levels of either sGC subunits in the aorta (Figure 4.15). Since both subunits are required for sGC function, the decrease in the protein expression level of one subunit ($sGC_{\beta 1}$ in the pulmonary artery) would impair sGC activity.

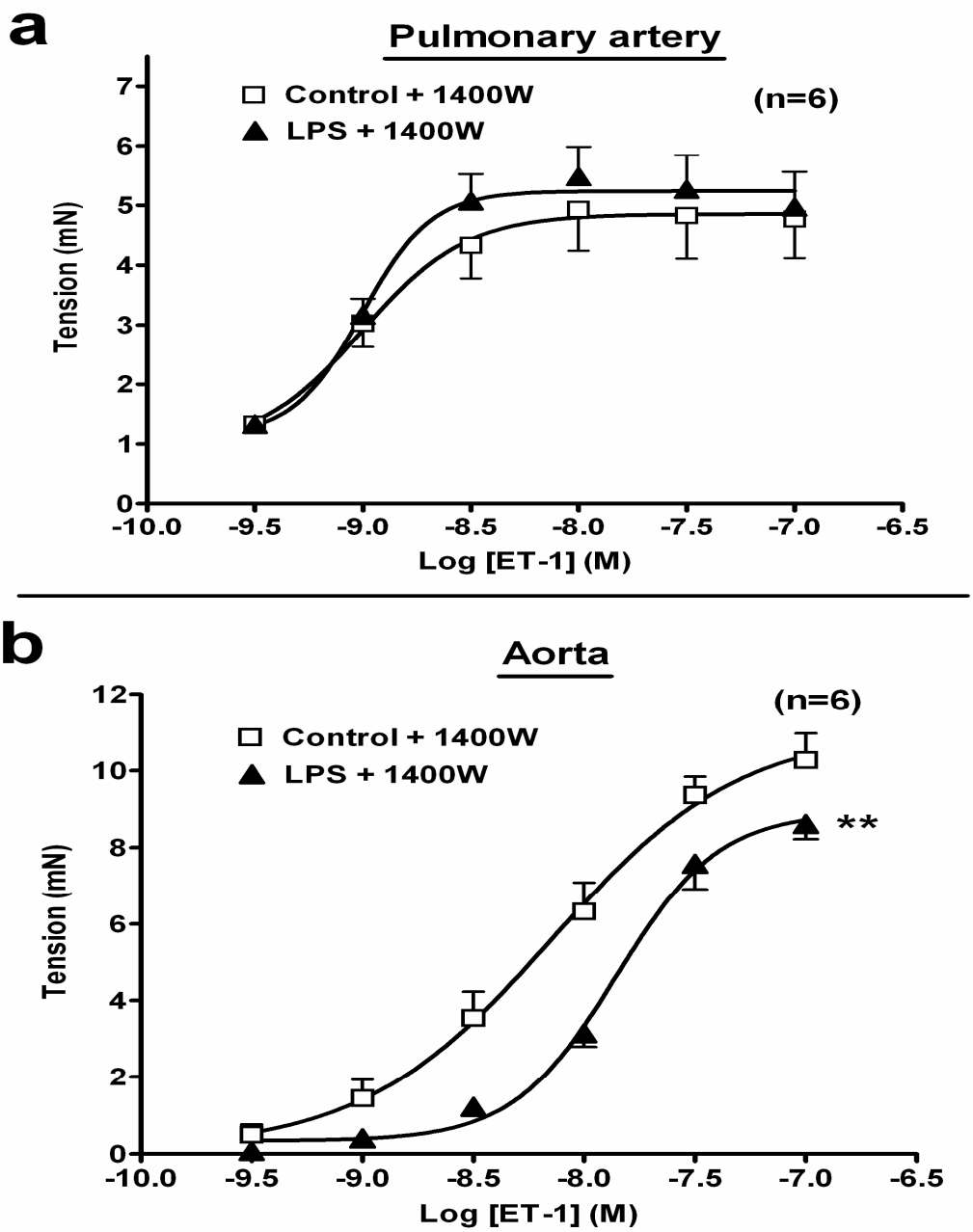

Figure 4.13 Effect of 1400W on LPS-induced changes in vascular reactivity to ET-1 in the pulmonary artery and the aorta. Contraction to ET-1 (0.3 nM-100 nM) was measured in the pulmonary artery (a) and the aorta (b) after incubation with LPS (10 µg ml^{-1}, 20 h) in the presence of 10 µM 1400W. Data are expressed as mean ± s.e.m., where (n) equals the number animals. ** $p<0.01$ for E_{max} and pEC_{50} values compared with control group using paired Student's *t*-test.

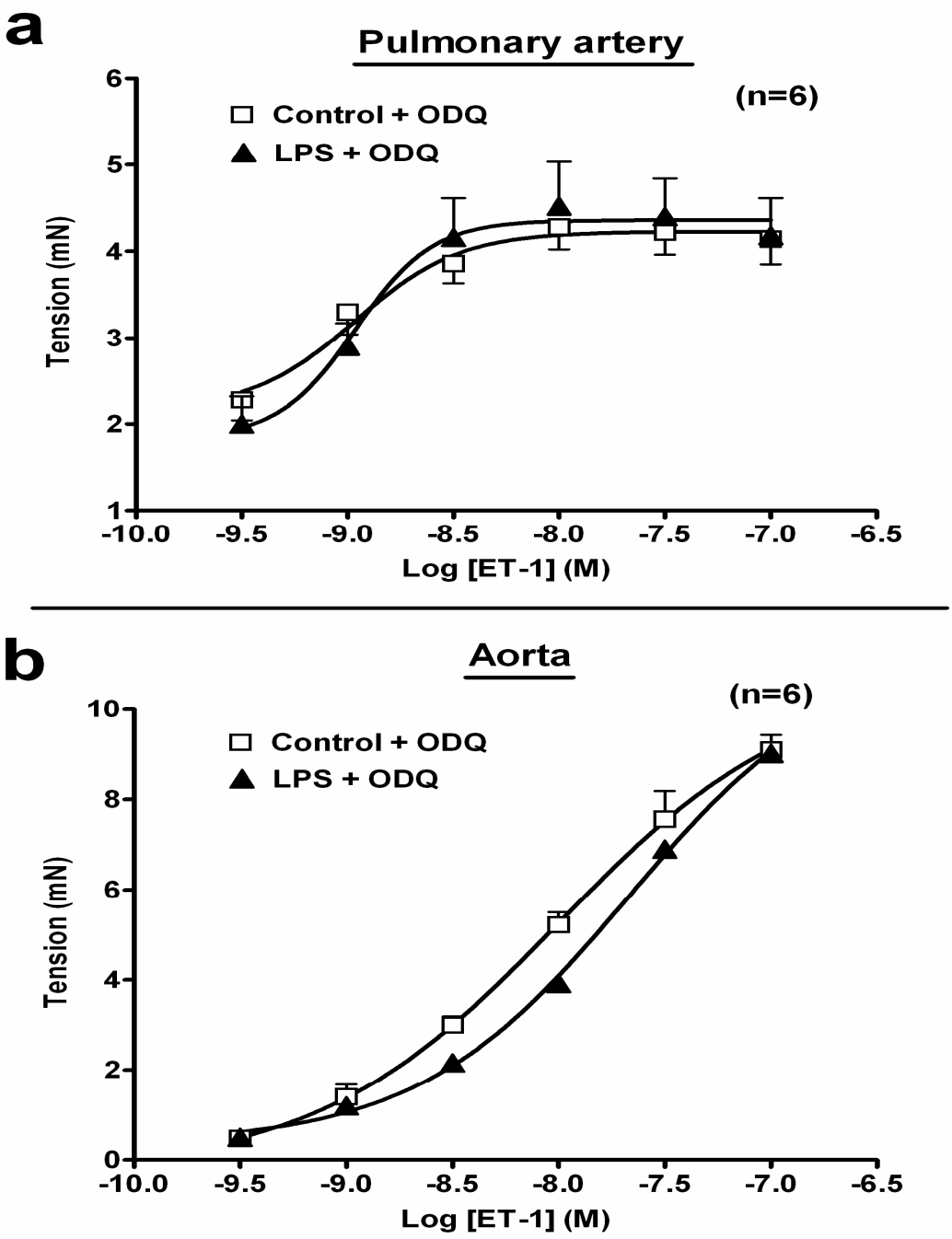

Figure 4.14 Effect of ODQ on LPS-induced changes in vascular reactivity to ET-1 in the pulmonary artery and the aorta. Contraction to ET-1 (0.3 nM-100 nM) was measured in the pulmonary artery (a) and the aorta (b) after incubation with LPS (10 µg ml^{-1}, 20 h) in the presence of 10 µM ODQ. Data are expressed as mean ± s.e.m., where (n) equals the number animals.

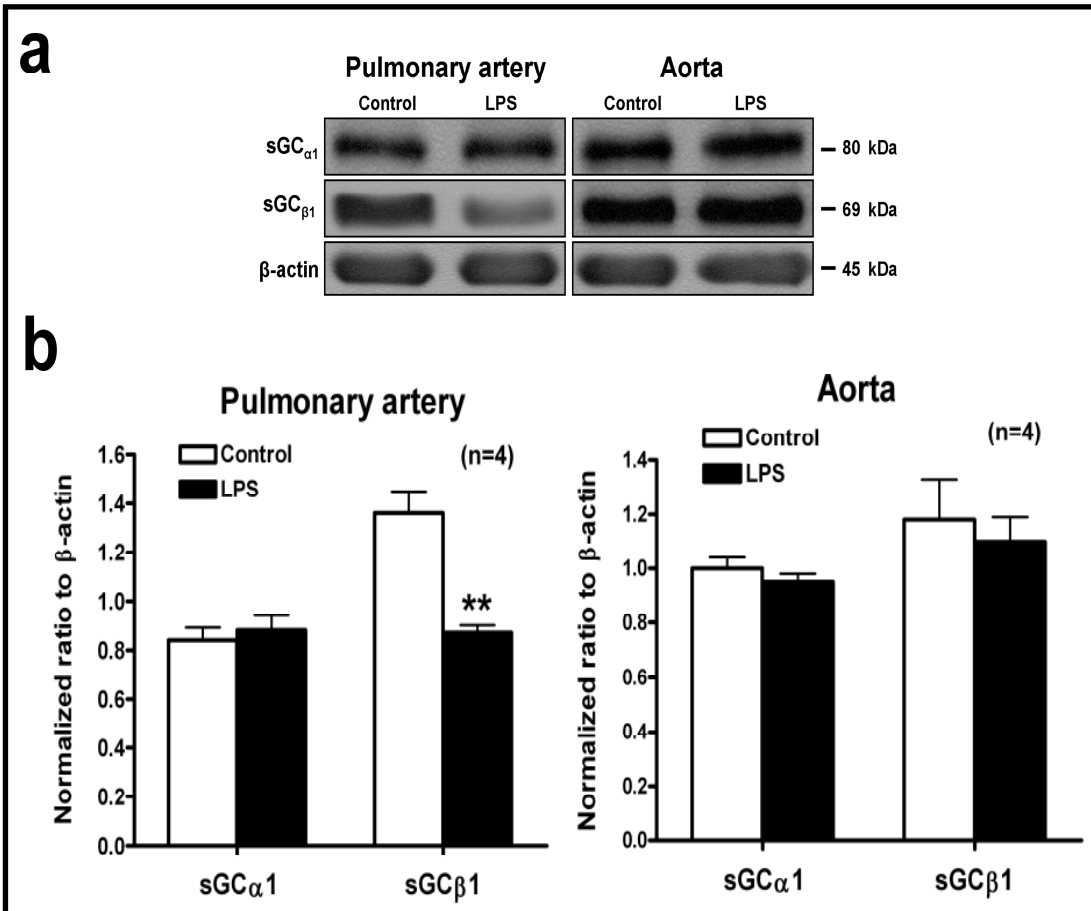

Figure 4.15 Effect of LPS on protein expression levels of sGC$_{\alpha1}$ and sGC$_{\beta1}$, in the pulmonary artery and the aorta. (a): representative immunoblots for sGC$_{\alpha1}$ and sGC$_{\beta1}$ in the pulmonary artery (left) and the aorta (right). (b): densitometric ratio of sGC protein subunits normalized to β-actin in the pulmonary artery (left) and the aorta (right). Data are expressed as mean ± s.e.m., where (n) equals the number animals. **p<0.01 compared with control group using paired Student's *t*-test.

4.6.11 Effect of LPS on relaxation responses induced by PDE5 inhibition

The role of PDE5 activity in LPS-induced impairment of vasorelaxation in the pulmonary artery was investigated using the potent and highly selective PDE5 inhibitor T-0156. Relaxation responses to T-0156 were significantly increased by LPS in the pulmonary artery, as manifested by an increase in E_{max} from 75±5 % to 94±2 % in the control and LPS-treated groups respectively ($p<0.01$, $n=6$) (Figure 4.16a). Conversely, LPS treatment did not have a significant effect on T-0156-induced relaxation in the aorta (Figure 4.16b). These results suggest that PDE5 expression or activity could be increased by LPS treatment in the pulmonary artery but not in the aorta.

4.6.12 Effect of LPS on protein expression level of PDE5

For the protein expression levels of PDE5, two bands were obtained at 95 and 85 kDa since PDE5 is dimeric (Lin *et al.*, 2006). LPS treatment of the pulmonary artery and the aorta did not significantly alter PDE5 protein expression levels in either vessel (Figure 4.17a and b). These results therefore suggest that the LPS-induced increase in the effects of T-0156 in the pulmonary artery is likely due to changes in PDE5 activity.

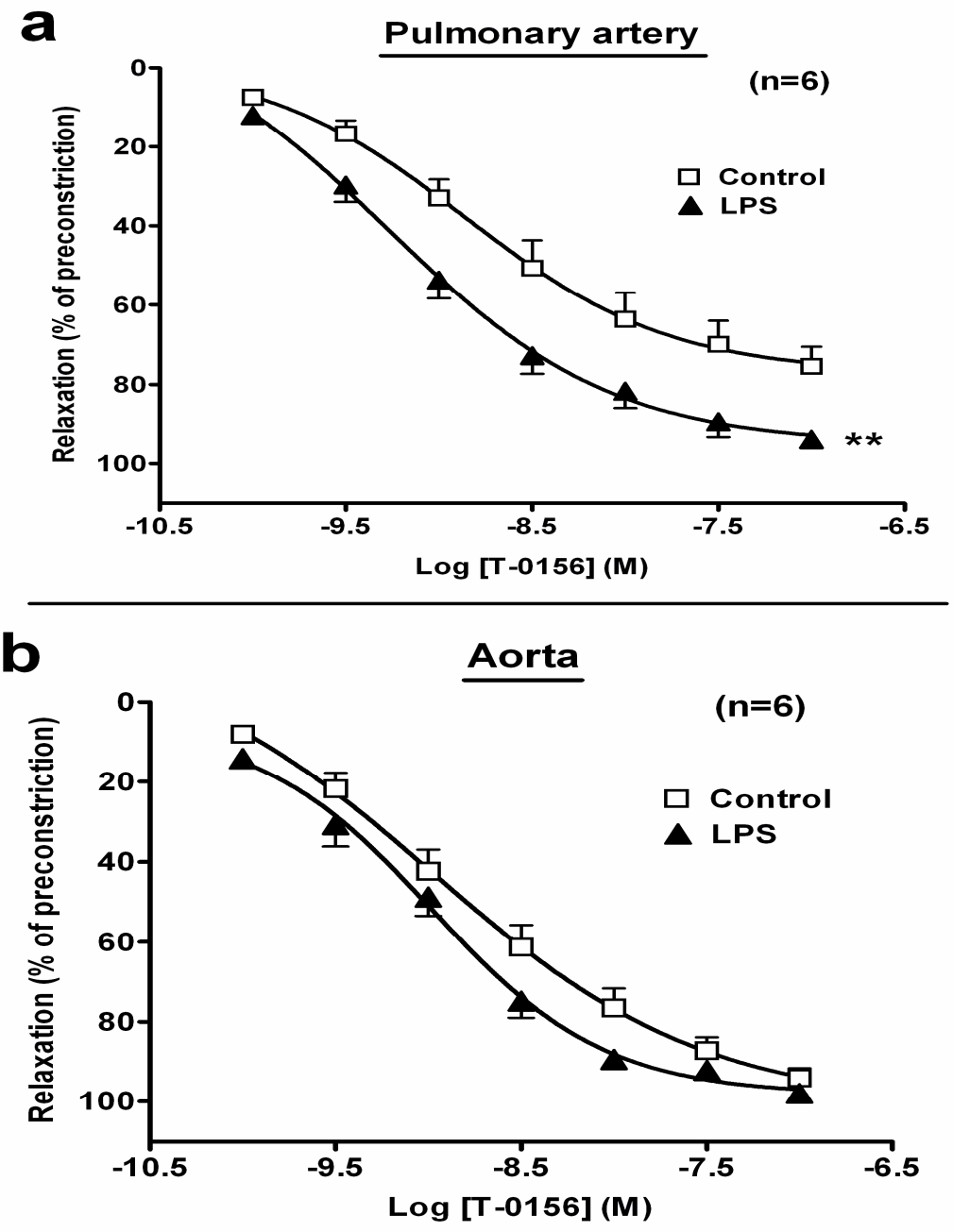

Figure 4.16 Effect of LPS treatment on T-0156-induced relaxation in the pulmonary artery and the aorta. LPS (10 µg ml^{-1}, 20 h)-treated pulmonary (a) and aortic (b) arterial rings were preconstricted with 30 nM ET-1 before measuring relaxation to T-0156 (0.1 nM-100 nM). Data are expressed as mean ± s.e.m., where (n) equals the number animals. **$p<0.01$ for E_{max} and pEC_{50} values compared with control group using paired Student's *t*-test.

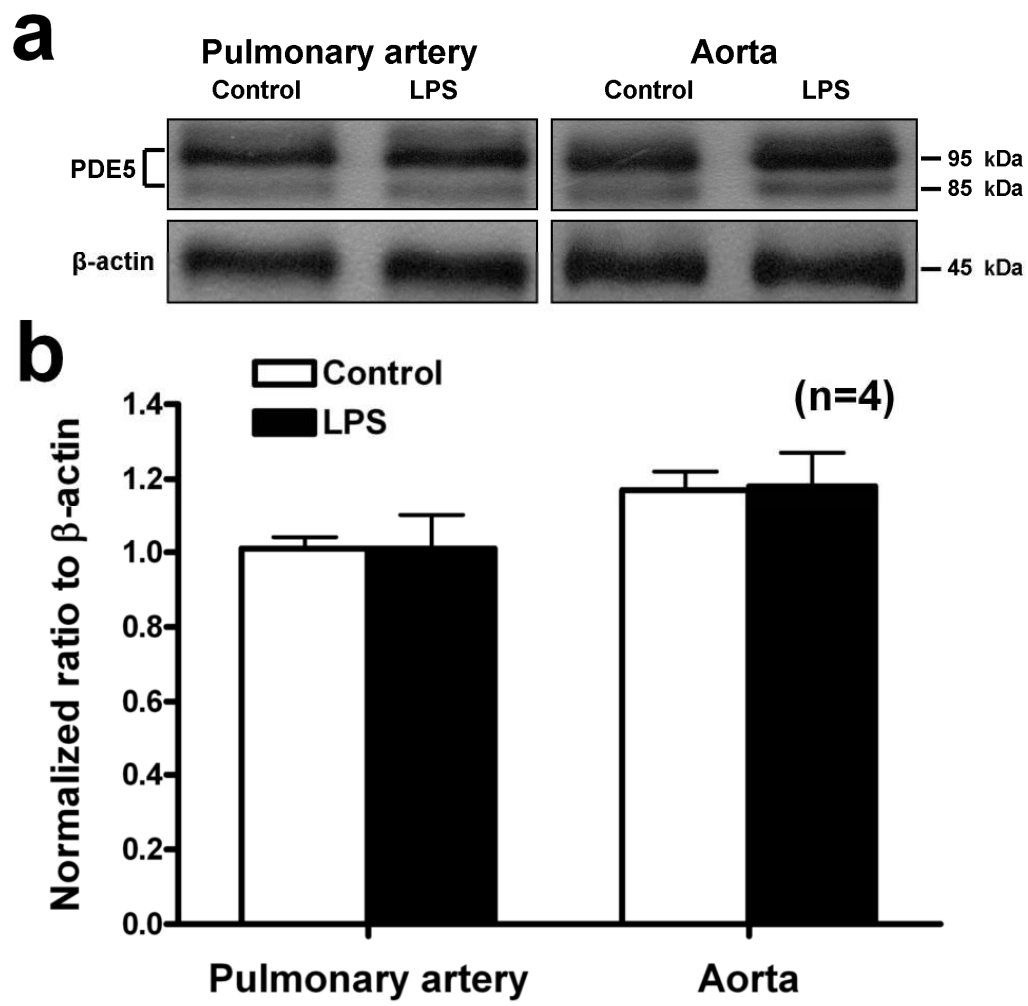

Figure 4.17 Effect of LPS on the protein expression levels of PDE5. (a) representative immunoblots for PDE5 in the pulmonary artery (left) and the aorta (right). (b) densitometric ratio of PDE5 protein subunits normalized to β-actin in the pulmonary artery and the aorta. Data are expressed as mean ± s.e.m., where (n) equals the number animals.

4.7 Discussion

The results presented in this chapter show that LPS activates sGC through a NO-independent pathway in the aorta. The effect of this activation is impaired in the pulmonary artery by decreasing protein expression of $sGC_{\beta 1}$ and by increasing PDE5 activity. As a consequence, LPS causes selective hypocontractility to ET-1 only in the aorta, while the pulmonary artery is not affected.

In both vessels, LPS significantly increased NO production via iNOS, as it was blocked by the selective iNOS inhibitor 1400W (1 μM). Such LPS-induced NO overproduction through iNOS was reported previously in the aorta (Griffiths *et al.*, 1995) and in the pulmonary artery (Bishop-Bailey *et al.*, 1997). We found, however, that ET-1 mediated contraction was significantly impaired only in the aorta but not in the pulmonary artery, a finding similar to observations in clinical sepsis where systemic vasodilation and pulmonary hypertension occurs (Manthous *et al.*, 1993; Lorente *et al.*, 1993) and to an *ex vivo* rat endotoxemic model using phenylephrine (McIntyre, Jr. *et al.*, 1997).

Endothelial removal did not affect vascular changes induced by LPS which is consistent with previous reports (McKenna, 1990; Hall *et al.*, 1996; O'Brien *et al.*, 2001), suggesting that endothelium does not play a major role in LPS-induced aortic hypocontractility to ET-1. Moreover, the expression of eNOS was not different between control and LPS-treated pulmonary and aortic vascular rings, while relaxation to ACh, an endothelium-dependent vasorelaxant, was impaired in both vessels. The impaired endothelium-dependent relaxations observed in endotoxemic blood vessels may result from several mechanisms including alteration in eNOS expression, activation, and signal transduction in addition to the mechanisms involved in NO release and degradation (Matsuda & Hattori, 2007). The eNOS expression has been shown to be diminished in blood vessels from rabbits (Matsuda *et al.*, 2003) and in lung tissues from mice (Matsuda *et al.*, 2004) following induction of sepsis with LPS. Furthermore, it has been demonstrated that sepsis causes a progressive and profound reduction in phosphorylation of eNOS in rabbit mesenteric arteries, possibly as a result of impaired phosphatidylinositol-3-kinase pathway (Matsuda *et al.*, 2006), suggesting less production of NO by eNOS in sepsis. Since

eNOS expression was not changed in this study, but ACh relaxation was decreased, it appears that either eNOS activity or the downstream signalling of NO is impaired. It is also worth noting that the impaired relaxation to ACh observed in both vessels is probably not involved in hypocontractility to ET-1 which was found only in the aorta.

LPS is also known to induce the expression of COX-2 (Bishop-Bailey *et al.*, 1997), suggesting that additional mechanisms are likely to contribute to LPS-induced changes in vascular reactivity. Inhibition of COX with indomethacin did not abolish the difference in contractile responses to ET-1 in LPS-treated aortic rings, indicating that COX may not play a major role in the present model. Similar results have been previously shown, where inhibition of COX-1 and/or COX-2 pathways does not reverse hypotension or vascular hyporeactivity induced by LPS (Bernard *et al.*, 1997; Leach *et al.*, 1998; O'Brien *et al.*, 2001). Similarly, inhibition of ROS, which could impair vascular reactivity, did not have a profound effect on LPS-induced changes in vascular reactivity to ET-1, suggesting a little role for ROS in the present system.

The selective inhibition of iNOS by 1400W was unable to prevent the aortic hypocontractility to ET-1, although the same concentration of 1400W did suppress the NO overproduction in both vessels. On the other hand, incubation with the sGC inhibitor ODQ prevented aortic LPS-induced hypocontractility to ET-1, leading to the conclusion that the hypocontractility is mediated through NO-independent regulator(s) of sGC activity. In addition, the aortic relaxation responses to the novel non-NO-based heme-dependent sGC activator BAY 41-2272 (Stasch *et al.*, 2001; Boerrigter & Burnett, Jr., 2007) were enhanced in the aorta, confirming that LPS treatment enhances NO-independent sGC activation in the aorta. These experiments show that inhibition of sGC could be more effective than NOS inhibition in preventing vascular hyporeactivity induced by LPS in systemic arteries.

LPS treatment in the present study decreased pulmonary artery relaxation responses to both the NO donor SNP and the sGC activator BAY 41-2272, suggesting that LPS treatment impairs sGC/cGMP pathway activation (both NO-dependent and independent) in the pulmonary artery. This impairment in sGC/cGMP pathway could be either due to an altered cGMP synthesis and/or

metabolism, or due to downstream changes in cGMP-effector signalling molecules such as PKG. Because the relaxation to the non-hydrolysable cGMP analogue 8-pCPT-cGMP was not affected in the LPS-treated vessels, cGMP-effector signalling molecules are not involved; leaving the likelihood that LPS modifies cGMP synthesis and/or degradation.

The involvement of the reduced synthesis of cGMP in the pulmonary artery is indicated by decreased sGC activity and was confirmed by a significant decrease in the expression of the $sGC_{\beta 1}$ subunit. Since both sGC subunits are required for the enzyme activity, reduced levels of either subunit lead to reduced sGC activity. Importantly, $sGC_{\beta 1}$ contains the major heme binding domain and seems to be more rapidly and robustly regulated after inflammatory stimuli (Takata *et al.*, 2001; Friebe & Koesling, 2003). Although previous studies demonstrate the involvement of sGC modulation in LPS-induced effects, these studies detected sGC in whole lung tissue or in isolated VSMCs, but not in isolated pulmonary arteries. For example, LPS decreases sGC activity and $sGC_{\beta 1}$ protein expression in rat lung (Fernandes *et al.*, 2006) and the expression of $sGC_{\beta 1}$ mRNA and both sGC protein subunits in mice lung (Glynos *et al.*, 2007). It is noteworthy that LPS decreases $sGC_{\alpha 1}$ but not $sGC_{\beta 1}$ expression in cultured rat aortic (Papapetropoulos *et al.*, 1996) or pulmonary (Scott & Nakayama, 1998) smooth muscle cells, raising the possibility that expression of sGC subunits may be influenced by cell isolation or culture.

Besides reduced cGMP synthesis by sGC, an increased degradation of cGMP by PDE5 could also contribute to NO hyporeactivity in the pulmonary artery. This was directly confirmed using T-0156, a potent and highly selective PDE5 inhibitor (Mochida *et al.*, 2002). Since the enhanced pulmonary artery relaxation to T-0156 in LPS-treated tissue was not associated with changes in protein expression of PDE5, the most likely explanation is that the activity of PDE5 was increased. An increased PDE5 activity was demonstrated in perfused rat lungs isolated from rats 18 h after LPS injection (Holzmann *et al.*, 1996) and 1 h after LPS inhalation in guinea pig lungs (Toward *et al.*, 2005) but was decreased after 48 h in the same model. The mechanism for increased PDE5 activity could include PKG-mediated phosphorylation and allosteric cGMP binding (either of which will upregulate PDE5 activity) and a decreased PP1 phosphatase activity and/or expression (Lin *et al.*,

2006). The latter will lead to a decreased dephosphorylation of PDE5, leading to maintained or enhanced PDE5 activity (Lin *et al.*, 2006). Since the results with the non-hydrolysable cGMP analogue suggest that downstream cGMP-effector signalling molecules are not affected by pre-treatment of vessels with LPS, downregulation of PP1 phosphatase activity and/or expression seems likely.

In sepsis, excessive vasodilation is counterbalanced by increased release of vasoconstrictors such as ET-1 and angiotensin II (Knotek *et al.*, 2000), therefore reduced sensitivity to sGC activation and increased PDE5 activity in pulmonary arteries could contribute to the development of pulmonary hypertension during sepsis. These mechanisms could also explain, at least in part, why a significant fraction (up to 30%) of pulmonary hypertensive patients fail to respond to therapeutic doses of inhaled NO (Holzmann *et al.*, 1996).

4.8 Summary and conclusions

By using an organ culture method and different inhibitors to the vasoactive mediators that could be involved in LPS-induced changes in vascular reactivity to ET-1 in the pulmonary artery and the aorta, the main findings are:

1- LPS-induced changes in vascular reactivity to ET-1 were not affected by endothelium removal, COX inhibition, ROS inhibition, or iNOS inhibition, but were abolished by sGC inhibition.

2- eNOS expression was not significantly affected by LPS, but iNOS expression was progressively increased leading to NO overproduction in both the pulmonary artery and the aorta.

3- Endothelium-dependent relaxation was impaired by LPS in both vessels, but endothelium-independent relaxation and cGMP production was impaired only in the pulmonary artery.

4- Relaxation responses to PDE-resistant cGMP analogue was not affected in either vessel, while relaxation to a direct sGC activator was decreased in the pulmonary artery and increased in the aorta.

5- The $sGC_{\beta 1}$ protein expression was decreased only in the pulmonary artery, while $sGC_{\alpha 1}$ expression was not affected in either vessel.

6- LPS increased relaxation responses to the PDE5 inhibitor T-0156 only in the pulmonary artery, but without changes in PDE5 protein expression.

In conclusion, LPS treatment *in vitro* causes a selective hypocontractility of rat aorta to ET-1, which is largely mediated by NO-independent activation of sGC. The pulmonary artery is not affected because LPS induces a desensitization of the sGC/cGMP dependent pathway by decreasing protein expression levels of $sGC_{\beta 1}$, and hence sGC activity, and increasing PDE5 activity. Neither endothelium, COX nor ROS are involved in these LPS effects. Therefore, sGC and/or PDE5-selective inhibitors could be important in controlling systemic and pulmonary vasomotor complications in sepsis.

Chapter 5

Result III: Molecular Mechanisms Involved in LPS-induced Changes in Vascular Reactivity

Chapter 5

5.1 Introduction

Numerous experimental studies of sepsis have clearly documented the presence of both *in vivo* and *in vitro* vascular hyporesponsiveness to α-adrenergic agonists (Guc *et al.*, 1990; O'Brien *et al.*, 2001; Farmer *et al.*, 2003), AngII (Umans *et al.*, 1993), KCl (Wakabayashi *et al.*, 1987; Umans *et al.*, 1993), ET-1 (Curzen *et al.*, 1997; Ishimaru *et al.*, 2001), serotonin (Wakabayashi *et al.*, 1987; Umans *et al.*, 1993), vasopressin (Guc *et al.*, 1990) and TxA_2 (Piepot *et al.*, 2002; Boer *et al.*, 2005). Vascular hyporesponsiveness could be mediated either by an increase in vasodilating or a decrease in vasoconstricting mechanisms. Excessive production of vasodilator molecules, such as NO, has been shown to contribute to the hypotension and vasoplegia in septic shock (Lorente *et al.*, 1993; Szabo *et al.*, 1995; Liu *et al.*, 1997), however inhibition of NO production yields conflicting results.

Membrane hyperpolarization by K^+ channel opening, mainly the BK and K_{ATP} channels, has been shown to account for the observed vascular hyporeactivity of septic shock (Chen *et al.*, 2000; Farias *et al.*, 2002; Wu *et al.*, 2004; O'Brien *et al.*, 2005; Pickkers *et al.*, 2006). Using different blockers for K_{ATP} and BK resulted in conflicting results. For example, the K_{ATP} channel inhibitor glibenclamide restored blood pressure in canine, porcine and rat *in vivo* models of LPS-induced shock (Wu *et al.*, 1995; Vanelli *et al.*, 1995; Gardiner *et al.*, 1999; Sorrentino *et al.*, 1999), but had no effect on vascular hyporeactivity in all ex vivo organ bath studies to date (Wu *et al.*, 1995; Taguchi *et al.*, 1996). Similarly, the BK channel inhibitor iberiotoxin restored aortic hyporeactivity to phenylephrine in endotoxemic rat *ex vivo* (Taguchi *et al.*, 1996), but did not protect against LPS-induced mortality in mice (Cauwels & Brouckaert, 2008).

Receptor-mediated vasoconstriction, which may also be affected in sepsis, could involve changes in receptor expression, Ca^{2+}-entry pathways, $[Ca^{2+}]_i$ and Ca^{2+} sensitization. Only a limited number of studies have examined the role of Ca^{2+} entry pathways in sepsis-induced vascular hyporeactivity without investigating Ca^{2+} sensitization or changes in receptor expression in the same model. For example, mesenteric hyporeactivity to the α-adrenergic agonist methoxamine in rat (Farmer *et*

al., 2003) or hyperreactivity to ET-1 in pig (Jones *et al.*, 1999) were not associated with changes in $[Ca^{2+}]_i$, while aortic vascular hyporeactivity to KCl was associated with enhanced Ca^{2+} uptake (Wakabayashi *et al.*, 1987) or with no change in $[Ca^{2+}]_i$ release (Biguad *et al.*, 1990).

The mechanisms involved in LPS-induced changes in vascular reactivity to ET-1 in the pulmonary artery and the aorta were evaluated by measuring changes in the expression levels of mRNA of ET-1, ET_A and ET_B and the expression levels of PKC and phosphorylation of MLC_{20}, ROKα, CPI-17 and MYPT1. The role of external Ca^{2+} and changes in $[Ca^{2+}]_i$ have also been studied.

5.2 Methods

Pulmonary and aortic arterial rings were incubated with LPS (10 µg ml^{-1}, 20 h) before measuring the following:

- mRNAs expression levels of ET-1 and its receptors (ET_A or ET_B) by qRT-PCR.
- contractile responses to ET-1 (0.3 nM-100 nM) in the presence or absence of external Ca^{2+}, K_{ATP} inhibitor glibenclamide (10 µM) or BK inhibitor iberiotoxin (100 nM).
- relaxation responses to the L-type VOCCs blocker nifedipine (1 nM- 30 µM), PKC inhibitor Ro-31-8425 (300 nM), ROKα inhibitor Y-27632 (100 nM- 30 µM) and the ROCCs and SOCCs blocker SKF-96365 (10 µM).
- the expression levels of PKC and phosphorylation of MLC_{20}, ROKα, CPI-17 and MYPT1 by Immunoblotting
- changes in aortic VSMCs $[Ca^{2+}]_i$ induced by ET-1 in the presence or absence of external Ca^{2+}, 20 µM diltiazem or 10 µM SKF-96365.
- contractile responses to ET-1 (0.3 nM-100 nM) in the presence of the protein synthesis inhibitor cycloheximide (10 µM)

5.3 Effect of LPS-pretreatment on gene expression of ET-1, ET_A and ET_B in pulmonary and aortic vascular rings

The PCR primers designed for ET-1, ET_A and ET_B together with the housekeeping gene β-actin were tested first by using normal PCR to detect presence of the expected products at 66, 71, 107 and 72 bp respectively (Figure 4.4). Melt-curve analyses, verifying specific amplification and absence of secondary primers products, and PCR standard curves of both the target (ET-1, ET_A and ET_B) and reference (β-actin) genes are shown in Figure 5.1.

Incubation of the pulmonary and aortic rings with LPS for 4, 8 or 20 h did not result in significant differences in the mRNAs expression levels of ET-1, ET_A or ET_B (Figure 5.2) when compared with the their matchged time-controls. This evidence argues against the involvement of changes in gene expression of ET-1 and its receptors in the observed LPS-induced aortic hyporeactivity to ET-1. However, it is acknowledged that the strength of this conclusion is limited by the small number of observations.

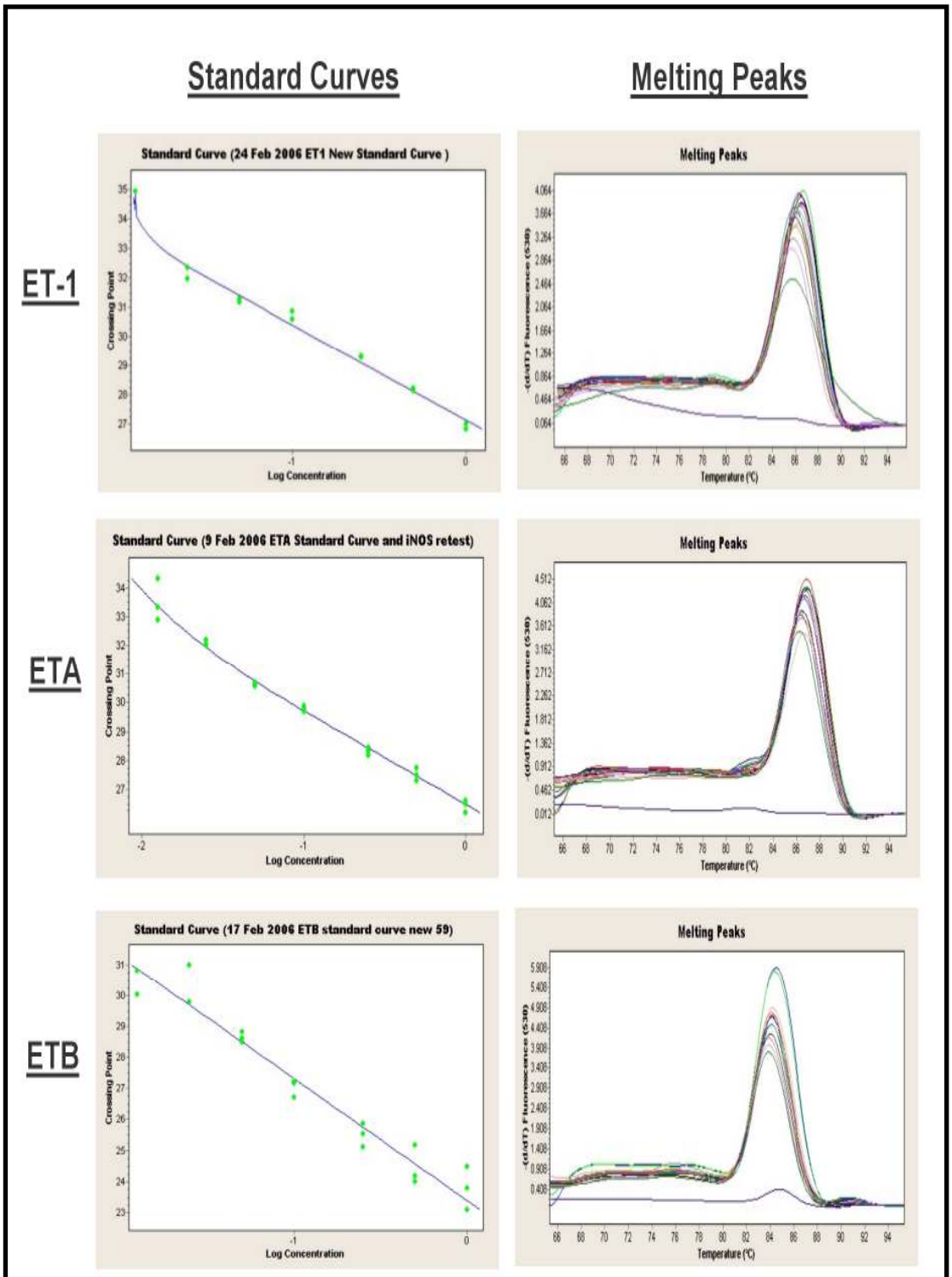

Figure 5.1 Representative qRT-PCR standard curves and melting peaks for ET-1, ET_A and ET_B. RNA was extracted from control and LPS (10 µg ml^{-1})-treated vascular rings at 0, 4, 8 and 20 h and reverse-transcribed into cDNA before carrying out quantitative RT-PCR using the Lightcycler.

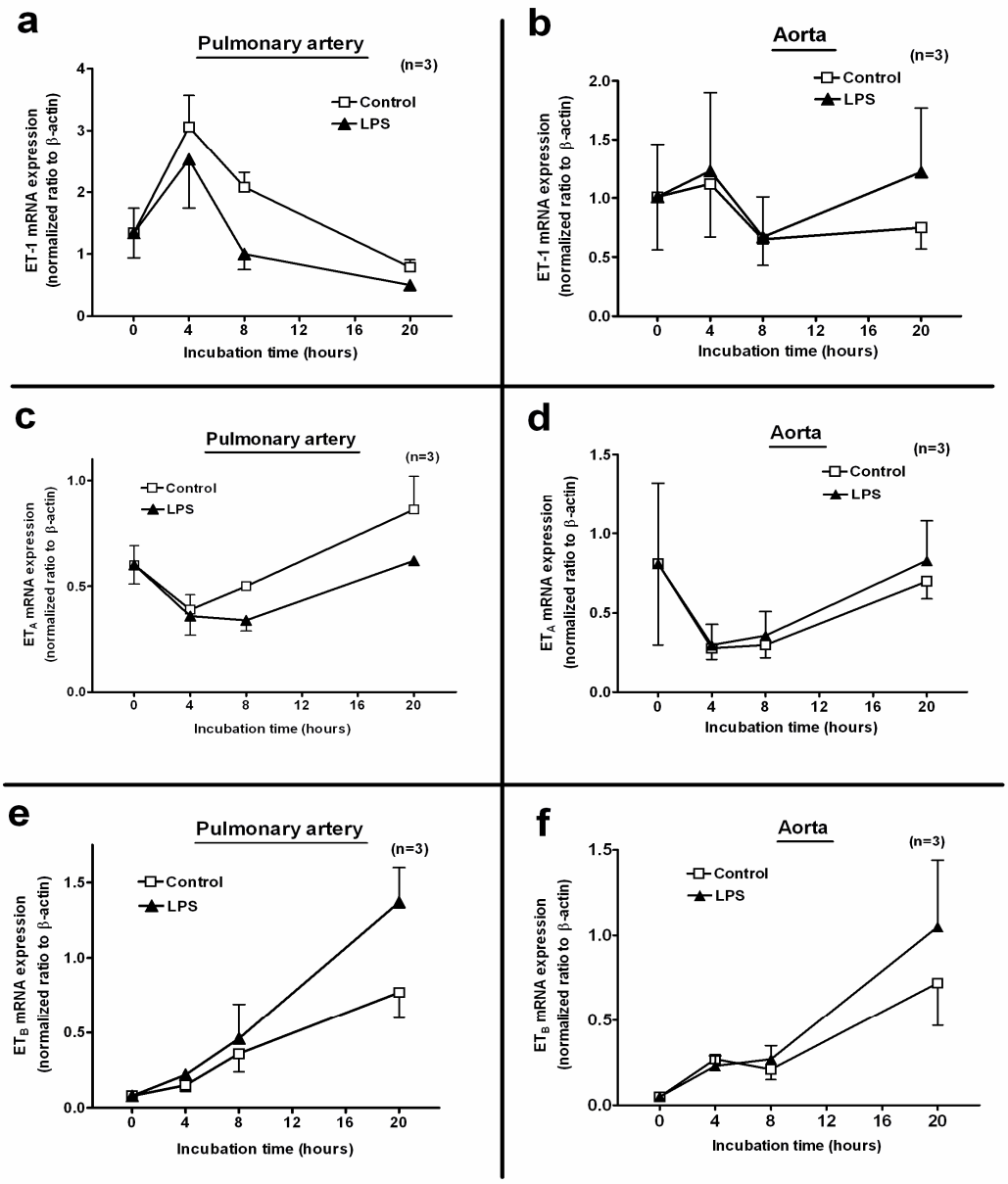

Figure 5.2 Effect of LPS on gene expression of ET-1, ET_A and ET_B in the pulmonary artery and the aorta. RNA was extracted from control and LPS (10 µg ml^{-1})-treated vascular rings at 0, 4, 8 and 20 h and reverse-transcribed into cDNA before carrying out qRT-PCR to detect changes in the gene expression of ET-1 (a and b), ET_A (b and c) and ET_B (e and f) in the pulmonary artery and aorta respectively. Data are expressed as mean ± s.e.m., where (n) equals the number of independent experiments, each using duplicate PCR reactions from the same sample prepared from pooled tissue lysates of 2 animals.

5.4 Effect of external Ca^{2+} removal on LPS-induced changes in vascular reactivity to ET-1

As previously mentioned in chapter 3, LPS selectively causes hyporeactivity to ET-1 in the aorta but not in the pulmonary artery (Figure 3.5). Removal of external Ca^{2+} had a significant effect on this selective LPS-induced vascular reactivity to ET-1. In the pulmonary artery, removal of external Ca^{2+} decreased maximal contractility to ET-1 as manifested by the decreased E_{max} for both the control (from 4.3±0.2 mN to 1.1±0.1 mN) and LPS-treated (from 4.4±0.2 mM to 1.0±0.1 mN) without revealing a difference between both of them (Figure 5.3a). Similarly, removal of external Ca^{2+} decreased E_{max} for both the control (from 8.0±0.4 mN to 4.0±0.4 mN) and LPS-treated (from 6.0±0.4 mN to 4.0±0.3 mN) aortic rings. However, this decrease in E_{max} in the aorta by removal of external Ca^{2+} abolished the difference in ET-1-induced contractions in the control and LPS-treated aortic rings (Figure 5.3b). This result suggests that external Ca^{2+} plays a major role in LPS-induced changes in vascular reactivity to ET-1.

5.5 Effect of external Ca^{2+} addition on LPS-induced changes in vascular reactivity to ET-1

In experiments performed to determine the role of Ca^{2+} influx, the addition of Ca^{2+} (0.1-10 mM) to pulmonary and aortic rings preconstricted with 100 nM ET-1 resulted in a stepwise increase in vessel contraction (Figure 5.4). The E_{max} values of this stepwise contractile response to Ca^{2+} addition was not affected by LPS-pretreatment in the pulmonary artery (Figure 5.5a), but it was significantly reduced by 56±8 % after LPS-pretreatment in aortic rings ($p<0.01$, $n=5$) (Figure 5.5b). The presence of the L-type VOCCs blocker nifedipine (10 µM) had no significant effect on contractile responses to external Ca^{2+}. This result suggests that external Ca^{2+} influx through non-VOCCs plays a major role in LPS-induced changes in vascular reactivity to ET-1.

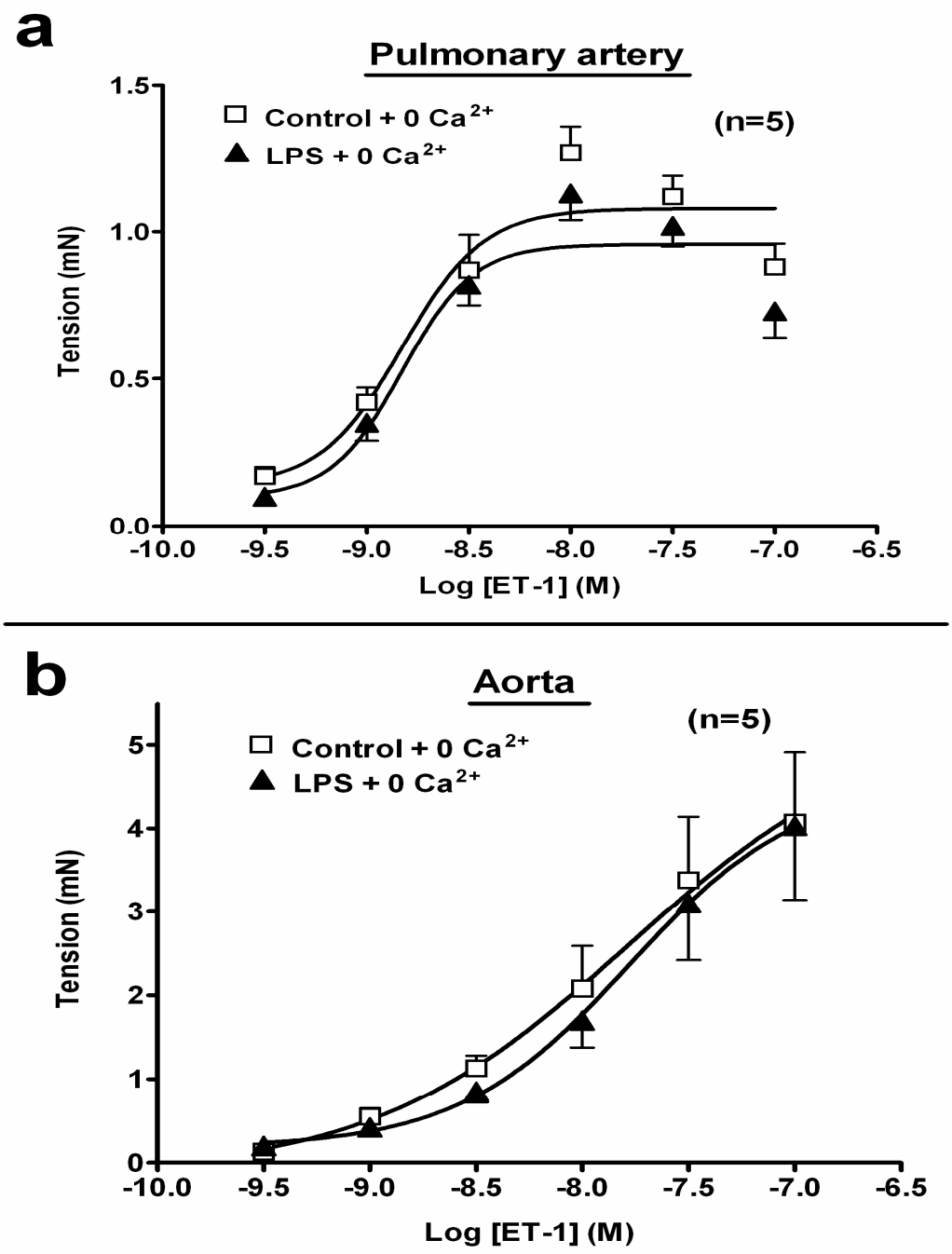

Figure 5.3 Effect of removal of external Ca^{2+} on LPS-induced changes in vascular reactivity to ET-1 in the pulmonary artery and the aorta. Contraction to ET-1 (0.3 nM-100 nM) was measured in the absence of external Ca^{2+} in the pulmonary artery (a) and aorta (b) after incubation with LPS (10 µg ml^{-1}, 20 h). Data are expressed as mean ± s.e.m., where (n) equals the number animals.

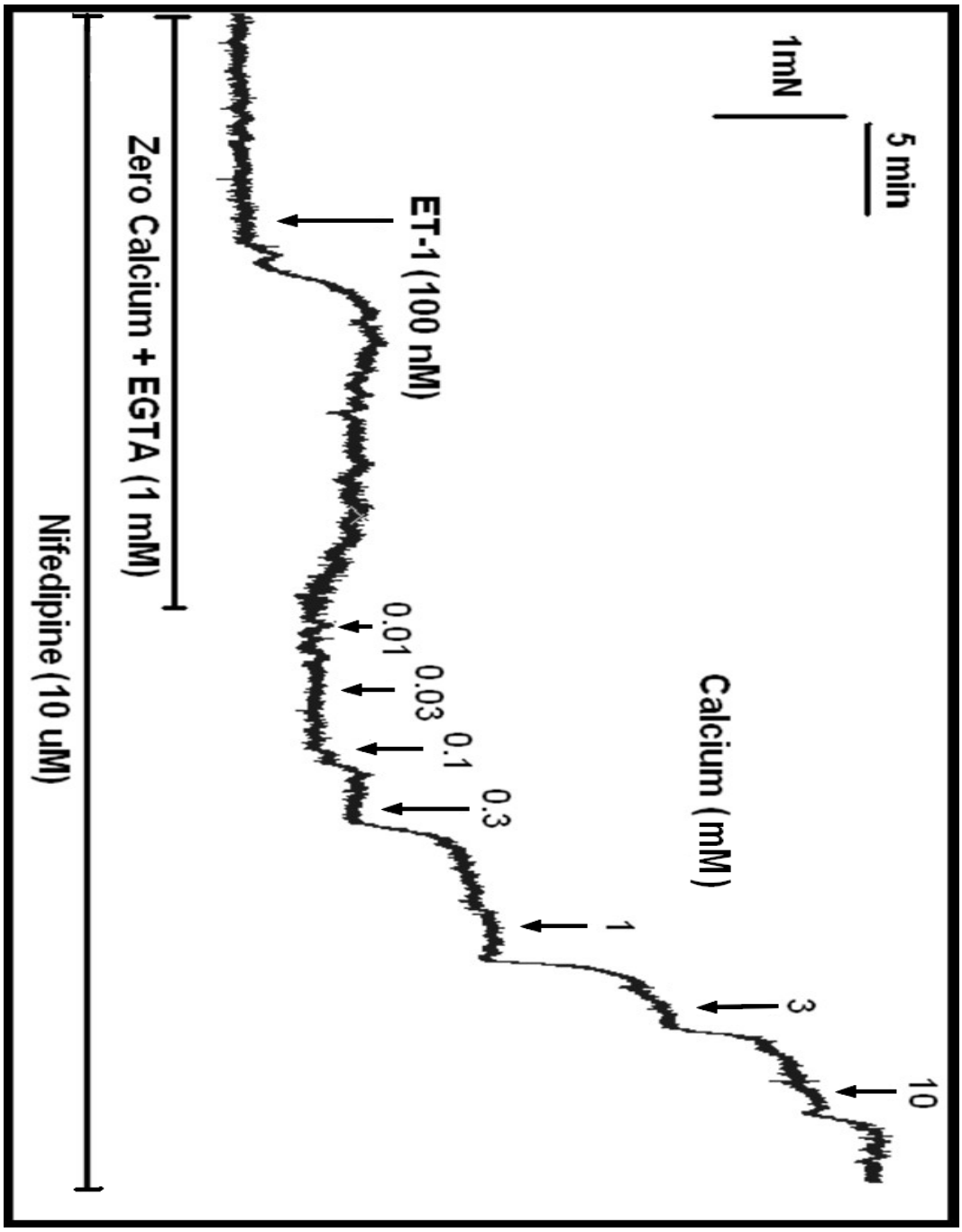

Figure 5.4 Representative control trace of contractile response to Ca^{2+} addition. This trace is showing the effect of subsequent increases in extracellular Ca^{2+} on the aorta preconstricted with 100 nM ET-1 in the presence of 10µM nifedipine. The starting point of Ca^{2+} addition at the plateau of ET-1 contraction was taken as the baseline for the Ca^{2+} response curve.

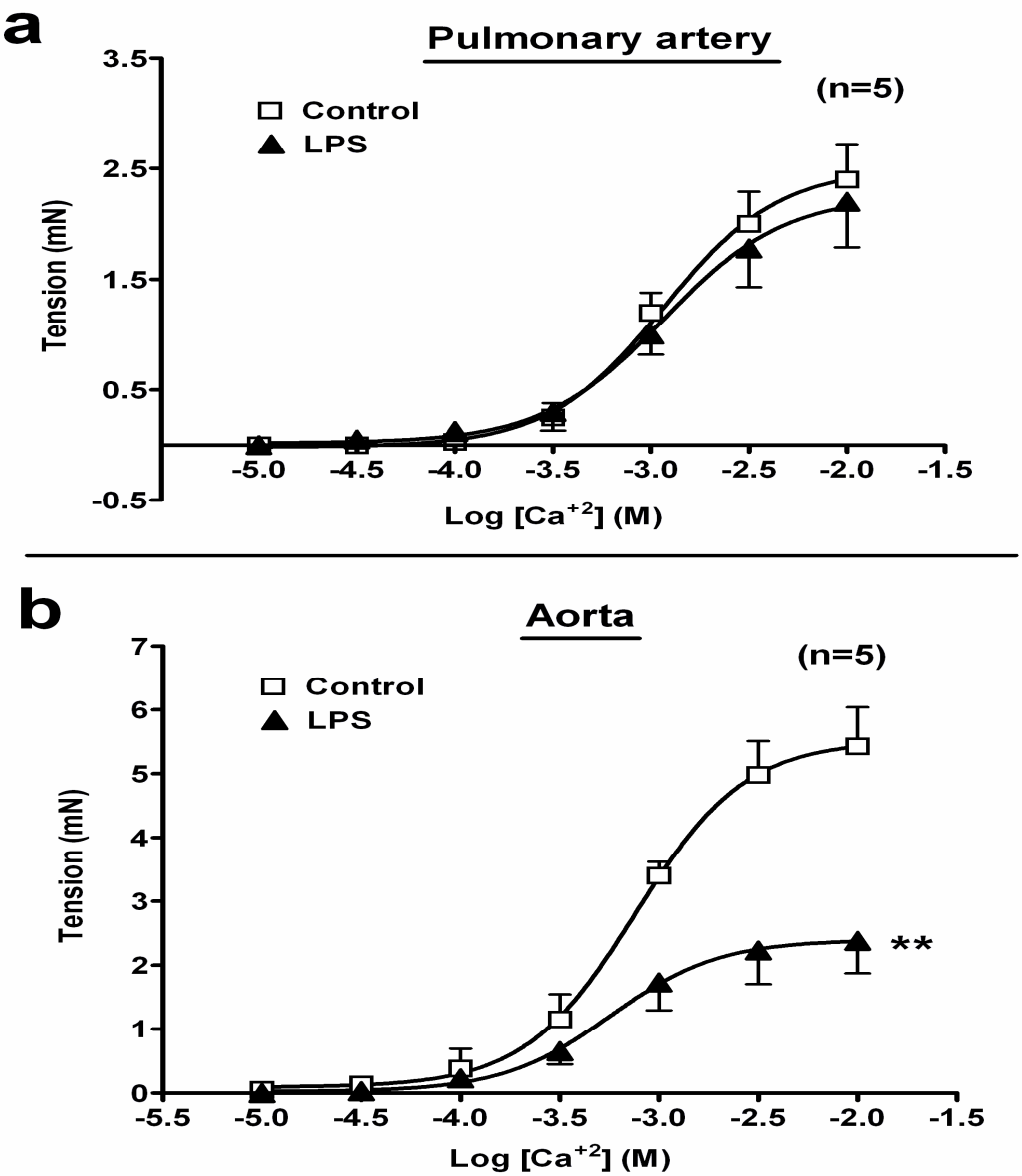

Figure 5.5 Effect of LPS on contractile responses to Ca^{2+} addition in the pulmonary artery and the aorta preconstricted with ET-1. Contraction responses to the addition of Ca^{2+} (0.1-10 mM) was measured in control and LPS (10 µg ml^{-1}, 20 h)- treated pulmonary (a) and aortic (b) rings preconstricted with 100 nM ET-1 in presence of 10µM nifedipine. The starting point of Ca^{2+} addition at the plateau of ET-1 contraction was taken as the baseline for the Ca^{2+} response curve. Data are expressed as mean ± s.e.m., where (n) equals the number animals. ** $p<0.01$ for E_{max} and pEC_{50} values compared with control group using paired Student's *t*-test.

5.6 Effect of VOCCs blocking on LPS-induced changes in vascular reactivity to ET-1

Blocking of L-type VOCCs by nifedipine caused approximately a 50% relaxation of both the pulmonary (Figure 5.6a) and aortic (Figure 5.6b) rings preconstricted with 30 nM ET-1, suggesting the presence of other types of Ca^{2+} channels that is involved in ET-1-induced contractions. In both the pulmonary artery and the aorta, no significant changes were found between the control and LPS-treated vascular rings preconstricted with 30 nM ET-1 in the relaxation responses to nifedipine (0.1-30 μM), suggesting that changes in VOCCs are not responsible for LPS-induced aortic hyporeactivity to ET-1.

5.7 Effect of blocking of ROCCs and SOCCs on LPS-induced changes in vascular reactivity to ET-1

By using 10 μM SKF-96365, which is a blocker of ROCCs and SOCCs, a similar 50% relaxation was obtained in both the pulmonary and aortic rings preconstricted with 30 nM ET-1 (Figure 5.7) suggesting the involvement of ROCCs and/or SOCCs in ET-1-induced contractions. In the pulmonary artery, there was no significant difference in the relaxation induced by 10 μM SKF-96365 between control and LPS-treated rings. However, LPS-pretreatment decreased SKF-6365-induced relaxation in the aorta ($p<0.05$, $n=4$), suggesting that ROCCs and/or SOCCs could be downregulated or deactivated by LPS.

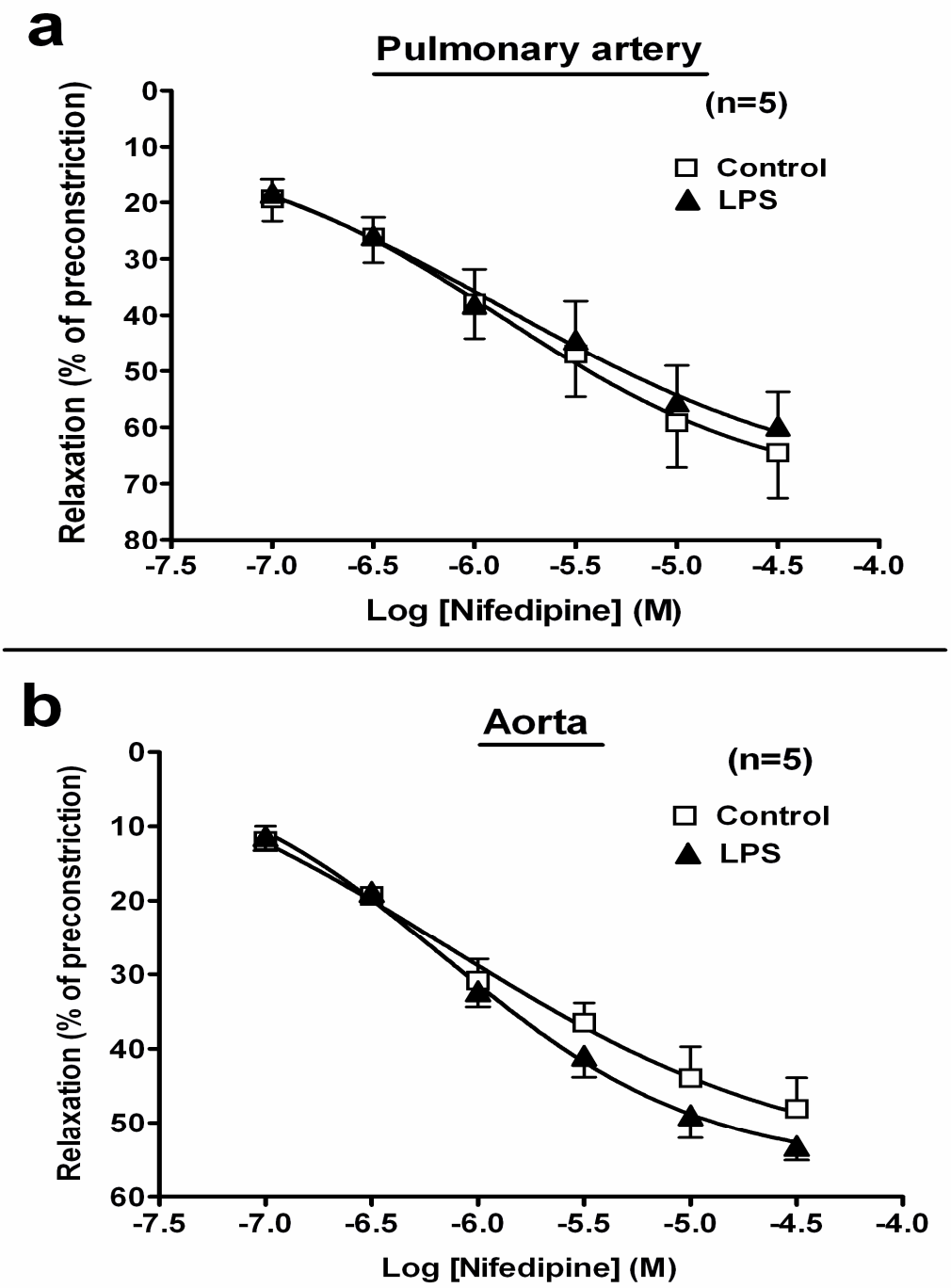

Figure 5.6 Effect of LPS on relaxation responses to nifedipine in the pulmonary artery and the aorta. Pulmonary (a) and aortic (b) arterial rings from control and LPS (10 μg ml^{-1}, 20 h)-treated groups were preconstricted with 30 nM ET-1 before measuring relaxation responses to nifedipine (1 nM- 30 μM). Data are expressed as mean ± s.e.m., where (n) equals the number animals.

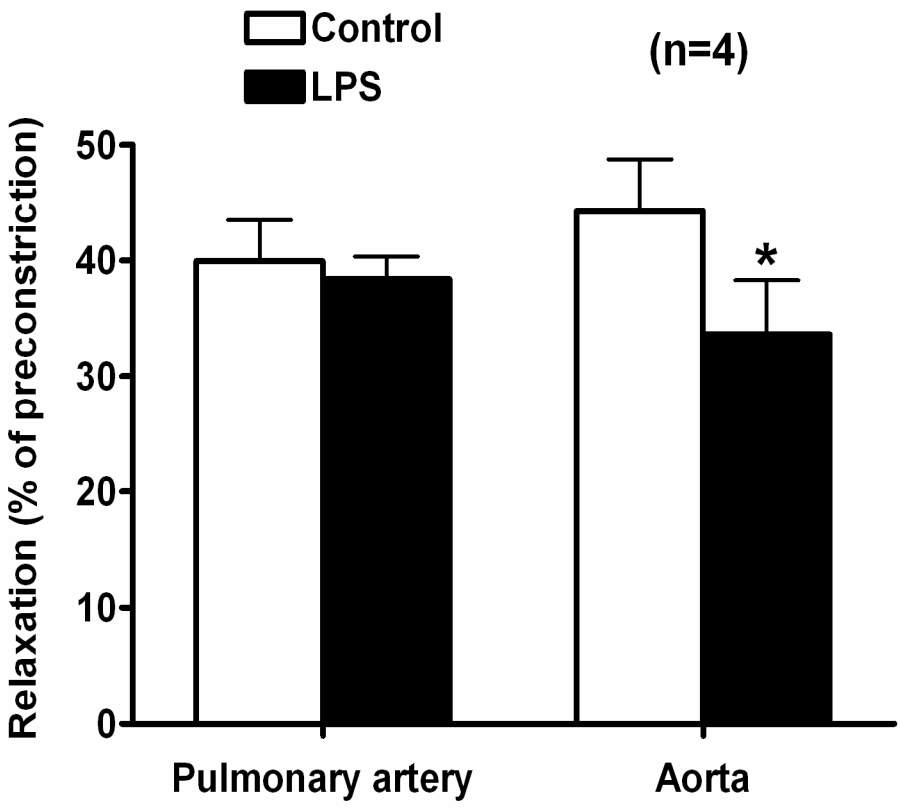

Figure 5.7 Effect of LPS on relaxation responses to 10 µM SKF-96365 in the pulmonary artery and the aorta. Pulmonary and aortic arterial rings from control and LPS (10 µg ml^{-1}, 20 h)-treated groups were preconstricted with 30 nM ET-1 before measuring relaxation to 10 µM SKF-96365. Data are expressed as mean ± s.e.m., where (n) equals the number animals. * $p<0.05$ compared with control group using paired Student's *t*-test.

5.8 Effect of K_{ATP} channels blocking on LPS-induced changes in vascular reactivity to ET-1

K_{ATP} channels represent a possible pathway that could be involved in LPS-induced vascular effects. Blocking of K_{ATP} channels by glibenclamide (10 μM, 30 min) caused no significance difference in ET-1-induced contraction between control and LPS-treated pulmonary artery (Figure 5.8a). In the aorta, glibenclamide did not abolished the LPS-induced hyporeactivity to ET-1 (Figure 5.8b), since there was still a 27±4 % decrease in E_{max} in the LPS group compared to control, suggesting that K_{ATP} channels are not affected by LPS treatment in this model.

5.9 Effect of BK channels blocking on LPS-induced changes in vascular reactivity to ET-1

BK channels are another important pathway that could play an important role in LPS-induced vascular hyporeactivity. Blocking of BK channels by incubation with 100 nM iberiotoxin for 30 min before measuring the contraction to ET-1 caused no significance difference in ET-1-induced contraction between control and LPS-treated pulmonary artery (Figure 5.9a). In the aorta, iberiotoxin did not abolish the LPS-induced hyporeactivity to ET-1 (Figure 5.9b), since there still a 25±4 % decrease in E_{max} in the LPS group compared to control, suggesting that BK channels are not involved in LPS-induced changes in contraction responses to ET-1.

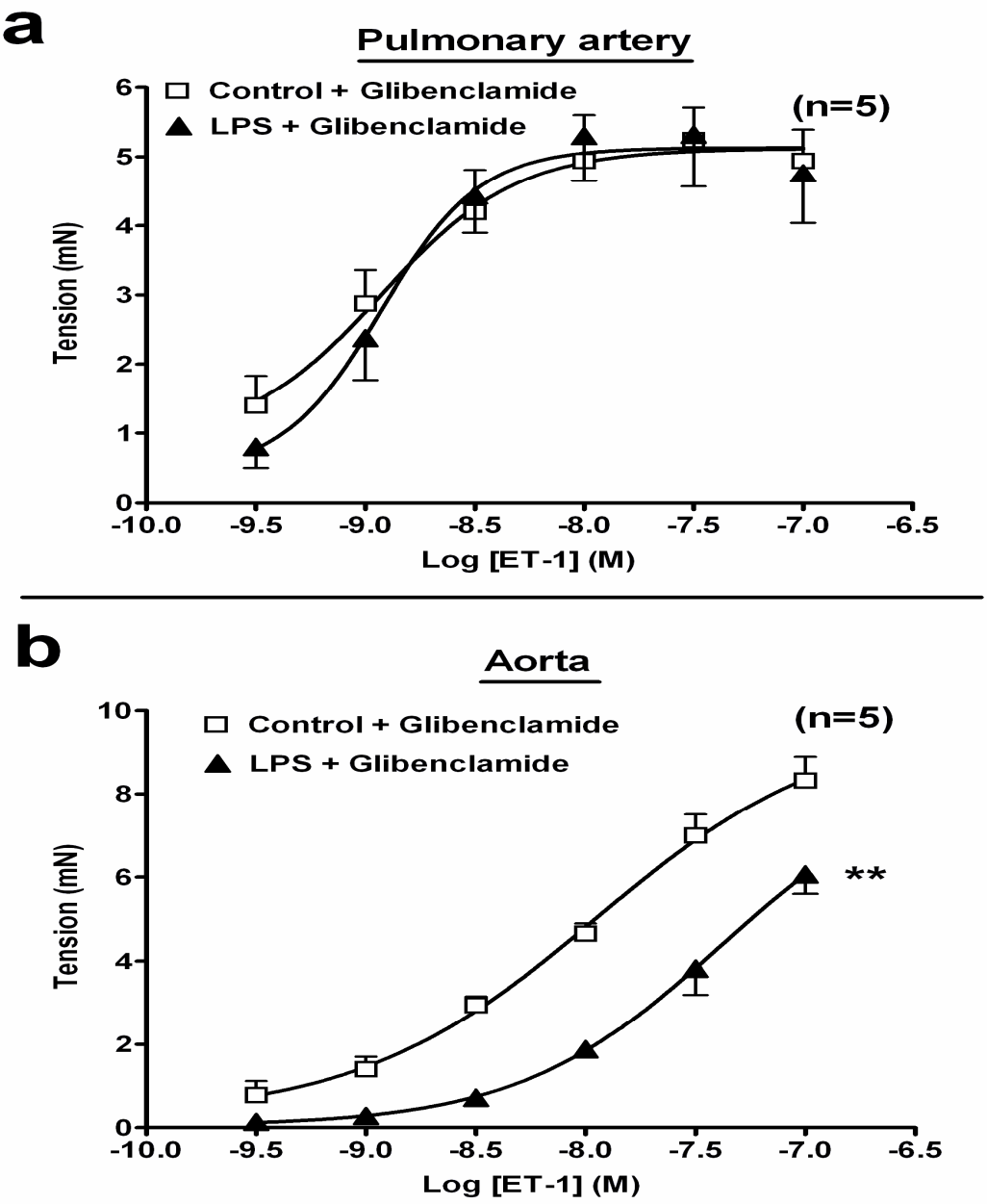

Figure 5.8 Effect of glibenclamide on LPS-induced changes in contractile responses to ET-1 in the pulmonary artery and aorta. Control and LPS (10 µg ml^{-1}, 20 h)-treated pulmonary (a) and aortic (b) rings were incubated with the K_{ATP} channel blocker glibenclamide (10 µM, 30 min) before measuring the contraction to ET-1 (0.3 nM-100 nM). Data are expressed as mean ± s.e.m., where (n) equals the number animals. ** $p<0.01$ for E_{max} and pEC_{50} values compared with control group using paired Student's *t*-test.

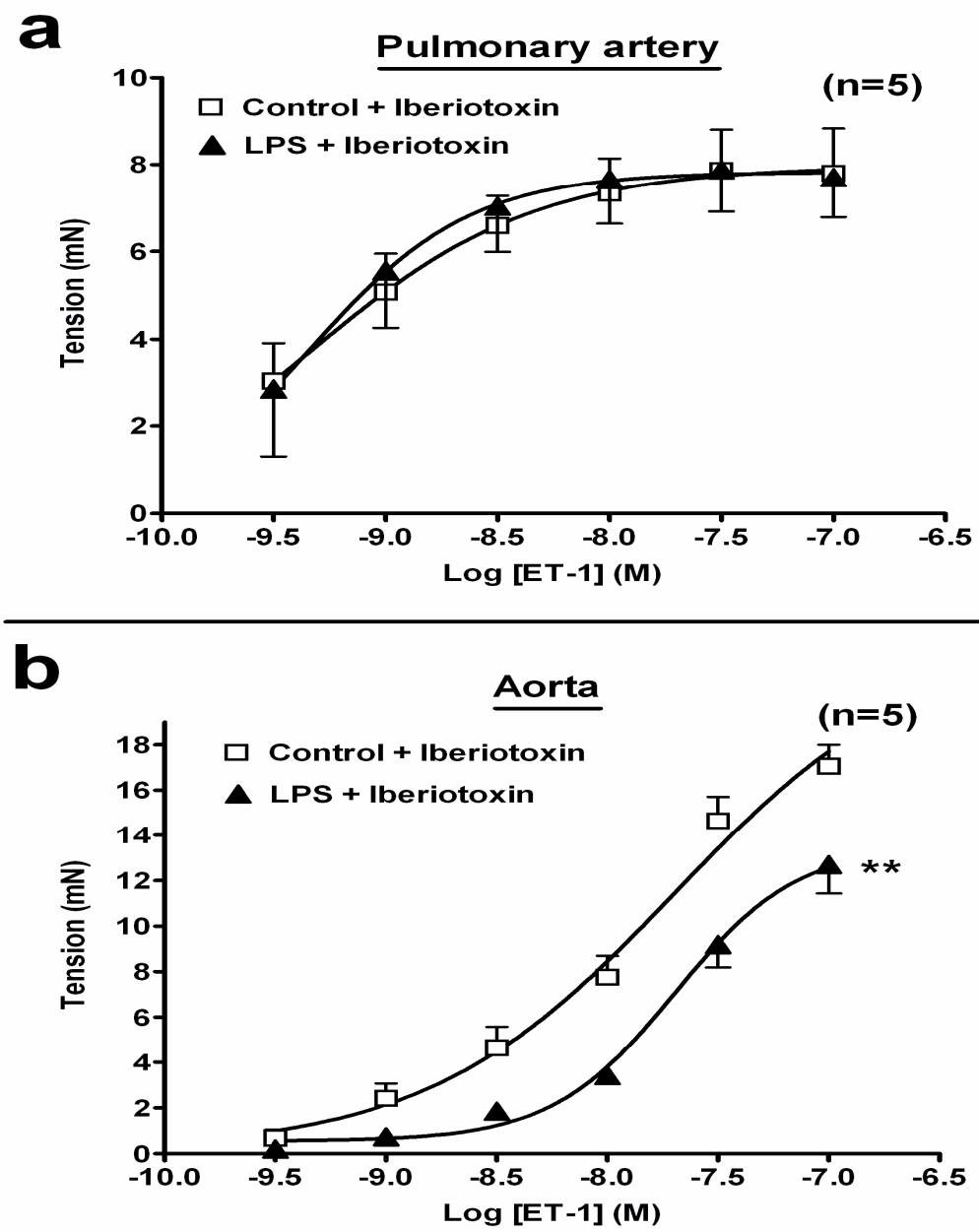

Figure 5.9 Effect of iberiotoxin on LPS-induced changes in contractile responses to ET-1 in the pulmonary artery and aorta. Control and LPS (10 µg ml^{-1}, 20 h)-treated pulmonary (a) and aortic (b) rings were incubated with the BK channel blocker iberiotoxin (100 nM, 30 min) before measuring the contraction to ET-1 (0.3 nM-100 nM). Data are expressed as mean ± s.e.m., where (n) equals the number animals. ** $p<0.01$ for E_{max} and pEC_{50} values compared with control group using paired Student's *t*-test.

5.10 Effect of ROKα inhibitor on LPS-induced changes in vascular reactivity to ET-1

Y-27632 is a selective inhibitor of ROKα that affects Ca^{2+} sensitization by removing the inhibitory effect of ROKα on MLCP leading to relaxation. ROKα is involved in several pathological conditions and could represent a possible pathway through which LPS can cause vascular hyporeactivity. Application of Y-27632 (100 nM- 30 μM) on pulmonary and aortic rings preconstricted with 30 nM ET-1 resulted in a full relaxation. In both vessels, there was no significance difference in the relaxation responses induced by Y-27632 between control and LPS-treated pulmonary artery (Figure 5.10a) and aorta (Figure 5.10b), suggesting that Ca^{2+} sensitization through the ROKα pathway is not affected by LPS treatment in this model.

5.11 Effect of PKC inhibitor on LPS-induced changes in vascular reactivity to ET-1

Ro-31-8425 is a non-selective PKC inhibitor that can cause relaxation similar to ROKα inhibitor by by removing the inhibitory effect of PKC on MLCP. PKC is an important pathway involved in the mechanism of contraction of several vasoactive agents, including ET-1. PKC inhibition or downregulation could be a possible pathway involved in LPS-induced vascular hyporeactivity. Inhibition of PKC by adding 300 nM Ro-31-8425 on pulmonary and aortic rings preconstricted with 30 nM ET-1 resulted in around 50 % relaxation of the vessels (Figure 5.11). The relaxation responses induced by Ro-31-8425 in control group were not significantly different from that of LPS-treated groups in both the pulmonary artery and the aorta, suggesting that changes in PKC are not involved in LPS-induced changes in contraction responses to ET-1.

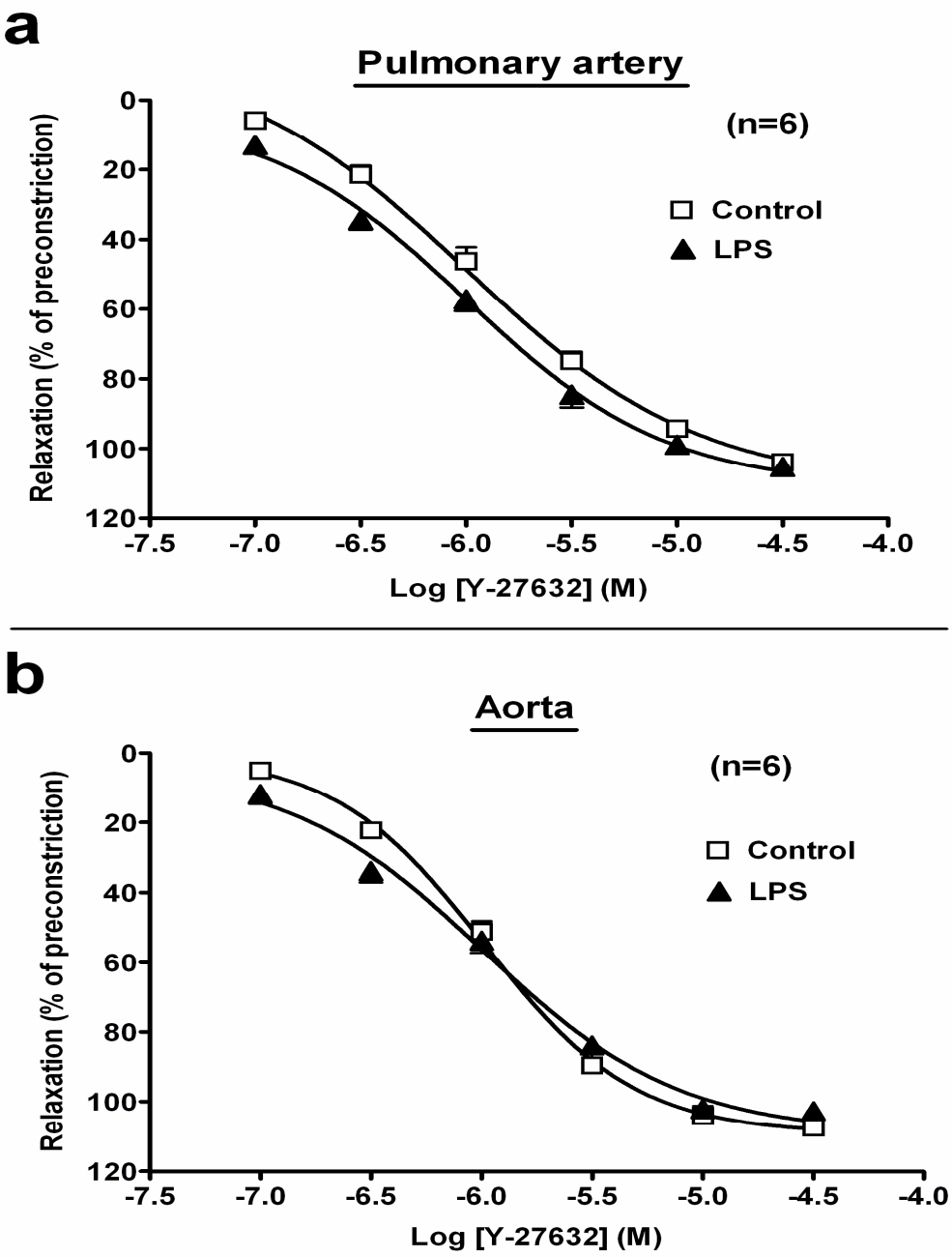

Figure 5.10 Effect of Y-27632 on LPS-induced changes in contractile responses to ET-1 in the pulmonary artery and aorta. Pulmonary (a) and aortic (b) arterial rings from control and LPS (10 µg ml^{-1}, 20 h)-treated groups were preconstricted with 30 nM ET-1 before measuring relaxation responses to Y-27632 (100 nM- 30 µM). Data are expressed as mean ± s.e.m., where (n) equals the number animals.

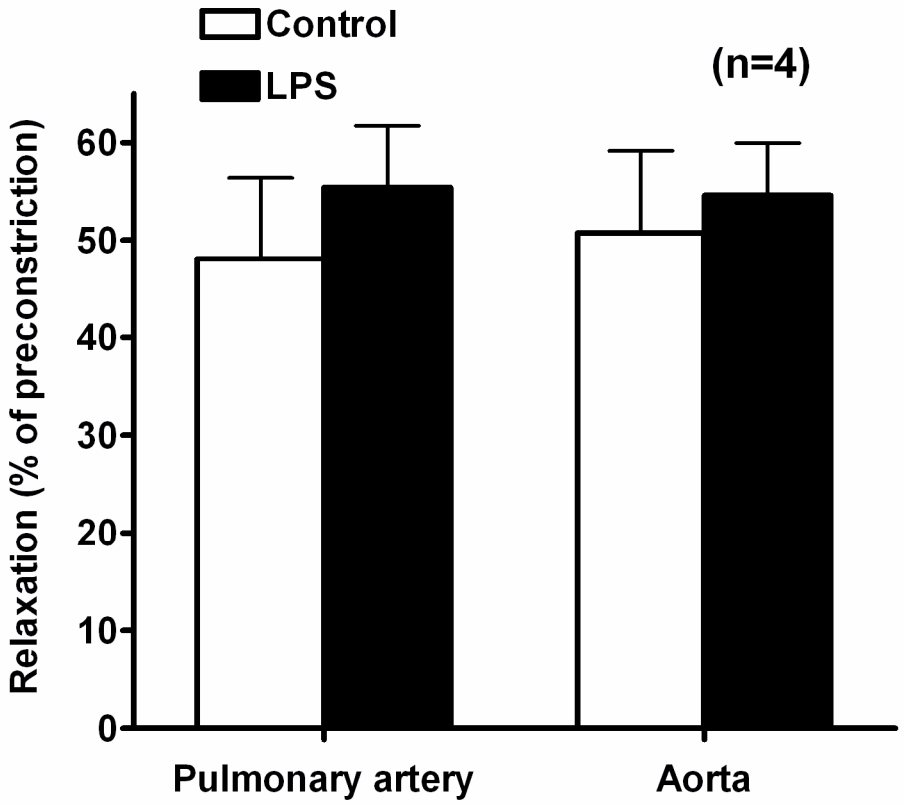

Figure 5.11 Effect of Ro-31-8425 on LPS-induced changes in contractile responses to ET-1 in the pulmonary artery and aorta. Pulmonary (a) and aortic (b) arterial rings from control and LPS (10 µg ml^{-1}, 20 h)-treated groups were preconstricted with 30 nM ET-1 before measuring relaxation responses to Ro-31-8425 (300 nM). Data are expressed as mean ± s.e.m., where (n) equals the number animals.

5.12 Effect of LPS-pretreatment on the expression of different proteins involved in Ca^{2+}-sensitization induced by ET-1

Phosphorylation of MLC_{20} is the major step leading to contraction of VSMCs, and this phosphorylation can be controlled by the level of $[Ca^{2+}]_i$ or through the Ca^{2+}-sensitization that depends mainly on the activity of MLCP. In both the pulmonary artery and the aorta, contraction with ET-1 caused a significant increase in the phosphorylation of MLC_{20} ($p<0.05$, $n=4$) (Figure 5.12). ET-1-stimulated phosphorylation of MLC_{20} was not affected by LPS-pretreatment in the pulmonary artery (Figure 5.12 a and b), but was significantly decreased in the aorta ($p<0.05$, $n=4$) (Figure 5.12 c and d), a result in line with the observed aortic hypocontractility to ET-1 (Figure 3.5).

To measure changes in the proteins involved in Ca^{2+}-sensitization, PKC, ROKα, CPI-17 and MYPT1 were investigated in both the pulmonary artery and the aorta. There were no significant changes in the ET-1-induced changes in the protein expression levels of PKC or the phosphorylation levels of ROKα, CPI-17 or MYPT1 between control and LPS-pretreated vascular rings (Figure 5.13). These results suggest that ET-1-induced sensitization to Ca^{2+} are not altered in LPS-pretreated pulmonary artery and aorta.

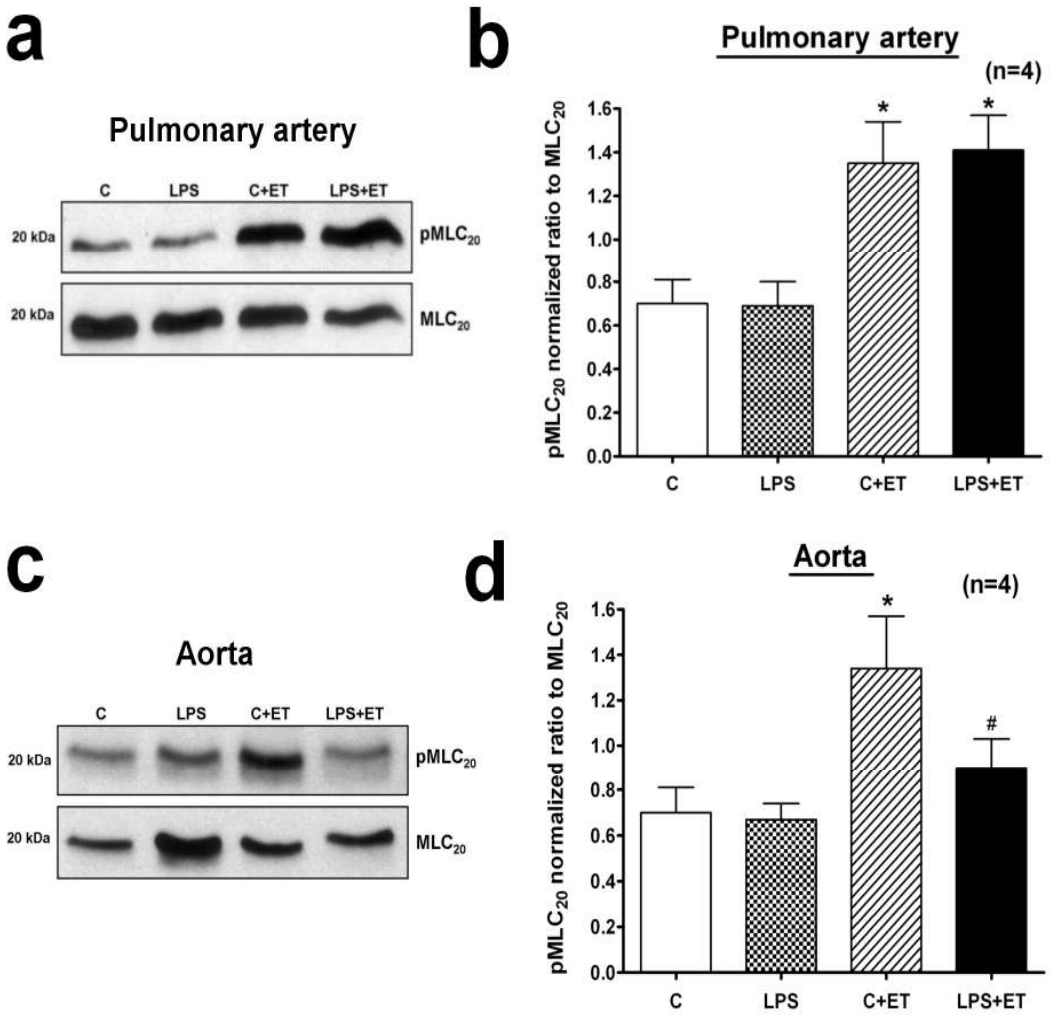

Figure 5.12 Effect of LPS on ET-1-induced phosphorylation of MLC_{20} in the pulmonary artery and aorta. (a, c) Representative immunoblots for $pMLC_{20}$ and MLC_{20} in the pulmonary artery and the aorta from control (C), (LPS), control + 100 nM ET-1 (C+ET) and LPS + 100 nM ET-1 (LPS+ET) groups. (b, d) densitometric ratio of $pMLC_{20}$ normalized to MLC_{20} in the pulmonary artery and the aorta. Data are expressed as mean ± s.e.m., where (n) equals the number animals. * $p<0.05$ compared with control or LPS groups, # $p<0.05$ compared with C+ET group using one-way ANOVA with Student-Newman-Keuls Multiple Comparisons *post-hoc* test.

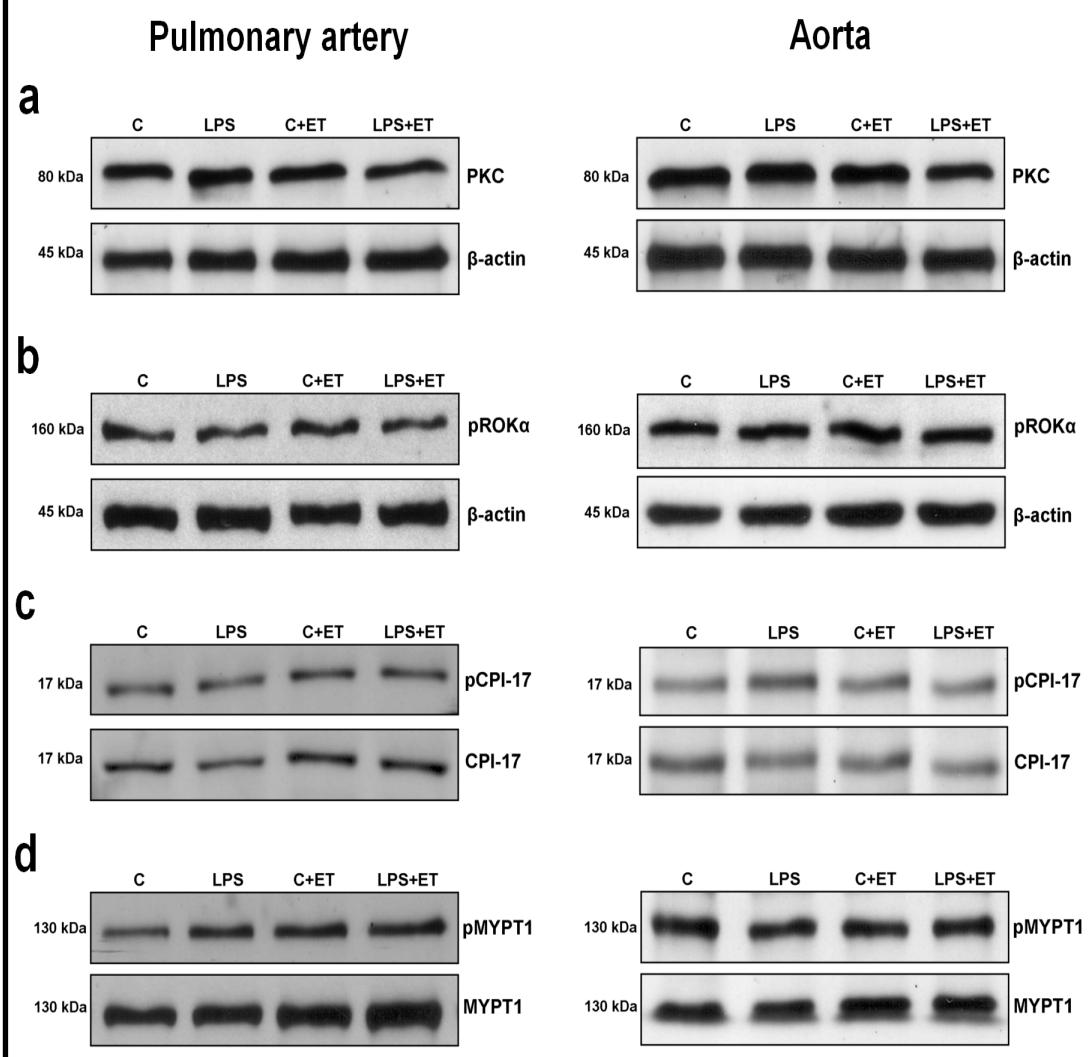

Figure 5.13 Effect of LPS on the protein expression levels of PKC and the phosphorylation levels of ROK*α*, CPI-17 and MYPT1 in the pulmonary artery and aorta. Representative immunoblots of PKC (a), pROKα (b), pCPI-17 (c) and pMYPT1 (d) in the pulmonary artery (left) and the aorta (right) from control (C), (LPS), control + 100 nM ET-1 (C+ET) and LPS + 100 nM ET-1 (LPS+ET) groups.

5.13 Effect of LPS-pretreatment on $[Ca^{2+}]_i$ changes induced by ET-1 in isolated aortic VSMCs

The resting level of $[Ca^{2+}]_i$ was significantly higher in LPS-treated VSMCs (106±5 nM) compared to control (94±5 nM) ($p<0.05$, n=12), but this difference was abolished when external Ca^{2+} was removed, where the baselines were 111±4 nM and 108±3 nM for LPS and control groups, respectively. Infusion of 100 nM ET-1 caused an initial increase in $[Ca^{2+}]_i$ (transient phase) followed by a continuous plateau elevation in $[Ca^{2+}]_i$ (sustained phase) (Figure 5.14b). There were no significant differences in the transient $[Ca^{2+}]_i$ increase induced by 100 nM ET-1 between control (111±10 nM) and LPS-treated (109±13 nM) aortic VSMCs. However, the sustained phase $[Ca^{2+}]_i$ level of control (26±3 % of transient phase in each cell) was significantly reduced to 15±2 % in the LPS-treated group ($p<0.001$, n=12) (Figure 5.14c). Removal of external Ca^{2+} had no significant effect on the transient phase $[Ca^{2+}]_i$ elevations in either the control (103±10 nM) or the LPS-treated (104±11 nM) group, but the sustained phase $[Ca^{2+}]_i$ was decreased in both control (11±1 %) and LPS-treated (11±2 %) groups which abolished the difference between control and LPS-treated groups (Figure 5.14c). Conversely, addition of 2.5 mM Ca^{2+} during the sustained phase, produced a continuous elevation in $[Ca^{2+}]_i$, which was significantly higher in control (210±17 %) compared to LPS-treated (155±12 %) groups ($p<0.05$, n=12) (Figure 5.15a and b). This continuous elevation in $[Ca^{2+}]_i$ was not significantly affected by incubation with 20 µM diltiazem for 5 minutes before the addition of the 2.5 mM Ca^{2+} (Figure 5.15b). However, incubation with 10 µM SKF-96365 significantly decreased the continuous elevation in $[Ca^{2+}]_i$ in both groups and abolished the difference between the control and LPS-treated groups (Figure 5.15b).

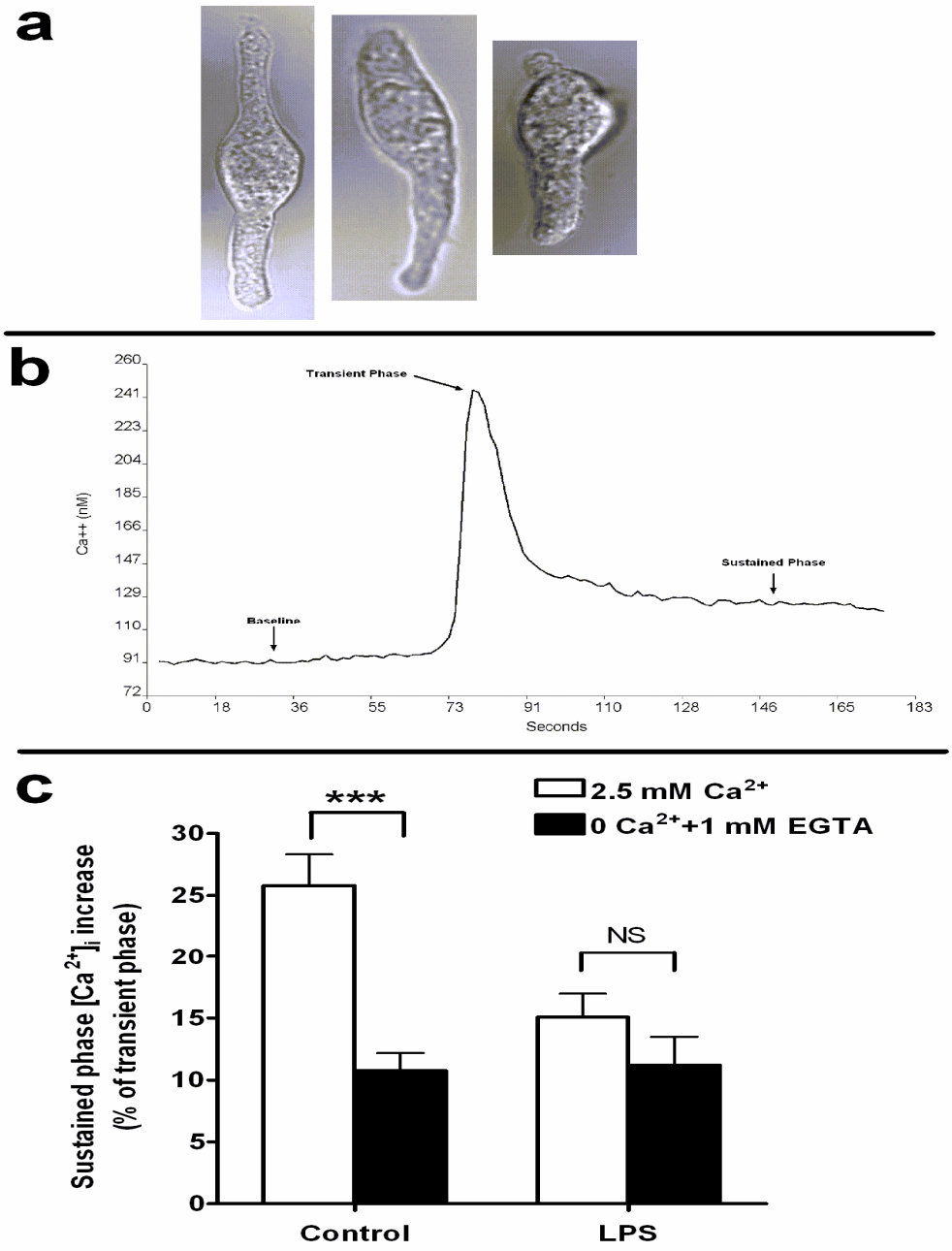

Figure 5.14 Effect of LPS on ET-1-induced changes of $[Ca^{2+}]_i$ in aortic VSMCs. (a) representative photos of the different shapes of isolated aortic VSMCs. (b) representative trace showing biphasic $[Ca^{2+}]_i$ changes induced by 100 nM ET-1 in control aortic VSMC. (c) The effect of external Ca^{2+} removal on sustained phase $[Ca^{2+}]_i$ induced by 100 nM ET-1. Data are expressed as % change from transient phase, n=12 cells prepared using tissue from 3 rats. ***p<0.01 compared with control group using paired Student's *t*-test.

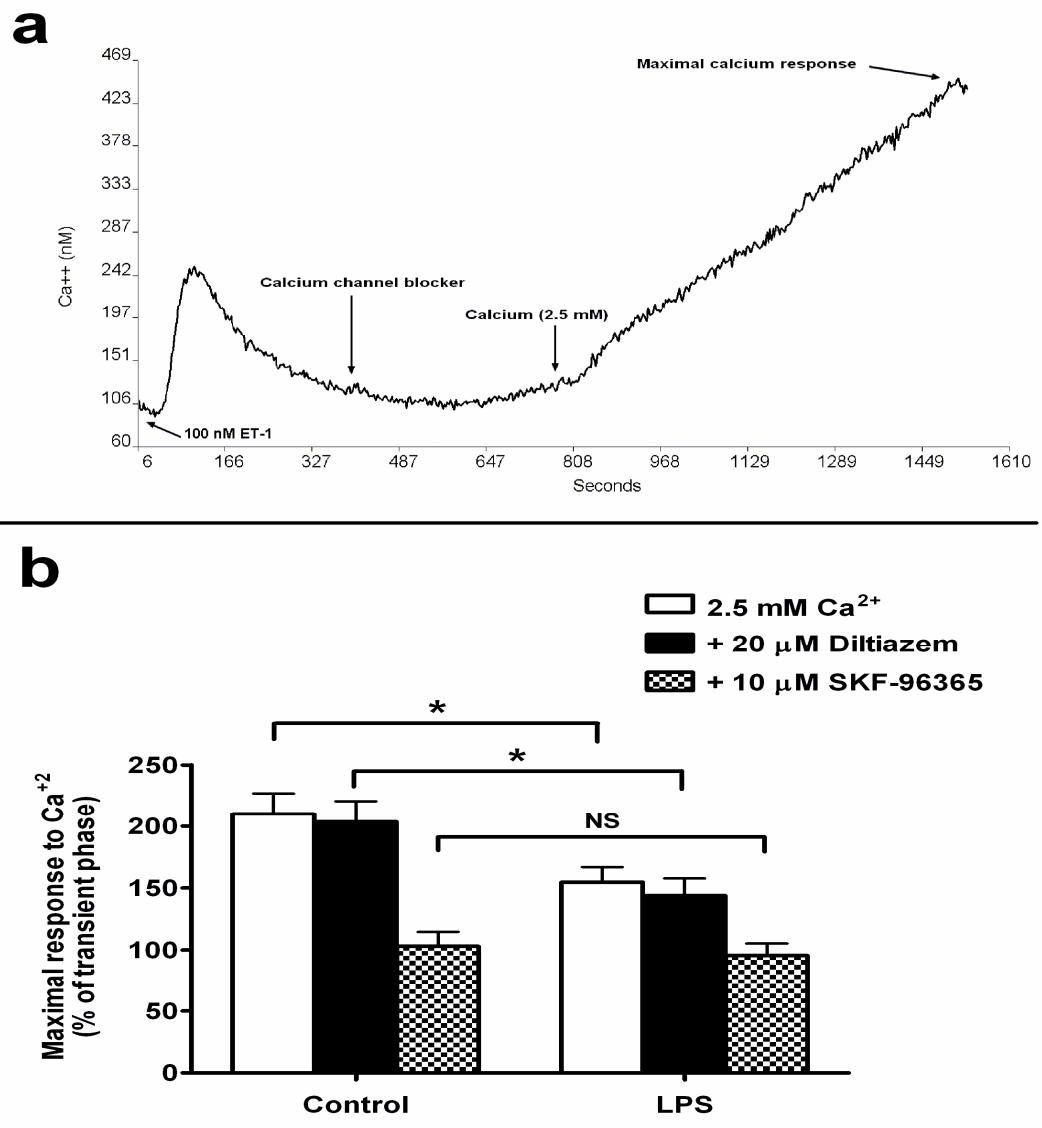

Figure 5.15 Effect of Ca^{2+} addition, diltiazem, and SKF-96365 on ET-1-induced changes of $[Ca^{2+}]_i$ in control and LPS-treated aortic VSMCs. (a) representative trace showing the effect of 2.5 mM Ca^{2+} addition on ET-1-induced biphasic $[Ca^{2+}]_i$ changes in control aortic VSMCs. (b) The effect of 20 µM diltiazem or 10 µM SKF-96365 on sustained phæse $[Ca^{2+}]_i$ induced by addition of 2.5 mM Ca^{2+} to aortic VSMCs preconstricted with 100 nM ET-1. Data are expressed as % change from transient phase, n=12 cells prepared using tissue from 3 rats. *$p<0.05$ using one-way ANOVA with Student-Newman-Keuls Multiple Comparisons *post-hoc* test.

5.14 Effect of protein synthesis inhibition on LPS-induced changes in vascular reactivity to ET-1

To determine if LPS-induced changes are dependent on protein synthesis or not, pulmonary and aortic rings were incubated with the protein synthesis inhibitor cycloheximide (10 µM) 1 h before and during the incubation with LPS. In the pulmonary artery, there was no significance difference in the contraction responses to ET-1 between control and LPS-treated vascular rings (Figure 5.16a). In the aorta, cycloheximide abolished the difference in contractile responses to ET-1 induced by LPS (Figure 5.16b), suggesting that LPS-induced aortic hyporeactivity to ET-depends on protein synthesis.

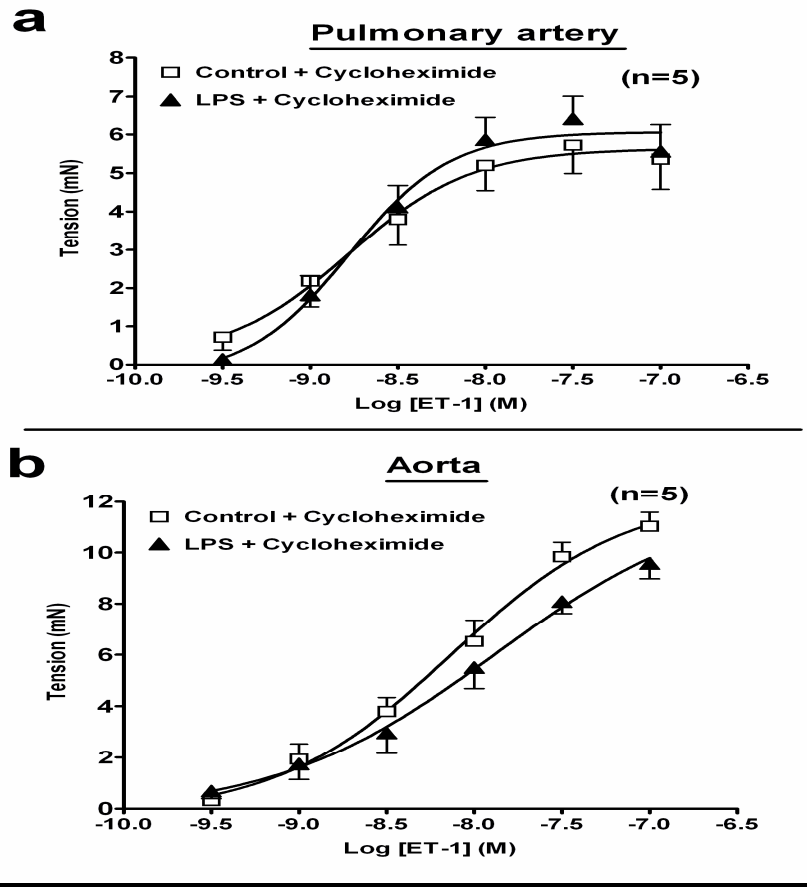

Figure 5.16 Effect of cycloheximide on LPS-induced changes in contractile responses to ET-1 in the pulmonary artery and aorta. Contraction to ET-1 (0.3 nM-100 nM) was measured in the pulmonary artery (a) and the aorta (b) after incubation with LPS (10 µg ml^{-1}, 20 h) in presence of 10 µM cycloheximide. Data are expressed as mean ± s.e.m., where (n) equals the number animals.

5.15 Discussion

The results presented in this chapter show that LPS-induced vascular hypocontractility to ET-1 in rat aorta is primarily dependent on Ca^{2+} influx through non-VOCCs, but not on changes in ET-1 receptor expression or Ca^{2+} sensitization.

In the present study, LPS treatment impaired contractile responses of rat aorta to both receptor-dependent and -independent vasoconstrictors. Although changed expression of ET-1 specific receptors ET_A and ET_B has been suggested as a mechanism of hypocontractility, no systematic study has evaluated this possibility in intact arteries. Previous studies have shown that LPS treatment decreases ET_A mRNA in rat heart (Ishimaru *et al.*, 2001; Hirata & Ishimaru, 2002), aortic VSM cell line A7r5 (Bucher & Taeger, 2002) and rat pulmonary VSM (Dschietzig *et al.*, 2008), but increases expression in septic pig heart (Forni *et al.*, 2005). Conversely, increased ET_B mRNA was observed in these previous studies but ET_B mRNA was decreased in rat pulmonary ECs (Dschietzig *et al.*, 2008). Few studies have examined ET-1 gene expression in intact arteries, where ET-1 mRNA is increased in mouse aorta (Shindo *et al.*, 1998) and in rat aorta and pulmonary artery (Curzen *et al.*, 1997), but was not affected in porcine aorta (Magder *et al.*, 2001) by LPS treatment. Since LPS had no effect on the ET-1, ET_A or ET_B receptors mRNA levels, changes in the gene expression of ET-1 system is unlikely to be involved in LPS-induced hyporeactivity in the present model. Using different animals for control and LPS-treated groups can influence the outcome due to the difference in genetic background, but in the present model all the time points representing LPS treatment have their respective controls which, for each sample, are pooled exactly from the same animals to eliminate any genetic background influence.

By using blockers for K_{ATP} (glibenclamide) and BK (iberiotoxin), LPS-induced changes in vascular reactivity to ET-1 were not affected in either the pulmonary artery or the aorta. These results are similar to previous *ex vivo* organ bath studies, where glibenclamide had no effect on vascular hyporeactivity (Wu *et al.*, 1995; Taguchi *et al.*, 1996) or even further reduced contractions (Sorrentino *et al.*, 1999) and to an *in vivo* model where both glibenclamide and iberiotoxin did not protect against LPS-induced mortality in mice (Cauwels & Brouckaert, 2008). In addition,

since K^+ channels activation causes hyperpolarization and closing of VOCCs, the absence of effects with either K^+ channels blockers or VOCCs blockers confirms that both K^+ channels and VOCCs are not involved in LPS-induced hyporeactivity to ET-1 in the aorta.

No previous studies are available where the role of different proteins involved in Ca^{2+}-sensitization was assessed in vascular hyporeactivity changes in animal models of sepsis. Therefore, the present results demonstrating the absence of significant changes between control and LPS-treated aortic rings in the protein expression levels of PKC or the phosphorylation levels of ROKα, CPI-17 or MYPT1, are an important evidence suggesting that Ca^{2+}-sensitization is not the primarily mechanism responsible for LPS-induced hyporeactivity to ET-1. These observations suggest that changes in Ca^{2+} mobilization or Ca^{2+} entry are more important.

Previous studies have mainly examined LPS-induced changes in depolarizing KCl (40-100 mM)-stimulated Ca^{2+}-entry via VOCCs. Increasing extracellular Ca^{2+} up to 30 mM reverses the diminished vascular reactivity to KCl in the aorta from septic rats (Wakabayashi *et al.*, 1987; Biguad *et al.*, 1990), an effect attributed to the impairment of either Ca^{2+} sensitization (Wakabayashi *et al.*, 1987) or Ca^{2+} influx (Biguad *et al.*, 1990), although specific mechanisms were not identified. The present results using the VOCCs blockers nifedipine or diltiazem suggest that VOCCs-dependent Ca^{2+}-entry is not responsible for LPS-induced hyporeactivity to ET-1. Furthermore, the difference in the sensitivity to external Ca^{2+} in the aorta preconstricted with ET-1 in the presence of nifedipine suggests that LPS impairs non-VOCCs Ca^{2+}-entry. Similarly, rat aorta from endotoxic rats display reduced sensitivity to Ca^{2+} in high K^+ depolarizing medium (Gray *et al.*, 1990; Ho *et al.*, 1996) and nitrendipine is not able to inhibit vascular hyporeactivity to phenylephrine in septic rat aorta (Biguad *et al.*, 1990). Conversely, pre-administration of verapamil and nifedipine (Sirmagul *et al.*, 2006) or nifedipine (Wu *et al.*, 1999) is able to prevent hypotension *in vivo* in endotoxin-shocked rats. Interestingly, amlodipine prevents LPS-induced hypotension *in vivo* but not *in vitro* (Salomone *et al.*, 1998), suggesting that results obtained with VOCCs modulators *in vivo* may be affected by other factors inside the body, such as metabolism, interaction with other mediators/cells and the presence of neuronal factors.

To study LPS-induced changes in Ca^{2+} influx further, changes in $[Ca^{2+}]_i$ levels in isolated aortic VSMCs were examined. The basal $[Ca^{2+}]_i$ levels were slightly higher in LPS-treated aortic VSMCs compared to control, a result consistent with previous studies using rat aorta (Song *et al.*, 1993) and rat mesenteric arteries (Martinez *et al.*, 1996). Since removal of external Ca^{2+} abolishes this difference in basal $[Ca^{2+}]_i$ levels, it is unlikely to result from an impairment of $[Ca^{2+}]_i$ storage (Hotchkiss & Karl, 1996; Farmer *et al.*, 2003), but probably from enhanced Ca^{2+} influx through VOCCs (Wilkinson *et al.*, 1996), or other Ca^{2+} channels.

The ET-1-induced biphasic increase in Ca^{2+} levels, comprising transient and sustained components, has been previously shown (Jones *et al.*, 1999; Zhang *et al.*, 1999). The transient phase of $[Ca^{2+}]_i$ increase was not affected by external Ca^{2+} removal, suggesting that it is mainly due to intracellular release of Ca^{2+} as previously demonstrated (Zhang *et al.*, 1999; Ko *et al.*, 2005). Since LPS treatment had no effect on the transient phase increase in $[Ca^{2+}]_i$, it is unlikely that Ca^{2+}-mobilization from intracellular stores was affected under the present experimental conditions. However, the ET-1-induced sustained phase $[Ca^{2+}]_i$ increase was significantly reduced in LPS-treated aortas. This difference was abolished by removal of external Ca^{2+}, suggesting that it is mediated by voltage-independent Ca^{2+} influx. Similar differences were observed in response to the addition of external Ca^{2+} in the presence of ET-1 and the lack of response to diltiazem confirms this conclusion. The complete inhibition of the difference in the sustained level of $[Ca^{2+}]_i$, by SKF-96365, an inhibitor of both ROCCs and SOCCs (Merritt *et al.*, 1990; Zhang *et al.*, 1999), indicates that LPS impairs Ca^{2+} influx through voltage-independent Ca^{2+} channels. Since Ca^{2+} mobilization was not affected by LPS, it is likely that ROCCs more than SOCCs are involved.

It should be noted that U46619 did not show hyporeactivity after LPS-treatment in contrast to ET-1, phenylephrine and KCl. U46619-mediated contraction of rat aortic rings through TP receptors was not affected by external Ca^{2+} removal (Dorn & Becker, 1993). In addition, U46619 induces RhoA activation higher than ET-1 and norepinephrine in rabbit aortic smooth muscle (Sakurada *et al.*, 2001). Therefore, U46619 resistance to LPS effects may be due its different mechanism of contraction, which depends on internal Ca^{2+} mobilization and Ca^{2+} sensitization more than on external Ca^{2+}.

5.16 Summary and conclusions

In this chapter, LPS-induced changes in ET-1 receptor expression, Ca^{2+}-entry pathways, $[Ca^{2+}]_i$ and Ca^{2+}-sensitization were examined in the pulmonary artery and aorta. The main findings are:

1- mRNA expression levels of ET-1, ET_A and ET_B are not affected by LPS in either vessel.

2- LPS-induced aortic hyporeactivity to ET-1 is dependent on external Ca^{2+} influx through voltage-independent Ca^{2+} channels.

3- Neither K_{ATP} nor BK have a major role in LPS-induced vascular effects.

4- The major proteins involved in Ca^{2+} sensitization, including ROKα, PKC, MYPT1 and CPI-17, are not affected by LPS treatment in either vessel.

5- LPS impairs ET-1-induced changes in $[Ca^{2+}]_i$ in aortic VSMCs by impairing Ca^{2+} influx mainly through ROCCs, although SOCCs could also be involved.

6- Inhibition of protein synthesis abolished LPS-induced aortic hypocontractility to ET-1

In conclusion, the mechanism of LPS-induced aortic hyporeactivity to ET-1 depends on external Ca^{2+} influx through non-VOCCs, but not on ET-1 receptor expression or Ca^{2+} sensitization. The effect of LPS on the non-VOCCs Ca^{2+} influx depends on protein synthesis. Therefore, Ca^{2+} homeostasis could be important in controlling systemic vasomotor complications in sepsis.

Chapter 6

Final Discussion & Conclusions

Chapter 6

Inflammation has incompletely characterized effects on cardiopulmonary vascular reactivity. One of the major diseases involving inflammation is sepsis, a complex dysregulation of inflammation arising when the host is unable to contain an infection successfully. Sepsis is associated with two main vasomotor complications, septic shock and pulmonary hypertension (Parsons *et al.*, 1989; Manthous *et al.*, 1993; Lorente *et al.*, 1993), suggesting that systemic and pulmonary vasculature respond differentially to inflammation.

The main aim of this study was to examine the molecular mechanisms involved in cardiopulmonary vascular reactivity changes induced during inflammation. By using LPS as a powerful inflammatory stimulus, the present study established a well-controlled *in vitro* model to study changes in vascular reactivity that allowed identification of the possible vasoactive mediators and the molecular mechanisms impaired by LPS in vascular tissues.

6.1 The model

The vascular effects of sepsis can be simulated by the administration of the bacterial endotoxin LPS, both in humans (Suffredini *et al.*, 1989) and in animals (Ruetten *et al.*, 1996; Peters & Lewis, 1996; Gardiner *et al.*, 1996b). The effect of endotoxemia on the vasculature has been studied by many different groups, using different models of *in vivo*, *in vitro* and *ex vivo* endotoxemia. However, the results are highly variable. Even in the same model, there is variability in LPS-induced changes in vascular reactivity between different blood vessels and towards different vasoconstrictors (Piepot *et al.*, 2002; Farmer *et al.*, 2003). This suggests that the type of blood vessel, mechanism of action of the vasoactive agent and the experimental conditions all affect the vascular reactivity observed in endotoxemic models.

The *in vivo* and *ex vivo* models, in contrast to *in vitro* models, represent real pathological conditions, but are difficult to control due to multiple interactions. The *in vitro* organ culture has been shown to preserve tissue structure and contractility (Adner *et al.*, 1998; Ozaki & Karaki, 2002; Guibert *et al.*, 2005), in contrast with *in*

vitro cultures of VSMCs, and its experimental conditions can be easily controlled. Therefore, the present study used an organ culture method as an endotoxemic model to investigate the effect of inflammation on vascular reactivity.

In the present model, the effect of *in vitro* incubation with LPS was examined in the pulmonary artery and the aorta, to represent pulmonary and systemic circulations respectively, under similar experimental conditions. The present study showed that LPS selectively induced vascular hyporeactivity to different vasoconstrictors in rat aorta but not in the pulmonary artery, similar to real *in vivo* observations in endotoxemia and sepsis. This aortic hyporeactivity was not due to organ culturing per se and was not affected by changing the LPS type. Therefore, this organ culture model is suitable to study LPS-induced changes in vascular reactivity and can be easily controlled to study the molecular mechanisms involved.

It should be noted that most *in vivo* and *ex vivo* studies used large bolus injection of LPS, with a few studies using continuous infusion of LPS (Guc *et al.*, 1990; Farmer *et al.*, 2003). This high single LPS bolus models are different from human infection where the bacterial toxins are continuously present in blood. In addition, high single LPS dose can cause a burst of inflammatory mediators such as cytokines, which may lead to altered results. The *in vitro* models, such as the present one, use LPS concentrations much higher than levels measured in clinical sepsis, which may be considered as a drawback. In addition, the role of circulating cells and other *in vivo* factors were not studied here.

6.2 The vasoactive mediators

Several mediators have been suggested to play a major role in sepsis-induced vascular complications, including NO, derivatives of COX, ROS and vasoconstrictors such as catecholamines, ET-1 and AngII. The present study focused on ET-1 and NO as major mediators that could be involved in vascular responses to LPS. Overproduction of NO, the major vasodilator, is suggested to be the responsible cause of vascular hyporeactivity in a large number of studies (Szabo *et al.*, 1995; Feihl *et al.*, 2001; Lopez *et al.*, 2004). Plasma levels of ET-1, the most powerful vasoconstrictor at present, are elevated in sepsis and its level correlates with the

severity of illness (Pittet *et al.*, 1991; Piechota *et al.*, 2007). Results with different blockers of NO pathway are conflicting and sometimes detrimental, while ET-1 antagonism attenuates pulmonary hypertension in endotoxic shock (Wanecek *et al.*, 1999; Kuklin *et al.*, 2004).

Interestingly, NO was increased in both the pulmonary artery and the aorta in the present study, but vascular responses to ET-1 were impaired only in the aorta, raising a doubt about the role of NO in this model. Moreover, inhibition of iNOS was unable to reverse aortic hyporeactivity, but inhibition of sGC prevented this hyporeactivity. These results suggest that LPS-induced aortic hypocontractility to ET-1 is largely mediated by NO-independent activation of sGC. The pulmonary artery did not show hyporeactivity to ET-1 because LPS induced a desensitization of the sGC/cGMP-dependent pathway by decreasing protein expression levels of $sGC_{\beta 1}$, and hence sGC activity, and increasing PDE5 activity. Importantly, previous studies examining sGC/cGMP pathway in sepsis examined whole lung tissue or cultured pulmonary VSMCs, but not isolated pulmonary artery, which may be more relevant and specific.

Although endothelium removal and COX or ROS inhibition were unable to prevent LPS-induced aortic hyporeactivity to ET-1, this does not exclude their role *in vivo*. In addition, the complexity of LPS action could involve other mediators not studied in the present work.

6.3 The mechanisms

Since LPS can induce vascular hyporeactivity *in vitro* to different vasoconstrictors, which is independent of LPS type, and also in vessels removed from LPS-treated animals, the defect in the vascular contractility is intrinsic to the vasculature. The mechanisms involved in VSM contraction is therefore affected by LPS, either directly or through mediators released by LPS.

Several mechanisms could be involved in LPS-induced vascular hyporeactivity, including changes in receptor expression, Ca^{2+}-entry pathways, $[Ca^{2+}]_i$ and

Ca^{2+}-sensitization, in addition to membrane hyperpolarization by K^+ channel opening, mainly the BK and K_{ATP} channels.

Only a limited number of studies have examined the effect of LPS on these mechanisms. Using different blockers for K_{ATP} and BK produced conflicting results in previous studies, similar to the case with NO inhibitors. The present results with BK and K_{ATP} channels blockers show that K^+ channels may not play a major role in this model. Similar to the endothelium, COX and ROS, this does not exclude the role of K^+ channels *in vivo*.

LPS treatment in the present study had no significant effect on ET_A or ET_B receptor mRNA levels, contrary to most studies showing that ET_A is decreased while ET_B is increased. It should be mentioned that no systematic study has evaluated ET-1 receptor expression in intact arteries in endotoxemia, which make the present results more specific than examining the whole organ like the heart or the lung. In addition, using different animals for control and LPS-treated groups can influence the outcome results due to the difference in genetic background. In contrast, all the time points in the present model representing LPS treatment have their respective controls which, for each sample, are pooled exactly from the same animals to eliminate any genetic background influence.

The exact role of Ca^{2+} homeostasis in LPS-induced vascular hyporeactivity is unknown. No previous studies examined the role of Ca^{2+}-entry pathways, $[Ca^{2+}]_i$ and Ca^{2+}-sensitization in LPS-induced vascular hyporeactivity in detail. The present results show that LPS impairs ET-1-induced Ca^{2+} influx without affecting different proteins involved in Ca^{2+}-sensitization (PKC, ROKα, CPI-17 or MYPT1) in the aorta. Previous studies have mainly examined LPS-induced changes in Ca^{2+}-entry via VOCCs stimulated by depolarizing KCl. The present study shows that LPS impairs ET-1-induced Ca^{2+} influx through voltage-independent Ca^{2+} channels, which may include SOCCs and ROCCs. Since Ca^{2+} mobilization was not affected by LPS, it is likely that ROCCs more than SOCCs are involved. These effects of LPS are dependent on protein synthesis. These results show the importance of Ca^{2+} homeostasis in LPS-induced vascular hyporeactivity. Figure 6.1 represents a simple scheme to highglight the findings of this study.

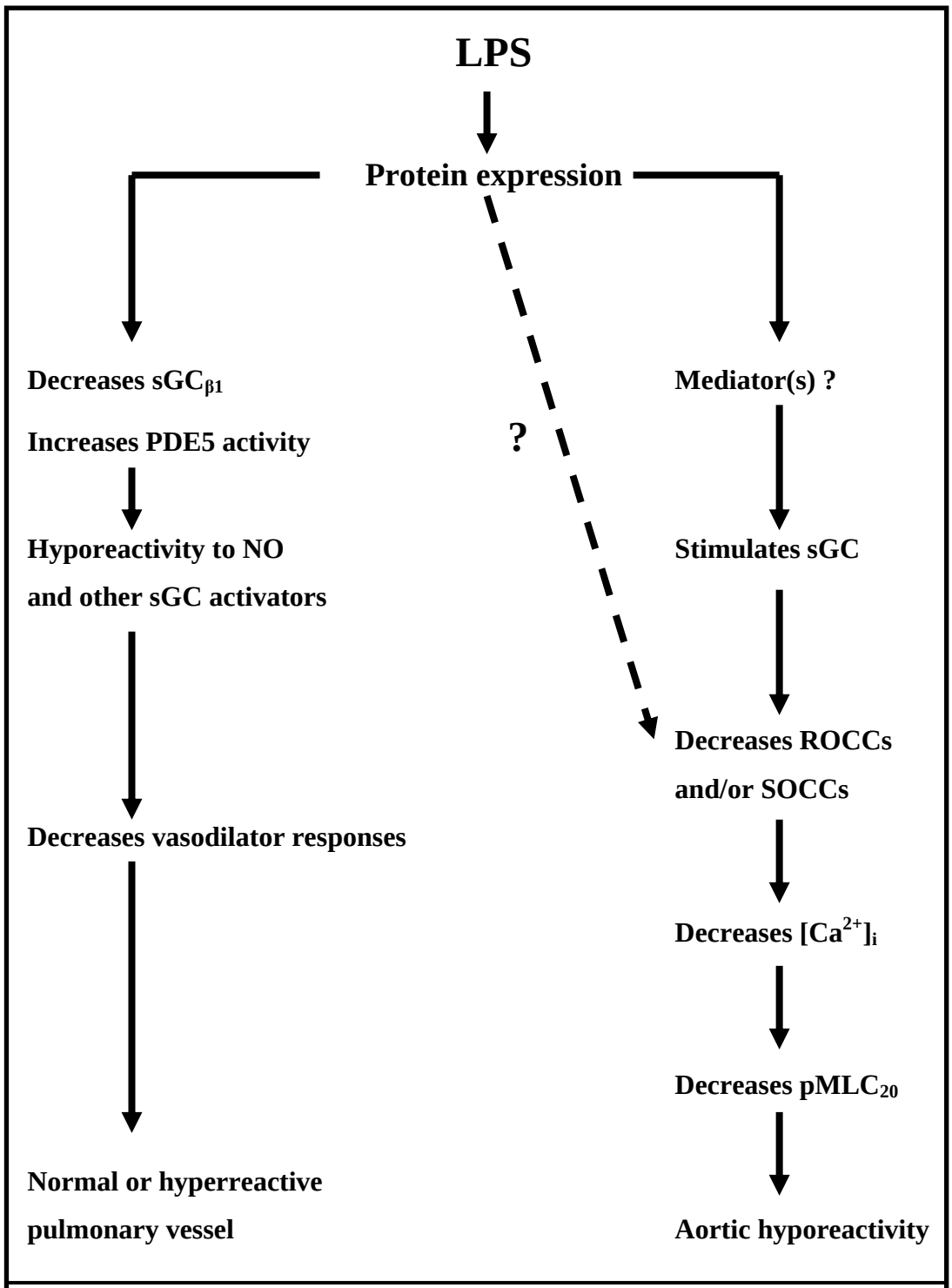

Figure 6.1 Simple scheme highlighting the findings of this study. $[Ca^{2+}]_i$, intracellular Ca^{2+}; NO, LPS, lipopolysaccharide;nitric oxide; PDE5, phosphodiesterase 5; $pMLC_{20}$, 20 kD phospho-myosin light chain; ROCCs, receptor-operated Ca^{2+} channels; SOCCs, store-operated Ca^{2+} channels; $sGC_{\beta1}$, soluble guanylyl cyclase β1.

6.4 Final conclusions

Inflammation can cause either vasoconstriction or vasodilation depending on the type of vascular tissue, vasoconstrictor and experimental conditions. The powerful inflammatory stimulus LPS causes selective aortic hypocontractility to different vasoconstrictors without affecting the pulmonary artery responses. In the aorta, LPS-induced hypocontractility to ET-1 may be due to NO-independent activation of sGC. In addition, LPS in the aorta may impair external Ca^{2+} influx through non-VOCCs, but not ET-1 receptors expression or Ca^{2+} sensitization, and these effects depend on protein synthesis. In the pulmonary artery, LPS does not affect pulmonary artery responses to different vasoconstrictors, since it causes desensitization of the sGC/cGMP pathway by decreasing protein expression levels of $sGC_{\beta 1}$, and hence sGC activity, and increasing PDE5 activity. In addition, LPS has no effect on ET-1 receptors expression or external Ca^{2+} influx induced by ET-1 in the pulmonary artery.

Therefore, it is likely that both Ca^{2+} homeostasis and the sGC/cGMP pathway play important roles in vasomotor complications in sepsis. sGC and/or PDE5-selective inhibitors, together with manipulating VSMC $[Ca^{2+}]_i$, could be important in controlling systemic and pulmonary vasomotor complications in sepsis.

6.5 Future work

Next steps may include determination of the nature of the NO-independent sGC activator stimulated by LPS, the mechanism by which LPS impairs PDE5 activity in pulmonary vessels and the type of Ca^{2+} channels involved in LPS actions. The mechanisms investigated in this study are related mainly to ET-1, other vasoconstricors can be investigated as well. The reproducibility of these results can be tested using *ex vivo* and then *in vivo* models. This could detect the applicability of the suggested pathways, such as sGC and/or PDE5 inhibitors, as therapeutic targets in sepsis.

References

Abassi ZA, Tate JE, Golomb E, Keiser HR (1992). Role of neutral endopeptidase in the metabolism of endothelin. *Hypertension*, **20**, 89-95.

Abu-Soud HM, Ichimori K, Presta A, Stuehr DJ (2000). Electron transfer, oxygen binding, and nitric oxide feedback inhibition in endothelial nitric-oxide synthase. *J Biol Chem*, **275**, 17349-17357.

Adelstein RS, Hathaway DR (1979). Role of calcium and cyclic adenosine 3':5' monophosphate in regulating smooth muscle contraction. Mechanisms of excitation-contraction coupling in smooth muscle. *Am J Cardiol*, **44**, 783-787.

Adner M, Erlinge D, Nilsson L, Edvinsson L (1995). Upregulation of a non-ETA receptor in human arteries in vitro. *J Cardiovasc Pharmacol*, **26 Suppl 3**, S314-S316.

Adner M, Uddman E, Cardell LO, Edvinsson L (1998). Regional variation in appearance of vascular contractile endothelin-B receptors following organ culture. *Cardiovasc Res*, **37**, 254-262.

Aird WC (2003). The role of the endothelium in severe sepsis and multiple organ dysfunction syndrome. *Blood*, **101**, 3765-3777.

Akira S, Uematsu S, Takeuchi O (2006). Pathogen recognition and innate immunity. *Cell*, **124**, 783-801.

Alderton WK, Cooper CE, Knowles RG (2001). Nitric oxide synthases: structure, function and inhibition. *Biochem J*, **357**, 593-615.

Alexander C, Rietschel ET (2001). Bacterial lipopolysaccharides and innate immunity. *J Endotoxin Res*, **7**, 167-202.

Alm R, Edvinsson L, Malmsjo M (2002). Organ culture: a new model for vascular endothelium dysfunction. *BMC Cardiovasc Disord*, **2**, 8.

Anggard E (1994). Nitric oxide: mediator, murderer, and medicine. *Lancet*, **343**, 1199-1206.

Arnold WP, Mittal CK, Katsuki S, Murad F (1977). Nitric oxide activates guanylate cyclase and increases guanosine 3':5'-cyclic monophosphate levels in various tissue preparations. *Proc Natl Acad Sci U S A*, **74**, 3203-3207.

Bachetti T, Pasini E, Suzuki H, Ferrari R (2003). Species-specific modulation of the nitric oxide pathway after acute experimentally induced endotoxemia. *Crit Care Med*, **31**, 1509-1514.

Bannerman DD, Goldblum SE (2003). Mechanisms of bacterial lipopolysaccharide-induced endothelial apoptosis. *Am J Physiol Lung Cell Mol Physiol*, **284**, L899-L914.

Battistini B, Chailler P, Orleans-Juste P, Briere N, Sirois P (1993). Growth regulatory properties of endothelins. *Peptides*, **14**, 385-399.

Beavo JA (1995). Cyclic nucleotide phosphodiesterases: functional implications of multiple isoforms. *Physiol Rev*, **75**, 725-748.

Beckman JS, Koppenol WH (1996). Nitric oxide, superoxide, and peroxynitrite: the good, the bad, and ugly. *Am J Physiol*, **271**, C1424-C1437.

Bernard GR, Wheeler AP, Russell JA, Schein R, Summer WR, Steinberg KP, Fulkerson WJ, Wright PE, Christman BW, Dupont WD, Higgins SB, Swindell BB (1997). The effects of ibuprofen on the physiology and survival of patients with sepsis. The Ibuprofen in Sepsis Study Group. *N Engl J Med*, **336**, 912-918.

Bialojan C, Ruegg JC, Di SJ (1985). Phosphatase-mediated modulation of actin-myosin interaction in bovine aortic actomyosin and skinned porcine carotid artery. *Proc Soc Exp Biol Med*, **178**, 36-45.

Biguad M, Julou-Schaeffer G, Parratt JR, Stoclet JC (1990). Endotoxin-induced impairment of vascular smooth muscle contractions elicited by different mechanisms. *Eur J Pharmacol*, **190**, 185-192.

Bishop-Bailey D, Larkin SW, Warner TD, Chen G, Mitchell JA (1997). Characterization of the induction of nitric oxide synthase and cyclo-oxygenase in rat aorta in organ culture. *Br J Pharmacol*, **121**, 125-133.

Bloch KD, Hong CC, Eddy RL, Shows TB, Quertermous T (1991). cDNA cloning and chromosomal assignment of the endothelin 2 gene: vasoactive intestinal contractor peptide is rat endothelin 2. *Genomics*, **10**, 236-242.

Boer C, Groeneveld AB, Scheffer GJ, de Lange JJ, Westerhof N, Sipkema P (2005). Induced nitric oxide impairs relaxation but not contraction in endotoxin-exposed rat pulmonary arteries. *J Surg Res*, **127**, 197-202.

Boerrigter G, Burnett JC, Jr. (2007). Nitric oxide-independent stimulation of soluble guanylate cyclase with BAY 41-2272 in cardiovascular disease. *Cardiovasc Drug Rev*, **25**, 30-45.

Bolton TB (1979). Mechanisms of action of transmitters and other substances on smooth muscle. *Physiol Rev*, **59**, 606-718.

Boulanger C, Luscher TF (1990). Release of endothelin from the porcine aorta. Inhibition by endothelium-derived nitric oxide. *J Clin Invest*, **85**, 587-590.

Boyle WA, III, Parvathaneni LS, Bourlier V, Sauter C, Laubach VE, Cobb JP (2000). iNOS gene expression modulates microvascular responsiveness in endotoxin-challenged mice. *Circ Res*, **87**, E18-E24.

Bradford MM (1976). A rapid and sensitive method for the quantitation of microgram quantities of protein utilizing the principle of protein-dye binding. *Anal Biochem*, **72**, 248-254.

Brandes RP, Koddenberg G, Gwinner W, Kim D, Kruse HJ, Busse R, Mugge A (1999). Role of increased production of superoxide anions by NAD(P)H oxidase and xanthine oxidase in prolonged endotoxemia. *Hypertension*, **33**, 1243-1249.

Brayden JE (1996). Potassium channels in vascular smooth muscle. *Clin Exp Pharmacol Physiol*, **23**, 1069-1076.

Bremnes T, Paasche JD, Mehlum A, Sandberg C, Bremnes B, Attramadal H (2000). Regulation and intracellular trafficking pathways of the endothelin receptors. *J Biol Chem*, **275**, 17596-17604.

Broillet MC (1999). S-nitrosylation of proteins. *Cell Mol Life Sci*, **55**, 1036-1042.

Bucher M, Taeger K (2002). Endothelin-receptor gene-expression in rat endotoxemia. *Intensive Care Med*, **28**, 642-647.

Buras JA, Holzmann B, Sitkovsky M (2005). Animal models of sepsis: setting the stage. *Nat Rev Drug Discov*, **4**, 854-865.

Buyukafsar K, Arikan O, Ark M, Kubat H, Ozveren E (2004). Upregulation of Rho-kinase (ROCK-2) expression and enhanced contraction to endothelin-1 in the mesenteric artery from lipopolysaccharide-treated rats. *Eur J Pharmacol*, **498**, 211-217.

Cai H, Harrison DG (2000). Endothelial dysfunction in cardiovascular diseases: the role of oxidant stress. *Circ Res*, **87**, 840-844.

Carbonell LF, Nadal JA, Llanos MC, Hernandez I, Nava E, Diaz J (2000). Depletion of liver glutathione potentiates the oxidative stress and decreases nitric oxide synthesis in a rat endotoxin shock model. *Crit Care Med*, **28**, 2002-2006.

Cauwels A, Brouckaert P (2008). Critical role for small and large conductance calcium-dependent potassium channels in endotoxemia and TNF toxicity. *Shock*, **29**, 577-582.

Chen SJ, Chen KH, Wu CC (2005). Nitric oxide-cyclic GMP contributes to abnormal activation of Na^+-K^+-ATPase in the aorta from rats with endotoxic shock. *Shock*, **23**, 179-185.

Chen SJ, Wu CC, Yang SN, Lin CI, Yen MH (2000). Abnormal activation of K^+ channels in aortic smooth muscle of rats with endotoxic shock: electrophysiological and functional evidence. *Br J Pharmacol*, **131**, 213-222.

Choudhury N, Khromov AS, Somlyo AP, Somlyo AV (2004). Telokin mediates Ca^{2+}-desensitization through activation of myosin phosphatase in phasic and tonic smooth muscle. *J Muscle Res Cell Motil*, **25**, 657-665.

Clapham DE, Runnels LW, Strubing C (2001). The TRP ion channel family. *Nat Rev Neurosci*, **2**, 387-396.

Clapp LH, Tinker A (1998). Potassium channels in the vasculature. *Curr Opin Nephrol Hypertens*, **7**, 91-98.

Clozel M, Gray GA, Breu V, Loffler BM, Osterwalder R (1992). The endothelin ETB receptor mediates both vasodilation and vasoconstriction in vivo. *Biochem Biophys Res Commun*, **186**, 867-873.

Coleman JW (2001). Nitric oxide in immunity and inflammation. *Internat Immunopharmacol*, **1**, 1397-1406.

Collins T, Cybulsky MI (2001). NF-κB: pivotal mediator or innocent bystander in atherogenesis? *J Clin Invest*, **107**, 255-264.

Cooke JP (2000). Does ADMA cause endothelial dysfunction? *Arterioscler Thromb Vasc Biol*, **20**, 2032-2037.

Curzen NP, Griffiths MJ, Evans TW (1995). Contraction to endothelin-1 in pulmonary arteries from endotoxin-treated rats is modulated by endothelium. *Am J Physiol*, **268**, H2260-H2266.

Curzen NP, Kaddoura S, Griffiths MJ, Evans TW (1997). Endothelin-1 in rat endotoxemia: mRNA expression and vasoreactivity in pulmonary and systemic circulations. *Am J Physiol*, **272**, H2353-H2360.

Cuzzocrea S, Mazzon E, Di PR, Esposito E, Macarthur H, Matuschak GM, Salvemini D (2006). A role for nitric oxide-mediated peroxynitrite formation in a model of endotoxin-induced shock. *J Pharmacol Exp Ther*, **319**, 73-81.

Dauphinee SM, Karsan A (2006). Lipopolysaccharide signaling in endothelial cells. *Lab Invest*, **86**, 9-22.

Davenport AP, O'Reilly G, Kuc RE (1995). Endothelin ETA and ETB mRNA and receptors expressed by smooth muscle in the human vasculature: majority of the ETA sub-type. *Br J Pharmacol*, **114**, 1110-1116.

Davis C, Fischer J, Ley K, Sarembock IJ (2003). The role of inflammation in vascular injury and repair. *J Thromb Haemost*, **1**, 1699-1709.

DelaTorre A, Schroeder RA, Kuo PC (1997). Alteration of NF-kappa B p50 DNA binding kinetics by S-nitrosylation. *Biochem Biophys Res Commun*, **238**, 703-706.

Dhaun N, Pollock DM, Goddard J, Webb DJ (2007). Selective and mixed endothelin receptor antagonism in cardiovascular disease. *Trends Pharmacol Sci*, **28**, 573-579.

Dorn GW, Becker MW (1993). Thromboxane A2 stimulated signal transduction in vascular smooth muscle. *J Pharmacol Exp Ther*, **265**, 447-456.

Dschietzig T, Alexiou K, Richter C, Bobzin M, Baumann G, Stangl K, Brunner F (2008). Endotoxin causes pulmonary hypertension by upregulating smooth muscle endothelin type-B receptors: role of aldose reductase. *Shock*, **30**, 189-196.

Emoto N, Yanagisawa M (1995). Endothelin-converting enzyme-2 is a membrane-bound, phosphoramidon-sensitive metalloprotease with acidic pH optimum. *J Biol Chem*, **270**, 15262-15268.

Ermert L, Ermert M, Merkle M, Goppelt-Struebe M, Duncker HR, Grimminger F, Seeger W (2000). Rat pulmonary cyclooxygenase-2 expression in response to endotoxin challenge: differential regulation in the various types of cells in the lung. *Am J Pathol*, **156**, 1275-1287.

Farias NC, Borelli-Montigny GL, Fauaz G, Feres T, Borges AC, Paiva TB (2002). Different mechanism of LPS-induced vasodilation in resistance and conductance arteries from SHR and normotensive rats. *Br J Pharmacol*, **137**, 213-220.

Farmer MR, Roberts RE, Gardiner SM, Ralevic V (2003). Effects of in vivo lipopolysaccharide infusion on vasoconstrictor function of rat isolated mesentery, kidney, and aorta. *J Pharmacol Exp Ther*, **306**, 538-545.

Faure E, Equils O, Sieling PA, Thomas L, Zhang FX, Kirschning CJ, Polentarutti N, Muzio M, Arditi M (2000). Bacterial Lipopolysaccharide Activates NF-kappa B through Toll-like Receptor 4 (TLR-4) in cultured human dermal endothelial cells. *J Biol Chem*, **275**, 11058-11063.

Feihl F, Waeber B, Liaudet L (2001). Is nitric oxide overproduction the target of choice for the management of septic shock? *Pharmacol Ther*, **91**, 179-213.

Felder CC, Singer-Lahat D, Mathes C (1994). Voltage-independent calcium channels. Regulation by receptors and intracellular calcium stores. *Biochem Pharmacol*, **48**, 1997-2004.

Feng J, Ito M, Ichikawa K, Isaka N, Nishikawa M, Hartshorne DJ, Nakano T (1999). Inhibitory phosphorylation site for Rho-associated kinase on smooth muscle myosin phosphatase. *J Biol Chem*, **274**, 37385-37390.

Fernandes D, da Silva-Santos JE, Duma D, Villela CG, Barja-Fidalgo C, Assreuy J (2006). Nitric oxide-dependent reduction in soluble guanylate cyclase functionality accounts for early lipopolysaccharide-induced changes in vascular reactivity. *Mol Pharmacol*, **69**, 983-990.

Forni M, Mazzola S, Ribeiro LA, Pirrone F, Zannoni A, Bernardini C, Bacci ML, Albertini M (2005). Expression of endothelin-1 system in a pig model of endotoxic shock. *Regul Pept*, **131**, 89-96.

Friebe A, Koesling D (2003). Regulation of nitric oxide-sensitive guanylyl cyclase. *Circ Res*, **93**, 96-105.

Fujii Y, Magder S, Cernacek P, Goldberg P, Guo Y, Hussain SN (2000). Endothelin receptor blockade attenuates lipopolysaccharide-induced pulmonary nitric oxide production. *Am J Respir Crit Care Med*, **161**, 982-989.

Furchgott RF, Zawadzki JV (1980). The obligatory role of endothelial cells in the relaxation of arterial smooth muscle by acetylcholine. *Nature*, **288**, 373-376.

Galizzi JP, Qar J, Fosset M, Van RC, Lazdunski M (1987). Regulation of calcium channels in aortic muscle cells by protein kinase C activators (diacylglycerol and phorbol esters) and by peptides (vasopressin and bombesin) that stimulate phosphoinositide breakdown. *J Biol Chem*, **262**, 6947-6950.

Galley HF, Howdle PD, Walker BE, Webster NR (1997). The effects of intravenous antioxidants in patients with septic shock. *Free Radic Biol Med*, **23**, 768-774.

Gardiner SM, Kemp PA, March JE, Bennett T (1995). Enhancement of the hypotensive and vasodilator effects of endotoxaemia in conscious rats by the endothelin antagonist, SB 209670. *Br J Pharmacol*, **116**, 1718-1719.

Gardiner SM, Kemp PA, March JE, Bennett T (1996a). Influence of aminoguanidine and the endothelin antagonist, SB 209670, on the regional haemodynamic effects of endotoxaemia in conscious rats. *Br J Pharmacol*, **118**, 1822-1828.

Gardiner SM, Kemp PA, March JE, Bennett T (1996b). Temporal differences between the involvement of angiotensin II and endothelin in the cardiovascular responses to endotoxaemia in conscious rats. *Br J Pharmacol*, **119**, 1619-1627.

Gardiner SM, Kemp PA, March JE, Bennett T (1999). Regional haemodynamic responses to infusion of lipopolysaccharide in conscious rats: effects of pre- or post-treatment with glibenclamide. *Br J Pharmacol*, **128**, 1772-1778.

Gardner PR, Costantino G, Szabo C, Salzman AL (1997). Nitric oxide sensitivity of the aconitases. *J Biol Chem*, **272**, 25071-25076.

Garthwaite J, Southam E, Boulton CL, Nielsen EB, Schmidt K, Mayer B (1995). Potent and selective inhibition of nitric oxide-sensitive guanylyl cyclase by 1H-[1,2,4]oxadiazolo[4,3-a]quinoxalin-1-one. *Mol Pharmacol*, **48**, 184-188.

Garvey EP, Oplinger JA, Furfine ES, Kiff RJ, Laszlo F, Whittle BJ, Knowles RG (1997). 1400W is a slow, tight binding, and highly selective inhibitor of inducible nitric-oxide synthase in vitro and in vivo. *J Biol Chem*, **272**, 4959-4963.

Gibson A, McFadzean I, Wallace P, Wayman CP (1998). Capacitative Ca^{2+} entry and the regulation of smooth muscle tone. *Trends Pharmacol Sci*, **19**, 266-269.

Glembot TM, Britt LD, Hill MA (1995). Lack of direct endotoxin-induced vasoactive effects on isolated skeletal muscle arterioles. *Shock*, **3**, 216-223.

Glynos C, Kotanidou A, Orfanos SE, Zhou Z, Simoes DC, Magkou C, Roussos C, Papapetropoulos A (2007). Soluble guanylyl cyclase expression is reduced in LPS-induced lung injury. *Am J Physiol Regul Integr Comp Physiol*, **292**, R1448-R1455.

Gonzalez JM, Jost LJ, Rouse D, Suki WN (1996). Plasma membrane and sarcoplasmic reticulum Ca-ATPase and smooth muscle. *Miner Electrolyte Metab*, **22**, 345-348.

Goode HF, Cowley HC, Walker BE, Howdle PD, Webster NR (1995). Decreased antioxidant status and increased lipid peroxidation in patients with septic shock and secondary organ dysfunction. *Crit Care Med*, **23**, 646-651.

Gow AJ, Luchsinger BP, Pawloski JR, Singel DJ, Stamler JS (1999). The oxyhemoglobin reaction of nitric oxide. *Proc Natl Acad Sci U S A*, **96**, 9027-9032.

Gray GA, Julou-Schaeffer G, Oury K, Fleming I, Parratt JR, Stoclet JC (1990). An L-arginine-derived factor mediates endotoxin-induced vascular hyposensitivity to calcium. *Eur J Pharmacol*, **191**, 89-92.

Griffith TM, Edwards DH, Lewis MJ, Newby AC, Henderson AH (1984). The nature of endothelium-derived vascular relaxant factor. *Nature*, **308**, 645-647.

Griffiths MJ, Curzen NP, Mitchell JA, Evans TW (1997). In vivo treatment with endotoxin increases rat pulmonary vascular contractility despite NOS induction. *Am J Respir Crit Care Med*, **156**, 654-658.

Griffiths MJ, Liu S, Curzen NP, Messent M, Evans TW (1995). In vivo treatment with endotoxin induces nitric oxide synthase in rat main pulmonary artery. *Am J Physiol*, **268**, L509-L518.

Griscavage JM, Hobbs AJ, Ignarro LJ (1995). Negative modulation of nitric oxide synthase by nitric oxide and nitroso compounds. *Adv Pharmacol*, **34**, 215-234.

Grisham MB, Jourd'Heuil D, Wink DA (1999). Nitric oxide. I. Physiological chemistry of nitric oxide and its metabolites:implications in inflammation. *Am J Physiol*, **276**, G315-G321.

Grynkiewicz G, Poenie M, Tsien RY (1985). A new generation of Ca^{2+} indicators with greatly improved fluorescence properties. *J Biol Chem*, **260**, 3440-3450.

Guc MO, Furman BL, Parratt JR (1990). Endotoxin-induced impairment of vasopressor and vasodepressor responses in the pithed rat. *Br J Pharmacol*, **101**, 913-919.

Guibert C, Ducret T, Savineau JP (2008). Voltage-independent calcium influx in smooth muscle. *Prog Biophys Mol Biol*, **98**, 10-23.

Guibert C, Savineau JP, Crevel H, Marthan R, Rousseau E (2005). Effect of short-term organoid culture on the pharmaco-mechanical properties of rat extra- and intrapulmonary arteries. *Br J Pharmacol*, **146**, 692-701.

Gunnett CA, Chu Y, Heistad DD, Loihl A, Faraci FM (1998). Vascular effects of LPS in mice deficient in expression of the gene for inducible nitric oxide synthase. *Am J Physiol*, **275**, H416-H421.

Gunnett CA, Lund DD, McDowell AK, Faraci FM, Heistad DD (2005). Mechanisms of Inducible Nitric Oxide Synthase-Mediated Vascular Dysfunction. *Arterioscler Thromb Vasc Biol*, **25**, 1617-1622.

Haeberle JR, Hathaway DR, Paoli-Roach AA (1985). Dephosphorylation of myosin by the catalytic subunit of a type-2 phosphatase produces relaxation of chemically skinned uterine smooth muscle. *J Biol Chem*, **260**, 9965-9968.

Hall S, Turcato S, Clapp L (1996). Abnormal activation of K^+ channels underlies relaxation to bacterial lipopolysaccharide in rat aorta. *Biochem Biophys Res Commun*, **224**, 184-190.

Hampton RY, Golenbock DT, Penman M, Krieger M, Raetz CR (1991). Recognition and plasma clearance of endotoxin by scavenger receptors. *Nature*, **352**, 342-344.

Hartshorne DJ (1998). Myosin phosphatase: subunits and interactions. *Acta Physiol Scand*, **164**, 483-493.

Hashimoto T, Hirata M, Itoh T, Kanmura Y, Kuriyama H (1986). Inositol 1,4,5-trisphosphate activates pharmacomechanical coupling in smooth muscle of the rabbit mesenteric artery. *J Physiol*, **370**, 605-618.

Hecht SS (1997). Approaches to cancer prevention based on an understanding of N-nitrosamine carcinogenesis. *Proc Soc Exp Biol Med*, **216**, 181-191.

Heine H, Rietschel ET, Ulmer AJ (2001). The biology of endotoxin. *Mol Biotechnol*, **19**, 279-296.

Heizmann CW (1992). Calcium-binding proteins: basic concepts and clinical implications. *Gen Physiol Biophys*, **11**, 411-425.

Hernanz R, Alonso MJ, Zibrandtsen H, Alvarez Y, Salaices M, Simonsen U (2004). Measurements of nitric oxide concentration and hyporeactivity in rat superior mesenteric artery exposed to endotoxin. *Cardiovasc Res*, **62**, 202-211.

Hiki N, Berger D, Prigl C, Boelke E, Wiedeck H, Seidelmann M, Staib L, Kaminishi M, Oohara T, Beger HG (1998). Endotoxin Binding and Elimination by Monocytes: Secretion of Soluble CD14 Represents an Inducible Mechanism Counteracting Reduced Expression of Membrane CD14 in Patients with Sepsis and in a Patient with Paroxysmal Nocturnal Hemoglobinuria. *Infect Immun*, **66**, 1135-1141.

Hirano K (2007). Current topics in the regulatory mechanism underlying the Ca^{2+} sensitization of the contractile apparatus in vascular smooth muscle. *J Pharmacol Sci*, **104**, 109-115.

Hirata Y, Ishimaru S (2002). Effects of endothelin receptor antagonists on endothelin-1 and inducible nitric oxide synthase genes in a rat endotoxic shock model. *Clin Sci (Lond)*, **103 Suppl 48**, 332S-335S.

Ho KH, Kwan CY, Bourreau JP (1996). Hyporesponsiveness to Ca^{2+} of aortic smooth muscle in endotoxin-treated rats: no-dependent and -independent in vitro mechanisms. *Res Commun Mol Pathol Pharmacol*, **92**, 275-284.

Hoesel LM, Ward PA (2004). Mechanisms of inflammatory response syndrome in sepsis. *Drug Discovery Today: Disease Mechanisms*, **1**, 345-350.

Hofmann F, Biel M, Flockerzi V (1994). Molecular basis for Ca^{2+} channel diversity. *Annu Rev Neurosci*, **17**, 399-418.

Hofmann F, Feil R, Kleppisch T, Schlossmann J (2006). Function of cGMP-dependent protein kinases as revealed by gene deletion. *Physiol Rev*, **86**, 1-23.

Hogg N, Kalyanaraman B (1999). Nitric oxide and lipid peroxidation. *Biochim Biophys Acta*, **1411**, 378-384.

Holzmann A, Bloch KD, Sanchez LS, Filippov G, Zapol WM (1996). Hyporesponsiveness to inhaled nitric oxide in isolated, perfused lungs from endotoxin-challenged rats. *Am J Physiol*, **271**, L981-L986.

Horowitz A, Menice CB, Laporte R, Morgan KG (1996). Mechanisms of smooth muscle contraction. *Physiol Rev*, **76**, 967-1003.

Hotchkiss RS, Karl IE (1996). Calcium: a regulator of the inflammatory response in endotoxemia and sepsis. *New Horiz*, **4**, 58-71.

Hoth M, Penner R (1992). Depletion of intracellular calcium stores activates a calcium current in mast cells. *Nature*, **355**, 353-356.

Hughes AD (1995). Calcium channels in vascular smooth muscle cells. *J Vasc Res*, **32**, 353-370.

Hughes MN (2008). Chemistry of nitric oxide and related species. *Methods Enzymol*, **436**, 3-19.

Hynynen MM, Khalil RA (2006). The vascular endothelin system in hypertension--recent patents and discoveries. *Recent Patents Cardiovasc Drug Discov*, **1**, 95-108.

Ignarro LJ, Buga GM, Wood KS, Byrns RE, Chaudhuri G (1987). Endothelium-derived relaxing factor produced and released from artery and vein is nitric oxide. *Proc Natl Acad Sci U S A*, **84**, 9265-9269.

Iino M (1990). Calcium release mechanisms in smooth muscle. *Jpn J Pharmacol*, **54**, 345-354.

Ikebe M, Hartshorne DJ, Elzinga M (1987). Phosphorylation of the 20,000-dalton light chain of smooth muscle myosin by the calcium-activated, phospholipid-dependent protein kinase. Phosphorylation sites and effects of phosphorylation. *J Biol Chem*, **262**, 9569-9573.

Ikeda U, Yamamoto K, Maeda Y, Shimpo M, Kanbe T, Shimada K (1997). Endothelin-1 inhibits nitric oxide synthesis in vascular smooth muscle cells. *Hypertension*, **29**, 65-69.

Inoue A, Yanagisawa M, Kimura S, Kasuya Y, Miyauchi T, Goto K, Masaki T (1989). The human endothelin family: three structurally and pharmacologically distinct isopeptides predicted by three separate genes. *Proc Natl Acad Sci U S A*, **86**, 2863-2867.

Ishimaru S, Shichiri M, Mineshita S, Hirata Y (2001). Role of endothelin-1/endothelin receptor system in endotoxic shock rats. *Hypertens Res*, **24**, 119-126.

Ito M, Nakano T, Erdodi F, Hartshorne DJ (2004). Myosin phosphatase: structure, regulation and function. *Mol Cell Biochem*, **259**, 197-209.

Itoh Y, Yanagisawa M, Ohkubo S, Kimura C, Kosaka T, Inoue A, Ishida N, Mitsui Y, Onda H, Fujino M, . (1988). Cloning and sequence analysis of cDNA encoding the precursor of a human endothelium-derived vasoconstrictor peptide, endothelin: identity of human and porcine endothelin. *FEBS Lett*, **231**, 440-444.

Jaggar JH, Wellman GC, Heppner TJ, Porter VA, Perez GJ, Gollasch M, Kleppisch T, Rubart M, Stevenson AS, Lederer WJ, Knot HJ, Bonev AD, Nelson MT (1998). Ca^{2+} channels, ryanodine receptors and Ca^{2+}-activated K^{+} channels: a functional unit for regulating arterial tone. *Acta Physiol Scand*, **164**, 577-587.

Janssen-Heininger YM, Poynter ME, Baeuerle PA (2000). Recent advances towards understanding redox mechanisms in the activation of nuclear factor kappaB. *Free Radic Biol Med*, **28**, 1317-1327.

Jones JJ, Rapps JA, Sturek M, Mattox ML, Adams HR, Parker JL (1999). Contractile function and myoplasmic free Ca^{2+} (Cam) in coronary and mesenteric arteries of endotoxemic guinea pigs. *Shock*, **11**, 64-71.

Juhaszova M, Shimizu H, Borin ML, Yip RK, Santiago EM, Lindenmayer GE, Blaustein MP (1996). Localization of the Na^{+}-Ca^{2+} exchanger in vascular smooth muscle, and in neurons and astrocytes. *Ann N Y Acad Sci*, **779**, 318-335.

Juilfs DM, Soderling S, Burns F, Beavo JA (1999). Cyclic GMP as substrate and regulator of cyclic nucleotide phosphodiesterases (PDEs). *Rev Physiol Biochem Pharmacol*, **135**, 67-104.

Kalra D, Baumgarten G, Dibbs Z, Seta Y, Sivasubramanian N, Mann DL (2000). Nitric oxide provokes tumor necrosis factor-alpha expression in adult feline myocardium through a cGMP-dependent pathway. *Circulation*, **102**, 1302-1307.

Karaki H, Ozaki H, Hori M, Mitsui-Saito M, Amano K, Harada K, Miyamoto S, Nakazawa H, Won KJ, Sato K (1997). Calcium movements, distribution, and functions in smooth muscle. *Pharmacol Rev*, **49**, 157-230.

Karne S, Jayawickreme CK, Lerner MR (1993). Cloning and characterization of an endothelin-3 specific receptor (ETC receptor) from Xenopus laevis dermal melanophores. *J Biol Chem*, **268**, 19126-19133.

Keaney JF, Jr., Simon DI, Stamler JS, Jaraki O, Scharfstein J, Vita JA, Loscalzo J (1993). NO forms an adduct with serum albumin that has endothelium-derived relaxing factor-like properties. *J Clin Invest*, **91**, 1582-1589.

Kedzierski RM, Yanagisawa M (2001). Endothelin system: the double-edged sword in health and disease. *Annu Rev Pharmacol Toxicol*, **41**, 851-876.

Kirkby NS, Hadoke PW, Bagnall AJ, Webb DJ (2008). The endothelin system as a therapeutic target in cardiovascular disease: great expectations or bleak house? *Br J Pharmacol*, **153**, 1105-1119.

Kitamura K, Yamazaki J (2001). Chloride channels and their functional roles in smooth muscle tone in the vasculature. *Jpn J Pharmacol*, **85**, 351-357.

Kitazawa T, Eto M, Woodsome TP, Brautigan DL (2000). Agonists trigger G protein-mediated activation of the CPI-17 inhibitor phosphoprotein of myosin light chain phosphatase to enhance vascular smooth muscle contractility. *J Biol Chem*, **275**, 9897-9900.

Kleschyov AL, Muller B, Schott C, Stoclet JC (1998). Role of adventitial nitric oxide in vascular hyporeactivity induced by lipopolysaccharide in rat aorta. *Br J Pharmacol*, **124**, 623-626.

Knotek M, Esson M, Gengaro P, Edelstein CL, Schrier RW (2000). Desensitization of soluble guanylate cyclase in renal cortex during endotoxemia in mice. *J Am Soc Nephrol*, **11**, 2133-2137.

Ko EA, Park WS, Ko JH, Han J, Kim N, Earm YE (2005). Endothelin-1 increases intracellular Ca^{2+} in rabbit pulmonary artery smooth muscle cells through phospholipase C. *Am J Physiol Heart Circ Physiol*, **289**, H1551-H1559.

Konrad D, Oldner A, Rossi P, Wanecek M, Rudehill A, Weitzberg E (2004). Differentiated and dose-related cardiovascular effects of a dual endothelin receptor antagonist in endotoxin shock. *Crit Care Med*, **32**, 1192-1199.

Koyama M, Ito M, Feng J, Seko T, Shiraki K, Takase K, Hartshorne DJ, Nakano T (2000). Phosphorylation of CPI-17, an inhibitory phosphoprotein of smooth muscle myosin phosphatase, by Rho-kinase. *FEBS Lett*, **475**, 197-200.

Kuklin VN, Kirov MY, Evgenov OV, Sovershaev MA, Sjoberg J, Kirova SS, Bjertnaes LJ (2004). Novel endothelin receptor antagonist attenuates endotoxin-induced lung injury in sheep. *Crit Care Med*, **32**, 766-773.

Kumar C, Mwangi V, Nuthulaganti P, Wu HL, Pullen M, Brun K, Aiyar H, Morris RA, Naughton R, Nambi P (1994). Cloning and characterization of a novel endothelin receptor from Xenopus heart. *J Biol Chem*, **269**, 13414-13420.

Landan G, Bdolah A, Wollberg Z, Kochva E, Graur D (1991). Evolution of the sarafotoxin/endothelin superfamily of proteins. *Toxicon*, **29**, 237-244.

Laporte R, Laher I (1997). Sarcoplasmic reticulum-sarcolemma interactions and vascular smooth muscle tone. *J Vasc Res*, **34**, 325-343.

Large WA, Wang Q (1996). Characteristics and physiological role of the Ca^{2+}-activated Cl^- conductance in smooth muscle. *Am J Physiol*, **271**, C435-C454.

Le Monnier de Gouville AC, Cavero I (1991). Cross tachyphylaxis to endothelin isopeptide-induced hypotension: a phenomenon not seen with proendothelin. *Br J Pharmacol*, **104**, 77-84.

Leach M, Hamilton LC, Olbrich A, Wray GM, Thiemermann C (1998). Effects of inhibitors of the activity of cyclo-oxygenase-2 on the hypotension and multiple organ dysfunction caused by endotoxin: a comparison with dexamethasone. *Br J Pharmacol*, **124**, 586-592.

Ledoux J, Werner ME, Brayden JE, Nelson MT (2006). Calcium-activated potassium channels and the regulation of vascular tone. *Physiology (Bethesda)*, **21**, 69-78.

Lesh RE, Nixon GF, Fleischer S, Airey JA, Somlyo AP, Somlyo AV (1998). Localization of ryanodine receptors in smooth muscle. *Circ Res*, **82**, 175-185.

Levin ER, Gardner DG, Samson WK (1998). Natriuretic peptides. *N Engl J Med*, **339**, 321-328.

Li D, Tomson K, Yang B, Mehta P, Croker BP, Mehta JL (1999). Modulation of constitutive nitric oxide synthase, bcl-2 and Fas expression in cultured human coronary endothelial cells exposed to anoxia-reoxygenation and angiotensin II: role of AT1 receptor activation. *Cardiovasc Res*, **41**, 109-115.

Li L, Eto M, Lee MR, Morita F, Yazawa M, Kitazawa T (1998). Possible involvement of the novel CPI-17 protein in protein kinase C signal transduction of rabbit arterial smooth muscle. *J Physiol*, **508 (Pt 3)**, 871-881.

Li YH, Yan ZQ, Brauner A, Tullus K (2002). Activation of macrophage nuclear factor-kappa B and induction of inducible nitric oxide synthase by LPS. *Respir Res*, **3**, 23.

Lin CS, Lin G, Xin ZC, Lue TF (2006). Expression, distribution and regulation of phosphodiesterase 5. *Curr Pharm Des*, **12**, 3439-3457.

Liu SF, Barnes PJ, Evans TW (1997). Time course and cellular localization of lipopolysaccharide-induced inducible nitric oxide synthase messenger RNA expression in the rat in vivo. *Crit Care Med*, **25**, 512-518.

Liu SF, Newton R, Evans TW, Barnes PJ (1996). Differential regulation of cyclo-oxygenase-1 and cyclo-oxygenase-2 gene expression by lipopolysaccharide treatment in vivo in the rat. *Clin Sci (Lond)*, **90**, 301-306.

Lopez A, Lorente JA, Steingrub J, Bakker J, McLuckie A, Willatts S, Brockway M, Anzueto A, Holzapfel L, Breen D, Silverman MS, Takala J, Donaldson J, Arneson C, Grove G, Grossman S, Grover R (2004). Multiple-center, randomized, placebo-controlled, double-blind study of the nitric oxide synthase inhibitor 546C88: effect on survival in patients with septic shock. *Crit Care Med*, **32**, 21-30.

Lorente JA, Landin L, Renes E, De PR, Jorge P, Rodena E, Liste D (1993). Role of nitric oxide in the hemodynamic changes of sepsis. *Crit Care Med*, **21**, 759-767.

Loscalzo J (2000). What we know and don't know about L-arginine and NO. *Circulation*, **101**, 2126-2129.

Lu JL, Schmiege LM, III, Kuo L, Liao JC (1996). Downregulation of endothelial constitutive nitric oxide synthase expression by lipopolysaccharide. *Biochem Biophys Res Commun*, **225**, 1-5.

Luscher TF, Barton M (2000). Endothelins and Endothelin Receptor Antagonists : Therapeutic Considerations for a Novel Class of Cardiovascular Drugs. *Circulation*, **102**, 2434-2440.

Maczewski M, Beresewicz A (2000). The role of endothelin, protein kinase C and free radicals in the mechanism of the post-ischemic endothelial dysfunction in guinea-pig hearts. *J Mol Cell Cardiol*, **32**, 297-310.

Magder S, Javeshghani D, Cernacek P, Giaid A (2001). Regional distribution of endothelin-1 and endothelin converting enzyme-1 in porcine endotoxemia. *Shock*, **16**, 320-325.

Manthous CA, Hall JB, Samsel RW (1993). Endotoxin in human disease. Part 2: Biologic effects and clinical evaluations of anti-endotoxin therapies. *Chest*, **104**, 1872-1881.

Marin J, Encabo A, Briones A, Garcia-Cohen EC, Alonso MJ (1999). Mechanisms involved in the cellular calcium homeostasis in vascular smooth muscle: calcium pumps. *Life Sci*, **64**, 279-303.

Marsault R, Vigne P, Breittmayer JP, Frelin C (1991). Kinetics of vasoconstrictor action of endothelins. *Am J Physiol*, **261**, C987-C993.

Martinez MC, Muller B, Stoclet JC, Andriantsitohaina R (1996). Alteration by lipopolysaccharide of the relationship between intracellular calcium levels and contraction in rat mesenteric artery. *Br J Pharmacol*, **118**, 1218-1222.

Mateo AO, De Artinano AA (1997). Highlights on endothelins: a review. *Pharmacol Res*, **36**, 339-351.

Matsuda N, Hattori Y (2007). Vascular biology in sepsis: pathophysiological and therapeutic significance of vascular dysfunction. *J Smooth Muscle Res*, **43**, 117-137.

Matsuda N, Hattori Y, Takahashi Y, Nishihira J, Jesmin S, Kobayashi M, Gando S (2004). Therapeutic effect of in vivo transfection of transcription factor decoy to NF-kappaB on septic lung in mice. *Am J Physiol Lung Cell Mol Physiol*, **287**, L1248-L1255.

Matsuda N, Hattori Y, Zhang XH, Fukui H, Kemmotsu O, Gando S (2003). Contractions to histamine in pulmonary and mesenteric arteries from endotoxemic rabbits: modulation by vascular expressions of inducible nitric-oxide synthase and histamine H1-receptors. *J Pharmacol Exp Ther*, **307**, 175-181.

Matsuda N, Hayashi Y, Takahashi Y, Hattori Y (2006). Phosphorylation of endothelial nitric-oxide synthase is diminished in mesenteric arteries from septic rabbits depending on the altered phosphatidylinositol 3-kinase/Akt pathway: reversal effect of fluvastatin therapy. *J Pharmacol Exp Ther*, **319**, 1348-1354.

Matsumoto H, Suzuki N, Onda H, Fujino M (1989). Abundance of endothelin-3 in rat intestine, pituitary gland and brain. *Biochem Biophys Res Commun*, **164**, 74-80.

Maurice DH, Palmer D, Tilley DG, Dunkerley HA, Netherton SJ, Raymond DR, Elbatarny HS, Jimmo SL (2003). Cyclic nucleotide phosphodiesterase activity, expression, and targeting in cells of the cardiovascular system. *Mol Pharmacol*, **64**, 533-546.

McIntyre RC, Jr., Sheridan B, Agrafojo J, Fullerton DA (1997). Endotoxin differentially impairs cyclic guanosine monophosphate-mediated relaxation in the pulmonary and systemic circulations. *Crit Care Med*, **25**, 318-323.

McKenna TM (1990). Prolonged exposure of rat aorta to low levels of endotoxin in vitro results in impaired contractility. Association with vascular cytokine release. *J Clin Invest*, **86**, 160-168.

McMillen MA, Sumpio BE (1995). Endothelins: polyfunctional cytokines. *J Am Coll Surg*, **180**, 621-637.

McNair LL, Salamanca DA, Khalil RA (2004). Endothelin-1 promotes Ca^{2+} antagonist-insensitive coronary smooth muscle contraction via activation of epsilon-protein kinase C. *Hypertension*, **43**, 897-904.

McPherson PS, Campbell KP (1993). The ryanodine receptor/Ca^{2+} release channel. *J Biol Chem*, **268**, 13765-13768.

Merritt JE, Armstrong WP, Benham CD, Hallam TJ, Jacob R, Jaxa-Chamiec A, Leigh BK, McCarthy SA, Moores KE, Rink TJ (1990). SK&F 96365, a novel inhibitor of receptor-mediated calcium entry. *Biochem J*, **271**, 515-522.

Michel T, Feron O (1997). Nitric oxide synthases: which, where, how, and why? *J Clin Invest*, **100**, 2146-2152.

Minami K, Fukuzawa K, Nakaya Y, Zeng XR, Inoue I (1993). Mechanism of activation of the Ca^{2+}-activated K^{+} channel by cyclic AMP in cultured porcine coronary artery smooth muscle cells. *Life Sci*, **53**, 1129-1135.

Mitaka C, Hirata Y, Yokoyama K, Nagura T, Tsunoda Y, Amaha K (1999). Improvement of renal dysfunction in dogs with endotoxemia by a nonselective endothelin receptor antagonist. *Crit Care Med*, **27**, 146-153.

Mitchell JA, Kohlhaas KL, Sorrentino R, Warner TD, Murad F, Vane JR (1993). Induction by endotoxin of nitric oxide synthase in the rat mesentery: lack of effect on action of vasoconstrictors. *Br J Pharmacol*, **109**, 265-270.

Mitchell JA, Paul-Clark MJ, Clarke GW, McMaster SK, Cartwright N (2007). Critical role of toll-like receptors and nucleotide oligomerisation domain in the regulation of health and disease. *J Endocrinol*, **193**, 323-330.

Mitolo-Chieppa D, Serio M, Potenza MA, Montagnani M, Mansi G, Pece S, Jirillo E, Stoclet JC (1996). Hyporeactivity of mesenteric vascular bed in endotoxin-treated rats. *Eur J Pharmacol*, **309**, 175-182.

Miwa S, Kawanabe Y, Okamoto Y, Masaki T (2005). Ca^{2+} entry channels involved in endothelin-1-induced contractions of vascular smooth muscle cells. *J Smooth Muscle Res*, **41**, 61-75.

Miyamoto A, Moriki H, Ishiguro S, Nishio A (2004). In vitro application of endotoxin to thoracic aortas from magnesium-deficient rats enhances vascular hyporeactivity to phenylephrine. *J Am Coll Nutr*, **23**, 518S-520S.

Mochida H, Takagi M, Inoue H, Noto T, Yano K, Fujishige K, Sasaki T, Yuasa K, Kotera J, Omori K, Kikkawa K (2002). Enzymological and pharmacological profile of T-0156, a potent and selective phosphodiesterase type 5 inhibitor. *Eur J Pharmacol*, **456**, 91-98.

Moncada S, Higgs A (1993). The L-arginine-nitric oxide pathway. *N Engl J Med*, **329**, 2002-2012.

Morgan KG, Gangopadhyay SS (2001). Invited review: cross-bridge regulation by thin filament-associated proteins. *J Appl Physiol*, **91**, 953-962.

Myers PR, Zhong Q, Jones JJ, Tanner MA, Adams HR, Parker JL (1995). Release of EDRF and NO in ex vivo perfused aorta: inhibition by in vivo E. coli endotoxemia. *Am J Physiol*, **268**, H955-H961.

Nakamura S, Naruse M, Naruse K, Demura H, Uemura H (1990). Immunocytochemical localization of endothelin in cultured bovine endothelial cells. *Histochemistry*, **94**, 475-477.

Nakamura T, Kasai K, Sekiguchi Y, Banba N, Takahashi K, Emoto T, Hattori Y, Shimoda S (1991). Elevation of plasma endothelin concentrations during endotoxin shock in dogs. *Eur J Pharmacol*, **205**, 277-282.

Nathan C, Xie QW (1994). Nitric oxide synthases: roles, tolls, and controls. *Cell*, **78**, 915-918.

Nathan CF, Hibbs JB, Jr. (1991). Role of nitric oxide synthesis in macrophage antimicrobial activity. *Curr Opin Immunol*, **3**, 65-70.

Nelson MT, Quayle JM (1995). Physiological roles and properties of potassium channels in arterial smooth muscle. *Am J Physiol*, **268**, C799-C822.

Neylon CB (1999). Vascular biology of endothelin signal transduction. *Clin Exp Pharmacol Physiol*, **26**, 149-153.

Niki I, Yokokura H, Sudo T, Kato M, Hidaka H (1996). Ca^{2+} signaling and intracellular Ca^{2+} binding proteins. *J Biochem*, **120**, 685-698.

Nilsson H (1998). Interactions between membrane potential and intracellular calcium concentration in vascular smooth muscle. *Acta Physiol Scand*, **164**, 559-566.

O'Brien AJ, Thakur G, Buckley JF, Singer M, Clapp LH (2005). The pore-forming subunit of the K(ATP) channel is an important molecular target for LPS-induced vascular hyporeactivity in vitro. *Br J Pharmacol*, **144**, 367-375.

O'Brien AJ, Wilson AJ, Sibbald R, Singer M, Clapp LH (2001). Temporal variation in endotoxin-induced vascular hyporeactivity in a rat mesenteric artery organ culture model. *Br J Pharmacol*, **133**, 351-360.

Opal SM (2007). The host response to endotoxin, antilipopolysaccharide strategies, and the management of severe sepsis. *Int J Med Microbiol*, **297**, 365-377.

Orallo F (1996). Regulation of cytosolic calcium levels in vascular smooth muscle. *Pharmacol Ther*, **69**, 153-171.

Ozaki H, Karaki H (2002). Organ culture as a useful method for studying the biology of blood vessels and other smooth muscle tissues. *Jpn J Pharmacol*, **89**, 93-100.

Papapetropoulos A, bou-Mohamed G, Marczin N, Murad F, Caldwell RW, Catravas JD (1996). Downregulation of nitrovasodilator-induced cyclic GMP accumulation in cells exposed to endotoxin or interleukin-1 beta. *Br J Pharmacol*, **118**, 1359-1366.

Parker JL, Myers PR, Zhong Q, Kim K, Adams HR (1994). Inhibition of endothelium-dependent vasodilation by Escherichia coli endotoxemia. *Shock*, **2**, 451-458.

Parmentier JH, Muthalif MM, Saeed AE, Malik KU (2001). Phospholipase D activation by norepinephrine is mediated by 12(s)-, 15(s)-, and 20-hydroxyeicosatetraenoic acids generated by stimulation of cytosolic phospholipase a2. tyrosine phosphorylation of phospholipase d2 in response to norepinephrine. *J Biol Chem*, **276**, 15704-15711.

Parsons PE, Worthen GS, Moore EE, Tate RM, Henson PM (1989). The association of circulating endotoxin with the development of the adult respiratory distress syndrome. *Am Rev Respir Dis*, **140**, 294-301.

Pasquet JP, Zou MH, Ullrich V (1996). Peroxynitrite inhibition of nitric oxide synthases. *Biochimie*, **78**, 785-791.

Peters K, Unger RE, Brunner J, Kirkpatrick CJ (2003). Molecular basis of endothelial dysfunction in sepsis. *Cardiovas Res*, **60**, 49-57.

Peters TS, Lewis SJ (1996). Lipopolysaccharide inhibits acetylcholine- and nitric oxide-mediated vasodilation in vivo. *J Pharmacol Exp Ther*, **279**, 918-925.

Pickkers P, Dorresteijn MJ, Bouw MP, van der Hoeven JG, Smits P (2006). In vivo evidence for nitric oxide-mediated calcium-activated potassium-channel activation during human endotoxemia. *Circulation*, **114**, 414-421.

Piechota M, Banach M, Irzmanski R, Barylski M, Piechota-Urbanska M, Kowalski J, Pawlicki L (2007). Plasma endothelin-1 levels in septic patients. *J Intensive Care Med*, **22**, 232-239.

Piepot HA, Boer C, Groeneveld AB, van Lambalgen AA, Sipkema P (2000). Lipopolysaccharide impairs endothelial nitric oxide synthesis in rat renal arteries. *Kidney Int*, **57**, 2502-2510.

Piepot HA, Groeneveld AB, van Lambalgen AA, Sipkema P (2002). The role of inducible nitric oxide synthase in lipopolysaccharide-mediated hyporeactivity to vasoconstrictors differs among isolated rat arteries. *Clin Sci (Lond)*, **102**, 297-305.

Piepot HA, Groeneveld AB, van Lambalgen AA, Sipkema P (2003). Endotoxin impairs endothelium-dependent vasodilation more in the coronary and renal arteries than in other arteries of the rat. *J Surg Res*, **110**, 413-418.

Pittet JF, Morel DR, Hemsen A, Gunning K, Lacroix JS, Suter PM, Lundberg JM (1991). Elevated plasma endothelin-1 concentrations are associated with the severity of illness in patients with sepsis. *Ann Surg*, **213**, 261-264.

Pleiner J, Mittermayer F, Schaller G, Marsik C, MacAllister RJ, Wolzt M (2003). Inflammation-induced vasoconstrictor hyporeactivity is caused by oxidative stress. *J Am Coll Cardiol*, **42**, 1656-1662.

Polson JB, Strada SJ (1996). Cyclic nucleotide phosphodiesterases and vascular smooth muscle. *Annu Rev Pharmacol Toxicol*, **36**, 403-427.

Pugin J, Schurer-Maly C, Leturcq D, Moriarty A, Ulevitch RJ, Tobias PS (1993). Lipopolysaccharide Activation of Human Endothelial and Epithelial Cells is Mediated by Lipopolysaccharide-Binding Protein and Soluble CD14. *PNAS*, **90**, 2744-2748.

Pulido EJ, Shames BD, Fullerton DA, Sheridan BC, Selzman CH, Gamboni-Robertson F, Bensard DD, McIntyre RC, Jr. (2000). Differential inducible nitric oxide synthase expression in systemic and pulmonary vessels after endotoxin. *Am J Physiol Regul Integr Comp Physiol*, **278**, R1232-R1239.

Putney JW, Jr. (1999). TRP, inositol 1,4,5-trisphosphate receptors, and capacitative calcium entry. *Proc Natl Acad Sci U S A*, **96**, 14669-14671.

Raeymaekers L, Eggermont JA, Wuytack F, Casteels R (1990). Effects of cyclic nucleotide dependent protein kinases on the endoplasmic reticulum Ca^{2+} pump of bovine pulmonary artery. *Cell Calcium*, **11**, 261-268.

Reddi BA, Carpenter RH (2005). Venous excess: a new approach to cardiovascular control and its teaching. *J Appl Physiol*, **98**, 356-364.

Rees DD, Monkhouse JE, Cambridge D, Moncada S (1998). Nitric oxide and the haemodynamic profile of endotoxin shock in the conscious mouse. *Br J Pharmacol*, **124**, 540-546.

Robin P, Boulven I, Desmyter C, Harbon S, Leiber D (2002). ET-1 stimulates ERK signaling pathway through sequential activation of PKC and Src in rat myometrial cells. *Am J Physiol Cell Physiol*, **283**, C251-C260.

Ros J, Leivas A, Jimenez W, Morales M, Bosch-Marce M, Arroyo V, Rivera F, Rodes J (1997). Effect of bacterial lipopolysaccharide on endothelin-1 production in human vascular endothelial cells. *J Hepatol*, **26**, 81-87.

Rubanyi GM, Polokoff MA (1994). Endothelins: molecular biology, biochemistry, pharmacology, physiology, and pathophysiology. *Pharmacol Rev*, **46**, 325-415.

Ruetten H, Thiemermann C (1996). Effect of selective blockade of endothelin ETB receptors on the liver dysfunction and injury caused by endotoxaemia in the rat. *Br J Pharmacol*, **119**, 479-486.

Ruetten H, Thiemermann C, Vane JR (1996). Effects of the endothelin receptor antagonist, SB 209670, on circulatory failure and organ injury in endotoxic shock in the anaesthetized rat. *Br J Pharmacol*, **118**, 198-204.

Rusch NJ, Liu Y, Pleyte KA (1996). Mechanisms for regulation of arterial tone by Ca^{2+}-dependent K^+ channels in hypertension. *Clin Exp Pharmacol Physiol*, **23**, 1077-1081.

Ryan GB, Majno G (1977). Acute inflammation. A review. *Am J Pathol*, **86**, 183-276.

Saida K, Mitsui Y, Ishida N (1989). A novel peptide, vasoactive intestinal contractor, of a new (endothelin) peptide family. Molecular cloning, expression, and biological activity. *J Biol Chem*, **264**, 14613-14616.

Sakurada S, Okamoto H, Takuwa N, Sugimoto N, Takuwa Y (2001). Rho activation in excitatory agonist-stimulated vascular smooth muscle. *Am J Physiol Cell Physiol*, **281**, C571-C578.

Sakurai T, Morimoto H, Kasuya Y, Takuwa Y, Nakauchi H, Masaki T, Goto K (1992). Level of ETB receptor mRNA is down-regulated by endothelins through decreasing the intracellular stability of mRNA molecules. *Biochem Biophys Res Commun*, **186**, 342-347.

Salamanca DA, Khalil RA (2005). Protein kinase C isoforms as specific targets for modulation of vascular smooth muscle function in hypertension. *Biochem Pharmacol*, **70**, 1537-1547.

Salomone S, Morel N, Godfraind T (1998). A therapeutic dosage of amlodipine prevents vascular hyporeactivity induced in rats by lipopolysaccharide. *Naunyn Schmiedebergs Arch Pharmacol*, **357**, 252-259.

Sanders KM (2001). Invited review: mechanisms of calcium handling in smooth muscles. *J Appl Physiol*, **91**, 1438-1449.

Satoh H (1995). Endothelin-1 inhibition of the ATP-sensitive K^+ channel in guinea-pig ventricular cardiomyocytes. *Gen Pharmacol*, **26**, 1549-1552.

Satoh M, Ando S, Shinoda T, Yamazaki M (2008). Clearance of bacterial lipopolysaccharides and lipid A by the liver and the role of argininosuccinate synthase. *Innate Immun*, **14**, 51-60.

Schmidt M, Kroger B, Jacob E, Seulberger H, Subkowski T, Otter R, Meyer T, Schmalzing G, Hillen H (1994). Molecular characterization of human and bovine endothelin converting enzyme (ECE-1). *FEBS Lett*, **356**, 238-243.

Schneider F, Schott C, Stoclet JC, Julou-Schaeffer G (1992). L-arginine induces relaxation of small mesenteric arteries from endotoxin-treated rats. *Eur J Pharmacol*, **211**, 269-272.

Schuetz P, Christ-Crain M, Morgenthaler NG, Struck J, Bergmann A, Muller B (2007). Circulating precursor levels of endothelin-1 and adrenomedullin, two endothelium-derived, counteracting substances, in sepsis. *Endothelium*, **14**, 345-351.

Schumann RR, Leong SR, Flaggs GW, Gray PW, Wright SD, Mathison JC, Tobias PS, Ulevitch RJ (1990). Structure and function of lipopolysaccharide binding protein. *Science*, **249**, 1429-1431.

Scott WS, Nakayama DK (1998). Escherichia coli lipopolysaccharide downregulates soluble guanylate cyclase in pulmonary artery smooth muscle. *J Surg Res*, **80**, 309-314.

Shaw MJ, Shennib H, Bousette N, Ohlstein EH, Giaid A (2001). Effect of endothelin receptor antagonist on lung allograft apoptosis and NOSII expression. *Ann Thorac Surg*, **72**, 386-390.

Shindo T, Kurihara H, Kurihara Y, Morita H, Yazaki Y (1998). Upregulation of endothelin-1 and adrenomedullin gene expression in the mouse endotoxin shock model. *J Cardiovasc Pharmacol*, **31 Suppl 1**, S541-S544.

Sirmagul B, Kilic FS, Tunc O, Yildirim E, Erol K (2006). Effects of verapamil and nifedipine on different parameters in lipopolysaccharide-induced septic shock. *Heart Vessels*, **21**, 162-168.

Somlyo AP, Somlyo AV (1994). Signal transduction and regulation in smooth muscle. *Nature*, **372**, 231-236.

Somlyo AP, Somlyo AV (2000). Signal transduction by G-proteins, rho-kinase and protein phosphatase to smooth muscle and non-muscle myosin II. *J Physiol*, **522 Pt 2**, 177-185.

Somlyo AV, Somlyo AP (1968). Electromechanical and pharmacomechanical coupling in vascular smooth muscle. *J Pharmacol Exp Ther*, **159**, 129-145.

Sommerville LE, Hartshorne DJ (1986). Intracellular calcium and smooth muscle contraction. *Cell Calcium*, **7**, 353-364.

Song SK, Karl IE, Ackerman JJ, Hotchkiss RS (1993). Increased intracellular Ca2+: a critical link in the pathophysiology of sepsis? *Proc Natl Acad Sci U S A*, **90**, 3933-3937.

Sorrentino R, d'Emmanuele d, V, Lippolis L, Sorrentino L, Autore G, Pinto A (1999). Involvement of ATP-sensitive potassium channels in a model of a delayed vascular hyporeactivity induced by lipopolysaccharide in rats. *Br J Pharmacol*, **127**, 1447-1453.

Stamler JS (1994). Redox signaling: nitrosylation and related target interactions of nitric oxide. *Cell*, **78**, 931-936.

Stasch JP, Becker EM, onso-Alija C, Apeler H, Dembowsky K, Feurer A, Gerzer R, Minuth T, Perzborn E, Pleiss U, Schroder H, Schroeder W, Stahl E, Steinke W, Straub A, Schramm M (2001). NO-independent regulatory site on soluble guanylate cyclase. *Nature*, **410**, 212-215.

Stasch JP, Schmidt PM, Nedvetsky PI, Nedvetskaya TY, AK HS, Meurer S, Deile M, Taye A, Knorr A, Lapp H, Muller H, Turgay Y, Rothkegel C, Tersteegen A, Kemp-Harper B, Muller-Esterl W, Schmidt HH (2006). Targeting the heme-oxidized nitric oxide receptor for selective vasodilatation of diseased blood vessels. *J Clin Invest*, **116**, 2552-2561.

Stuehr DJ (1999). Mammalian nitric oxide synthases. *Biochim Biophys Acta*, **1411**, 217-230.

Stull JT, Tansey MG, Tang DC, Word RA, Kamm KE (1993). Phosphorylation of myosin light chain kinase: a cellular mechanism for Ca2+ desensitization. *Mol Cell Biochem*, **127-128**, 229-237.

Sudjarwo SA, Hori M, Takai M, Urade Y, Okada T, Karaki H (1993). A novel subtype of endothelin B receptor mediating contraction in swine pulmonary vein. *Life Sci*, **53**, 431-437.

Suffredini AF, Fromm RE, Parker MM, Brenner M, Kovacs JA, Wesley RA, Parrillo JE (1989). The cardiovascular response of normal humans to the administration of endotoxin. *N Engl J Med*, **321**, 280-287.

Szabo C, Dawson VL (1998). Role of poly(ADP-ribose) synthetase in inflammation and ischaemia-reperfusion. *Trends Pharmacol Sci*, **19**, 287-298.

Szabo C, Salzman AL, Ischiropoulos H (1995). Endotoxin triggers the expression of an inducible isoform of nitric oxide synthase and the formation of peroxynitrite in the rat aorta in vivo. *FEBS Lett*, **363**, 235-238.

Taguchi H, Heistad DD, Chu Y, Rios CD, Ooboshi H, Faraci FM (1996). Vascular expression of inducible nitric oxide synthase is associated with activation of Ca(++)-dependent K+ channels. *J Pharmacol Exp Ther*, **279**, 1514-1519.

Takahashi K, Silva A, Cohen J, Lam HC, Ghatei MA, Bloom SR (1990). Endothelin immunoreactivity in mice with gram-negative bacteraemia: relationship to tumour necrosis factor-alpha. *Clin Sci (Lond)*, **79**, 619-623.

Takata M, Filippov G, Liu H, Ichinose F, Janssens S, Bloch DB, Bloch KD (2001). Cytokines decrease sGC in pulmonary artery smooth muscle cells via NO-dependent and NO-independent mechanisms. *Am J Physiol Lung Cell Mol Physiol*, **280**, L272-L278.

Takuwa Y (1996). Regulation of vascular smooth muscle contraction. The roles of Ca2+, protein kinase C and myosin light chain phosphatase. *Jpn Heart J*, **37**, 793-813.

Tan P, Luscinskas FW, Homer-Vanniasinkam S (1999). Cellular and Molecular Mechanisms of Inflammation and Thrombosis. *Eur J Vasc Endovasc Surg*, **17**, 373-389.

Teder P, Noble PW (2000). A Cytokine Reborn? . Endothelin-1 in Pulmonary Inflammation and Fibrosis. *Am J Respir Cell Mol Biol*, **23**, 7-10.

Tedgui A, Mallat Z (2001). Anti-Inflammatory Mechanisms in the Vascular Wall. *Circ Res*, **88**, 877-887.

Toescu EC (1995). Temporal and spatial heterogeneities of Ca2+ signaling: mechanisms and physiological roles. *Am J Physiol*, **269**, G173-G185.

Toward TJ, Nials AT, Johnson FJ (2005). Guinea-pig lung adenylyl and guanylyl cyclase and PDE activities associated with airway hyper- and hypo-reactivity following LPS inhalation. *Life Sci*, **76**, 997-1011.

Traaseth NJ, Ha KN, Verardi R, Shi L, Buffy JJ, Masterson LR, Veglia G (2008). Structural and dynamic basis of phospholamban and sarcolipin inhibition of Ca(2+)-ATPase. *Biochemistry*, **47**, 3-13.

Tsai BM, Wang M, Pitcher JM, Kher A, Meldrum DR (2006). Disparate IL-1beta and iNOS gene expression in the aorta and pulmonary artery after endotoxemia. *Surg Infect (Larchmt)*, **7**, 21-27.

Umans JG, Wylam ME, Samsel RW, Edwards J, Schumacker PT (1993). Effects of endotoxin in vivo on endothelial and smooth-muscle function in rabbit and rat aorta. *Am Rev Respir Dis*, **148**, 1638-1645.

Vaandrager AB, de Jonge HR (1996). Signalling by cGMP-dependent protein kinases. *Mol Cell Biochem*, **157**, 23-30.

Van Amersfoort ES, Van Berkel TJC, Kuiper J (2003). Receptors, Mediators, and Mechanisms Involved in Bacterial Sepsis and Septic Shock. *Clin Microbiol Rev*, **16**, 379-414.

Vanelli G, Hussain SN, Aguggini G (1995). Glibenclamide, a blocker of ATP-sensitive potassium channels, reverses endotoxin-induced hypotension in pig. *Exp Physiol*, **80**, 167-170.

Vila E, Salaices M (2005). Cytokines and vascular reactivity in resistance arteries. *Am J Physiol Heart Circ Physiol*, **288**, H1016-H1021.

Virdis A, Colucci R, Fornai M, Blandizzi C, Duranti E, Pinto S, Bernardini N, Segnani C, Antonioli L, Taddei S, Salvetti A, Del TM (2005). Cyclooxygenase-2 inhibition improves vascular endothelial dysfunction in a rat model of endotoxic shock: role of inducible nitric-oxide synthase and oxidative stress. *J Pharmacol Exp Ther*, **312**, 945-953.

Wakabayashi I, Hatake K, Kakishita E, Nagai K (1987). Diminution of contractile response of the aorta from endotoxin-injected rats. *Eur J Pharmacol*, **141**, 117-122.

Waldron GJ, Cole WC (1999). Activation of vascular smooth muscle K+ channels by endothelium-derived relaxing factors. *Clin Exp Pharmacol Physiol*, **26**, 180-184.

Walker RL, Hume JR, Horowitz B (2001). Differential expression and alternative splicing of TRP channel genes in smooth muscles. *Am J Physiol Cell Physiol*, **280**, C1184-C1192.

Walsh MP, Horowitz A, Clement-Chomienne O, Andrea JE, Allen BG, Morgan KG (1996). Protein kinase C mediation of Ca(2+)-independent contractions of vascular smooth muscle. *Biochem Cell Biol*, **74**, 485-502.

Wanecek M, Oldner A, Rudehill A, Sollevi A, Alving K, Weitzberg E (1997). Cardiopulmonary dysfunction during porcine endotoxin shock is effectively counteracted by the endothelin receptor antagonist bosentan. *Shock*, **7**, 364-370.

Wanecek M, Oldner A, Rudehill A, Sollevi A, Alving K, Weitzberg E (1999). Endothelin(A)-receptor antagonism attenuates pulmonary hypertension in porcine endotoxin shock. *Eur Respir J*, **13**, 145-151.

Wanecek M, Weitzberg E, Rudehill A, Oldner A (2000). The endothelin system in septic and endotoxin shock. *Eur J Pharmacol*, **407**, 1-15.

Webster NR, Galley HF (2003). Inflammation and immunity. *BJA CEPD Reviews*, **3**, 54-58.

Weitzberg E, Hemsen A, Rudehill A, Modin A, Wanecek M, Lundberg JM (1996). Bosentan-improved cardiopulmonary vascular performance and increased plasma levels of endothelin-1 in porcine endotoxin shock. *Br J Pharmacol*, **118**, 617-626.

Weitzberg E, Lundberg JO (1998). Nonenzymatic nitric oxide production in humans. *Nitric Oxide*, **2**, 1-7.

Wiel E, Pu Q, Corseaux D, Robin E, Bordet R, Lund N, Jude B, Vallet B (2000). Effect of L-arginine on endothelial injury and hemostasis in rabbit endotoxin shock. *J Appl Physiol*, **89**, 1811-1818.

Wilkinson MF, Earle ML, Triggle CR, Barnes S (1996). Interleukin-1beta, tumor necrosis factor-alpha, and LPS enhance calcium channel current in isolated vascular smooth muscle cells of rat tail artery. *FASEB J*, **10**, 785-791.

Winder SJ, Allen BG, Clement-Chomienne O, Walsh MP (1998). Regulation of smooth muscle actin-myosin interaction and force by calponin. *Acta Physiol Scand*, **164**, 415-426.

Woodsome TP, Polzin A, Kitazawa K, Eto M, Kitazawa T (2006). Agonist- and depolarization-induced signals for myosin light chain phosphorylation and force generation of cultured vascular smooth muscle cells. *J Cell Sci*, **119**, 1769-1780.

Wu CC, Chen SJ, Garland CJ (2004). NO and KATP channels underlie endotoxin-induced smooth muscle hyperpolarization in rat mesenteric resistance arteries. *Br J Pharmacol*, **142**, 479-484.

Wu CC, Chen SJ, Yen MH (1998a). Nitric oxide-independent activation of soluble guanylyl cyclase contributes to endotoxin shock in rats. *Am J Physiol*, **275**, H1148-H1157.

Wu CC, Thiemermann C, Vane JR (1995). Glibenclamide-induced inhibition of the expression of inducible nitric oxide synthase in cultured macrophages and in the anaesthetized rat. *Br J Pharmacol*, **114**, 1273-1281.

Wu CC, Wang JH, Chiao CW, Yen MH (1999). Comparison between effects of dantrolene and nifedipine on lipopolysaccharide-induced endotoxemia in the anesthetized rats. *Chin J Physiol*, **42**, 211-217.

Wu X, Haystead TA, Nakamoto RK, Somlyo AV, Somlyo AP (1998b). Acceleration of myosin light chain dephosphorylation and relaxation of smooth muscle by telokin. Synergism with cyclic nucleotide-activated kinase. *J Biol Chem*, **273**, 11362-11369.

Xia Y, Tsai AL, Berka V, Zweier JL (1998). Superoxide generation from endothelial nitric-oxide synthase. A Ca2+/calmodulin-dependent and tetrahydrobiopterin regulatory process. *J Biol Chem*, **273**, 25804-25808.

Xie Q, Nathan C (1994). The high-output nitric oxide pathway: role and regulation. *J Leukoc Biol*, **56**, 576-582.

Yamazaki J, Duan D, Janiak R, Kuenzli K, Horowitz B, Hume JR (1998). Functional and molecular expression of volume-regulated chloride channels in canine vascular smooth muscle cells. *J Physiol*, **507 (Pt 3)**, 729-736.

Yanagisawa M, Kurihara H, Kimura S, Tomobe Y, Kobayashi M, Mitsui Y, Yazaki Y, Goto K, Masaki T (1988). A novel potent vasoconstrictor peptide produced by vascular endothelial cells. *Nature*, **332**, 411-415.

Yen MH, Chen SJ, Wu CC (1995). Comparison of responses to aminoguanidine and N omega-nitro-L-arginine methyl ester in the rat aorta. *Clin Exp Pharmacol Physiol*, **22**, 641-645.

Zhang XF, Iwamuro Y, Enoki T, Okazawa M, Lee K, Komuro T, Minowa T, Okamoto Y, Hasegawa H, Furutani H, Miwa S, Masaki T (1999). Pharmacological characterization of Ca2+ entry channels in endothelin-1-induced contraction of rat aorta using LOE 908 and SK&F 96365. *Br J Pharmacol*, **127**, 1388-1398.

Zingarelli B, Hasko G, Salzman AL, Szabo C (1999). Effects of a novel guanylyl cyclase inhibitor on the vascular actions of nitric oxide and peroxynitrite in immunostimulated smooth muscle cells and in endotoxic shock. *Crit Care Med*, **27**, 1701-1707.

Zor T, Selinger Z (1996). Linearization of the Bradford protein assay increases its sensitivity: theoretical and experimental studies. *Anal Biochem*, **236**, 302-308.

Appendix